Effects of anthropogenic stressors on temperate mesophotic ecosystems

Valerio Micaroni

A thesis submitted to the Victoria University of Wellington

in fulfilment of the requirements for the degree of

Doctor of Philosophy

Victoria University of Wellington

2022

This thesis was conducted under the supervision of:

Prof James J. Bell

(Primary supervisor, Victoria University of Wellington)

&

Prof Rob McAllen

(Co-supervisor, University College Cork, Cork, Ireland)

&

Prof John Turner

(Co-supervisor, Bangor University, Wales - UK)

Victoria University of Wellington

Wellington, New Zealand

Abstract

Coastal ecosystems are among the most productive biomes on the planet, but also the most vulnerable. A wide range of anthropogenic impacts are threatening the integrity of coastal systems, and therefore their capability to provide goods and ecosystem services. Despite their importance and vulnerability, many coastal ecosystems remain poorly studied. Mesophotic ecosystems lie between the shallow euphotic waters and the aphotic deep-sea. While these ecosystems have been relatively well-studied in tropical regions, the importance of temperate mesophotic ecosystems (TMEs) has only recently been recognised. TMEs extend from the lower limit of the euphotic zone to the limit of benthic primary production, which usually correspond to ~30–150 m. However, in particular conditions, mesophotic ecosystems can occur in shallower waters. Lough Hyne (Ireland) is a fully marine sea lough, designated as Europe's first Marine Nature Reserve in 1981 for its extraordinary biodiversity. This reserve hosts particularly diverse sponge-dominated mesophotic communities as shallow as 10 m. Unfortunately, during the last decade, the lough's underwater communities have undergone drastic changes, which have been attributed to changes in water quality and in particular, an increase in dissolved nitrogen. My research aimed to investigate the effects of anthropogenic stressors on temperate mesophotic ecosystems using Lough Hyne as a model system. My thesis aims to: 1) characterise the changes that have occurred in the subtidal communities at Lough Hyne; 2) investigate the possible causes of these changes through tolerance experiments; and 3) investigate community dynamics and any recovery of Lough Hyne's mesophotic communities.

In my first chapter, I collated 30 years (1990-2019) of scientific surveys and opportunistic observations of the subtidal (6–30 m) communities at Lough Hyne to investigate the long-term stability and vulnerability of TMEs. I then explored the potential causes of the observed changes. I found significant changes in the overall biological community and sponge assemblages at all sites within Lough Hyne. However, these changes were not consistent across sites and mainly affected the innermost areas of the lough. Changes were also not consistent between taxa and functional groups, suggesting differential vulnerability of TME organisms to stress events. The main finding was a marked decline in most three-dimensional sponges in the inner part of the lough, which was likely the result of one or more mass mortality events between 2010 and 2015. These changes did not seem to be related to either thermal or rainfall anomalies. The only factor known to have changed over this period is nitrogen, which has increased threefold during the last 20-30 years. Therefore, I hypothesised that the sponge mortality at Lough Hyne is linked to eutrophication. Importantly, this chapter shows the potential vulnerability of TMEs to short-term

disturbance events, and highlights the importance of monitoring mesophotic habitats globally to ensure they are appropriately conserved.

In my second chapter, I investigated the possible causes of the mass sponge mortality at Lough Hyne through laboratory experiments. One of the most common and severe consequences of eutrophication in aquatic ecosystems is hypoxia. Therefore, I investigated the response of sponges to moderate and severe simulated hypoxic events. I ran three laboratory experiments on four species from two different temperate oceans (NE Atlantic and SW Pacific). I exposed sponges to a total of five hypoxic treatments, with increasing severity (3.3, 1.6, 0.5, 0.4 and 0.13 mg O_2 L^{-1}, over 7–12 days). The main finding was that sponges are generally very tolerant of hypoxia. All sponges survived under the experimental conditions, except *Polymastia croceus*, which showed significant mortality at the lowest oxygen concentration (0.13 mg O_2 L^{-1}, median lethal time: 12 days). In all species except *Suberites carnosus*, respiration rate was unaffected down to 0.4 mg O_2 L^{-1}. Importantly, sponges showed species-specific phenotypic changes in response to hypoxic treatments, likely representing adaptive strategies for living in low oxygen water. Compared to other sessile organisms, sponges generally showed a much higher tolerance to hypoxia, suggesting that sponges may be favoured and survive in future deoxygenated oceans. These results also indicate that hypoxia alone was probably not the cause of sponge mortality at Lough Hyne.

In my third data chapter, I investigated the resilience and temporal dynamics of shallow-water (~ 17 m) mesophotic communities at Lough Hyne, following the mass mortality event. In June 2018, I established five replicate permanent quadrats (0.25 m^2) on the rocky cliffs (18 m) at five sites inside the lough. My collaborators and I took photoquadrats twice a year until June 2021 (36 months, 5–7 time points), from which I extracted data on the percentage cover of sessile organisms identified to the lowest practical taxonomic level. In addition, I analysed historical photoquadrats collected with a similar methodology between 1994 and 1995, from two internal sites at Lough Hyne. Historical data were used to assess if differences in temporal patterns between sites were exclusive to impacted communities or also occurred in the past. Multivariate analysis did not detect any directional community or assemblage changes over time in the internal and innermost sites, suggesting that recovery of benthic communities and sponge assemblages is either occurring very slowly or not at all. In contrast, I found significant community changes at the entrance site, where barnacles suffered a mass mortality event in 2018, perhaps due to a heatwave. Univariate analysis revealed weak signs of recovery for some of the three-dimensional sponges and anemones that were highly affected by the disturbance,

represented by a small increase in percentage cover. In general, temporal dynamics (turnover, diversity and percentage cover of benthic groups) were found to be different between: 1) sites experiencing very distinct environmental conditions; and 2) between sites that shared similar conditions and communities. Most importantly, sponges seem to be recovering only in one of the three internal sites, where I detected a positive trend in the three-dimensional sponges affected by the 2010–2015 mortality event. This finding indicates that small variations in environmental conditions can affect the dynamics and recovery of mesophotic subtidal ecosystems.

Overall, my thesis shows that mesophotic ecosystems are vulnerable to environmental stressors and slow recovery rates. Most temperate mesophotic taxa are long-lived and slow-growing organisms, likely to have limited resilience to human-induced impacts. Despite sponges being generally considered tolerant of stressors, the mass mortality at Lough Hyne shows that this is not always the case. My results suggest that three-dimensional mesophotic sponges are among the most sensitive species and the slowest growing. Any decline in these habitat-forming species will likely affect important ecosystem functions (e.g., nutrient cycling, bentho-pelagic coupling, habitat provisioning), with detrimental effects on the associated ecosystem services. My study also shows that, as some sites, recovery is underway. However, at the current rate, whole-lough recovery is likely to be in the order of decades. Given the vulnerability and importance of TMEs, research and management of these habitats should be prioritised at Lough Hyne and elsewhere. In particular, long-term monitoring of biotic and abiotic factors will be crucial to understand TME long-term dynamics, recovery and how these ecosystems respond to environmental variations and anthropogenic disturbances. Monitoring will improve our ability to make evidence-based decisions for the management of TMEs in a fast-changing world. In addition, we also need more research on how mesophotic organisms respond to stressors and how they contribute to ecosystem functioning. Better knowledge of these ecosystems will increase awareness of the value of TMEs among decision-makers and the general public, which will be essential to ensure their conservation.

...to Mother Nature

Acknowledgements

I wish to thank James, my primary supervisor at Victoria University of Wellington for his amazing support, the invaluable guidance, the cool field trips, for sharing his passion for the marine environment, and for the many opportunities he has offered me. I thank Rob, my secondary supervisor, for always being supportive, for making all the work at Lough Hyne super smooth and for bear all my fussy demands. I am also thankful to John, my external supervisor for his support, encouragement, and his valuable input to my manuscripts.

This research was possible thanks to National Parks and Wildlife Service of Ireland (An tSeirbhís Páirceanna Náisiúnta agus Fiadhúlra) that provided research funding and support. A particular thanks to Cliona O'Brien, Declan O'Donnell, and Patrick Graham. I also thank Victoria University of Wellington for providing my scholarship, covering my university fees, as well as resources and support for my research and training. I thank also the University College Cork for providing access to their facilities in Cork and at Lough Hyne.

Special thanks go to Christine Morrow and Bernard Picton for the amazing moral support, for the good time spent together, for all the knowledge about sponge taxonomy and Irish biodiversity they shared with me; Julia Nunn and Nick Owen for sharing their precious knowledge, photos and videos of Lough Hyne, their work has been unvaluable; Luke Harmann, for his amazing technical support in Ireland, and for all the great time had together; Daniel "Snout" McNaughtan, for the precious technical advice, the amazing diving training and support and for the good time spent at VUCEL; John Van Der Sman for all the boating teaching and the fantastic all his craftsman's creations he realised for my PhD project; Dr Lisa Woods, for all the statistical help and for teaching me so much about statistics; Prof Iacopo Bertocci, and Prof Marti Jane Anderson and Dr Alberto Rovellini for the unvaluable statistical advice; Charli Mortimer, for her support and company during the 2018 Lough Hyne field trip. Tracey Saxby and Jane Thomas, IAN Image Library (https://ian.umces.edu/imagelibrary), for some of the images used in the thesis.

Thanks to all the old and new members of the "Sponge club", for the good time spent at uni and at the lab, for the fantastic BYOs and for all the constructive discussions about those amazing creatures with holes and spicules. Thank you, Albi, Alice, Ben, Charli, Fra, Emily, Meg, Nora, Imke, Rama, Sandeep, and Valeria. I also thank the all the VUCEL faithful, for brightening up the PhD days; in particular all the other PhDs and MSc that shared this path with me: Ali, Andy, Andrea, Erik, Luia and Sergio. A special thanks to my Italian friends aka "Nouzo". A super

thanks also to Jaime for the best welcome to New Zealand I could desired (together with Zoe!) and for introducing me to Kaitiakitanga and Manaakitanga.

I am grateful for the unvaluable support of my parents Giulia and Pietro. You have always encouraged me to follow my passions. None of what I have done would have been possible without your unconditional love and faith in me. I finally thanks Francesca for being always with me for having followed me on the other side of world, for teaching me new things every day. The life with you if amazing, no matter where we are and what we are doing.

Chapter contributions and publications

Chapter 2:

Study design: Valerio Micaroni, Prof James J. Bell (Victoria University of Wellington - VUW - New Zealand)

Data collection: VM, JJB, Prof Rob McAllen and Luke Harman (University College Cork - Ireland)

Data analyses: VM

Chapter writing and editing: VM, JJB, RM, John Turner (Bangor University – Wales, UK)

Publication: **Micaroni, V**., McAllen, R., Turner, J., Strano, F., Morrow, C., Picton, B., Harman, L., Bell, J.J. (2021). Vulnerability of Temperate Mesophotic Ecosystems (TMEs) to environmental impacts: Rapid ecosystem changes at Lough Hyne Marine Nature Reserve, Ireland. *Science of The Total Environment* 789: 147708. https://doi.org/10.1016/j.scitotenv.2021.147708

Chapter 3:

Study design: VM, JJB

Data collection: VM, Francesca Strano (VUW)

Data analyses: VM, under the guidance of Lisa Woods (VUW)

Chapter writing and editing: VM, JJB, FS, RM, JT

Publication: **Micaroni, V**., Strano, F., McAllen, R., Woods, L., Turner, J., Harman, L., Bell, J.J. (2022). Adaptive strategies of sponges to deoxygenated oceans. *Global Change Biology* 28, 1972–1989. https://doi.org/10.1111/gcb.16013

Chapter 4:

Study design: VM, JJB

Data collection: VM, JJB, RM, LH, FS

Data analyses: VM with assistance from Dr Alberto Rovellini (NOAA – US)

Chapter writing and editing: VM, JJB, RM

Publication: **Micaroni, V**., McAllen, R., Strano, F., Rovellini, A., Morrow, C., Picton, B., Woods, L., Turner, J., Harman, L., Bell, J.J. (*In preparation*). Resilience to disturbance and interannual dynamics of a rocky temperate mesophotic ecosystem.

Table of Contents

Figures

Tables

1. Chapter 1 - General Introduction

The Renouf Laboratory at dawn, Lough Hyne

1.1. Coastal Ecosystems

Coastal ecosystems lie at the interface between terrestrial and marine environments and are characterised by great complexity and spatial variability (MAE, 2005; Granek, *et al.*, 2009). These include a heterogeneous range of habitat types, including estuaries, rocky reefs, bays, nearshore coastal waters, mangrove forests, coastal marshes, seagrass beds, sand dunes, bivalve reefs, mud flats, and inshore coral reefs (NRC, 1995; MAE, 2005; Barbier *et al.*, 2011).

Coastal ecosystems are among the most important biomes on the planet due to the reliance of human populations on the resources they provide (Barbier *et al.*, 2011; Cloern *et al.*, 2014). Despite occupying only 7.4% of the world's seas, they account for a large part of ocean productivity and host a high proportion of the world's marine biodiversity (Gray, 1997; Martínez *et al.*, 2007; Cloern *et al.*, 2014). According to estimates from 2011, the global economic value of coastal ecosystem services is around $27.7 trillion/year, the highest among the world's biomes (de Groot *et al.*, 2012; Costanza *et al.*, 2014). Marine areas within the continental shelf alone account for 25% of global primary productivity, 90–95% of the world's fish catches, 50% of global denitrification, and 90% of global sedimentary mineralization (UNEP, 1992; MAE, 2005). Other important goods and services provided by these ecosystems include the provision of raw materials and pharmaceuticals, gas and climate regulation, protection from wave action and flooding, bioremediation of wastes and nutrient cycling, along with human wellbeing, recreational, cultural, and spiritual values (Costanza *et al.*, 1997; Beaumont *et al.*, 2007; Barbier *et al.*, 2011).

1.2. Threats to Coastal Ecosystem

The importance of coastal areas has been recognised since ancient times. It is no coincidence that many of the first human settlements were established in proximity to the coast (MAE, 2005; Neuman *et al.*, 2015). Currently, around 40% of the global population lives within 100 km of the coast, and half of the world's major cities (> 500,000 people) are located within 50 km of the ocean (MAE, 2005; Kummu *et al.*, 2016). Furthermore, demographic trends indicate that coastal populations are increasing at a higher rate than inland ones (Neuman *et al.*, 2015). For these reasons, coastal ecosystems are among the most threatened biomes in the world (Islam and Tanaka, 2004). Despite their recognised importance, a wide range of anthropogenic impacts threaten their structural and functional integrity, and consequently, their capability to provide goods and services (Worm *et al.*, 2006).

Among threats to coastal ecosystems, habitat loss is one of the biggest and the second leading cause of marine species extinction (Dulvy *et al.*, 2003; Crain *et al.*, 2009). This phenomenon has been occurring for centuries, although it has increased substantially since the industrial revolution (Lotze *et al.*, 2006). Since the rise of human civilisation, we have lost 67% of wetlands, 65% of seagrasses, and 48% of other habitat-forming aquatic vegetation (Lotze *et al.*, 2006). The loss of important habitat-forming organisms can have major ecosystem-level consequences and typically facilitates regime shifts from complex, productive, and highly diverse habitats to simpler, less productive and diverse ones (Hughes *et al.*, 2003; Folke *et al.*, 2004).

Another important impact on coastal systems is overfishing, which has already led to the ecological extinction (*sensu* Estes *et al.*, 1989) of many key species, and in some cases, to the loss of entire trophic levels (Jackson *et al.*, 2001). Overfishing is not only reducing the capacity of the oceans to feed a growing human population, but its indirect effects are compromising the functioning of many coastal ecosystems with cascading effects through food webs (Sheffer *et al.*, 2005).

Since the beginning of the industrial revolution, new major threats, including pollution and eutrophication, have emerged (Crain *et al.*, 2009). Coastal areas are being extensively degraded by both point and nonpoint sources of pollution (Kennish, 2017). The ocean is often a sink for a wide range of substances discharged deliberately or accidentally via human activities (Islam and Tanaka, 2004). These include heavy metals, microplastics, hydrocarbons, biocides, endocrine disruptors, and many other toxic compounds (Porte *et al.*, 2006; Crain *et al.*, 2009; Cole *et al.*, 2011; Kennish, 2017). Eutrophication is one of the leading causes of declines in environmental quality in many coastal marine ecosystems across the world (Smith *et al.*, 1999). It results from nutrient enrichment, generally resulting from the release of agricultural fertilisers, livestock and human wastes, and fossil fuel combustion (Nixon, 1995). Eutrophication can have many effects on the marine ecosystems spanning from changes in species composition to the occurrence of Harmful Algal Blooms (HABs). In the worst cases, it can lead to mass mortality events due to anoxia (Smith *et al.*, 1999). Pollution and eutrophication are particularly relevant impacts to consider in coastal areas due to the deep interconnections between the coast and terrestrial ecosystems (MAE, 2005). Pollutants can originate far from the coast and be transported over long distances by rivers that ultimately link the continental landmass to the oceans (Meybeck and Vörösmarty, 1999). This means that coastal management needs a whole-of-system perspective involving the entire water catchment (MAE, 2005).

Global climate change resulting from human activities is now recognised as one of the major environmental challenges of the 21st century (Heip *et al.*, 2009). The global mean ocean surface temperature is predicted to increase between 0.3°C and 4.8°C by the end of the century (IPCC, 2014). Climate change can affect ecosystems at different levels of organisation, from organisms to populations, and all the way through communities (Crain *et al.*, 2009). Among the main effects detected so far are shifts in species distributions, decreased ocean productivity, an increase in the incidence of diseases, alteration of food web dynamics (e.g., increasing the speed of biomass transfer between trophic levels), and the reduction in the abundance of habitat-forming species (Cheung *et al.*, 2009; Hoegh-Guldberg and Bruno, 2010; Poloczanska *et al.*, 2013; Bell *et al.*, 2018).

Biological invasions are another threat to coastal ecosystems that has been exacerbated by globalization and industrialization (Occhipinti-Ambrogi and Savini, 2003). During the last century, the movement of goods and people around the world has increased exponentially (Ruiz *et al.*, 1997). This has led to an increase in the movement and spread of organisms among geographic regions (Carlton, 1989). Non-indigenous species now occur across the planet, and the extent and cumulative impact of these invasions have been enormous (Elton, 1958; Occhipinti-Ambrogi and Savini, 2003). While many non-indigenous species become part of the local flora and fauna without major effects, others become invasive, reaching high densities and, in some cases, outcompeting native organisms with severe ecological and economic consequences (Bax *et al.*, 2003).

1.3. Temperate mesophotic ecosystems

Despite the recognised importance of the coastal environment, many coastal ecosystems are still poorly studied. Temperate mesophotic ecosystems (TMEs) lie between the shallow euphotic waters and the aphotic deep-sea, in the so-called twilight zone. TMEs extend from the lower limit of the euphotic zone (<1%, of the surface irradiance) to the limit of benthic primary production (Cerrano *et al.*, 2019). In most areas, TMEs are found between 30 and 150 m of depth (Turner *et al.*, 2019). While mesophotic ecosystems have attracted significant attention in tropical regions (mesophotic coral ecosystems, MCEs), we still know very little about these ecosystems in temperate waters.

Rocky temperate mesophotic ecosystems are dominated by benthic invertebrates, including sponges, cnidarians, bryozoans, and ascidians, and shade-adapted algae (Fig. 1.1; Ballesteros, 2006; Rossi *et al.*, 2017; Turner *et al.*, 2019; Bell et al, *in review*). In the upper mesophotic zone

(< 50 m), the dominant organisms are usually algae, mainly coralline and other calcifying red algae (e.g., *Peyssonnelia*). In some mesophotic ecosystems, calcifying algae can produce extensive biogenic reefs up to 3–4 m thick (e.g., Mediterranean Sea; Ballesteros, 2006). At greater depths, algal dominance decreases. At its lowest boundary (~ 150 m), TMEs are almost exclusively dominated by sessile invertebrates (Piazzi *et al.*, 2019; Heyns *et al.*, 2016).

Across all the mesophotic zones, the most dominant sessile invertebrates are usually sponges, which occupy on average ~13–19% of the substrate (Bell et al, *in review*). Most of the sponge coverage is due to encrusting forms, but arborescent and massive forms can be also locally abundant. The most abundant group after sponges is cnidarians, which occupy ~ 9–12% of the substrate on average (Bell et al, *in review*). Octocorals are particularly important because they create extensive and dense "forests", of high ecological and economic value (Rossi, 2013; Gori *et al.*, 2017). Among the other abundant organisms, we find bryozoans, which can be locally very abundant and form complex biogenic reefs, and turf (Cocito, 2004; Piazzi *et al.*, 2019). Turf can occupy a large portion of the substrate, especially in the lower mesophotic zone. At mesophotic depths, turf is generally composed of filamentous algae and small invertebrates such as hydroids and bryozoans (Bell *et al.*, *in review*). With respect to sessile invertebrates, there are generally large increases in upright morphologies with depth, which creates higher habitat complexity (e.g., Heyns *et al.*, 2016; Harris *et al.*, 2021) and is the result of greater morphological complexity of sponges (Harris *et al.*, 2021), bryozoans (Bradstock and Gordon, 1983) and cnidarians (Cerrano *et al.*, 2009), when compared to their shallower counterparts.

The mesophotic zone represents a vertical transition belt between shallow and deeper waters (Cerrano *et al.*, 2019). This area is characterised by several environmental gradients, which are relatively constant worldwide (Bell *et al.*, *in review*). In general, temperature decreases with depth, while salinity can slightly increase or decrease, depending on the geographic area (Ingleby and Huddleston, 2007; Bell *et al.*, in review). Both temperature and salinity become more stable with depth and show less variability (Montero-Serra *et al.*, 2018). While oxygen generally decreases with depth, the decrease is small and is therefore unlikely to be biologically important (Bell *et al.*, *in review*). Important nutrients such as phosphate and nitrate substantially increase with depth (Lazzari *et al.*, 2016), while dissolved organic matter (DOC), particulate organic matter (POC), and chlorophyll-*a* decrease with depth (Tanaka and Rassoulzadegan, 2002). These are particular important factors because they are likely to be food sources for TME organisms (Stuart and Klumpp, 1984; Riisgård *et al.*, 2000). Finally, turbidity and pH generally decrease with depth, although the change in pH between 30 and 150 m of depth is only around 0.1–0.2

units (Bell *et al.*, *in review*). The structure and the functioning of TME communities are probably driven by the complex interactions of these gradients and other local abiotic factors such as currents, sedimentation, and type of substrate. (Bell *et al.*, in review).

TMEs provide important ecosystem services, including supporting fisheries, and providing raw materials (e.g., pharmaceuticals), genetic resources, and a range of cultural and recreational values (e.g., SCUBA diving and angling) (Tonin, 2018). Since TMEs are mostly dominated by filter feeders, these ecosystems might play a key role in bentho-pelagic coupling and recycling nutrients in deeper waters (Maldonado *et al.*, 2012). Furthermore, many benthic organisms inhabiting TMEs have long life spans (Montero-Serra *et al.*, 2018), so they may act as important carbon sinks (Coppari *et al.*, 2019). The complex "animal forests" supported by stable rocky TMEs can provide substrate, refuge and shelter for an array of organisms (Rossi *et al.*, 2017), including commercially important fish and crustaceans (Paoli *et al.*, 2017). Mesophotic systems have also been hypothesised to act as refugia from anthropogenic stressors including fishing. For example, in temperate Australia, mesophotic reefs provide habitat for larger fish compared to shallow waters (Williams *et al.*, 2019), one interpretation of which is refuge effect. In addition, mesophotic depths might also act as refugia from ocean warming in response to climate change, since temperature is generally cooler and more stable (Idan *et al.*, 2020).

Recent research has highlighted how TMEs are threatened by a wide range of anthropogenic stressors. Increased sea temperatures and thermal anomalies due to climate change can be particularly detrimental to mesophotic organisms, as already reported from the Mediterranean Sea (Cerrano *et al.*, 2000; Garrabou *et al.*, 2019).. Since TMEs are dominated by suspension feeders, they are particularly susceptible to increased sedimentation. Some TME organisms have been shown to be relatively tolerant of sedimentation, while others seem to be very sensitive (Tseng *et al.*, 2011; Piazzi *et al.*, 2012; Bell *et al.*, 2015a; Topçu *et al.*, 2019). Increases in sedimentation are mainly caused by bottom-fishing activity (e.g., trawling), changes in land use, and sea-bed mining (Jones, 1992; Jankowski *et al.*, 1996; Vaalgamaa, 2004). Industrial, artisanal, and recreational fisheries are also recognised as a major threat to rocky TMEs in the Mediterranean (Bo *et al.*, 2014, Angiolillo *et al.*, 2015; Yıldız and Karakulak, 2016), but little information is available for other geographical areas. Other important stressors that could treat TMEs include eutrophication, acidification, and the arrival of non-indigenous species (Piazzi *et al.*, 2011; Swezey *et al.*, 2017; Sempere-Valverde *et al.*, 2021).

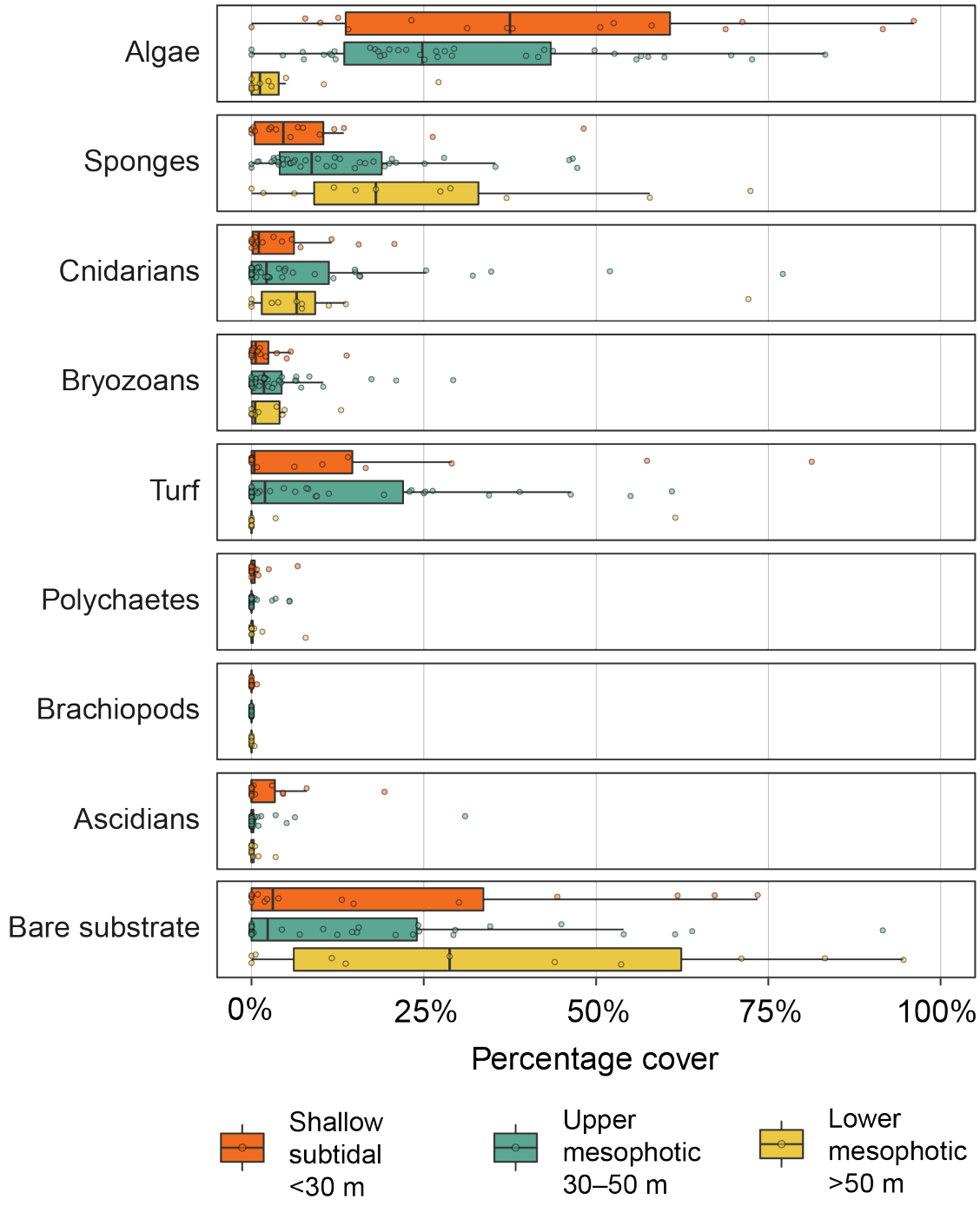

Figure 1.1. Percentage cover of the main benthic organisms in the upper and lower mesophotic zones and shallow water of world oceans. Horizontal bars inside the boxplots represent medians; the symbol × represents means. Lower and upper hinges of the boxplots correspond to the first and third quartiles, respectively. Points represent individual data points. Shallow subtidal (0-15 m), Upper mesophotic (20-50 m), Lower mesophotic (51-150 m). Made by the author for Bell *et al.* (*in review*).

1.4. Ecosystem resilience

Resilience is a key concept in ecology and conservation biology to understand and predict ecosystem responses to human and natural disturbance (Capdevila *et al.*, 2021). Resilience in ecological sciences has been defined several times and is now a broad, multifaced, and loosely organized cluster of concepts (Strunz, 2012). In its original definition, resilience describes the persistence of systems and of their ability to absorb change and disturbance (Holling, 1973). For other authors, resilience is a measure of how fast ecosystems return to their original state following disturbance (Pimm, 1984; Tilman and Downing, 1994). The first definition implies the existence of alternative stable states, where instabilities can flip a system into another regime of stability domain, while the second definition focuses on stability near an equilibrium steady state (Holling, 1973). In its most modern sense, resilience encompasses elements from both definitions and is determined by: 1) the capacity to reduce the impact of a disturbance (ecological resilience or resistance); and 2) the ability to recover from the impact of disturbance (engineering resilience or recovery capacity) (Hodgson *et al.*, 2015; Ingrisch and Bahn, 2018).

Assuming the existence of multiple stable states, if a disturbance drives the system beyond a tipping point, the system may transition to an alternative state (Scheffer *et al.*, 2009). This new system state is characterized by substantially different structures and is maintained by hysteresis (from Greek delay, lag) processes or feedbacks (Capdevila *et al.*, 2021). The concept of hysteresis recognizes that localized short-term reductions of disturbance will not ensure recovery to a pristine state (Hughes *et al.*, 2005).

The resilience of benthic communities to disturbance has been investigated in a wide range of marine habitats, from coral reefs to seagrass meadows and soft sediment communities (Sherman and Coull, 1980; Halford *et al.*, 2004; Unsworth *et al.*, 2015). However, studies on recovery require repeated sampling over time of the same areas, which can be difficult to perform in deep waters (Turner *et al.*, 2019). Furthermore, estimating patterns and recovery trajectories requires baseline data, which are extremely rare due to the challenges of studying deep- and cold-water habitats (Bianchi *et al.*, 2017). Consequently, despite information about mass mortality episodes having increased in recent decades, our knowledge about temperate mesophotic communities is still inadequate (Cerrano *et al.*, 2000; Coma *et al.*, 2009; Garrabou *et al.*, 2009). Indeed, resilience in mesophotic communities has only been speculated from single-species studies (Marschal *et al.*, 2004; Teixidó *et al.*, 2011; Rossi, 2013; Bramanti *et al.*, 2014; Hitt *et al.*, 2020). These previous studies found low dynamics, high longevity, and the persistence of

many structuring species, suggesting a low resilience to disturbance (Teixidó *et al.*, 2011). However, population recovery is not necessarily indicative of ecosystem recovery (Lotze *et al.*, 2011). Hence, better estimation of resilience of temperate mesophotic communities to disturbance remains of paramount importance for both science and management (Bianchi *et al.*, 2017).

1.5. Eutrophication

Among all the impacts on marine ecosystems, eutrophication is considered one of the main drivers of change, especially in coastal areas (Halpern *et al.*, 2007). Eutrophication is defined as "an increase in the rate of supply of organic matter to an ecosystem" (Nixon, 1995). This increase is more often mediated by nutrient enrichment caused by the leaching of agricultural fertilizers, the discharge of human and livestock waste, and fossil fuel combustion (Howarth *et al.*, 2000). At the end of the 20th century, estimates suggest that half of the total nitrogen (N) and phosphorus (P) input into aquatic ecosystems originated from agriculture (Oenema *et al.*, 2018). The contribution of agriculture started to be particularly important from the 1960s, following the post-WWII technological and economic boom that led to a rapid increase in fertilizer use and manure production (Oenema *et al.*, 2018). In other countries, this problem has occurred more recently (PCE, 2013). In New Zealand for example, eutrophication is becoming of increasing concern since dairy farming has intensified and expanded dramatically in the past two decades leading to a decline in water quality in many areas of the country (PCE, 2013; Foote *et al.*, 2015). In less than 40 years in New Zealand, due to anthropogenic inputs, the total N and P exported to the ocean has increased by 74% and 48%, respectively (Snelder *et al.*, 2018). Globally, human population size is expected to increase to 9.7 billion by 2050, and 11.2 billion by 2100, and the global agricultural production (based on data from 2005) needs to increase by 70–110% to meet demand in 2050 (Tilman *et al.*, 2011; UN, 2015). This will likely lead to an increase in eutrophication in the future (Ray *et al.*, 2013).

Eutrophication of aquatic ecosystems can have many direct and indirect consequences (Nixon, 1995). The first effect of the increase of nutrients in the water is higher primary production (Justić, 1987). In coastal ecosystems, phytoplankton growth is limited by nutrient availability, in particular by N, and to a lesser extent by P (Howarth and Marino, 2006). A limited increase of nutrients and primary production can have positive effects on ecosystems, increasing species richness and biomass (Boström *et al.*, 2002; Grall and Chauvaud, 2002). However, more often, eutrophication leads to severe or catastrophic consequences (Van Beusekom, 2018). The

excess of phytoplankton and benthic algae, not grazed by primary consumers, once dead, accumulates in the sediment and leads to oxygen depletion as it is broken down by heterotrophic bacteria (Heip, 1995). The ultimate effect of severe eutrophication is anoxia (Diaz and Rosenberg, 2008). If this state persists, sulphur-oxidizing bacteria start to produce H_2S with devastating effects on the biota (Jørgensen, 1980; Faganeli *et al.*, 1985; Cockcroft, 2001; Luther *et al.*, 2004).

One of the largest zones of coastal hypoxia on Earth is in the northern Gulf of Mexico adjacent to the Mississippi and Atchafalaya estuaries, the so-called "Dead Zone" (Malakoff, 1998). In 2001 it reached the record area of 20,700 km^2 (Rabalais *et al.*, 2001). The high nutrient input from the Mississippi River substantially increased after the 1950s, and led to the annual formation of a hypoxic water mass, persistent from spring through late summer (Rabalais *et al.*, 2002). The consequences have been devastating, with regime shifts in benthic communities and the disappearance of many marine invertebrates such as pericaridean crustaceans, bivalves, gastropods, and ophiuroids (Rabalais *et al.*, 2002).

In the Black Sea, in the 1960s, following a rapid increase in local industrial and agricultural activities, a huge area (up to 40,000 km^2 in 1980) started to become seasonally hypoxic (Rabotyagov *et al.*, 2012). This resulted in mass mortalities of many marine organisms, and the local extinction of many species including commercially important species (Zaitsev, 1992). During this period, the Black Sea fishery that was worth around US$2 billion was reduced by 90 % and the tourism industry losses were estimated at around US$500 million (Battaglini, 2008).

Hypoxic areas resulting from human activities have more than doubled since the 1960s (Van Beusekom, 2018). Other relevant examples of eutrophication-induced hypoxic systems are: the Baltic Sea, now persistently hypoxic, where the missing biomass in the dead zones is estimated to be around 264,000 tons, roughly 30% of total Baltic secondary production (Diaz and Rosenberg, 2008); Chesapeake Bay, where seasonally occurring hypoxia leads to a drastic reduction in the benthic diversity and in the overall productivity of the area (Officer *et al.*, 1984; Boesch *et al.*, 2001; Kemp *et al.*, 2005); and the northern Adriatic Sea, where the seasonal occurrence of hypoxia between the 1970s and the 1980s, led to a 90% reduction in the benthic biomass in some areas (Justić, 1987; Justić, 1991; Stachowitsch, 1991).

Other than hypoxia, eutrophication may have several other consequences (Heip, 1995). Changes in nutrient concentrations and ratios can lead to a change in phytoplankton composition and dynamics and in some case to the occurrence of harmful algal blooms (HABs) (Anderson *et*

al., 2002; Davidson *et al.*, 2014). In addition, eutrophication can profoundly change rocky shore communities, for example with the replacement of perennial, canopy-forming algae by ephemeral turf-forming algae (Worm and Lotze, 2006).

Other factors can intensify the negative effects of eutrophication in marine ecosystems, particularly global warming (Moss *et al.*, 2011). It has been suggested that increased water temperature can both promote HABs, by selectively favouring noxious thermo-tolerant species, and facilitating the occurrence of hypoxia through enhanced stratification, decreased oxygen solubility, increased metabolism, and increased production of organic matter (Rabalais *et al.*, 2009; O'neil *et al.*, 2012). However, although the interactive effects of global warming and eutrophication have been considered, there is a lack of empirical evidence, and further studies are needed (Van Beusekom, 2018).

Reductions in nutrient inputs have allowed some estuarine and coastal ecosystems to recover rapidly from eutrophication (Paerl *et al.*, 2004; Schindler and Vallentyne, 2008). In some systems, however, the recovery has been slow or negligible (Smith and Schindler, 2009). Therefore, it is important to implement holistic integrated management, that takes into consideration the entire watershed and includes land use planning to prevent further occurrences of the negative effect of eutrophication (MAE, 2005).

1.6. Effect of Hypoxia/anoxia on marine animals

In marine ecosystems, normal dissolved oxygen (DO) concentrations range from 100% air saturation (about 8–10 mg O_2 L^{-1}, depending on temperature and salinity) to 2.0 mg L^{-1} (Diaz and Rosenberg, 1995). When values decrease below 2.0 mg O_2 L^{-1}, the system is considered hypoxic, and when values are around 0 mg O_2 L^{-1}, it is considered anoxic (Diaz and Rosenberg, 1995).

Many marine invertebrates and ectothermic vertebrates can cope with decreasing concentrations of ambient DO, through different behavioural, physiological, and molecular adaptations (Gorr *et al.*, 2010). A common behavioural response of mobile animals is to come out from sediment or to migrate to more oxygenated areas (Wu, 2002). At the physiological level, the first response is metabolic down-regulation, through a wide range of biological mechanisms (Guppy and Withers, 1999). If the DO concentration decreases below a certain value, termed the critical PO_2 (variable depending on the organism), the metabolism shifts from aerobic to anaerobic (Pörtner and Grieshaber, 1993; Pörtner *et al.*, 2005). The genetic response

to decreasing DO has been found to be mediated by the hypoxia-inducible transcription factor (HIF) (Gorr *et al.*, 2010). HIF regulates the transcription of many genes involved in the short-term and long-term cellular and systemic responses to hypoxia, enabling better survival under low DO regimes (Wu, 2002; Li and Brouwer, 2007). Recent molecular analysis has shown that HIF is an evolutionarily conserved gene found in all metazoans, even though sponge and ctenophore genomes lack key components of the HIF pathway (Kaelin and Ratcliffe, 2008; Mills *et al.*, 2018).

Although many marine organisms can tolerate low DO, the thresholds of oxygen concentrations for hypoxia can vary significantly among and within different taxa (Vaquer-Sunyer and Duarte, 2008). Comparative studies on infaunal ophiuroids, decapods and bivalves in NE Atlantic have shown that the tolerance range was in the order of 0.7–1.3 mg $O_2\ L^{-1}$ (8 to 15 % saturation), which they could tolerate in experimental conditions for several days to weeks (Rosenberg *et al.*, 1991). A recent meta-analysis, covering selected marine groups, showed that crustaceans and fish are the most sensitive organisms, while molluscs, cnidarians and priapulids are the most tolerant (Vaquer-Sunyer and Duarte, 2008). In general, more mobile organisms are less tolerant to low DO than sessile and slow-moving ones as they can move to avoid hypoxic conditions (Vaquer-Sunyer and Duarte, 2008). The general results of the meta-analysis are shown in Figure 1.2.

Tolerance to hypoxia can also differ among different life stages of the same species. For example, DO levels well above hypoxia (2.8 mg L^{-1}) have a significant impact on gastropod veliger development, even though molluscs are among the most tolerant animals (Chan *et al.*, 2008). Furthermore, tolerance can vary according to different hydrological conditions: in stagnant or semi-stagnant areas (fjords, sea lochs, protected embayments), critical DO concentrations appear to be around 1.9 mg L^{-1}, while in estuaries and open coasts this is closer to 0.9 mg L^{-1} (Llanso, 1992; Llanso and Diaz, 1994). This difference could be related to the different stability and duration of hypoxia in the two kinds of environments (Diaz and Rosenberg, 1995).

Global warming will likely exacerbate the problem of hypoxia in the sea (Matear and Hirst, 2003; Huey and Ward, 2005). An increase in water temperature not only facilitates the occurrence of hypoxia in the oceans but it increases the vulnerability of benthic fauna to hypoxia (Vaquer-Sunyer and Duarte, 2010; Bendtsen and Hansen, 2013). Results of a meta-analysis showed that survival times under hypoxia were reduced by on average 74% and that median

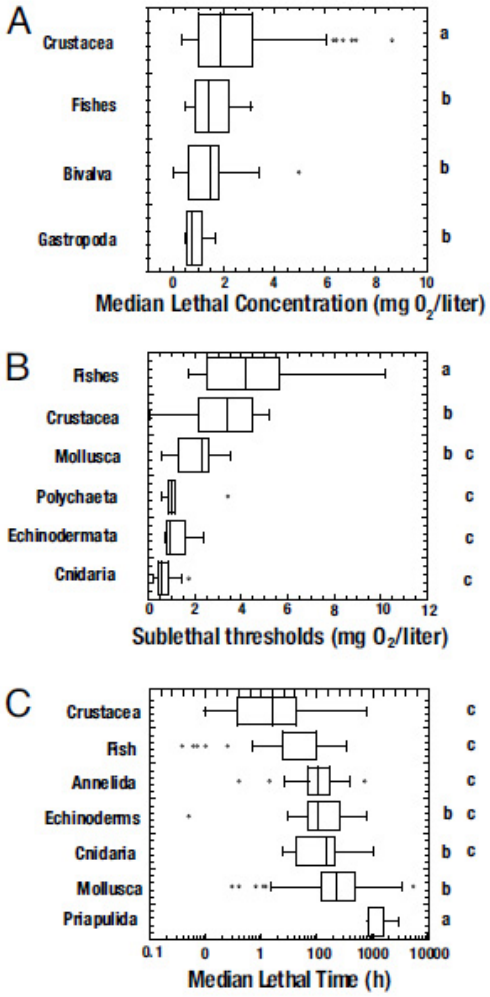

Figure 1.2. Box plot showing the distributions of oxygen thresholds among taxa for (A) LC_{50} (median lethal dose at which 50% of the population is killed in a given period of time), (B) SCL_{50} (median sublethal dose at which 50% of the population exhibit sublethal responses in a given period of time), and (C) LT_{50} (median lethal time after exposure of an organism to a toxic substance) (reproduced from Vaquer-Sunyer & Duarte, 2008).

lethal concentration (LC_{50}) increased by on average 16% when marine benthic organisms were exposed to warmer temperatures (Vaquer-Sunyer and Duarte, 2011).

1.7. Sponges

Sponges (Phylum Porifera) are among the simplest animals on Earth and probably the oldest extant multicellular organisms (Brusca *et al.*, 2016). Their body is composed of an outer surface of cells, called the pinacoderm, an internal system of chambers covered by a "choanoderm",

composed of flagellated cells called choanocytes, and the "mesohyl", a jellylike layer of variable thickness found between these two thin cellular sheets (Miller and Harley, 2011). Various types of amoeboid cells move around in the mesohyl and are specialized for secreting skeletal elements, reproduction, transporting and storing food, and many other important functions (Marshall *et al.*, 1972). Sponges have no organs or true tissues, they have not evolved a nervous system or sense organs and they possess only the simplest of contractile elements (Hickman *et al.*, 2011). Sponges are supported by a skeleton that may be formed by calcareous or siliceous spicules, and spongin, which is a fibrous protein made of collagen (Brusca *et al.*, 2016). Most traditional sponge taxonomy is based on the nature, shape, and arrangement of these skeletal elements (Hooper and Van Soest, 2012).

Sponges are sessile, suspension-feeding animals whose life depends on the water currents that their choanocytes create (Miller and Harley, 2011). Water currents bring food and oxygen, and excrete metabolic and digestive wastes (Marshall *et al.*, 1972). The body openings consist of pores, usually tiny ones called ostia, where the water flows in, and a few large ones called oscula through which the water comes out (Brusca *et al.*, 2016). Sponges can feed on dissolved organic carbon (DOC), picoplankton, nanoplankton and microplankton (Reiswig, 1971, Riisgård *et al.*, 1993; Pile *et al.*, 1996; Ribes *et al.*, 1999; Yahel *et al.*, 2003; de Goeij *et al.*, 2008). Sponges can filter up to 72,000 times their body volume per day and can retain particles with an efficiency of up to 99% (Reiswig, 1971; Koopmans *et al.*, 2010).

Sponges are hosts for a wide range of symbiotic microorganisms such as archaea, bacteria, fungi, cyanobacteria, and microalgae, which can account for over 50% of a sponge's mass (Brantley *et al.*, 1995; Lee *et al.*, 2001). Usually, these associations are mutualistic, with the sponge matrix providing a rich medium for microorganism growth, and the host benefiting by obtaining food and important secondary metabolites (Usher, 2008; Brusca *et al.*, 2016). Some tropical sponges can obtain more than 50% of their energy requirements from carbon fixed by cyanobacterial and zooxanthellae symbionts (Hill, 1996; Webster and Taylor, 2012). A recent molecular study on the nature of sponge microbiota found that most of the bacteria are species-specific, while a very few of them, the core bacterial community, are conserved across almost all the species (Schmitt *et al.*, 2012).

Sponges can reproduce sexually or asexually (Ereskovsky, 2010). Most sponges are monoecious, but they produce eggs and sperm at different times (Brusca *et al.*, 2016). In oviparous sponges, embryos are typically released as mature lecithotrophic larvae, that, depending on the species, can settle directly, can swim for a few hours to a couple of days before

settling, or can crawl about the benthos to find suitable substrate (Maldonado, 2006). Asexual reproduction is very common in sponges and can occur through fragmentation, formation of gemmules, budding, and possibly through the formation of asexual larvae (Sivaramakrishnan, 1951; Ayling, 1980; Wulff, 1991). Gemmules are a type of resting stage observed in most freshwater and a few marine sponges, produced to withstand harsh conditions, such as cold and desiccation (Simpson and Fell, 1974). When favourable conditions return, the gemmules hatch giving rise to a new sponge (Manconi and Pronzato, 2007).

Currently, the phylum Porifera is comprised of around 8,500 species divided into four classes: Desmospongiae, Hexactinellida, Calcarea, and Homoscleromorpha (Gazave *et al.*, 2011; Van Soest *et al.*, 2012). Desmospongiae is the largest class (83% of all living sponges) and includes sponges found in marine, brackish, or freshwater environments, characterised by the presence of siliceous spicules and/or spongin (Van Soest *et al.*, 2012; Morrow and Cárdenas, 2015; Brusca *et al.*, 2016). Calcarea is comprised of around 700 species, whose mineral skeleton is entirely composed of calcium carbonate, consisting of free, rarely linked, or cemented spicules, to which a solid basal calcitic skeleton can be added (Van Soest *et al.*, 2012). Hexactinellida or glass sponges are exclusively marine, and they are mainly found on hard and soft substrates in deeper waters, with a few exceptions in the British Columbia, the Mediterranean Sea, and in Fiordland, New Zealand, where they occasionally occur in shallower waters (Krautter *et al.*, 2001; Bakran-Petricioli *et al.*, 2007; Cook, 2010; Van Soest *et al.*, 2012). The Homoscleromorpha is a recently introduced class that comprises a small group of encrusting or cushion-shaped marine sponges with a unique feature: a basement membrane lining both the choanoderm and pinacoderm (Gazave *et al.*, 2011; Van Soest *et al.*, 2012).

1.8. Sponge ecology and threats

Sponges are ubiquitous organisms in aquatic environments, found in high abundance in temperate, tropical, and polar marine ecosystems where they perform many functional roles (Dayton *et al.*, 1974; Bell and Smith, 2004; Bell, 2008). In temperate seas, these include nutrient cycling, the transfer of energy from the water column to the benthos, bioerosion, substrate stabilisation, provision of microhabitats for a wide range of commensals and symbionts, and enhancement of biodiversity (Bell, 2008).

Due to their great filtering capacity and their remarkable abundance, sponges can be significant contributors to nutrient cycling, by linking benthic and pelagic environments in marine ecosystems (Bell, 2008). Marine sponges process a variety of dissolved and particulate

carbon, nitrogen, phosphorus, and silicon compounds, influencing nutrient availability in the water column (Maldonado *et al.*, 2012; Colman, 2015). Furthermore, the symbiosis of sponges with a wide range of microorganisms makes their functional role more complex than just heterotrophy (Maldonado *et al.*, 2012). Bacteria, fungi, and archaea associated with sponges are capable of a wide range of aerobic and anaerobic metabolism that substantially affects the biogeochemical cycling of key nutrients (Li *et al.*, 2016; Pita *et al.*, 2018). In addition, due to their high retention efficiency of small particles (< 10 μm) sponges can significantly influence the ultraplankton abundance and control the occurrence of phytoplankton blooms (Peterson *et al.*, 2006; Perea-Blázquez *et al.*, 2012).

Sponge bioerosion is known to be especially important in tropical areas where boring sponges play a key role in the balance between erosion and accretion of the coral reefs (Glynn and Manzello 2015). However, bioerosion is also important in temperate seas, such as the Mediterranean Sea, where boring sponges are one of the strongest forces modelling coralligenous bioconcretions, and deep-sea coral reefs (Cerrano *et al.*, 2001; Ballesteros, 2006; Beuck *et al.*, 2010). Other than erosion, sponges can contribute to substrate stabilisation (Bell, 2008). This has been particularly studied in the tropics, but it could be also true in temperate seas, where it has been suggested that by growing between boulders, sponges can stabilise the habitat and reduce disturbance (Bell and Barnes, 2003).

In addition to microorganisms, sponges are hosts for a broad spectrum of macroorganisms (Bell, 2008). The porous nature of sponges makes them ideally suited for colonisation by opportunistic organisms, like crustaceans, ophiuroids, and various worms (Brusca *et al.*, 2016, Bell *et al.*, 2020). A single specimen of *Spheciospongia vesparia* from Florida was found to have over 16,000 shrimps living in it, and a study from the Aegean Sea found 104 different species associated with the sponge *Verongia aerophoba* (Voultsiadou-Koukoura *et al.*, 1987). Furthermore, many sponge assemblages form three-dimensional habitats that provide architectural complexity that favour increased abundance and diversity of other organisms (Rossi *et al.*, 2017).

Despite their importance in benthic ecosystems, our understanding of the impacts of most environmental stressors on sponges is still poor (Bell *et al.*, 2015b). Global warming is one of the main impacts on sponges and many studies have reported mass mortality events following thermal anomalies (which typically increase in frequency and severity with climate change, see Vicente, 1989; Cerrano *et al.*, 2000; Garrabou *et al.*, 2009). However, sensitivity to increased temperature seems to vary among different species and it has been predicted that global warming

may even favour sponges over corals on tropical coral reefs, at least in the short term (Bell *et al.*, 2013; Bennett *et al.*, 2017; Carballo and Bell, 2017). Studies on the effect of ocean acidification on sponges have given contrasting results to date. Some studies report low abundance and diversity at acidified sites (Goodwin *et al.*, 2014), while others suggest that some species tolerate low-pH conditions well (Morrow *et al.*, 2015), or are even favoured by them, as is the case of boring species (Wisshak *et al.*, 2012). Increased sedimentation has been suggested to be a stressor for sponges, however this seems true only for some species, while others can tolerate or even thrive in sedimented environments (Bell and Barnes, 2000a, b, c; 2002; Carballo, 2006; Cerrano *et al.*, 2007; Bell *et al.*, 2015a; Schönberg, 2016). Anoxia events have been shown to be detrimental for sponge assemblages: in 1983 in the northern Adriatic Sea, sponges were among the first organisms to die following the development of oxygen-deficient waters (Stachowitsch, 1984). Other documented cases of impacts on sponges have occurred as a result of diseases (Webster, 2007), anoxia events, the introduction of non-indigenous species (Baldacconi and Corriero, 2009; de Caralt and Cebrian, 2013), destructive fishing practices (Wassenberg *et al.*, 2002), and overexploitation of commercial species (Pronzato and Manconi, 2008).

1.9. Sponge response to hypoxia

The response of sponges to hypoxia has been poorly investigated, and the few published studies have only been conducted on Demospongiae (Gunda and Janapala, 2009; Mills *et al.*, 2014; Mills *et al.*, 2018). The tropical species *Haliclona pigmentifera,* from the Gulf of Mannar, India, showed growth for 42 days when incubated in hypoxic conditions (1.5-2.0 mg O_2 L^{-1}), but complete mortality occurred within 2 days when exposed to [O_2] below 0.3 mg L^{-1} (Gunda and Janapala, 2009). A protein band corresponding to human HIF-1α-like protein was found in sponges exposed to hypoxic conditions, but not in the ones exposed to normoxic conditions (Gunda and Janapala, 2009). Mills *et al.*, (2014) investigated the response of *Halichondria panicea*, from the brackish Kerteminde Fjord (Denmark), to different concentrations of DO, finding that the sponges were able to both respire and feed when exposed to DO levels cycling between 0.5% and 4% of present atmospheric levels (~0.04–0.35 mg L^{-1}), but died at lower levels. The same research group investigated the molecular response of the tropical species *Tethya wilhelma* (see Sarà *et al.*, 2001), exposed to 4 days of variable hypoxic conditions (lower O_2 concentration: 0.04–0.3 mg L^{-1}), without finding any significant difference in the transcriptome between the treatment and the normoxic controls (Mills *et al.*, 2018). Despite the high tolerance of sponges to oxygen deprivation in laboratory experiments, evidence from field observations depicts another scenario. Following an anoxia event in the NE Adriatic Sea sponges

were among the first organisms to die (Stachowitsch, 1984). In coastal waters of British Columbia, glass sponges become very rare when oxygen levels fall below 2 mg L^{-1} (Leys *et al.*, 2004).

1.10. Study Site: Lough Hyne

Lough Hyne is a small (~ 0.5 km^2), fully marine (salinity 34.3–34.9) semi-enclosed lough on the southwest coast of Ireland (Bassindale *et al.*, 1957). The presence of many rare species, the high number of habitats within a small area (~0.5 km^2) and the high species richness have highlighted this site as a globally important biodiversity hotspot (Wilson and Picton, 1983; Kitching, 1987; Bell and Barnes, 2000a, Bell, 2007; Rae *et al.*, 2013; Hiscock, 2014). For these reasons, it was designated as Europe's first statutory marine reserve in 1981 and is now included in a Special Area of Conservation (SAC) under the Natura2000 network (Sullivan and Emmerson, 2011; NPWS, 2014). Lough Hyne is one of the most well studied marine environments in the world, investigated intensively since the 19th Century, with hundreds of papers published and extensive quantitative data (Wilson, 1984; Lawson *et al.*, 2004).

Lough Hyne is approximately 0.8 km long by 0.6 km wide (McAllen *et al.*, 2009). It consists of a north and south basin (both approximately 20 m at their deepest points) and a deeper Western Trough (48 m) that connects these shallower areas (Fig. 1.3) (Kitching, 1987). The lough is connected to the adjacent Atlantic coast by a narrow (~ 25 m wide) channel called the Rapids. Water-flow into the lough is essentially unidirectional due to a sill (maximum depth 3 m) in the Rapids, meaning the incoming tide must reach the level of the sill before the water inflow can begin (Kitching, 1987). As a result, water flows in for four hours, with currents reaching > 300 cm s^{-1} and flows out for eight hours when currents are low (< 5 cm s^{-1}) in all parts of the lough, except in the Rapids. Current speed decreases rapidly as in-flowing water moves across the lough resulting in an east-west sedimentation gradient (Bell and Barnes, 2002).

A seasonal thermocline also develops in the Western Trough (20–30 m) over the summer months (Kitching, 1987), although there is inter-annual variation in its duration. In general, the

thermocline starts forming in April, reaching maximum intensity in August/September and then dissipates between September/November, depending on the temperature and storm activity (McAllen *et al.*, 2009; Sullivan *et al.*, 2013). This stratification leads to a hypoxic/anoxic deeper layer that becomes isolated from the surface water mass for several months (McAllen *et al.*, 2009). When the thermo-oxycline begins forming, the oxygen content decreases progressively

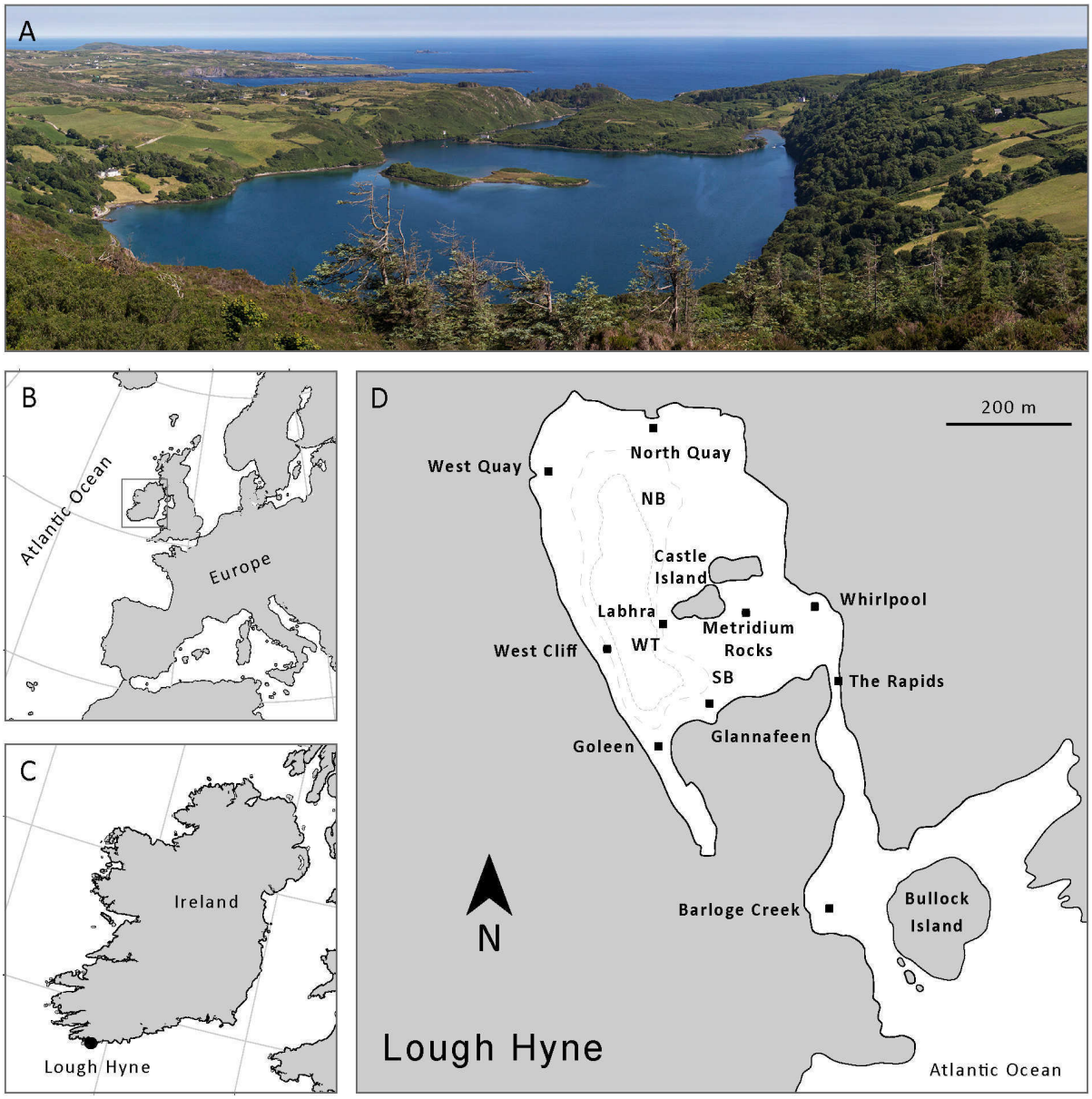

Figure 1.3. Lough Hyne. **(A)** Panoramic photo of Lough Hyne from the north-west looking towards the Atlantic coast (SSE). **(B)** Map of western Europe. **(C)** Location of Lough Hyne in Ireland. **(D)** Map of Lough Hyne. NB, North Basin; SB, South Basin; WT, Western Trough. Inside Lough Hyne, the 25 and 35 m bathymetric contours around the Western Trough are indicated by the short-dashed and dotted line, respectively. Made by the author for McAllen *et al.* (2021).

from 15-20 m to the bottom of the Western Trough. During the summer months, the oxycline becomes steeper, and the oxygen concentration of the water changes from 100% air saturation (a.s.) at 15–25 m to 0% a.s. at 25–35 m (Kitching, 1987). Hydrogen sulphide has also been recorded (but not quantified) in the deeper anoxic water (Kitching, 1987). Although the influence of this thermocline on the subtidal communities is dramatic, several sponge species have been reported to live on the cliffs below 30 m of depth all year round (Bell, 2007).

The presence of different environmental gradients within Lough Hyne has led to the occurrence of high habitat and species diversity. In addition to cold-boreal, North Atlantic species, many Lusitanian and Mediterranean species occur in the lough, from fishes and seaweeds to sea slugs and other invertebrates (Kitching, 1987; Myers *et al.*, 1991; Costello and Emblow, 1997). The subtidal cliffs at Lough Hyne once supported highly diverse reef communities, which were dominated by sponges (Fig. 1.4; Bell, 2007; Bell and Barnes, 2000b, c). More than 70 species of sponges have been found inside the boundary reserve (Bell, 2007). The "Lough Hyne Nature Reserve and Environs SAC" was established with the aim of conserving the lough's biodiversity, and specifically three important habitats included in the Habitat Directive: Large shallow inlets and bays (1160), Reefs (1170) and Submerged or partly submerged sea caves (8330); and six biological community types: Muds to mixed sediment with polychaetes, bivalves and oligochaetes community complex, *Zostera*-dominated community, Intertidal reef community complex, Subtidal community complex, Laminaria-dominated community complex, and Sea cave community complex (NPWS, 2014).

Unfortunately, while Lough Hyne has been well recognised in the past as a biodiversity hotspot, major changes have occurred in recent years and this ecosystem is under threat (Trowbridge *et al.*, 2011; 2017a; Gallagher *et al.*, 2017; Little *et al.*, 2018). Benthic assemblages have experienced dramatic changes across multiple locations and depths, suggesting some large-scale environmental impacts. Regime shifts in Lough Hyne during the last decade were firstly recognized for intertidal and shallow subtidal rocky benthic communities. Major changes in algal composition have occurred during the last 30 years, with the proliferation of the non-indigenous *Sargassum muticum,* and the native warm-water *Cystoseira foeniculacea*, along with ephemeral algae (Trowbridge *et al.*, 2011; 2013; Salvaterra *et al.*, 2013). In the intertidal, the non-indigenous barnacle *Austrominius modestus* has become the dominant species leading to a reduction in the abundance of the native species (Gallagher *et al.*, 2017). Changes have also occurred in many shallow subtidal invertebrates: bryozoans and hydrozoans, with the proliferation of more tolerant species and the decline of the sensitive ones; echinoderms, with

the decline of the once abundant *Paracentrotus lividus* and the recent increase in the spiny starfish *Marthasterias glacialis*; and ascidians whose abundance has increased (Sullivan and Emmerson, 2011; Trowbridge *et al.*, 2011; 2018; Little *et al.*, 2018). In addition, many authors have reported the occurrence of algal blooms, that seem to be increasing in their frequency (Jessopp *et al.*, 2011; Trowbridge *et al.*, 2017b). Critical changes, undescribed until now, have also occurred in deeper areas of the lough. There have been large declines in sponges on the subtidal cliffs, across many species, where large old sponges have disappeared.

The possible causes of these changes are unclear, but some authors have hypothesized that indirect effects of eutrophication such as extreme oxygen fluctuations and an extension of the period of hypoxia/anoxia might have been the main drivers (Jessopp *et al.*, 2011; Trowbridge *et al.*, 2011; 2017a; Sullivan and Rega,n 2013; Gallagher *et al.*, 2017; Little *et al.*, 2018). Based on monitoring of dissolved oxygen levels in shallow water and the spread of ephemeral algae such as ectocarpoids and ulvoids, typical of eutrophic habitats, the decline in water quality started around 2010 (Trowbridge *et al.*, 2011; 2013; 2017a). It is worth noting that the total nitrogen in the waters of the lough has increased from 37–190 mg/m^3 in 1992 to 335–735 mg/m^3 in 2018 (Johnson *et al.*, 1995; McAllen, personal communication). According to current literature, coastal waters with a total nitrogen content greater than 350 mg/m^3 are considered eutrophic (Smith *et al.*, 1999). However, many other factors may be involved in the major changes occurring in the lough, including an increase in number of tourists, increased sedimentation, extreme temperature events and the occurrence of a toxic event. Some authors have suggested that ocean warming is a possible cause of the lough-wide changes (Trowbridge *et al.*, 2018). A study in Northern Ireland has shown that rising sea surface temperatures in recent decades has been responsible for changes in species distribution patterns for several species (Goodwin *et al.*, 2013). In contrast, Gallagher *et al.*, (2017) reported higher levels of mortality for *Austrominius modestus* following the winters of 2009/2010 and 2010/2011, which were among the coldest of the last few decades. A toxic event could also be responsible for the changes at Lough Hyne since harmful algal blooms (HABs) have been recently reported along with the presence in the lough of biotoxins produced by dinoflagellates including pinnatoxin G and spirolides (Jessopp *et al.*, 2011; McCarthy *et al.*, 2014; 2015; Trowbridge *et al.*, 2017b).

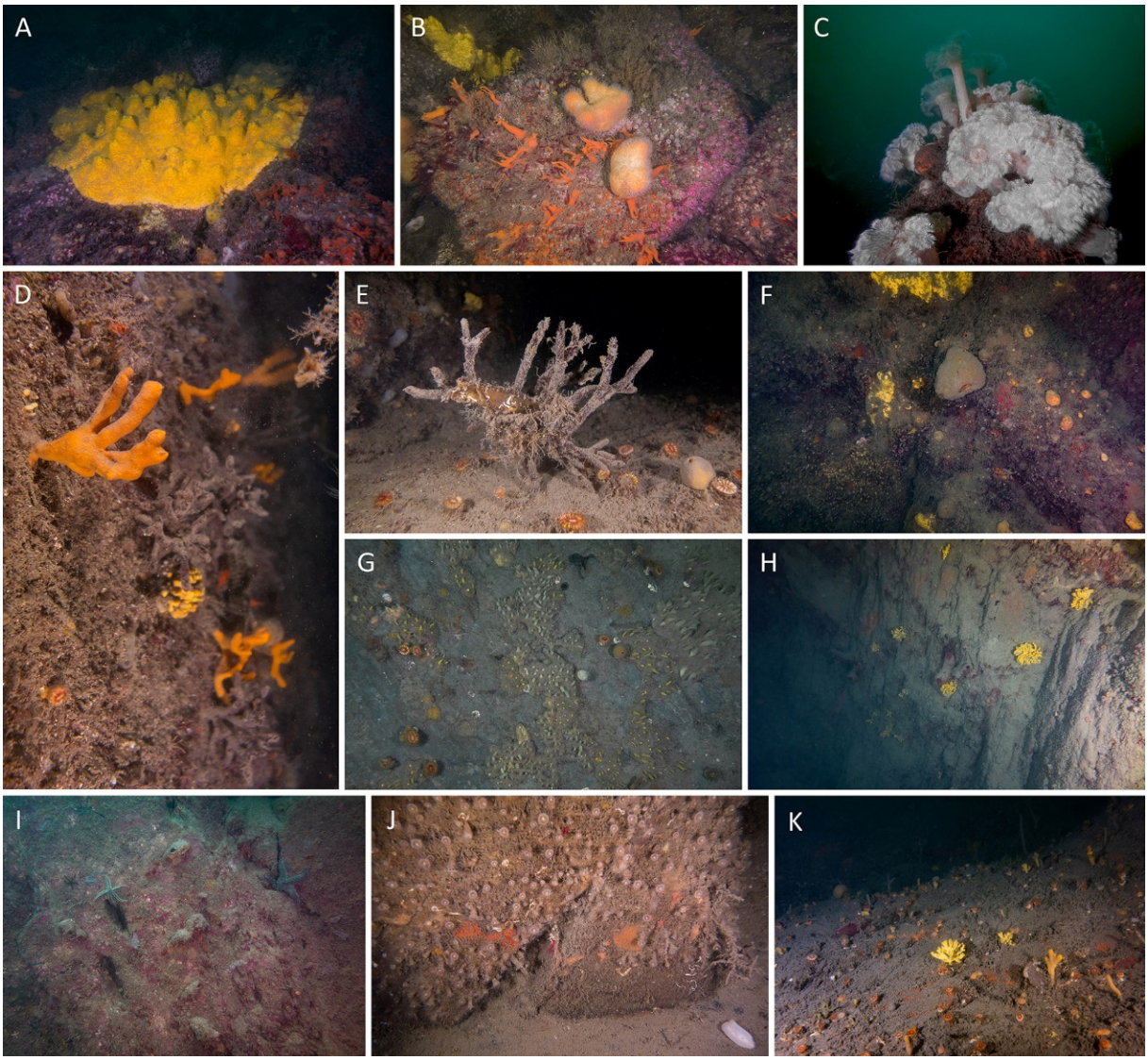

Figure 1.4. Examples of the subtidal sessile species and communities of Lough Hyne. **(A)** Large specimen of the sponge *Cliona celata* at Whirlpool Cliff. **(B)** typical community found at Whirlpool Cliff (18 m) dominated by cnidarians and sponges. **(C)** Large specimens of the anemone *Metridium senile.* **(D)** Small area at Glannafeen (12 m) where branching sponges are still abundant. **(E)** Catshark (*Scyliorhinus* sp.) egg case anchored to the sponge *Raspailia ramosa.* **(F)** Typical cliffs at Labhra (15 m), dominated by *Corynactis viridis*, large specimens of the sponge *Suberites carnosus* and *Cliona celata*. **(G)** Large specimens of Polymastidae sponges, almost disappeared in the lough, but still abundant at McAllen mount (21 m), Labhra. **(H)** Small area at Goleen cliff where the flabellate sponges *Axinella damicornis* survived the mass mortality event (20 m). **(I)** West cliff (12 m), now dominated by ascidians, coralline algae, and turf. **(J)** Deep cliff at Labhra (28 m), inhabited by the colonial anemone *Epizoanthus couchii*, and several species of crustose sponges of the family Raspailiidae. **(K)** Small recruits of sponges. Made by the author for McAllen *et al.* (2021)

1.11. Aims of the thesis

The overall aim of this thesis is to investigate anthropogenic disturbance in temperate mesophotic ecosystems (TMEs), using Lough Hyne as a model system since its shallow TME communities allow easy access. This thesis is divided into three data chapters with the following aims:

1 - To describe changes in the Lough Hyne subtidal communities, to gain insights into the long-term stability and vulnerability of TMEs. In this chapter, I collated 30 years (1990-2019) of scientific surveys and opportunistic observations on the subtidal communities of Lough Hyne, which were analysed with a variety of univariate and multivariate statistical analyses. In addition, I explored available environmental data (temperature and precipitation) that might explain the changes observed.

2 - To identify potential drivers of the change through laboratory experiments. In this chapter, I explored the potential contribution of hypoxia to the mass mortality of sponges observed in Chapter 1. I exposed four sponge species from Lough Hyne and New Zealand to a total of five hypoxic treatments, with increasing severity (3.3– 0.13 mg O_2 L^{-1}) over 7–12 days.

3 - To investigate the resilience and dynamics of TMEs to disturbance events. In this chapter, I analysed the dynamics of sessile organisms from two time series taken before (1994–1995) and after (2018–2021) the disturbance events at Lough Hyne.

2. Chapter 2 - Changes in the subtidal benthic communities of Lough Hyne

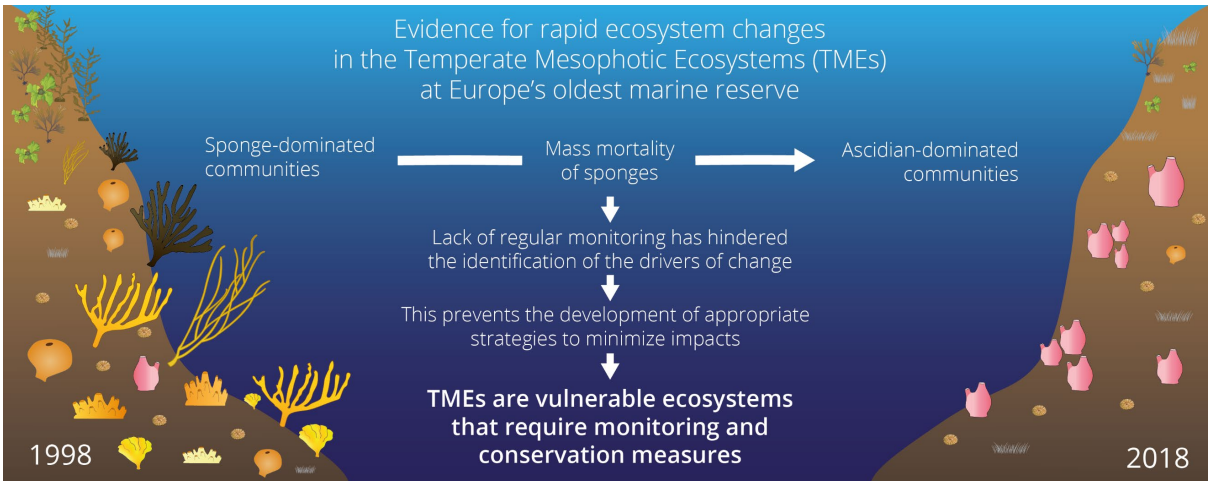

The results presented in this chapter are published in: **Micaroni, V.**, McAllen, R., Turner, J., Strano, F., Morrow, C., Picton, B., Harman, L., Bell, J.J. (2021). Vulnerability of Temperate Mesophotic Ecosystems (TMEs) to environmental impacts: Rapid ecosystem changes at Lough Hyne Marine Nature Reserve, Ireland. *Science of The Total Environment* 789: 147708. https://doi.org/10.1016/j.scitotenv.2021.147708. Reprinted with permission (altered version). Elsevier is the copyright holder for this article.

Abstract

Temperate Mesophotic Ecosystems (TMEs) are stable habitats, usually dominated by slow-growing, long-lived sessile invertebrates and shade-adapted algae. Organisms inhabiting TMEs can form complex three-dimensional structures and support many commercially important species. However, TMEs have been poorly studied, with little known about their vulnerability to environmental impacts. Lough Hyne Marine Nature Reserve (Ireland) supports TMEs in shallower waters (12–40 m) compared with other locations (30–150+ m) as a result of the unusual hydrodynamic conditions. Here, I investigate changes that have occurred on the sponge-dominated cliffs at Lough Hyne between 1990 and 2019, providing insights into TME long-term stability and vulnerability to environmental impacts. My main finding was a marked decline in most three-dimensional sponges at the internal sites of the lough. This was likely the result of one or more mass mortality events that occurred between 2010 and 2015. I also found an increase in ascidians, which might have been more tolerant and benefited from the space freed by the sponge mortality. Finally, in the most recent surveys, I found a high abundance of sponge recruits, indicating that a natural recovery may be underway. The possible factors involved in these community changes include eutrophication, increased temperature, and a toxic event due to an anomaly in the oxy-thermocline breakdown. However, the absence of comprehensive monitoring of biotic and abiotic variables makes it impossible to identify the cause with certainty. My Lough Hyne example shows the potential vulnerability of TMEs to short-term disturbance events, highlighting the importance of monitoring these habitats globally to ensure they are appropriately conserved.

2.1. Introduction

Coastal ecosystems are among the most important biomes on the planet because of the reliance of human populations on the resources they provide (Costanza *et al.*, 2014). However, many coastal ecosystems remain poorly studied. Mesophotic ecosystems lie between the shallow euphotic waters and the aphotic deep-sea. While these ecosystems have been relatively well-studied in some tropical regions, termed mesophotic coral ecosystems (MCEs), the importance of temperate mesophotic ecosystems (TMEs) has only recently been recognised (see Cerrano *et al.*, 2019; Turner *et al.*, 2019).

TMEs extend from the lower limit of the euphotic zone (<1%, of the surface irradiance, ~ 20-30 m) to the limit of benthic primary production (150-300 m) (Cerrano *et al.*, 2019). These ecosystems host rich and diverse communities typically dominated by invertebrates, including sponges, cnidarians, bryozoans, and ascidians, or by shade-adapted (sciaphilous) algae (Rossi *et al.*, 2017; Turner *et al.*, 2019). TMEs provide important ecosystem services, including supporting commercial fisheries, providing raw materials (e.g., pharmaceuticals), genetic resources, and a range of cultural and recreational values (e.g., SCUBA diving and angling) (Tonin, 2018). To date, only 20% of studies on mesophotic ecosystems are from temperate seas. Of those, 67% are from the Mediterranean Sea and temperate Australasia, with little known about TMEs in other regions (Bongaerts *et al.*, 2019).

Importantly, like shallow-water ecosystems, TMEs are also threatened by a wide range of anthropogenic stressors, including ocean warming, ocean acidification, urbanisation, the arrival of non-indigenous species, and fishing activity including trawling (Gennaro and Piazzi, 2011; Cerrano *et al.*, 2013; Bo *et al.*, 2014; Rossi *et al.*, 2017, Ferrigno *et al.*, 2018; Marzloff *et al.*, 2018; Enrichetti *et al.*, 2019a; Turner *et al.*, 2019; Betti *et al.*, 2020). Nonetheless, there have been only a few reports of changes in TME communities, which have been linked to wastewater discharge (Hong, 1983; Roberts *et al.*, 1998), heatwaves (Cerrano *et al.*, 2000; Garrabou *et al.*, 2009), shifts in species distribution patterns due to climate change (Perkins *et al.*, 2020) and aquaculture-related eutrophication (Haeussermann *et al.*, 2013). However, as TMEs are challenging to access, many changes may have gone unnoticed due to limited baseline data. Furthermore, there is very little information on TME species and community ecology and how these organisms respond to anthropogenic stressors (Turner *et al.*, 2019).

In recent decades, legislative efforts by governments to protect TMEs have increased substantially. In Europe, under the EU Marine Strategy Framework Directive 2008/56/EC,

important mesophotic habitats, including coralligenous reefs, coral gardens (e.g., gorgonian and alcyonarian forests) and deep-sea sponge aggregations have been formally given special protection (OSPAR, 2008; UNEP-MAP-RAC/SPA, 2008). To date, very few countries have implemented long-term monitoring programmes in mesophotic habitats. The best examples are the coralligenous assemblage monitoring in the Mediterranean Sea (UNEP-MAP-RAC/SPA, 2008) and the Automated Underwater Video benthic monitoring program run by Australia's Integrated Marine Observing System (IMOS) (Williams *et al.*, 2010; Pizarro *et al.*, 2013). However, for most TMEs, there is still a lack of baseline data, inhibiting our ability to distinguish between population fluctuations and anthropogenic impacts (Thurstan *et al.*, 2017).

Lough Hyne Marine Nature Reserve (est. 1981) is a fully marine, semi-enclosed lough in southwest Ireland, one of the most well studied marine environments in the world (Lawson *et al.*, 2004). Lough Hyne hosts many rare species and contains a very high number of habitats within a small area (~0.5 km^2) and has been highlighted as a globally important biodiversity hotspot (Kitching, 1987; Bell and Barnes, 2000a; Bell, 2007). Lough Hyne is particularly well known for its rich and abundant mesophotic cliff communities, which occur in much shallower water than areas in the Atlantic because of the elevated water turbidity and sheltered conditions (Picton, 1990). These communities were previously dominated by sponges, including many three-dimensional forms that provided habitat complexity to the subtidal cliffs and formed extensive sponge gardens (Picton, 1990; Bell and Barnes, 2000a). Similar ecosystems are only found in a few other areas in the world, for example, Bathurst Channel in Tasmania, Fiordland in New Zealand, and on the southwest coast of Chile (Schiel and Hickford, 2001; Barrett *et al.*, 2010; Försterra *et al.*, 2017). Because of the small sizes, environmental conditions, the high level of endemism, highly restricted distribution patterns and limited populations, these ecosystems are considered among the most threatened on Earth (Barrett and Edgar, 2010).

In recent years, major community changes have occurred at Lough Hyne in intertidal and shallow-subtidal (<1 m) habitats, suggesting some large-scale environmental impact (Trowbridge *et al.*, 2013; Little *et al.*, 2018). These include shifts in algal assemblages (Trowbridge *et al.*, 2011, 2013), invasions by non-indigenous species (Salvaterra *et al.*, 2013, Gallagher *et al.*, 2017), and changes in the abundance and composition of many intertidal and shallow subtidal invertebrates, such as echinoderms, bryozoans, hydrozoans, and molluscs (Trowbridge *et al.*, 2011; O'Sullivan and Emmerson, 2011; Little *et al.*, 2018, 2020; Trowbridge *et al.*, 2018). Moreover, some authors have reported the occurrence of algal blooms, that appear to be increasing in frequency (Jessopp *et al.*, 2011). While anecdotal reports have suggested

changes have also occurred on deeper subtidal rocky cliffs, this has never been quantified as no long-term monitoring programme exists (unlike for the intertidal and shallow subtidal habitats; see Trowbridge *et al.*, 2013; Little *et al.*, 2018).

My study provides an example of how to investigate spatial and temporal variability in TME communities in the absence of long-term monitoring, with data from a range of quantitative and qualitative sources. I collated 30 years (1990-2019) of scientific surveys and opportunistic observations on the subtidal communities of Lough Hyne to gain insights on the long-term stability and vulnerability of TMEs. I then explored the available environmental data and considered the possible causes of the changes observed. Finally, I discussed the limits of the methodology used and the importance of regular monitoring of biotic and abiotic variables for TME conservation globally.

2.2. Materials and Methods

2.2.1. Study sites

My study focused on six sites within the boundaries of Lough Hyne Marine Nature Reserve, five of them located inside the lough and one located on the adjacent Atlantic coast (Fig. 2.1). See Chapter 1, section 1.10 for a more details on the study area.

Among the sites inside the lough, the four internal sites (Glannafeen, Labhra Cliff, Goleen and West Cliff) share similar environmental conditions, which is reflected in the similar biological communities found at these sites (Picton 1990; Bell and Barnes, 2000a, b, c). During the incoming tide, the internal sites experience low to moderate current flow (5–50 cm s^{-1}), and

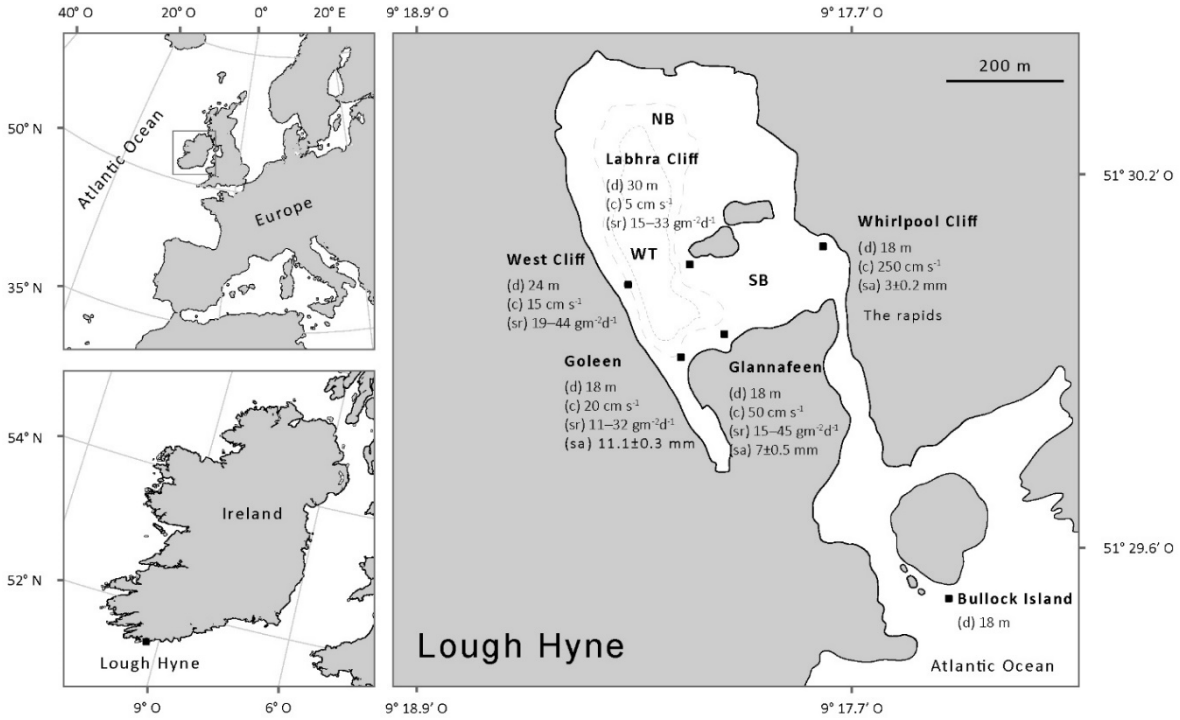

Figure 2.1. Lough Hyne map showing its position in the North-East Atlantic (top left corner) and Ireland (bottom left corner). NB, North Basin; SB, South Basin; WT, Western Trough. For each site, the maximum depth (d), maximum current speed (c, from Bell and Barnes, 2002), sedimentation rate (sr, from Bell and Barnes, 2002) and accumulated sediment on surfaces (sa, from Bell and Turner, 2000) are shown. Inside Lough Hyne, the 25 and 35 m bathymetric contours around the Western Trough are indicated by the short-dashed and dotted line, respectively (from Sullivan *et al.*, 2013).

most of the time, there is little or no water movement at all (Bell and Barnes, 2002). These internal sites are characterised by high sedimentation rates and considerable sediment accumulation upon cliff surfaces (7–11 mm) (Bell and Turner, 2000; see Figure 2.1 for more details). Shallow cliff areas are characterised by coralline algae and other macroalgae, although algae quickly decline below 6-10 m, where the substrate becomes dominated by sponges and turf algae (Bell, 2007).

The site at the entrance of the lough (Whirlpool Cliff) is subjected to strong flow conditions (up to 250 cm s^{-1} during in-flow) and negligible sediment accumulation on rocky surfaces (3 ± 0.2 mm) (Bell and Barnes, 2002; Fig. 2.1). The deeper areas of Whirlpool Cliff are dominated by suspension-feeders (cnidarians and sponges), while macroalgae, including the kelp species *Laminaria*, mostly dominate the shallower parts (< 12–15m).

My final site (Bullock Island) is located outside the lough and contrasts with the other sites as it is subjected to strong oceanic wave action, with waves exceeding 10 m during storms. The benthic communities of this site are characteristic of the open Atlantic coast, with the kelp *Laminaria* dominating to 10–12 m depth, and encrusting filter feeders, coralline algae and turf algae dominating in the deeper areas (Kitching, 1987; Bell, 2007).

2.2.2. Spatial variation and temporal changes in benthic communities and sponge assemblages

My study focused on the benthic sessile component of communities of the subtidal cliffs of Lough Hyne and the adjacent Atlantic coast. I used the same sampling design for investigating spatial variation and temporal changes between 1998 and 2018 for both the overall benthic communities and sponge assemblages. Abundance data of sponge taxa and benthic organisms were collected in July/August 1998 and July 2018 at the six sites described above (Fig. 2.1). Each site was sampled at 6 m intervals, from 6 to 18, 24 or 30 m depth depending on the maximum depth of each site (see Fig. 2.1 for maximum depths). Data from 1998 at Glannafeen 12 m were missing, and therefore could not be included in the analysis. At each site, five replicate photoquadrats (0.25 m^2) were recorded on vertical (~ 90°) and inclined (~ 40–50°) surfaces. This distinction was necessary since substrate inclination has been shown to structure sponge assemblages and benthic communities at Lough Hyne (Bell, 2007) and other mesophotic reefs (Bridge *et al.*, 2011). In 1998, photographs were taken on slide film using a Sea and Sea Motormarine II and YS-50 Strobe. A Sony Rx100 I digital camera with two 12 000 lumen photo

lights (Diving Torches Powerpro 100w) was used in 2018. Sediment was wafted from surfaces prior to taking photographs in both 1998 and 2018 as many sponges are buried beneath this layer.

The abundance of the dominant sessile organisms was estimated from the photoquadrats using a random point count method in Coral Point Count with Excel extensions (CPCe; Kohler and Gill, 2006). This software randomly allocates points over a picture, and the user manually identifies the organism beneath each point. For each photograph, 120 randomly generated points (480 points/m^2) were used. Preliminary trials indicated that this number of points was appropriate to estimate the benthic cover accurately. The benthic categories used were: macroalgae, sponges, bryozoans, anthozoans, hydrozoans, ascidians, polychaetes, barnacles, turf-forming organisms (i.e., turf-forming algae and small invertebrates, as hydroids and bryozoans) and bare substrate.

For the sponge assemblages, photoquadrats were analysed using the area/length analysis tool in CPCe. Every sponge was manually outlined using a freehand drawing tool to measure the planar area occupied by the sponge in the photo. Each sponge was assigned to a taxon/operational taxonomic unit (OTU) group and a morphological type. Additional close-up photos and voucher specimens were also used for the identification of species and morphological types. Due to technological differences in the photographic equipment used between years, particularly the lower resolution of photoquadrats in 1998, measures were taken to make the data comparable. A minimum cut-off sponge size of 1 cm^2 was used, a slightly higher value than the minimum 1998 detection limit. Furthermore, all the photographs from 1998 and 2018 were analysed to a common taxonomic resolution. When possible, sponges were identified to species level. However, due to the indistinguishable external morphology of some specimens (especially in photos from 1998), some species were combined into OTUs that included multiple species. OTUs as are known to be generally effective for identifying patterns of distribution of benthic invertebrates (Brind'Amour *et al.*, 2014), and marine sponges (Strano *et al.*, 2020), at the same time avoiding the need for destructive sampling in concerned habitats. The list of OTUs/taxa and associated species is provided in Table S2.1.

2.2.3. Statistical analysis

Differences in benthic community and sponge assemblage structure were analysed using permutational multivariate analysis of variance (PERMANOVA, Anderson, 2001) based on Bray-Curtis dissimilarities. The models were run using 9999 unrestricted permutations of raw data. When the number of unique permutations was lower than 100, Monte Carlo *p*-values were used instead of permutation *p*-values. Because of the difference in the number of levels for the

depth factor among sites, both 3 and 4-way PERMANOVAs were performed. Four-way PERMANOVAs included the factors year, site, depth (only the depths common for all the sites: 6 m and 18 m) and inclination. Three-way PERMANOVAs were then conducted separately for each site and included the factors year, depth (including all the levels available), and inclination. Year and site were treated as random factors, while depth and inclination were treated as fixed factors. Cover data of both the benthic organisms and sponges were Log transformed to reduce the influence of the most abundant groups. I conducted pairwise comparisons of significant multivariate differences between years. *P*-values for the pairwise analyses were corrected using the Benjamini-Hochberg procedure to reduce the chance of type I errors (Benjamini and Hochberg, 1995). Effect size (omega squared, ω^2) was calculated for PERMANOVA tests made for each combination of site and depth, with data from vertical and inclined surfaces pooled (Lakens, 2013). Differences in multivariate assemblages were graphically displayed using non-metric multidimensional scaling (nMDS) based on Bray-Curtis dissimilarities and Principal Component Analysis (PCA). All the multivariate analyses were performed by the software PRIMER v6 (with the PERMANOVA+ add-on).

Differences in the abundance and richness of the main benthic organisms and sponge morphologies (following Bell and Barnes, 2001) between 1998 and 2018 were analysed using an unequal variance *t*-test on ranked data. This test was chosen due to the unequal variance and non-normal distribution of data, even after transformation (Ruxton, 2006). The Benjamini-Hochberg procedure was used to correct for multiple comparisons for each family of analysis. *T*-tests were performed using the software IBM SPSS Statistics v26. Statistical significance was set to $p < 0.05$. All the data and the detailed results of all the statistical tests are reported in the Appendix A.

2.2.4. High-resolution sponge diversity comparison between 1998 and 2019

A detailed taxonomic survey was conducted involving extensive photographic sampling and sponge fragments collection to compare the species diversity before and after the changes. In 2019, 213 sponge samples and > 3000 photos were collected during 15 dives (3 dives at each site, except the site outside). Sponge taxa were identified through a combination of external and internal morphological characteristics. Species lists from 1998 were taken from Bell and Barnes (2001), where the authors used a similar sampling effort. However, in Lough Hyne, there are still many undescribed sponge species of the genera *Eurypon* and *Haliclona* and from the family Polymastiidae and Suberitidae. To avoid biases in the comparison, undescribed or

indistinguishable members of these genera/families were combined (e.g., *Eurypon* spp., encrusting Suberitidae).

2.2.5. Long-term sponge abundance reconstruction

To reconstruct and estimate the long-term changes that may have occurred on the subtidal cliffs at Lough Hyne, I gathered all the published and unpublished data available, along with opportunistic observations made by researchers between 1990 and 2019. These include:

1) Scientific surveys: twenty-five Hi8 video transects (20–35 min each), collected in 1990, 1993, 1995, 1996 and 1997 at Whirlpool Cliff, Glannafeen, Goleen, West Cliff and Labhra Cliff; in each video, the same video operator conducted transects across each cliff at 2 m depth intervals, from 18 m to the surface. Photoquadrats that were taken in 1998 and 2018 (see previous sections).

2) Opportunistic surveys: observations, photos and videos from researchers diving at Lough Hyne for other projects in 2005, 2010, 2012 and 2015 (material by Julia Nunn and Nick Owen), and surveys conducted by other members of the research group and me in 2017 and 2019.

Due to differences in sites and species recorded, different analyses were performed on these data. For papillate (family Polymastiidae) and arborescent sponges (*Raspailia* spp., *Axinella dissimilis* and *Stelligera stuposa*) at Goleen, I was able to determine the presence of adults (> 10 cm) and recruits (< 2 cm) from all the time points mentioned above. For *Raspailia ramosa* at West Cliff, I was able to determine the presence of adults and recruits from all the time points mentioned above, except 2010 and 2012. For all the other sites, I was only able to extrapolate presence data for 8 easily distinguishable sponge taxa: *Axinella damicornis*, *A. dissimilis*, *Cliona celata*, *Polymastia* spp., *Raspailia ramosa*, *Stelligera rigida* and "other branching sponges" (this latter category included *Raspailia hispida* and *Stelligera stuposa*). Data used were from the video transects 1990–1997, the scientific surveys (1998 and 2018), and opportunistic surveys conducted by me and other members of my research group in 2017 and 2019.

2.2.6. Environmental data analysis

Local environmental data (sea surface temperature, air temperature and rainfall) were acquired from different sources and analysed for deviation from the expected climatology in order to evaluate their potential contribution to the biotic changes. Mean daily sea surface temperature (SST) data from 01/01/1982 to 31/12/2019, for 51° 22' 30" N, 9° 22' 30" W, were retrieved from the NOAA's Optimum Interpolation Sea Surface Temperature (OISST) version

2 (Reynolds *et al.*, 2007). Maximum and minimum daily air temperature from 01/07/1974 to 31/12/2019, at the Sherkin Island weather station (51° 28’ 33.6” N, 9° 25’ 40.8” W) were retrieved from Met Éireann (www.met.ie). Daily rainfall from 01/07/1974 to 31/12/2019 at the Sherkin Island weather station was retrieved from Met Éirean.

Sea surface and air temperature were analysed in R to detect heatwaves and cold spells using the package *HeatwaveR* (Schlegel and Smit, 2018), based on the marine heatwave (MHW) and cold spell (MCS) definition and categorisation by Hobday *et al.* (2016; 2018) and Schlegel *et al.* (2017). To investigate extreme precipitation events, I examined short periods of time (24, 48, 72 and 96 h long) for which rainfall exceeded a threshold value set at the 99.5^{th} and 99.9^{th} percentile. When two or more extreme precipitation events shared the same daily rainfall data, only the event with the highest rainfall was considered. The climatology data resulting from these analyses were finally used to compare the time frame when the biotic changes were estimated to have occurred (estimated from the long-term sponge abundance reconstruction) with the period preceding it.

2.3. Results

2.3.1. Spatial variation in benthic communities and sponge assemblages

Both benthic communities and sponge assemblages from 1998 and 2018 showed significant differences among sites and depths (Tab. S2.2; Fig. 2.2–3). In addition, significant interactions were found between site and depth (p = 0.0001–0.0002, F = 5.9–10.1), depth and inclination (p = 0.0001–0.0002, F = 2.3–6.0), and site, depth, and inclination (p = 0.0001–0.0005, F = 2.3–3.6; but not significant for benthic communities in 2018) (Tab. S2.2). These interactions indicate that changes between sites and depths were not homogeneous and depended on the substrate's inclination. Sites represented the main sources of variation, explaining 16.3–30.4% and 29–32% of the variation (not considering interactions), respectively, for the overall benthic sessile communities and sponge assemblages (Tab. S2.2). For sponges, three different assemblages could be identified: Bullock Island, Whirlpool Cliff, and the internal sites: Glannafeen, Labhra Cliff, Goleen and West Cliff, while for wider benthic sessile communities, these differences were less evident (Fig. 2.2). Depth was another important factor that alone accounted for 28.6–34.7% of variation in the benthic communities and 7.4–7.6% in the sponge assemblages. Depth also interacted with site accounting for another 9.9–12.4% and 12.1–14.1% of the variation, respectively.

The overall biological communities of the internal sites were generally characterised by a higher abundance of sponges (more marked in 1998) and ascidians (mostly in 2018), compared to the other sites (Fig. 2.5). Both sponges and ascidians increased with depth, reaching a peak around 18 m for sponges and 12 m for ascidians. Bare substrate was also generally more common at the internal sites, and steadily increased with depth. In contrast, Whirlpool Cliff and Bullock Island had a higher abundance of macroalgae, especially at 12 and 18 m. At the internal sites, macroalgae were abundant (up to 70% mean coverage) but only at 6 m, but abundance decreased sharply with depth (Fig. 2.5). Whirlpool Cliff was also characterised by a higher abundance of anthozoans compared to all the other sites. Concerning the sponge assemblages, the internal sites had a higher abundance of encrusting sponges than the other sites, both in 1998 and 2018 (Fig. 2.6). Arborescent, papillate, and pedunculate sponges were the main feature of the internal sites in 1998, but not in 2018 (see following sections). Whirlpool Cliff was characterised by a high abundance of the repent sponge *Amphilectus fucorum* and the massive sponge *Cliona celata* (occupying up to 28% of some quadrats). Bullock Island was instead characterised by a relatively high abundance of *Haliclona* sp.

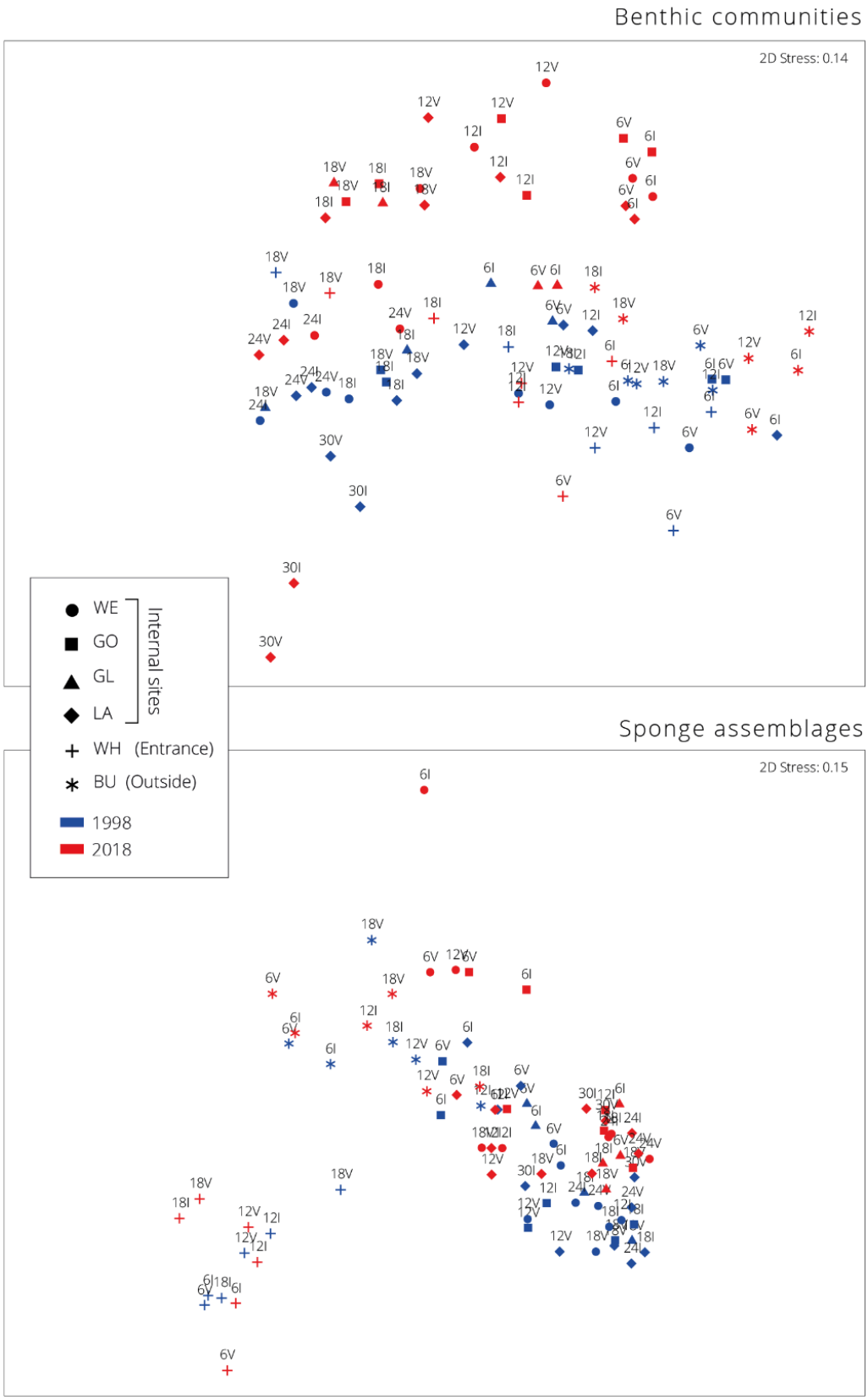

Figure 2.2. Non-metric multidimensional scaling (nMDS) of centroids of benthic communities (top) and sponge assemblages (bottom) for each combination of year, site depth and inclination at all sites at Lough Hyne. Site key: WE West Cliff, GO Goleen, GL Glannafeen, LA Labhra Cliff, WH Whirlpool Cliff, BU Bullock Island.

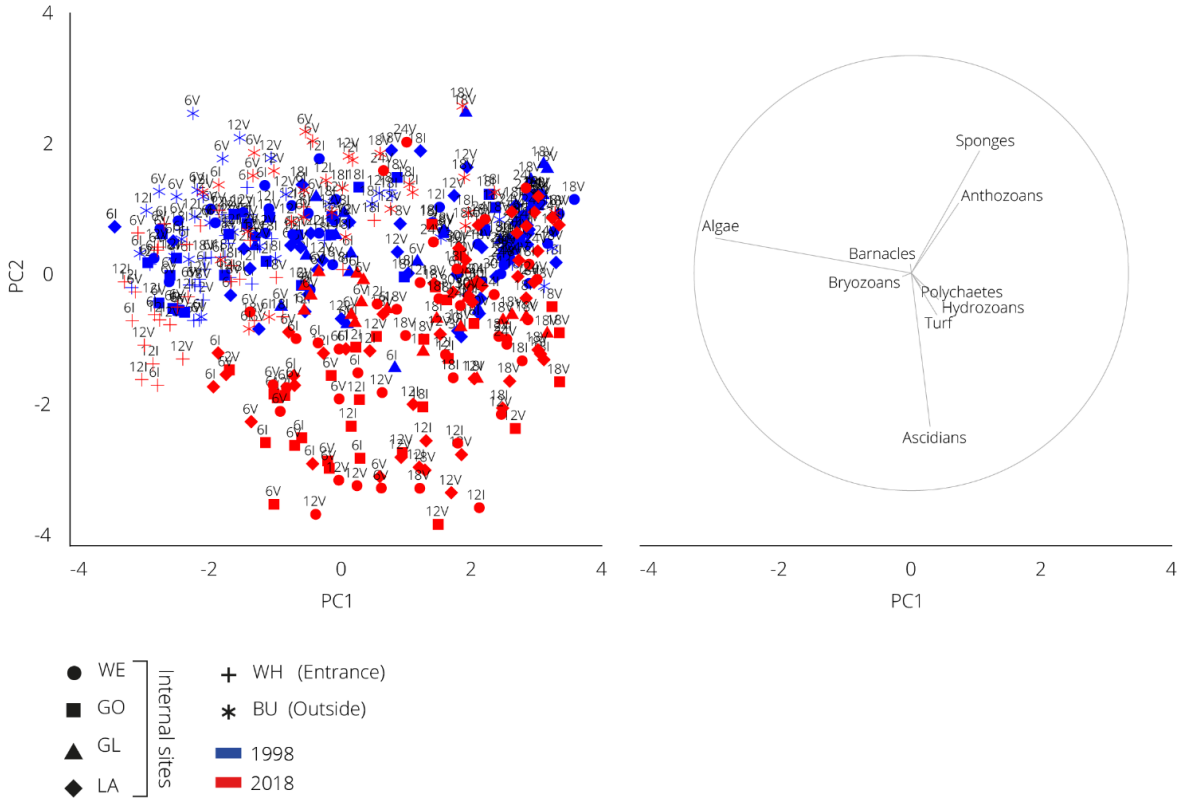

Figure 2.3. Principal Component Analysis (PCA) of benthic communities for each combination of year, site depth and inclination at all sites at Lough Hyne. Site key: WE West Cliff, GO Goleen, GL Glannafeen, LA Labhra Cliff, WH Whirlpool Cliff, BU Bullock Island

2.3.2. Temporal changes in benthic sessile communities between 1998 and 2018

Benthic communities were highly variable among sites, depths, and inclination. However, three main different communities could be identified: the internal sites (Glannafeen, Labhra Cliff, Goleen and West Cliff), the site at the entrance of Lough Hyne (Whirlpool Cliff) and the site outside the lough (Bullock Island) (Fig. 2.2–3)

I found significant changes between 1998 and 2018 benthic communities data at all sites, but these differences were greater at the internal sites. The four-way PERMANOVA (considering all the sites) showed significant differences in benthic communities between years, sites, and depths, with significant interactions between year and site ($p = 0.0001$, $F = 10.5$), year, site, and depth ($p = 0.0001$, $F = 5.2$), year, site and inclination ($p = 0.0003$, $F = 3.6$), and site depth and inclination ($p = 0.0002$, $F = 9.5$) (Tab. S2.3). These interactions indicate significant changes between the 1998 and 2018 data, but these changes varied with sites. Furthermore, within the

individual sites, changes were not homogeneous for each depth and between vertical and inclined surfaces. Three-way PERMANOVAs on the individual sites showed significant changes between years at all sites, with interactions between year and depth, and depth and inclination at most sites (Tab. S2.4). Both nMDS and PCA show clear spatial gradients in benthic communities, with the internal sites separating from the site at the entrance and outside the lough (Fig. 2.2–3, S2.1–2). However, temporal changes at the internal sites were similar and generally greater than at the entrance and outside the lough (Fig. 2.2–4, S2.1–2). Pairwise PERMANOVA comparisons between 1998 and 2018 showed significant differences for most combinations of site, depth, and inclination, except for the site at the entrance, where significant differences were found at 6 m on vertical surfaces (Tab. S2.2).

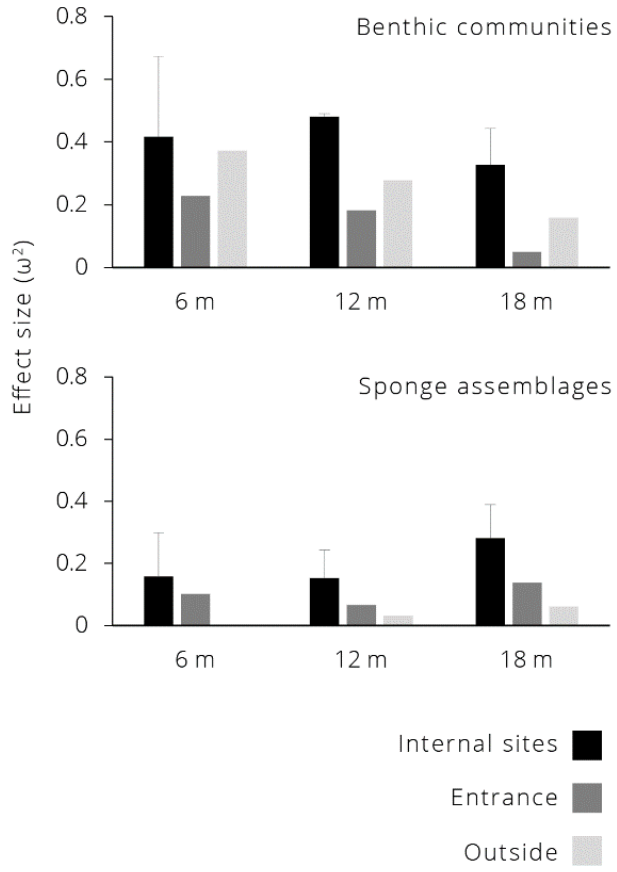

Figure 2.4. Effect size (ω^2) quantifying the magnitude of temporal changes in benthic communities and sponge assemblages at 6, 12 and 18 m at the internal sites (Glannafeen, Labhra Cliff, Goleen and West Cliff pooled together), entrance (Whirlpool Cliff) and outside the lough (Bullock Island). For the internal sites, the bars indicate the mean value among sites, and the error bars indicate the standard deviation.

The benthic organisms that changed the most between 1998 and 2018 were sponges and ascidians, followed by turf-forming organisms and macroalgae (Fig. 2.5; S2.3). Sponge abundance generally decreased between 1998 and 2018 at the internal sites, while it increased at the entrance of the lough (Fig. 2.5; S2.3). At the internal sites, mean sponge abundance in 1998 was up to 25.3%, while in 2018, it never exceeded 12.9%. Changes were more pronounced on vertical surfaces than inclined ones and at the innermost sites (West Cliff and Goleen). No changes were found outside the lough. Ascidian abundance increased significantly at all sites, except at the entrance of the lough. At the internal sites, mean ascidian abundance changed from a maximum of 0.8% in 1998 to 19.2% in 2018 (Fig. 2.5; S.2.3). Outside the lough, ascidian abundance also increased (from 0% in 1998 to 0.2–2.7% in 2018). In contrast, turf-forming organisms generally increased at the internal sites of the lough but decreased outside (Fig. 2.5; S2.3). Univariate statistical analyses are provided in supplementary Table S2.5 and summarised in Figure S2.3.

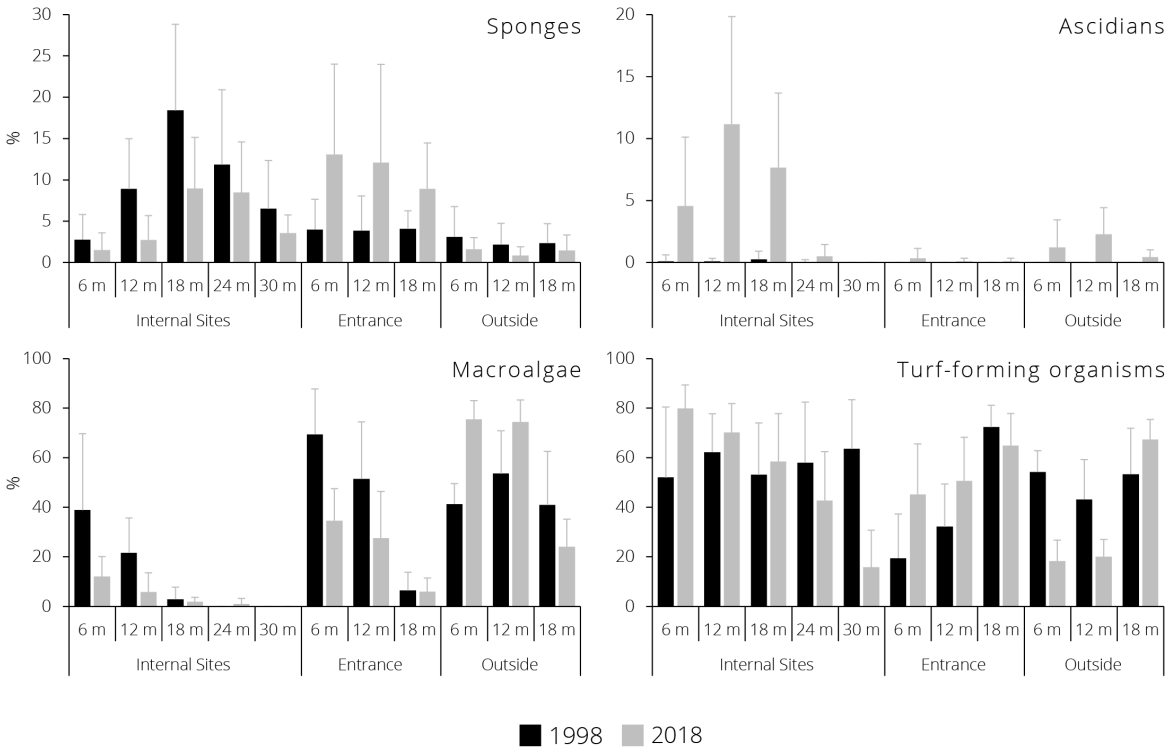

Figure 2.5. Mean percentage cover of main benthic organisms in 1998 and 2018 for each depth at the internal sites (Glannafeen, Labhra Cliff, Goleen, and West Cliff pooled together), entrance (Whirlpool Cliff) and outside Lough Hyne (Bullock Island). Error bars indicate standard deviation. Note the different y-axis scales.

2.3.3. Temporal changes in sponge assemblages between 1998 and 2018

Similarly to the overall benthic communities, the sponge assemblages showed high heterogeneity among sites, depths and, to a lesser extent, inclination. The separation between internal sites, entrance and outside the lough was evident and even more marked than for the benthic communities (Fig. 2.2; S2.1–2).

Significant temporal changes between 1998 and 2018 were found at all sites in the lough (more marked at the internal sites), but not outside. The PERMANOVA test showed significant changes in sponge assemblages between sites, and significant interactions between year and site ($p = 0.0001$, $F = 4.9$), year and depth ($p = 0.034$, $F = 2.8$), year, site, and depth ($p = 0.0001$, $F = 3.5$), year, site and inclination ($p = 0.0008$, $F = 1.9$) and year, site, depth and inclination ($p = 0.0001$, $F = 2.2$) (Tab. S2.3). These interactions suggest that changes occurred between years, but these were not homogeneous. Three-way PERMANOVAs showed significant changes at all sites, except the site outside the lough (Bullock Island). Significant interactions were also found between year and depth for all the sites inside the lough and for year and inclination at most sites inside the lough (Tab. S2.4). However, temporal changes were greater for the internal sites than at the entrance of the lough (Whirlpool Cliff) (Fig. 2.2, 2.4). Pairwise comparisons between 1998 and 2018 showed differences in sponge assemblages for most combinations of site, depth, and inclination at the internal sites. At the entrance, there were significant differences only at 6 m on vertical surfaces and 18 m on inclined surfaces, while no differences were found outside the lough (Tab. S2.3).

The major change in the sponge assemblage between 1998 and 2018 was a decline in three-dimensional morphologies (papillate, arborescent, flabellate, pedunculate and massive) at the internal sites of the lough (Fig. 2.6–7, S.2.4). Papillate sponges (family Polymastiidae) were one of the most affected groups. In 1998, papillate sponges were found at the internal sites with mean coverage up to 6.3%, while in 2018, the highest mean coverage (at any site/depth) was 0.2% (Fig. 2.6, S2.4). The cover of arborescent sponges has also decreased significantly at the inner sites. In 1998, arborescent sponges covered up to 2.6% of the substrate, while in 2018, they were not found at the innermost sites (West Cliff and Goleen), and their cover ranged between 0 and 0.5% at the other two internal sites (Labhra Cliff and Glannafeen) (Fig. 2.6, S2.4). Flabellate sponges decreased significantly at the internal sites (except Glannafeen, closer to the entrance). Pedunculate sponges from the genus *Suberites* also showed a general decrease, especially at the innermost sites (Fig. 2.6, S2.4).

Pairwise comparisons of massive sponge abundance only showed some local decreases (Fig. 2.6, S2.4). However, when pooling across depth and inclination there was a significant decrease in massive sponge cover at most of the internal sites (West Cliff, $p < 0.0001$, $t = 4.5$; Goleen; $p = 0.001$, $t = 3.6$; Labhra Cliff; $p = 0.021$, $t = 2.4$). Globular sponges (*Tethya citrina*) did not show any significant changes between 1998 and 2018 (Tab S2.6).

Unlike most three-dimensional sponges, encrusting sponges were relatively abundant both in 1998 and 2018. These, however, showed some local significant decreases at most of the internal sites, except Glannafeen (Fig. A4). Univariate statistical analyses are provided in Table S2.6 and summarised in Figure S2.6.

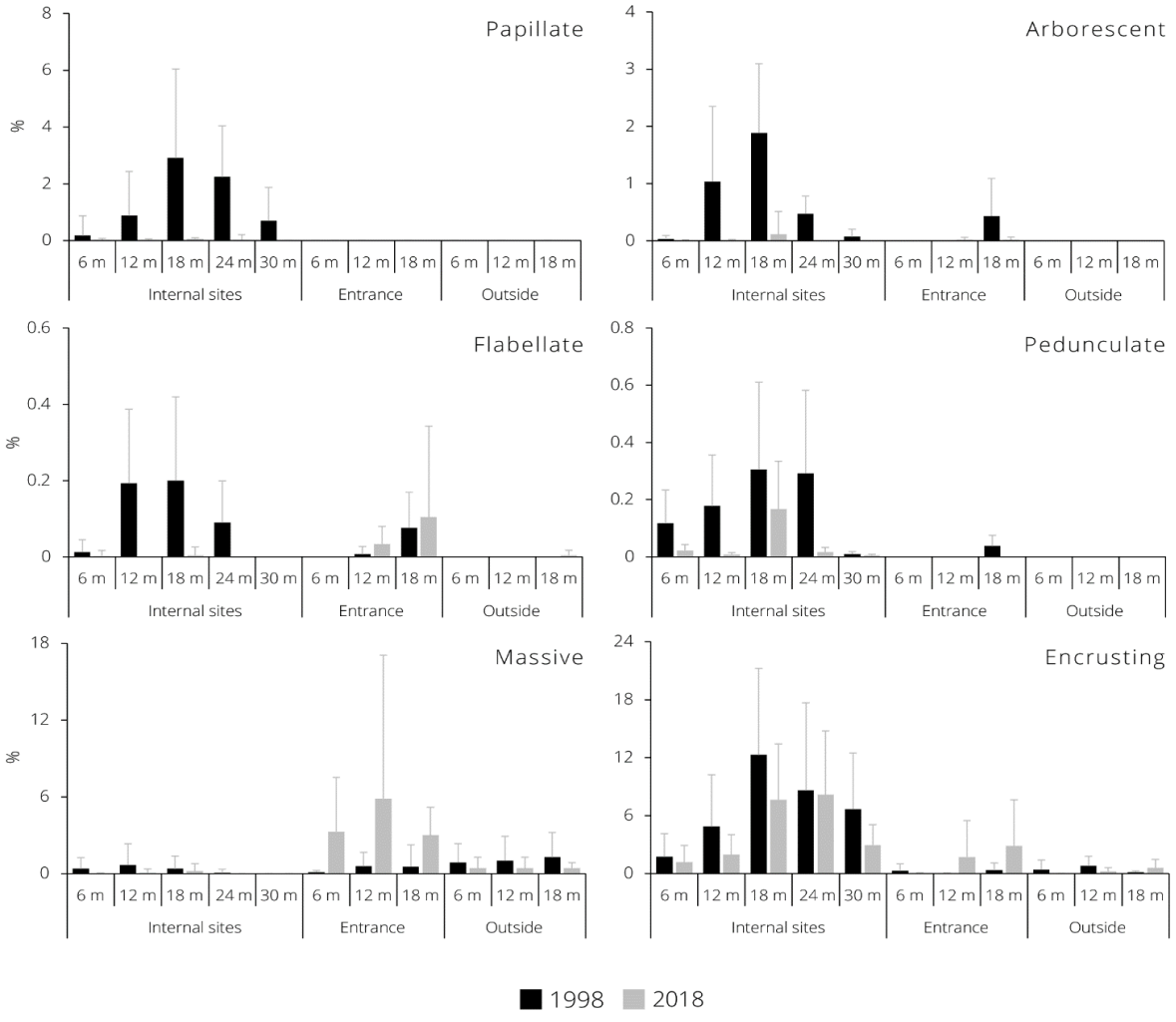

Figure 2.6. Mean percentage cover of main sponge morphologies in 1998 and 2018 for each depth at the internal sites (Glannafeen, Labhra Cliff, Goleen and West Cliff pooled together), entrance (Whirlpool Cliff) and outside Lough Hyne (Bullock Island). Error bars indicate standard deviation. Note the different y-axis scales.

2.3.4. High-resolution sponge diversity comparison between 1998 and 2019

From the detailed taxonomic survey, the number of sponge taxa reported in Lough Hyne decreased from 49 in 1998 to 44 in 2019 (Tab. S2.7). At the internal sites, the taxa richness decreased by between 6 and 49%, with the innermost site (West Cliff) experiencing the greatest reduction. The total number of taxa did not change at the entrance of the lough (32 species). Ten taxa were found only in 1998, while five taxa were found only in 2019 (Tab. S2.7).

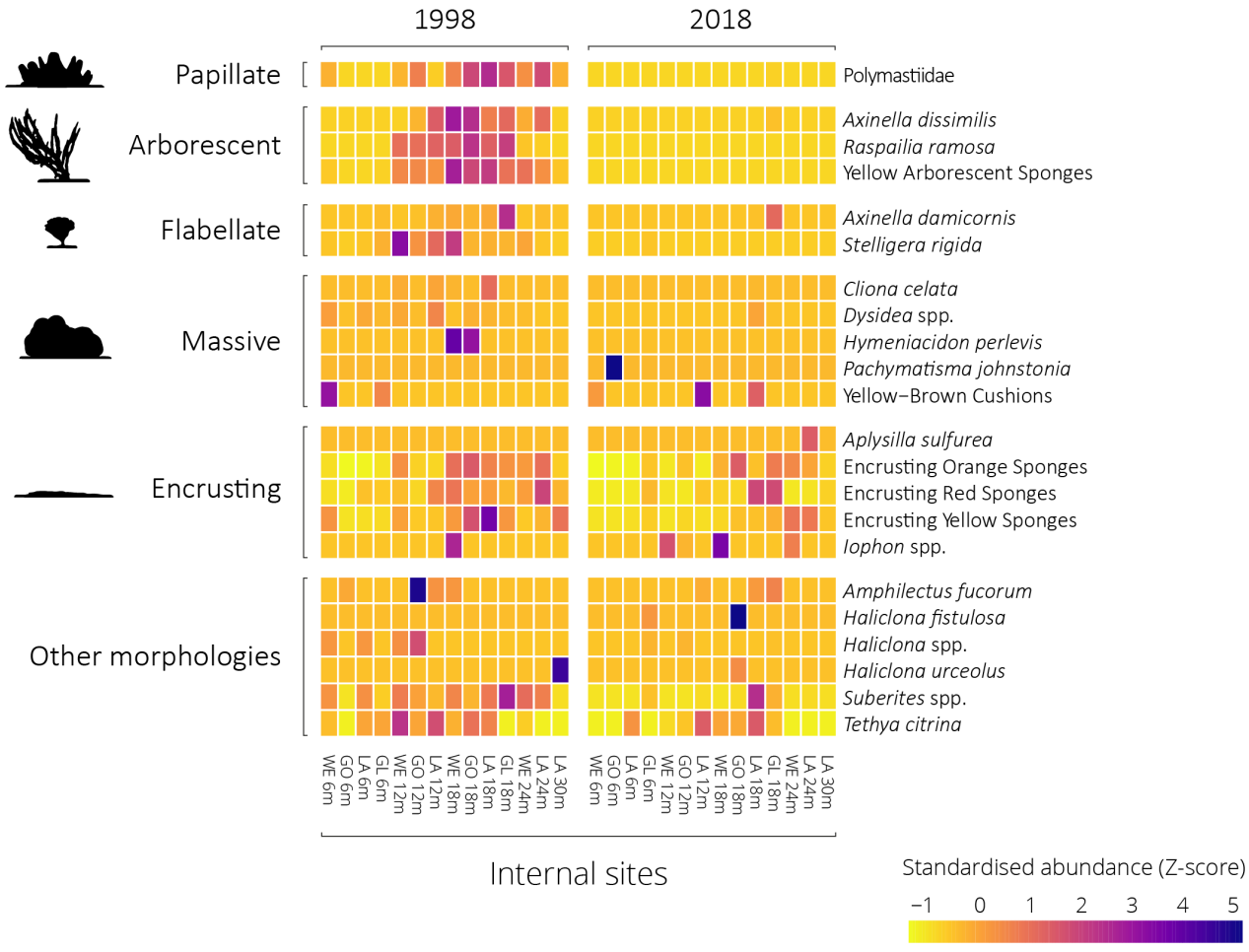

Figure 2.7. Heat map of the mean abundance of sponge taxa at the internal sites for each combination of site and depth in 1998 and 2018. Site Key: WE West Cliff, GO Goleen, LA Labhra Cliff and GL Glannafeen. Abundance data (percentage cover) are standardised (Z-score normalisation) on the taxon axes (i.e., each taxon is given equal weight). Data from vertical and inclined surfaces were pooled.

2.3.5. Long-term sponge abundance reconstruction

The available data indicate that the decline of papillate and arborescent sponges occurred between 2010 and 2015 (Fig. 2.8–9). At Goleen (internal site), adult individuals of papillate and arborescent sponges were commonly found during all eight surveys conducted between 1990 and October 2010 (Fig. 2.8). In July 2012, papillate sponge assemblage was noticeably depleted (only one adult was found), but large arborescent sponges were still present. In August 2015, no papillate and arborescent sponges were found at the innermost sites of the lough (Goleen and West Cliff), and other conspicuous sponges had almost disappeared (Nick Owen, Julia Nunn,

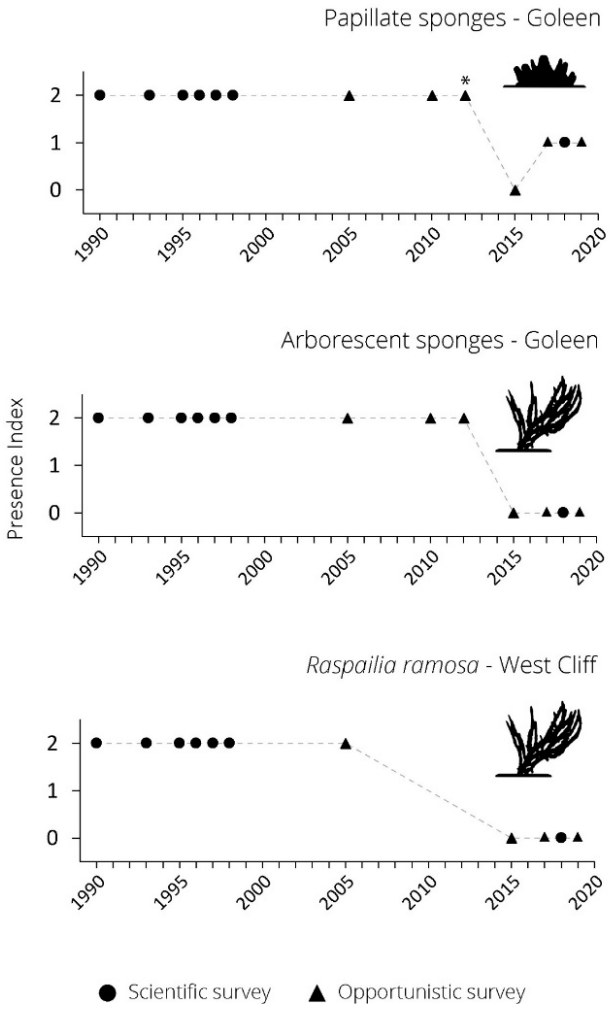

Figure 2.8. Temporal variation of papillate and arborescent sponges at Goleen, and *Raspailia ramosa* at West Cliff, between 1990 and 2019. Legend to the presence index: 0 = No sponge recorded; 1 = Only recruits recorded (< 2 cm); 2 = adult recorded (> 10 cm). *Only one adult was found.

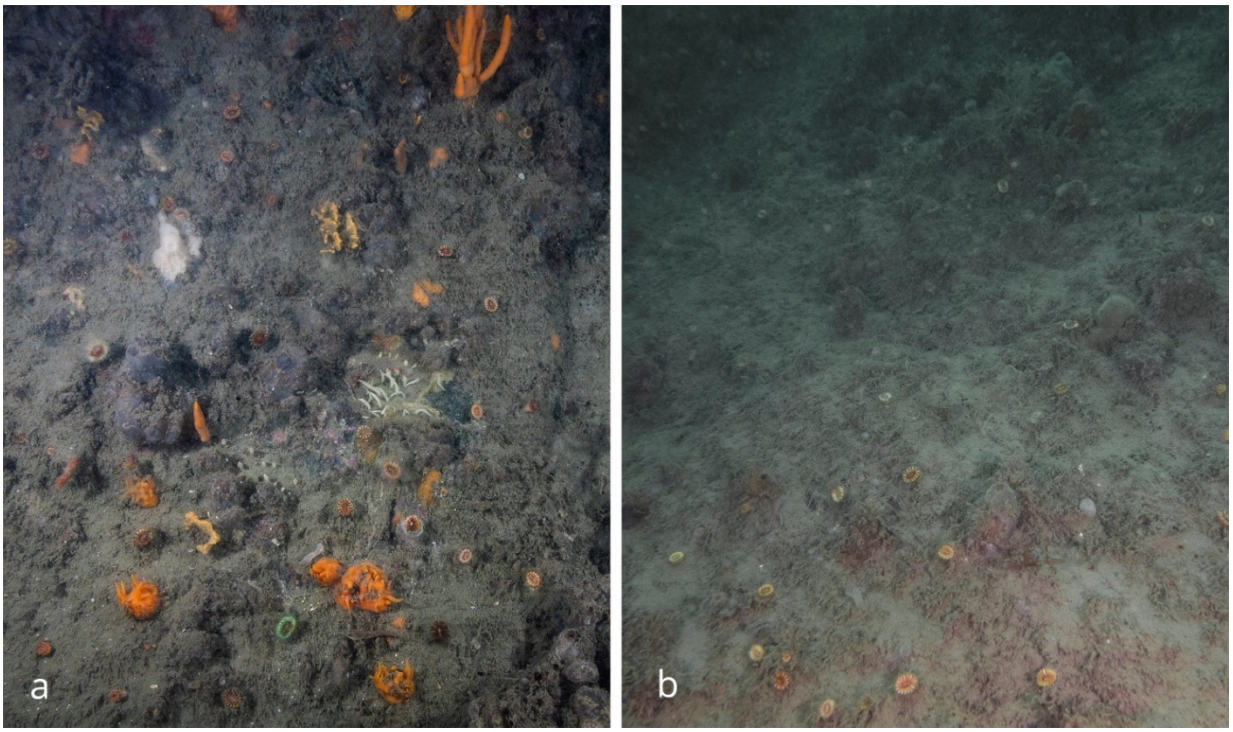

Figure 2.9. Examples of subtidal cliffs (~15 m) at Goleen in 2010 (a), the last time it was seen in a 'healthy' condition and 2018 (b). Notice the abundance and diversity of three-dimensional sponges in 2010 that are absent in 2018. Among the species present in the photo from 2010 are the branching sponges *Axinella dissimilis*, several papillates sponges of the genus *Polymastia* and *Sphaerotylus*, the flabellate sponges *Axinella damicornis* and *Stelligera rigida*. In contrast, ascidians and cup corals dominate in the photo from 2018. The photo from 2010 is courtesy of Nick Owen.

personal communication). During surveys carried out between 2017 and 2019, I was not able to record any arborescent sponge from Goleen and West Cliff, while I recorded papillate sponges, but only small recruits. *Raspailia ramosa* at West Cliff followed a similar trend as the arborescent sponges at Goleen, but information for the 2010–2012 period was not available.

At the other sites, all the eight species investigated (*Axinella damicornis*, *A. dissimilis, Cliona celata, Polymastia* spp., *Raspailia ramosa*, *Stelligera rigida* and other branching sponges) were present every year sampled at all study sites from 1990 to 1998 (except *Axinella damicornis,* that has never been recorded at the entrance of the lough). In 2017, 2018 and 2019, these species were still present at all sites, except the innermost ones (West Cliff and Goleen). At West Cliff (innermost site), only *Polymastia* spp. was recorded (only small recruits). While at Goleen

(internal site), only *Polymastia* spp. (only small recruits), *S. rigida* (only small recruits), and *A. damicornis* were recorded.

2.3.6. Environmental data analysis

Twenty-three summer heatwaves (*sensu* Hobday *et al.*, 2016) and 20 winter cold spells (*sensu* Schlegel *et al.*, 2017) were found in the SST analysis between 1982 and 2019 (Fig. S2.5a, b, c). Among the heatwaves, 78% could be considered moderate (Cat I), and 22% strong (Cat II), while for the cold spells, 85% were moderate and 15% strong; no severe (Cat III) or extreme (Cat IV) events were reported for the period investigated. Four heatwaves (one of which was strong) and one cold spell (strong) occurred in the period recognised as the potential time frame for change in biological communities at Lough Hyne (October 2010 – August 2015). The strong heatwave occurred between 15 June and 3 July 2014 and had a maximum intensity of 3.3 °C and cumulative intensity of 49.9 °C. Before October 2010, this cumulative intensity value has been exceeded by five other heatwaves with values up to 125 °C. The strong cold spell occurred between 16 December 2010 and 10 January 2011 with a maximum intensity of -1.8 °C and cumulative intensity of -28.7 °C. Before October 2010, this latter value was exceeded by 4 other cold spells with cumulative intensity up to -181.3 °C. Analyses of the air temperature reflect the SST data, with only moderate and strong events reported (Fig. S2.5d, e, f).

Regarding rainfall, the threshold values for the 24, 48, 72 and 96-hour-long extreme events were calculated as 31.7, 44.4, 55.3, 66.2, and 74.8 mm, respectively for the 99.5th percentile, and 42.9, 58.8, 70.6, 82.4, and 89.5 m, respectively for the 99.9th percentile. In total, 83 (24 h), 60 (48 h), 50 (72 h) and 44 (96 h) events exceeded the 99.5th percentile threshold, of which 6 (24 h) and 4 (48 h, 72 h and 96 h) occurred during the likely time frame for the change (Fig. S2.6). Seventeen (24 h), 14 (48 h), and 11 (72 h and 96 h) events exceeded the 99.9th percentile threshold, but none occurred during that timeframe when the biological changes might have occurred. The maximum rainfall recorded between October 2010 and August 2015 was 39.9, 53.1, 63, and 74.3 mm, respectively for 24, 48, 72 and 96h time frames. During the period between July 1974 and October 2010, those values were exceeded 22 (24 h), 18 (48 and 72 h) and 14 (96 h) times, with values up to 63.3 (24 h), 77 (48 h), 88.5 (72 h), 96.3 (96 h) mm.

2.4. Discussion

The unusual environmental conditions inside Lough Hyne support TMEs in much shallower water than other locations creating a rare opportunity to study TMEs using SCUBA. Despite early video surveys showing stability in the subtidal hard substratum communities at Lough Hyne, a major change has occurred between 1998 and 2018, characterised by a marked decline of predominantly three-dimensional sponge species and an increase in ascidians. These changes were generally restricted to the internal sites of Lough Hyne, suggesting a localised impact. Opportunistic observations suggest that the decline of sponges mostly likely occurred between 2010 and 2015, following one or more mortality events. I explored several potential drivers, but the absence of regular monitoring has made it impossible to identify the causative factor(s) confidently.

2.4.1. Spatial variation in benthic sessile communities and sponge assemblages at Lough Hyne

The results of the spatial variation analysis are consistent with previous studies at Lough Hyne. The three different sponge assemblages found in the present study (all internal sites, Whirlpool Cliff and Bullock Island) are similar to the assemblages described by Picton (1990) and Bell and Barnes (2000a). These differences result from the very different environmental conditions characterising the different sites (Bell, 2007). However, for the overall benthic communities, the spatial separation between sites was present but less pronounced. This is probably due to the low-taxonomical resolution used to identify the organisms, which was sufficient for discriminating temporal changes.

West Cliff, Goleen, Labhra Cliff, and Glannafeen share similar conditions (weak water movement, high sedimentation) that is reflected in similar biological communities (Picton, 1990). The higher abundance of sessile invertebrates on the subtidal cliffs of the internal sites is probably correlated with the sharp decrease in algae due to increased sedimentation with depth that limits light penetration (Bell and Barnes, 2002; Eriksson and Johansson, 2005). Bullock Island and Whirlpool Cliff are high-energy sites with less sediment accumulation than the internal sites, which explains the higher abundance of algae at lower depths, and the absence of delicate sponge morphologies (Palumbi, 1984; Bell and Turner, 2000). The different type of water movement can explain the differences between these two sites. Whirlpool Cliff experiences periodic unidirectional fast water flow that is destructive to some delicate organisms,

but is exploited by others such as algae and anthozoans, and some sponge species (Bell and Barnes, 2000a; Wildish and Kristmanson, 2005). In contrast, Bullock Island experiences extreme wave action (especially in winter) that only allows the growth of encrusting or seasonal organisms (Hiscock, 1983).

2.4.2. Temporal changes in subtidal benthic sessile communities at Lough Hyne

Between 1998 and 2018, I found changes in the overall biological community at all sites and sponge assemblage changes at all sites, except the site outside the lough. These changes were not consistent across the sites and mainly affected the internal sites, especially the innermost ones. Changes were also not consistent between taxa and functional groups, suggesting a differential vulnerability of TME organisms to stressful events.

At the internal sites, the general trend was a decrease in sponges and macroalgae and an increase in ascidians and turf-forming organisms. The most significant change was the strong decline, and in some cases the disappearance, of most three-dimensional sponges at the inner lough sites. Papillate, arborescent and flabellate sponges that once characterised the mesophotic cliffs of Lough Hyne were the most affected. Pedunculate and massive sponges also decreased, but to a lesser extent, while globular sponges did not show any change. At present, it is unclear if different morphologies were more tolerant to the factor/s that caused the sponge declines, or their life-history traits allowed substrate recolonisation quicker than other species. In contrast to the loss of three-dimensional forms, encrusting sponges were still relatively abundant in Lough Hyne in 2018, although they also decreased at the inner sites. Given the considerable size of some of the patches of encrusting sponges (mostly *Eurypon* spp. and encrusting suberitids) found in 2018, and their very slow growth rate (Fowler and Laffoley, 1993; Bernard Picton, unpublished data), it is very likely that most of these sponges were decades old and not new recruits. This differential response of sponges is consistent with previous research that found some sponge taxa to be very tolerant and others very sensitive to anthropogenic disturbance (Carballo and Naranjo, 2002).

I believe this marked decline in three-dimensional sponges is more likely the result of a mass mortality event than natural fluctuations. Although based on opportunistic observations of just a few species, my long-term sponge abundance reconstruction suggests that the sponge assemblages had been relatively constant for at least 20 years (1990–2010). Furthermore, most of the sponges that characterised the internal cliffs of Lough Hyne (including all the conspicuous species that disappeared) are long-lived and slow-growing, changing little from year to year. For

example, Fowler and Laffoley (1993), in the UK, reported less than 1 cm of growth in 6 years for Axinellid sponges (the same species that drastically declined at Lough Hyne). This is also supported by Perkins *et al.*, (2017), who found erect and massive sponge populations are reasonably constant on mesophotic temperate reefs in Australia.

Sponge abundance decreased at all depths, but changes were more evident at 18 and 24 m, than 6, 12 and 30 m, and more often on vertical surfaces than on inclined ones (except for papillate sponges that decreased more on inclined surfaces). This may result from the high level of variability of the sponge assemblages, which is supported by the significant interaction found in most analyses. Hence, it does not necessarily mean that sponges at 18 m and 24 m and on vertical surfaces were more impacted. With respect to the species recorded only in 1998 or 2018, most were rare, and the differences could be explained by species being missed when sampling. None of these rare species constituted a single OTU/taxon in the quantitative analyses, so they did not influence them. In contrast, the branching sponge *Raspailia hispida* was relatively abundant in 1998 and has likely become locally extinct in the lough. The most recent surveys carried out at the lough found a high abundance of sponge recruits at most sites, which could mean that, at least for some species, natural recovery is underway.

Sponge declines inside the lough correlated with a marked increase in ascidian abundance, which might be the result of the free space that became available after the sponges died. Ascidians may also have a higher tolerance to stressors that affected the sponges (Naranjo *et al.*, 1996). However, the ascidian increase could also result from their opportunistic nature and their considerable seasonal and interannual variability (Caputi *et al.*, 2015; Lynch *et al.*, 2016). This would be consistent with findings from the Bathurst Channel in Tasmania, where most of the species show high temporal stability, while others, including ascidians, showed considerable interannual variability (Barrett *et al.*, 2010).

The increase in turf-forming organism abundance and the decrease in macroalgal cover inside the lough at shallow depths (6 and 12 m) is consistent with the changes in the algal assemblages that have occurred over the last few decades in the intertidal and shallow subtidal. Trowbridge *et al.*, (2013) reported a recent increase in ephemeral filamentous algae, potentially driven by the reduction in primary consumers and the total nitrogen increase in the area (Jessopp *et al.*, 2011). These ephemeral algae often form continuous blankets that coat other algal species, which explains the lower cover of macroalgae found in 2018 (Trowbridge *et al.*, 2013). Changes in spatial dominance of various foundation species to turf-forming algae are common features of degraded temperate rocky subtidal reefs globally, often caused by a complex interaction of

factors including climate change and eutrophication (Strain *et al.*, 2014; Filbee-Dexter and Wernberg, 2018; O'Brien and Scheibling, 2018).

Less clear is the reason for the increase in sponge abundance (mainly massive sponges) at the site at the entrance of the lough. I believe this more likely represents natural population fluctuations as the changes were smaller compared to the inner sites. Furthermore, some of the sponge species that increased in abundance in 2018 at this site are fast-growing and highly dynamic, particularly *Amphilectus fucorum* and *Cliona celata* (Fowler and Laffoley, 1993; Van Soest and Hajdu, 2002).

Changes in communities (but not sponge assemblages) were also found outside the lough. In this case, the main changes were an increase in ascidians and macroalgae, and the consequent decrease in the coverage of turf-forming organisms. These changes are more likely due to seasonal variations. Concerning ascidians, the only species found in 2018 was *Clavelina lepadiformis*, a seasonal species whose zooids disappear at the end of the summer (Berrill, 1951). It is possible that in 1998, this species was missed because all the zooids had disappeared before sampling. The same could be true for algae, as one of the most abundant algae found in 2018 was *Delesseria sanguinea*. Reports from the Normandy coasts show that this species loses its fronds in June (Nabil and Cosson, 1996); so, it might not have been recorded in 1998 because the fronds had disappeared before sampling.

2.4.3. Potential causes of biological changes at Lough Hyne

There are many potential explanations for the changes I report at Lough Hyne (see Table S2.1 for a summary of the possible causes). However, the limited biological and environmental monitoring makes it very difficult to identify the exact cause or the timing. I explored available environmental data, but I could not determine with certainty any causal processes responsible for the observed mass mortality event of three-dimensional sponges.

Opportunistic observations indicate that the decline of sponges mostly likely occurred between 2010 and 2015, in one or more mortality events. This change most strongly affected the innermost sites, suggesting that the cause of the change has either originated from inside the lough or that the sheltered conditions of the Lough Hyne basin have amplified a driver originating from the surrounding coast. Similar mass mortality events in temperate waters, involving several orders of sponges, have only been reported in the Mediterranean Sea, caused

Table 2.1. Possible Causes of the changes occurred at the mesophotic communities of Lough Hyne.

Possible causes	Estimated likelihood and explanation.
Toxic event	**Plausible**. A toxic event due to an anomaly in the oxy-thermocline breakdown might explain a mass mortality event. During the seasonal stratification, anoxic water accumulates in the deeper areas of the lough. In autumn, the oxy-thermocline is usually eroded by the surface waters that become cold and dense (Kitching, 1987). However, in the case of a severe storm, the oxy-thermocline might break quickly, allowing the anoxic, acidic, and H_2S-rich water to spread across the shallower part of the basin. A similar situation seems to have happened in September 2011, due to the effects of Hurricane Katia (Grams and Blumer, 2015), which caused strong winds and the sudden drop of water temperature (Fig. S2.7) and an early breakage of the oxycline (as reported by Sullivan *et al.*, 2013). Hydrogen sulphide might have been above the tolerance level of many sponge species. Furthermore, pH, low oxygen, and H_2S might have acted synergistically, increasing the event's toxicity (Vaquer-Sunyer and Duarte, 2010). In contrast, sponges closer to the entrance of the lough might have survived due to the higher influx of water from the open sea (Kitching, 1987). Such an event might explain the scale of change that has occurred, and why some sites were more affected than others. In support of this hypothesis is the encrusting sponges of the family Raspailidae remaining relatively abundant in 2018. These sponges are the only ones abundant in the deeper, periodically anoxic/hypoxic areas of the lough and are better adapted to acidic, hypoxic, H_2S-rich conditions (Schuster *et al.*, 2021). While this kind of oceanographic event could occur naturally in systems like Lough Hyne, the nutrient increase recorded at Lough Hyne and the coastal areas of SW Ireland between the 1990s and 2000s could have contributed to the intensification of the anoxic/hypoxic regime as reported in many other areas of the world (Diaz and Rosenberg, 2008).

Eutrophication	**A likely contributor**. Jessopp *et al.*, (2011) reported a high degree of nitrogen enrichment at Lough Hyne and the surrounding coast. Total nitrogen inside the lough has increased from a maximum monthly of 210 mg m^{-3} in the 1990s (Johnson *et al.*, 1995) to 720 mg m^{-3} in the late 2000s (Jessopp *et al.*, 2011). Eutrophic conditions might have intensified the naturally occurring anoxic/hypoxic regime and the diel oxygen fluctuations (Plowman *et al.*, 2020) at Lough Hyne, contributing to the mass mortality of sponges (Diaz and Rosenberg, 2008). Increased nutrients promote the growth of ephemeral algae, which, at the end of their life cycle, die and accumulate on the seafloor inducing anoxia and the release of hydrogen sulphide (Lyons *et al.*, 2014). Furthermore, some ephemeral algae (e.g., *Ulva*) can also affect sessile invertebrates by releasing toxic compounds (Nelson *et al.*, 2003). In the absence of strong currents, such as in the innermost sites of the lough, decaying algae can settle and accumulate on erect sponges (personal observations). The decomposition products might have stressed the sponges beyond the tolerance limit.
Heatwave	**Unlikely to be the main driver, but a possible contributor**. No heatwaves occurred during the time frame when the change was firstly recognised (11/2010–07/2012) (Fig. S2.5). However, the 2013 and 2014 heatwaves might have contributed to a possible later phase of the change.
Increased sedimentation	**Possible but unlikely to be the main driver**. Sediment generally has negative impacts on sponges (Gerrodette and Flechsig, 1979). However, many sponge species show specific adaptations allowing them to survive and often thrive in sedimented habitats (Bell, 2004, 2015; Schönberg, 2016; Strehlow *et al.*, 2017; Cummings *et al.*, 2020). For example, at Lough Hyne, highly sedimented sites were previously described as having higher sponge abundance and diversity than less sedimented sites (Bell and Barnes 2000a, b, c). Furthermore, sponge morphologies that

	were affected the most (arborescent and papillate polymastid sponges) are considered the most suited to highly sedimented environments (Bell, 2007, Schönberg, 2016). Finally, to the best of my knowledge, no mass mortality of temperate sponges following increased sedimentation has been reported before.
Cold spell	**Possible but unlikely**. Ireland and the British Isles experienced an extremely cold winter in 2010/2011, with a strong cold spell (SST) occurring between 16/12/2010 and 10/01/2011 (Fig. S2.5). However, on that occasion, the temperature did not go below 8.4 °C. During other cold spells occurring in February–April (the coolest period), between 1983 and 1987, the temperature decreased down to 7.4 °C. Furthermore, cold-related mortality in temperate sponges has never been reported, and it is unlikely that this has affected the deeper sponge assemblages.
Algal bloom	**Possible but unlikely**. In recent decades, records of phytoplankton blooms at Lough Hyne have increased (Jessopp *et al.*, 2011; Trowbridge *et al.*, 2017b). Although a direct effect of phytoplankton clogging or toxins has never been demonstrated, some authors suggested that it might be possible (Wall *et al.*, 2012).
Pathogen outbreak	**Possible but unlikely**. Reports of sponge disease have increased in recent years and are often associated with environmental factors such as temperature anomalies and urban/agricultural runoff (Webster, 2007). However, a mass mortality event due to a pathogen outbreak would likely have been more uniform around the lough. Furthermore, pathogens usually affect phylogenetically related sponges (Webster, 2007), while the sponges affected at Lough Hyne were from several different orders.
Competition with other organisms	**Unlikely**. Sponges are regarded as strong space competitors, but in some cases, they can be outcompeted by ascidians and cnidarians (Wulff, 2006). Furthermore, sponge food sources can overlap with other filter feeders, such as ascidians (Petersen, 2007).

Decreased salinity	**Unlikely**. Salinity in the water column below 3 m of depth shows a very little variation (Kitching, 1987). Furthermore, extreme precipitation events that occurred during the time frame of the change were minor compared to the ones that occurred in the period before the change (Fig. S2.6).
Industrial Pollution	**Unlikely.** Pollution by heavy metals, hydrocarbons, and other toxic chemical compounds can be excluded as no major industrial centres are present in the area.
Increased tourist frequentation	**Unlikely**. Tourism in the area has increased (official figures are not available), but the type of tourism (mainly kayakers, swimmers, and hikers) is not compatible with the change that has occurred.
Damage from fishing activities	**Unlikely**. Lough Hyne is a statutory Marine Nature Reserve, and no collections of marine organisms can be made without a permit. Only a few local fishermen are allowed to use pots for fishing shrimp. Even though fishing pots have the potential to damage benthic organisms (Johnson, 2002), this was unlikely the cause of the mass mortality occurred as pots are generally placed in shallow (<10 m) water.
Recreational diving	**Unlikely**. Diving activities at Lough Hyne are regulated by the National Parks and Wildlife Service and only allowed under a permit. Although recreational divers can potentially impact benthic communities (Garrabou *et al.*, 1998), the annual number of dives in the lough has not increased markedly over the last 20 years (National Parks and Wildlife Service, personal communication). Furthermore, damage from diving activity is not compatible with the striking changes occurred.

by disease outbreaks (Gaino *et al.*, 1992), heatwaves (Garrabou *et al.*, 2009; Di Camillo and Cerrano, 2015) and eutrophication-related anoxia (Stachowitsch, 1984), and in Australia as a result of sewage discharge (Roberts *et al.*, 1998). Other catastrophic changes in similar environments have been reported from the Chilean Patagonian fjord region, where the cold-water coral *Desmophyllum dianthus* experienced a mass die-off in 2012 following eutrophication due to salmon farming pollution (Försterra *et al.*, 2014). However, mass mortalities in benthic ecosystems usually remain undocumented or poorly described due to difficulties in responding rapidly to unforeseen events and a lack of baseline data, especially in remote marine systems (Jurgens *et al.*, 2015).

Sponge mass mortalities have been often attributed to disease outbreaks, but I think this is unlikely to be the cause of the changes that occurred at Lough Hyne. Usually, pathogen outbreaks infect broad geographic areas (Webster, 2007), so I believe the effects would have likely been more uniform around the lough. Furthermore, pathogens usually affect a specific group of sponges (a species, a family or more rarely an order; Webster, 2007), while in Lough Hyne, several orders of sponges were involved. Heatwaves are also unlikely to be the main cause, considering that no significant heatwaves occurred during the period when the changes were first recognised (October 2010 – July 2012; Fig S2.5). In contrast, winter 2010/2011 was characterised by a moderate cold spell which probably caused the death of some intertidal gastropods at Lough Hyne (Little *et al.*, 2020). In tropical coral reefs, cold-water events are known to be a cause of mortality of sponges and other benthic invertebrates (Colella *et al.*, 2012). However, cold-related mortality has never been reported for temperate sponges.

At this stage, eutrophication seems to be one of the most likely contributors to the changes. There has been a marked increase in nutrients both inside the lough and the surrounding coast in recent years. Total nitrogen inside the lough increased from a maximum monthly concentration of 210 mg m^{-3} in the 1990s (Johnson *et al.*, 1995) to 720 mg m^{-3} in the late 2000s (Jessopp *et al.*, 2011). Eutrophication appears to be central to the changes seen in the shallow water communities of the lough (Trowbridge *et al.*, 2017a; Plowman *et al.*, 2020). Similarly to other coastal systems worldwide, the high nitrogen levels have stimulated the proliferation of ephemeral macroalgae (particularly ulvoids and ectocarpoids) and phytoplankton blooms (Jessopp *et al.*, 2011, Trowbridge *et al.*, 2011, Lyons *et al.*, 2014). Some of these algae (e.g., *Ulva*) can produce chemicals that negatively affect benthic species (Nelson *et al.*, 2003). When large quantities of blooming algae settle on the seafloor, they increase the organic load of the sediment, inducing

anoxia and the release of hydrogen sulphide (Lyons *et al.*, 2014). At Lough Hyne, this excess of organic matter might also influence the duration of the oxy-thermocline in the lough, promoting earlier formation and greater persistence of anoxic conditions (Diaz and Rosenberg, 2008, Jessopp *et al.*, 2011). Furthermore, other factors, such as increased temperatures and the occurrence of a toxic event caused by an anomaly in the oxy-thermocline break, might have contributed to the stress of the benthic communities culminating in the sponge mass mortality.

The small number of laboratory experiments that have tested the effects of increased nutrients on sponges have found no or little effect (Luter *et al.*, 2014; Beepat *et al.*, 2020; Ramsby *et al.*, 2020). However, the effects of eutrophication on heterotrophic organisms are mainly caused by cascading effects rather than the actual nutrients themselves (Grall and Chauvaud, 2002, Gray *et al.*, 2002). One of the most severe consequences of eutrophication is a decrease in oxygen, but, in laboratory conditions, sponges have been found to be tolerant of severe hypoxia (Mills *et al.*, 2014; 2018; see Chapter 3). However, the severity of hypoxia could be different in the natural environment, and threshold values can be highly influenced by temperature and the presence of hydrogen sulphide (Gamenick *et al.*, 1996; Vaquer-Sunyer and Duarte, 2008; Vaquer-Sunyer and Duarte, 2011). For example, Stachowitsch (1984) found that during a eutrophication-related hypoxia/anoxia event sponges were among the first organisms to die.

Unfortunately, there is still very little information about TME species and community ecology, or the vulnerability of these systems to anthropogenic stressors. Basic information on life cycles, connectivity patterns, population dynamics and responses to stressors for most TMEs species is often still inferred from related shallow-water species. However, the very different environmental conditions of shallow and mesophotic waters (i.e., temperature, light, hydrodynamics, and food availability), mean the ecology and TME organisms and their response to stressors could differ (Cerrano *et al.*, 2019). Therefore, more research is needed to understand TME ecology in the context of global and local changes, and to predict potential changes to TME species and communities.

2.4.4. Implications for the conservation of TMEs

My study highlights the vulnerability of mesophotic habitats to environmental change, and how major changes can occur, which are easily overlooked. What has happened in Lough Hyne could also have happened or might be happening in other areas without being noticed. TMEs are comprised mainly of long-living and slow-growing organisms, which are likely to have limited resilience to human-induced impacts (Deter *et al.*, 2012). Despite the high tolerance of some

shallow-water sponges to anthropogenic disturbance, my study suggests that three-dimensional mesophotic sponges are among the most sensitive species (see also Carballo and Naranjo, 2002). Any decline in these habitat-former species will likely affect important ecosystem functions with detrimental effects on related ecosystem services (Gómez-Gras *et al.*, 2021). Given the vulnerability and importance of TMEs, the management and conservation of these habitats should be prioritised by management agencies.

Successful management and conservation of TMEs can only be achieved through fit-for-purpose monitoring of biotic and abiotic factors, including environmental stressors (Borja, 2014). To date, TMEs are monitored in only a few regions of the world (e.g., Mediterranean Sea and Australia), while very little is known about them elsewhere. Furthermore, MPA management plans rarely consider TMEs and often, as in the case of Lough Hyne, protection only results from shallow MPA designation extending into deeper waters (Kitching, 1987; Turner *et al.*, 2019). TMEs need specific consideration in current MPA monitoring programmes, and new TME monitoring schemes should be established to monitor particularly rich and vulnerable habitats and communities. Together with monitoring, current baselines need to be established, against which potential changes can be measured and evaluated in relation to natural variation in the system (Borja *et al.*, 2012). Furthermore, historical baselines need to be reconstructed to assess if changes have already occurred as this information is critical to set future conservation targets.

Quantitative data for TMEs are rarely available, so, as in my case, it can be useful to combine scientific data with opportunistic observations to consolidate time-series and document long-term changes. Photos, videos, historical descriptions from all possible sources including the internet and social media (Di Camillo *et al.*, 2018), local fishers, SCUBA divers and naturalists, can provide essential information to reconstruct earlier environmental and biological conditions (Drew 2005; Ferretti *et al.*, 2015; Thurstan *et al.*, 2017). In my study, the use of opportunistic observations considerably improved my ability to reconstruct historical baselines at Lough Hyne and in the evaluation of long-term community dynamics. However, this approach does not replace the need for long-term monitoring programmes in the evaluation of environmental impacts. The absence of regular subtidal monitoring of Lough Hyne's TMEs resulted in almost a decade between the occurrence of the change and its recognition, which has significantly reduced the chances of identifying the drivers. This consequently hinders the implementation of appropriate measures aimed at restoring the original status and eliminating or minimising the impacts.

The main factors limiting the research and monitoring of TMEs globally are the depth and the availability of technology, as these ecosystems are usually out of range of conventional scientific diving (Turner *et al.*, 2019). However, recent rapid technological advances have led to the development of a wide range of tools that can now facilitate exploring deeper ocean areas at low cost. For example, small remotely operated vehicles (ROVs), autonomous underwater vehicles (AUVs) and closed-circuit rebreathers, together with advanced acoustic and optical imaging techniques, are now available for a wide range of management and conservation applications for TMEs (e.g., UNEP-MAP-RAC/SPA, 2008; Williams *et al.*, 2010, Pizarro *et al.*, 2013).

If TMEs are monitored regularly in Lough Hyne Marine Reserve, then the lough could become an important reference site due to the accessibility of its TMEs, and its relative isolation from external drivers. However, the shallowness of the Lough Hyne TMEs may also contribute to their vulnerability to internal drivers, which, if monitored, could be recorded and identified relatively easily.

2.5. Conclusions

This study at Lough Hyne demonstrates the potential fragility of TMEs and how changes can happen without being detected if adequate monitoring is not in place. The monitoring of TMEs will contribute to our scientific understanding of these poorly-studied systems and improve our ability to make evidence-based decisions for TME management and conservation (Turner *et al.*, 2019; Sukhotin and Berger, 2013). A better knowledge of these ecosystems will also raise the awareness of the value of TMEs among decision-makers and the general public, which is essential to ensure their conservation (Inglehart, 1995). Finally, this study is a small-scale example, that even if dramatic ecological changes happen, most species and functional groups persist, leaving space for a potential recovery (Lotze *et al.*, 2006).

3. Chapter 3 - Adaptive strategies of sponges to deoxygenated oceans

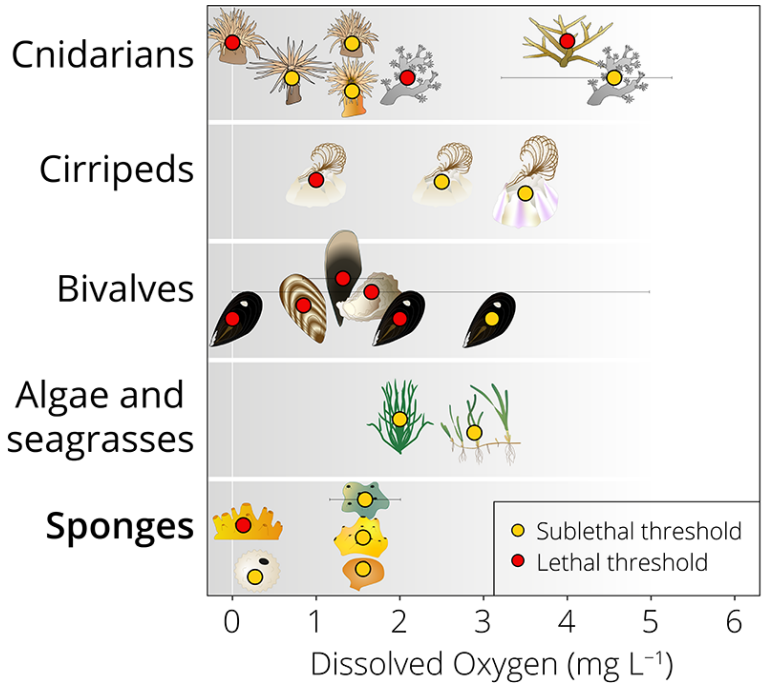

The results presented in this chapter are published in: **Micaroni, V.**, Strano, F., McAllen, R., Woods, L., Turner, J., Harman, L., Bell, J.J. (2022). Adaptive strategies of sponges to deoxygenated oceans. *Global Change Biology* 28, 1972-1989. Reprinted with permission (altered version). John Wiley and Sons, Inc is the copyright holder for this article.

Abstract

Ocean deoxygenation is one of the major consequences of climate change. In coastal waters, this process can be exacerbated by eutrophication, which is contributing to an alarming increase in so-called "dead zones" globally. Despite its severity, the effect of reduced dissolved oxygen has only been studied for a very limited number of organisms, compared to other climate change impacts such as ocean acidification and warming. Here I experimentally assessed the response of sponges to moderate and severe simulated hypoxic events. I ran three laboratory experiments on four species from two different temperate oceans (NE Atlantic and SW Pacific). Sponges were exposed to a total of five hypoxic treatments, with increasing severity (3.3, 1.6, 0.5, 0.4 and 0.13 mg O_2 L^{-1}, over 7–12-days). I found that sponges are generally very tolerant of hypoxia. All the sponges survived in the experimental conditions, except *Polymastia crocea,* which showed significant mortality at the lowest oxygen concentration (0.13 mg O_2 L^{-1}, lethal median time: 286 h). In all species except *Suberites carnosus*, hypoxic conditions do not significantly affect respiration rate down to 0.4 mg O_2 L^{-1}, showing that sponges can uptake oxygen at very low concentrations in the surrounding environment. Importantly, sponges displayed species-specific phenotypic modifications in response to the hypoxic treatments, including physiological, morphological, and behavioural changes. This phenotypic plasticity likely represents an adaptive strategy to live in reduced or low oxygen water. My results also show that a single sponge species (i.e., *Suberites australiensis*) can display different strategies at different oxygen concentrations. Compared to other sessile organisms, sponges generally showed higher tolerance to hypoxia, suggesting that sponges could be favoured and survive in future deoxygenated oceans.

3.1. Introduction

Anthropogenic emissions of carbon dioxide and other greenhouse gasses have increased exponentially since the industrial revolution, causing significant changes in the Earth's climate (Raupach and Canadell, 2010; IPCC, 2021). Climate change has three main effects on the marine environment: warming, acidification, and oxygen decline (Bijma *et al.*, 2013). While most ecological and physiological research has targeted the first two stressors, deoxygenation remains comparatively neglected (Limburg *et al.*, 2017). Despite the scant attention, recent research shows that oxygen loss is a major anthropogenic stressor for marine biota that may exceed the severity of the combined effects of ocean warming and acidification (Sampaio *et al.*, 2021).

Oxygen is essential to all aerobic life, and ocean deoxygenation has the potential to affect all biogeochemical and biological processes within the oceans (Semenza, 2007; Levin and Breitburg, 2015). In the open sea, warming is considered the main cause of O_2 reduction: an increase in sea temperature leads to decreased O_2 solubility, increased water stratification, and alterations to oceanic circulation, which reduces O_2 supply to the ocean interior (Doney, 2010; Keeling *et al.*, 2010). Higher temperatures also enhance microbial respiration, which can further deplete oxygen in marine ecosystems (Altieri and Diaz, 2019; Robinson, 2019). Oxygen levels in the global oceans have already declined by 2% during the last 50 years, with more significant O_2 declines in the North Pacific and tropical oxygen minimum zones (OMZ) (Levin and Breitburg, 2015). This is likely to get worse in the future, with models predicting a global ocean reduction in O_2 of up to 7% by the end of the century (Keeling *et al.*, 2010).

In coastal waters, climate-driven deoxygenation can be intensified by eutrophication (Nixon, 1995; Altieri and Gedan, 2015). The input of anthropogenic nutrients, such as fertilizers and human/livestock wastes, can increase algal growth resulting in an accumulation of organic material on the seafloor. This excess of organic matter is then degraded by bacteria, causing O_2 depletion that can lead to hypoxic conditions (Smith *et al.*, 2006). In shallow and well-mixed waters, eutrophication-driven hypoxia is generally caused by nocturnal heterotrophic respiration, resulting in daily oscillations in oxygen concentration. In contrast, long-term hypoxic events are more likely to occur in enclosed seas or basins (Levin *et al.*, 2009). Hypoxia has widespread and severe impacts across taxonomic and functional groups. The intensity and duration of oxygen depletion are the main factors influencing the severity of hypoxic events on benthic organisms (Levin *et al.*, 2009; Altieri and Diaz, 2019). Mild hypoxia can alter behavioural patterns, decrease feeding rates and cause changes in physiological processes such as metabolic rate, ventilation,

etc. (Vaquer-Sunyer and Duarte, 2008). Severe hypoxic events can cause mass mortalities, leading to the formation of so-called "dead zones", which are areas largely devoid of macrofauna (Diaz and Rosenberg, 2008). Dead zones have been reported in small water bodies such as harbours, fjord and inlets, and large basins, such as the Baltic Sea, spreading over 60,000 km^2 (Altieri and Diaz, 2019). As climate and land use continue to change, coastal hypoxia is expected to worsen, with the increased occurrence, frequency, intensity, and duration of hypoxic events (Diaz and Rosenberg, 2011).

Despite the extent of the problem and the dramatic effects caused by ocean deoxygenation, the response of many groups of organisms to hypoxia is still poorly studied. This lack of knowledge limits our ability to model the effects of declining oxygen availability on marine ecosystems (Seibel, 2011). To date, research on tolerance to reduced levels of dissolved oxygen has primarily focused on fish, crustaceans, and molluscs (Vaquer-Sunyer and Duarte, 2008), while very little is known about most other groups, especially sessile organisms. Sessile organisms could be considered particularly vulnerable to hypoxic events because they cannot move or migrate to well-oxygenated water. Furthermore, sessile organisms include many important habitat-forming species, so any change in their abundance could have major consequences for the components of ecosystems they support (Vergés *et al.*, 2019; Woodhead *et al.*, 2019; Piazzi *et al.*, 2021). Therefore, it is critical to understand how these organisms respond to hypoxia to predict possible future changes and better manage threats to marine ecosystems.

Sponges are the dominant sessile organisms in many marine ecosystems and are found in high abundance in tropical, temperate, and polar ecosystems (Ayling, 1983, Bell *et al.*, 2020). They perform many important ecological functions, including contributing to nutrient cycling, bioerosion, enhancing ecosystem complexity and providing habitats for a wide range of associated organisms (Wulff, 2006; Bell, 2008; Maldonado *et al.*, 2012). Despite being important components of marine ecosystems, sponge tolerance to hypoxia has been poorly investigated to date. Mills *et al.*, (2014) showed that *Halichondria panicea* can feed and respire with oxygen levels down to 4% of air saturation. However, the authors did not provide information on the duration of the treatments and replication; furthermore, in the same study, information on the temperature and salinity of the water was unavailable, so it is not possible to derive the actual oxygen concentrations to which sponges were exposed. Two other relevant experiments have investigated the short-term response of sponges to hypoxia. Mills *et al.*, (2018) exposed *Tethya wilhelma* to a step decreasing oxygen concentration (30–40 h with O_2 lower than 10% a.s., 0.7 mg L^{-1}). They found that sponges continued to perform periodic full-body contractions down to

0.27 mg O_2 L^{-1}, but ceased below that concentration. Leys and Kahn (2018) exposed *Geodia barretti* to 6.5 h of hypoxia (7% air saturation, 0.6 mg O_2 L^{-1}), and found that sponge respiration rate remained largely unchanged. However, filtration rates dropped almost immediately after the oxygen level was reduced. Despite these earlier studies, we still have very little insight into how sponges may cope with hypoxic events caused by ocean and coastal deoxygenation.

Here I provide an assessment of sponge response to hypoxia. Specifically, I experimentally investigated the physiological, behavioural, and morphological responses of four temperate sponge species to moderate and severe hypoxic conditions. I ran the first experiment to expose sponges to moderate hypoxic conditions for seven days, including a wide range of dissolved oxygen concentrations (0.5, 1.6 and 3.3 mg O_2 L^{-1}). Subsequently, I investigated sponge response to severe hypoxia (0.13 and 0.4 mg O_2 L^{-1}) for 12 days with two additional experiments. Finally, I discuss sponge tolerance to low dissolved oxygen compared to other sessile organisms in the context of future climatic conditions.

3.2. Materials And Methods

3.2.1. Study area and species

Experiment 1 (moderate hypoxia) was performed in Ireland (Renouf Laboratory, Lough Hyne) on two abundant North-East Atlantic sponge species: *Cliona celata* Grant, 1826 and *Suberites carnosus* (Johnston, 1842). Experiments 2 and 3 (severe hypoxia) were performed in New Zealand (Wellington University Coastal Ecology Laboratory, Wellington) on two abundant temperate Australasian species: *Polymastia crocea* Kelly-Borges and Bergquist, 1997 and *Suberites australiensis* Bergquist, 1968.

3.2.2. Experiment 1: moderate hypoxia

In the first experiment, I investigated the response of *Cliona celata* and *Suberites carnosus* to a wide range of oxygen concentrations, using an air-tight system with a continuous flow of seawater. Sponges were exposed to ~95% (7.71 ± 0.19 mg O_2 L^{-1}), ~40% (3.34 ± 0.17 mg O_2 L^{-1}), ~20% (1.56 ± 0.19 mg O_2 L^{-1}) and ~6% (0.48 ± 0.09 mg O_2 L^{-1}) air saturation (a.s.) for seven days (a summary of the seawater parameters is provided in Table S3.1).

The experimental set-up (see scheme in Figure S3.1) consisted of two independent replicate modules for each treatment, randomly distributed in the experimental set-up. To condition water, I used two header tanks for each experimental module: one providing water and one reservoir. Header tanks were filled with 10-µm-filtered seawater. The oxygen level was then lowered and maintained to the desired dissolved oxygen concentration by bubbling specific mixtures of N_2 (BOC, food-grade) and air, through glass-ceramic diffusers. Hypoxic gas blends were prepared by decanting food-grade N_2 and air in 15 L scuba cylinders using an oxygen decanting assembly (Undersea Ltd, 5215) with a DPM-300 digital gauge (0.25% accuracy). Oxygen concentration was then checked with a Nuvair Pro O_2 Analyser and adjusted, if necessary.

Conditioned water was delivered to two replicate experimental chambers (2.3 L) for each system at a rate of 25 L per day, ensuring 100% water replacement every 2 h and 15 min. Water circulation within each experimental chamber was provided by the gravity-driven water flow (~3 cm/s). Temperature was kept constant using a water bath controlled by an aquarium chiller.

Cliona celata was collected from the Kedges (51°27’41.4 “N 9°20’44.2 "W), whereas *Suberites carnosus* was collected from the rocky cliffs of Lough Hyne (51°30'00.4"N 9°18'03.9"W). For both species, sampling was carried out at 10–18 m in June 2019 and sponges

collected were at least 2 m apart. Sponges were then left to recover for two months from harvesting stress in a 1 m^3 underwater cage placed at 8 m depth.

Sponges were then transferred to the experimental system and randomly distributed across the experimental chambers. The experimental design consisted of 32 experimental chambers (two replicate chambers for each species for each replicate module, and two replicate modules for each treatment). A diagram of the experimental design is reported in Figure S2. Three sponges were placed in each chamber (6 sponges in total for each replicate module and 12 for each treatment). Sponges belonging to different species were not mixed but kept in separate chambers. Sponges were left to acclimate with oxygen saturated air for five days before oxygen was lowered by introducing hypoxic water into the chambers. Oxygen concentration was lowered in 24 h and was then maintained for seven days until the end of the experiment (a graph showing the oxygen concentration in the different treatments over time is provided in Figure S3). In natural ecosystems, hypoxic conditions can develop in short times ranging from hours to a few days (Breitburg, 1990; Nezlin *et al.*, 2009), so I consider these acclimation times appropriate and ecologically relevant. Temperature, salinity and oxygen concentration inside the experimental chamber were measured twice a day using a Fibox 4 oxygen meter with a dipping probe (Presence GmbH, Germany). A two-spot calibration was performed on the oxygen probe every three days, using sodium dithionite for 0 % oxygen and air-saturated water for 100% oxygen.

3.2.3. Experiments 2 and 3: severe hypoxia

I also investigated the response of sponges (*Polymastia crocea* and *Suberites australiensis*) to severe hypoxia through two separate experiments using an air-tight system. In experiment 2, sponges were exposed to ~5% (0.4 ± 0.04 mg O2 L^{-1}), and ~100% a.s. (8.34 ± 0.13 mg O_2 L^{-1}), while in experiment 3, sponges were exposed ~1.5% (0.13 ± 0.02 mg O_2 L^{-1}), and ~100% a.s. (8.15 ± 0.16 mg O_2 L^{-1}). The different oxygen concentration in the controls was due to the small difference in temperature between the two experiments (13.3 ± 0.5 °C in experiment 2 compared to 14.3 ± 0.6 °C in experiment 3). A summary of the seawater parameters is provided in Table S3.1.

Sponges were kept in independent cylindrical air-sealed polypropylene chambers (10 L), randomly distributed inside a water bath. Every two days, ~70% of the water was replaced using 10-µm-filtered seawater, preconditioned to the desired oxygen concentration in independent conditioning tanks. Oxygen concentration was then maintained by bubbling air or air-N_2 blends

through glass-ceramic diffusers (see section 2.1.2 for more details on gas blends). Custom made de-bubbler devices were used to eliminate bubbles coming from the ceramic diffusers that could affect sponges (Figure S4). The sponges were fed twice a day with *Nannochloropsis* microalgae (1–2 µm cell diameter; Nanno 3600™ Reed Mariculture, US.). Water circulation within each experimental chamber was provided by the de-bubbler device and an additional water pump located on the side of the chamber, which provided a constant circular water flow. The chambers were placed in a water bath to control water temperature.

Polymastia crocea was collected from Barrett Reef (Wellington South Coast, 41°20'31.1"S 174°50'09.7"E) by cutting fragments (~8 cm^3) from separate sponges (at least 5 m apart). Whole specimens of *Suberites australiensis* were collected from Mahanga Bay (Wellington Harbour, 41°17'32.2"S 174°50'06.5"E), attached to a fragment of their respective substrate. Sponges were then left to recover for three weeks after sampling and cutting stress in water tables with 10-µm-filtered flow-through seawater.

Sponges were then transferred to the experimental system, consisting of 12 experimental chambers (3 independent replicate chambers for each species and treatment combination). Five sponges were placed in each chamber (15 sponges in total for each treatment). Sponges were left to acclimate with oxygen saturated air for five days. Oxygen was then lowered by bubbling a specific Air-N_2 mixture. In experiment 2, oxygen was lowered in ~24 hours and then maintained at 5% a.s. (0.4 mg O_2 L^{-1}) for 12 days until the end of the experiment. While in experiment 3, oxygen was lowered to 1.5% a.s. (0.13 mg O_2 L^{-1}) in ~72 hours (which included a preacclimation at 10% a.s., 1 mg O_2 L^{-1}) and maintained for 12 days until the end of the experiment (Fig. S3.3). This further acclimation in hypoxic conditions was made because of the very low O_2 concentration of the treatment. In experiment 3, due to the very low concentration of O_2 (0.13 ± 0.02 mg L^{-1}), O_2 increased to ~0.3 mg L^{-1} for about 20 minutes during daily examinations. Temperature, salinity and oxygen concentration inside the experimental chamber were measured twice a day using Fibox 4 oxygen meter with a dipping probe (Presence GmbH, Germany). A two-spot calibration was performed on the oxygen probe every three days, using sodium dithionite for 0% oxygen and air-saturated water for 100% oxygen.

3.2.4. Response variables

3.2.4.1. Survival and health monitoring

Sponge health was monitored daily during the experiment. Sponges showing ≥ 25% of external necrosis were considered dead and removed from their treatment tanks during the daily

checks, so as not to impact other sponges in the treatments. At the end of the experiments, all sponges were sectioned to assess the presence of any internal necrosis.

3.2.4.2. Respiration Rate

For all the experiments, respiration rate was measured on the same specimens at *T*0 (before the beginning of the experiment), *T*1/2 (after two days from the beginning of the final treatment in experiment 1, and after five days in experiments 2 and 3) and *T-end* (end of the experiment). In experiment 1 (moderate hypoxia), I measured respiration rates of three sponges in each replicate module (n = 6 for each treatment). In experiments 2 and 3 (severe hypoxia), respiration rates were measured on three sponges in each experimental chamber (n = 9 for each treatment). To measure respiration rate, sponges were placed in sealed cylindrical glass respiration chambers (150 ml for *Cliona celata*; 80 ml for *Suberites carnosus*; 250 ml for *Polymastia crocea* and *Suberites australiensis*) with PreSens oxygen sensor spots (SP-PSt3-NAU) attached to their inner surface. Experimental chambers contained either oxygen saturated water (pre-experimental measurements and controls) or water at a slightly higher oxygen concentration than the experimental treatment (+20–50%, depending on the treatment) collected from the respective header tanks. Respiration rates were not performed on sponges from experiment 3 (1.5% a.s.). The incubations were performed in controlled temperature (water bath) and dark conditions. The water inside the respirometry chambers was gently stirred using a magnetic stir bar. After 20 min of acclimation, oxygen concentration inside the chambers was measured every 10 min for 1 hour, using a Fibox 4 oxygen meter with a polymer optical fibre (POF). Respiration measurements were ended prematurely if the oxygen level fell below 70% of the treatment concentration to avoid any detrimental effect on the sponges. Blank incubations, containing only seawater were performed every respiration run and used to correct for any microbial community respiration in the seawater. A two-point calibration was performed on the oxygen sensor spots before each measurement session.

Respiration measurements were standardized to sponge ash-free dry weight (*AFDW*) from buoyant weight (*BW*) measurements (Fig. S3.5). For *Suberites australiensis*, it was not possible to estimate *AFDW* from *BW* due to the abundant external material accumulated by the sponge inside the tissue that influences the *BW*. For this species, I measured the *AFDW* of all the specimens used in the respirations at the *T-end*, and I assumed that sponges had the same weight at *T*0 and *T*1/2.

3.2.4.3. Changes in weight, size, and morphology

Changes in weight and size over time relative to the initial values were estimated by calculating the buoyant weight variation (*BWV*) and contracted area variation (*CAV*). For all of the experiments, buoyant weights (*BW*) of all experimental sponges (except *Suberites australiensis*) were taken at *T*0 and *T-end* and used to calculate relative buoyant weight variation as $BWV = [(BW_{T\text{-}end} - BW_{T0}) / BW_{T0}] \cdot 100$. Buoyant weight was measured with a digital scale (AandD FX-200i) following the methods of Osinga *et al.*, (1999). For experiments 2 and 3 (severe hypoxia), photographs of contracted sponges were taken at *T*0 and *T-end* to measure sponge contracted area (*CA*) and calculate contracted area variation as $CAV = [(CA_{T\text{-}end} - CA_{T0}) / CA_{T0}] \cdot 100$ (following Osinga *et al.*, 1999). Contraction was achieved by disturbing sponges with a blunt plastic rod (being careful not to damage the sponge) and waiting for one hour for the sponge to react to the stimulus. All the photographs were analysed using ImageJ (US National Institutes of Health, Bethesda, Md, USA).

During experiments 2 and 3, treatment conditions induced the development of peculiar morphological structures in some specimens of both *Polymastia crocea* and *Suberites australiensis*. Sponges were photographed and monitored daily to calculate the percentage of specimens developing these structures and the median time of occurrence.

3.2.4.4. Sponge contractile behaviour

During experiments 2 (5% a.s.) and 3 (1.5% a.s.), sponge contractile behaviour was monitored daily from *T*0 to *T-end*, on all experimental sponges through photographic analysis. For *Suberites australiensis*, the contractile behaviour was estimated using an "expansion ratio" (*EXPR*) calculated as $EXPR = A_{Ti} / CA_{T0}$, where A_{Ti} is the area occupied at T_i and CA_{T0} is the contracted area at *T*0. Area was preferred over volume because of the low invasiveness of the measurements. In *Polymastia crocea,* contraction/expansion mainly occur at the papillae level, so the contractile behaviour was estimated from the ratio of expanded papillae (*REP*) calculated as $REP = P_E/P_{tot}$, where P_E is the number of visible expanded papillae and P_{tot} is total number of visible papillae. Expanded papillae were defined as papillae whose length was at least two and a half times the width.

3.2.4.5. Pumping rate

Pumping rate was only calculated for *Suberites australiensis* from experiments 2 and 3 (severe hypoxia). Having only one osculum of relatively large size, this species was particularly

suitable for investigating changes in pumping rate. To minimize sponge disturbance during the experiment, pumping rate (PR) was derived from the measurement of the sponge osculum cross-sectional area (OSA). In sponges, pumping rate (PR) is correlated with OSA (e.g., Goldstein *et al.*, 2019; Morganti *et al.*, 2021). In the case of *S. australiensis*, this relationship was calculated on 20 sponges (following Yahel *et al.*, 2005) and was found as $PR = 6.55 \cdot OSA^{1.43}$ (Fig. S3.6). Photographs of the oscula with scale were taken daily from *T*0 to *T-end*, on three sponges in each experimental chamber (the same specimens each time point, n = 9 per treatment). Since *S. australiensis* has only one osculum, pumping rate was then standardized per sponge volume.

3.2.4.6. Histology

Histological sections of *Suberites australiensis* from the severe hypoxia experiments were analyzed to calculate the percentage of the sponge body occupied by the aquiferous system (system of connected water channels inside the sponge). At *T-end*, two contracted sponges for each experimental chamber (n = 6 per treatment) were fixed in Davidson's solution at room temperature for 12 h and then preserved in 70% ethanol. A fragment of about 0.5 cm^3 was cut from each sample and dehydrated in an ethanol series (70%, 80%; 90%, 95%, 100%), washed in xylene (50% xylene in ethanol and 100% xylene) and included in paraffin under vacuum with an automated tissue processor (Leica Biosystems TP1020). Samples were then embedded in paraffin wax using an embedding station (EG1160). Sections (10 µm) were manually cut with a rotary microtome (Leica Biosystems RM2235), stained with haematoxylin and eosin, and mounted on microscope slides with DePeX mounting medium (Strano *et al.*, 2021). Three replicate sections for each sponge were then photographed under a dissecting microscope (Olympus SZ61) and photographed using a Canon EOS 70D digital camera. To calculate the area occupied by the aquiferous system, pictures were analyzed using ImageJ.

3.2.5. Data analysis

All the statistical data analyses were performed in R version 3.1.3 (R Core Team, 2013), except PERMANOVA models, which were performed using PRIMER v7 with PERMANOVA+ add-on (Anderson *et al.*, 2008; Clarke and Gorley, 2015). Experiments 2 and 3 were analyzed separately. To investigate respiration rate, pumping rate and expansion ratio in *Suberites australiensis* from experiment 2, I used linear mixed-effects models with normally distributed errors and random intercepts (lmer, *lme4* package; Bates *et al.*, 2015). For pumping rate, I added a constant variance function structure (varIdent) to the linear mixed-effects models to allow different variances for each treatment at each time point (lme, *R* package *nlme*; Pinheiro *et al.*,

2021). The constant variance function structure was necessary because the variance of the response variable differed across treatments and experimental days. To investigate the effect of time and treatment on the expansion ratio of *Polymastia crocea* in experiment 3, I used a generalized linear mixed model with beta regression and logit link (*glmmTMB*, Brooks *et al.*, 2017). In all the mixed models, treatment and time were considered fixed effects, while experimental chamber and sponge specimen were considered random effects. The experimental chamber effect was included to address pseudo-replication. For these models, fixed- and random-effect terms were tested using the functions *anova* and *ranova* (*R* package *lmerTest*, Kuznetsova *et al.*, 2017), respectively; while *post hoc* pairwise comparisons were computed on estimated marginal means using emmeans (*R* package *emmeans*; Lenth, 2021). The ratio of expanded papillae in *P. crocea* from experiment 2 and expansion ratio in *S. australiensis* from experiment 3 were investigated using repeated measure univariate PERMANOVA (Anderson, 2001; 2014), because did not meet the normality assumption for mixed-effects models. Pairwise tests were then calculated using permutation *t*-tests (*R* package *RVAideMemoire*; Hervé, 2021). PERMANOVA and permutation *t*-tests were also used to supplement mixed-effects models when there were concerns about the normality of the residuals (pumping rate in *S. australiensis*). Change over time relative to the initial value of buoyant weight and contracted area, and differences in percentage occupied by the aquiferous system were investigated using Kruskal–Wallis H tests, Welch's *t*-tests or Wilcoxon Signed-Rank Tests, depending on the variable. Respiration rates from experiment 1 were log (x + 1) transformed, and pumping rates were square-root transformed to meet normality assumptions. The goodness of fit, normality and homoscedasticity of the errors were checked for all models by inspecting plots of the normalized residuals and the quantile-quantile plots. All the multiple comparisons were corrected using Benjamini-Hochberg Procedure, but uncorrected *p*-values are reported in the text. All the statistical analyses made for each variable are reported and summarized in Table S3.2**.**

Time to event analysis for sponge survival and development of peculiar morphological structures (modified papillae and protruding oscular membranes) was performed using the Kaplan-Meier Method, and *p*-values were calculated using the Log Rank Test implemented in the survival *R* package (Therneau, 2021). Median lethal time (LT_{50}) and median time to the development of modified morphological structures were calculated using a logistic model.

3.3. Results

3.3.1. Sponge responses to moderate hypoxia

All the sponges of experiment 1 survived the seven days of treatment, except one specimen of *Suberites carnosus* in the lower DO treatment (6% a.s.), which exhibited internal necrosis on the final day of the experiment.

Mean buoyant weight variation between *T*0 and *T-end* ranged between -1% and -1.6% for *Cliona celata* and +2.1% and -0.5% in *Suberites carnosus*. There were no differences in buoyant weight variation among treatments for both species, but for *C. celata* there was a significant slight decrease in weight in the 40% a.s. (-1.6%, $p = 0.008$) and 20% a.s. (-1.4%, $p = 0.008$) treatments (Tab. S3.3; Fig. S3.7).

For *Cliona celata*, there was no significant effect of time or treatment on the respiration rate (Tab. S3.4). However, pairwise comparisons revealed a significant decrease ($p = 0.028$) in the 20% a.s. treatment between day 0 and 7, and a significant increase ($p = 0.029$) in the 6% a.s. treatment between day 2 and day 7, but both became non-significant after the correction for multiple comparisons (Tab. S3.4). However, the data suggest a coherent temporal pattern in the respiration rate in both 20% a.s. and 6% a.s. treatments. *C. celata* respiration rate decreased after two days from the start of the experiment and then increased until the end of the experiment. In contrast, in both the 100% a.s. and 40% a.s. treatments, respiration rate remained stable for the whole duration of the experiment (Fig. 3.1a).

For *Suberites carnosus*, there was a significant interaction of time and treatment ($p = 0.007$) on the respiration rate (Tab. S3.5). Pairwise comparisons revealed a significant decrease in respiration rate between day 0 and 7 ($p < 0.0001$), and day 2 and 7 ($p < 0.0001$) (Tab. S3.5). The respiration rate showed a non-significant decrease towards the end of the experiment in the 20% a.s. treatment, while in both the 100% a.s. and 40% a.s. treatments, respiration rate remained stable for the duration of the experiment (Fig. 3.1b).

3.3.2. Sponge responses to severe hypoxia

3.3.2.1. Survival

Sponge survival differed among species, with *Suberites australiensis* more tolerant than *Polymastia crocea*. No mortality was observed for *S. australiensis* in both experiments 2 (5%

a.s.) and 3 (1.5% a.s.). In contrast, for *P. crocea*, significant mortality ($p = 0.001$) was observed in sponges exposed to the 1.5% a.s. treatment, starting from day 10 (day 12 when including the hypoxic acclimation), and with a median lethal time of 11.9 ± 0.3 days (Fig S8–9). Eight out of 15 sponges had died by the end of the experiment. No mortality was observed for *P. crocea* in the 5% a.s. treatment.

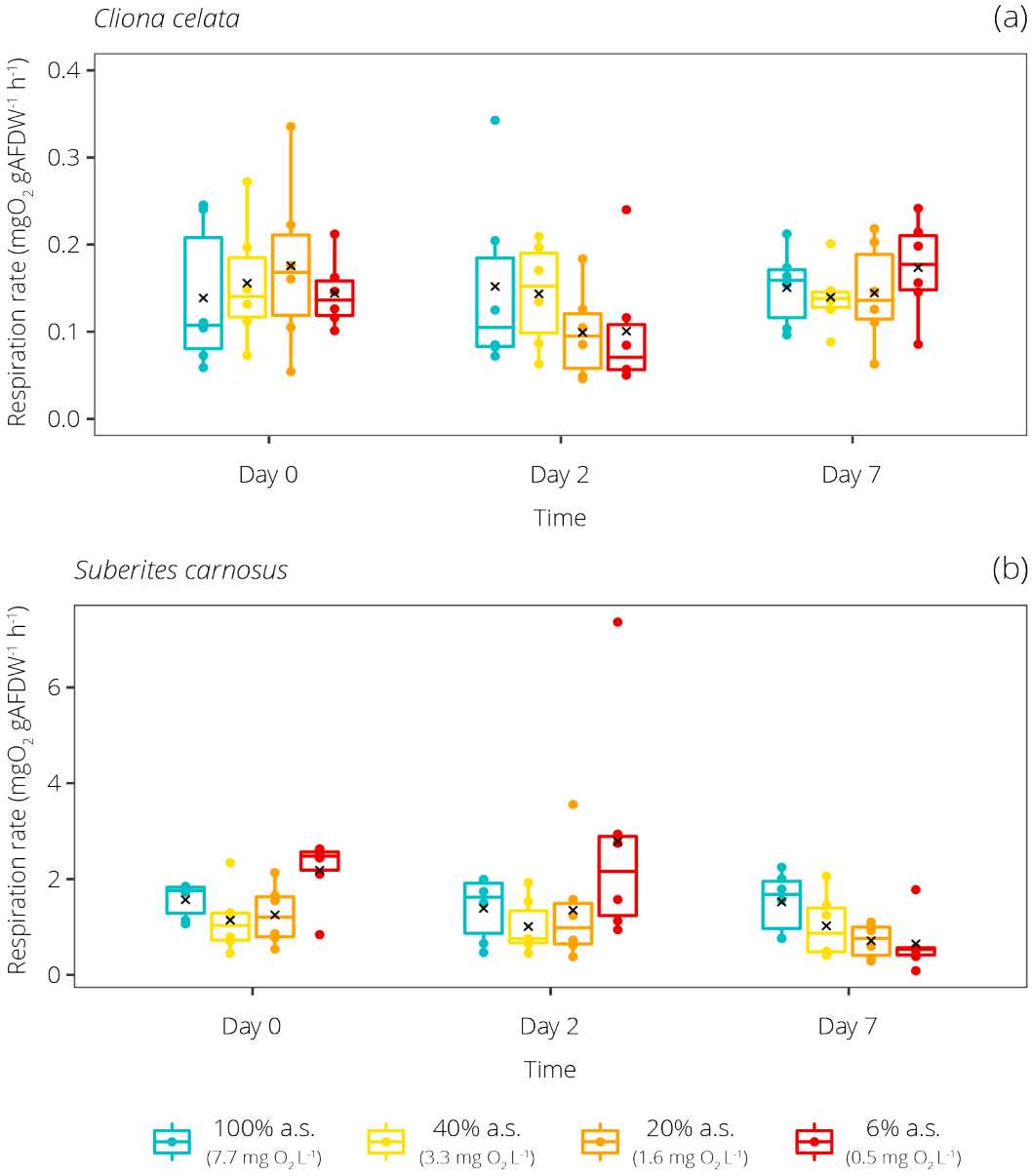

Figure 3.1. Respiration rates in (a) *Cliona celata* and (b) *Suberites carnosus* from experiment 1 (moderate hypoxia) measured at *T*0, *T*1/2 and *T-end*. Note: x-axis and y-axis scales differ between species. Horizontal bars inside the boxplots represent medians; the symbol × represents means. Lower and upper hinges of the boxplots correspond to the first and third quartiles, respectively. Points represent data points.

3.3.2.2. Change in weight and size

For *Polymastia crocea*, buoyant weight variation between *T*0 and *T-end* differed among treatments in experiment 3 (1.5% a.s.) ($t = 2.82$, $p = 0.012$), but not in experiment 2 (5% a.s.). Sponges from the 1.5% a.s. treatment showed a significant decrease in buoyant weight (-7.1%, $t = -5.17$, $p = 0.002$), while the controls did not significantly change (Tab. S3.6; Fig. S3.10).

The relative variation in area of contracted sponges (after stimulating contraction) between *T*0 and *T-end* differed significantly between treatments and controls for both *Polymastia crocea* ($W = 12$, $p < 0.0001$) and *Suberites australiensis* ($W = 13$, $p < 0.0001$), but only in experiment 2 (5% a.s.). Both *P. crocea* and *S. australiensis*, from the 5% a.s. treatment, experienced an increase in contracted area (+18.9%, $W = 120$, $p = 0.0001$ and +18.4%, $W = 105$, $p = 0.008$, respectively). While *S. australiensis* from the control treatment (experiment 2) experienced a decrease in contracted area (-15.3%, $W = 3$, $p = 0.0003$) (Tab. S3.7; Fig. S3.11).

3.3.2.3. Sponge contractile behaviour

Low DO treatments generally induced sponge expansion, but the response differed between species, and it was generally more marked in the 5% a.s. treatment. In *Polymastia crocea*, the ratio of expanded papillae was significantly affected by the interaction between time and treatment in both experiments 2 ($p = 0.0001$) and 3 ($p < 0.0001$ and $p = 0.03$) (Tab. S3.8–9). During experiment 2 (5% a.s.), the treatment induced a progressive expansion of papillae from day 2. The ratio of expanded papillae in sponges from the hypoxic treatment became significantly higher than control sponges from day 6 to the end of the experiment ($p = 0.0002$–0.005) (Tab. S3.8; Fig. 3.2a). A similar trend was found in experiment 3 (1.5% a.s.), but the ratio of expanded papillae of the treatment sponges was more variable and became significantly different only at day 9 ($p = 0.003$) (Tab. S3.9; Fig. 3.2b). In this experiment, I also found a correlation between the ratio of expanded papillae and mortality. Sponges that survived the treatment had a significantly higher maximum ratio of expanded papillae compared to sponges that died, both when the maximum ratio was calculated at the end of the experiment (Welch *t*-test: $t = 5.3$, $p = 0.0005$) and at day ten, before sponges started to die (Welch *t*-test: $t = 4.6$, $p = 0.0007$).

In *Suberites australiensis*, there was a significant interactive effect of treatment and time ($p < 0.0001$) on the expansion ratio in experiment 2 (5% a.s.), but only an effect of time ($p = 0.01$) in experiment 3 (1.5% a.s.) (Tab. S3.10–11). For experiment 2 (5% a.s.), pairwise comparisons

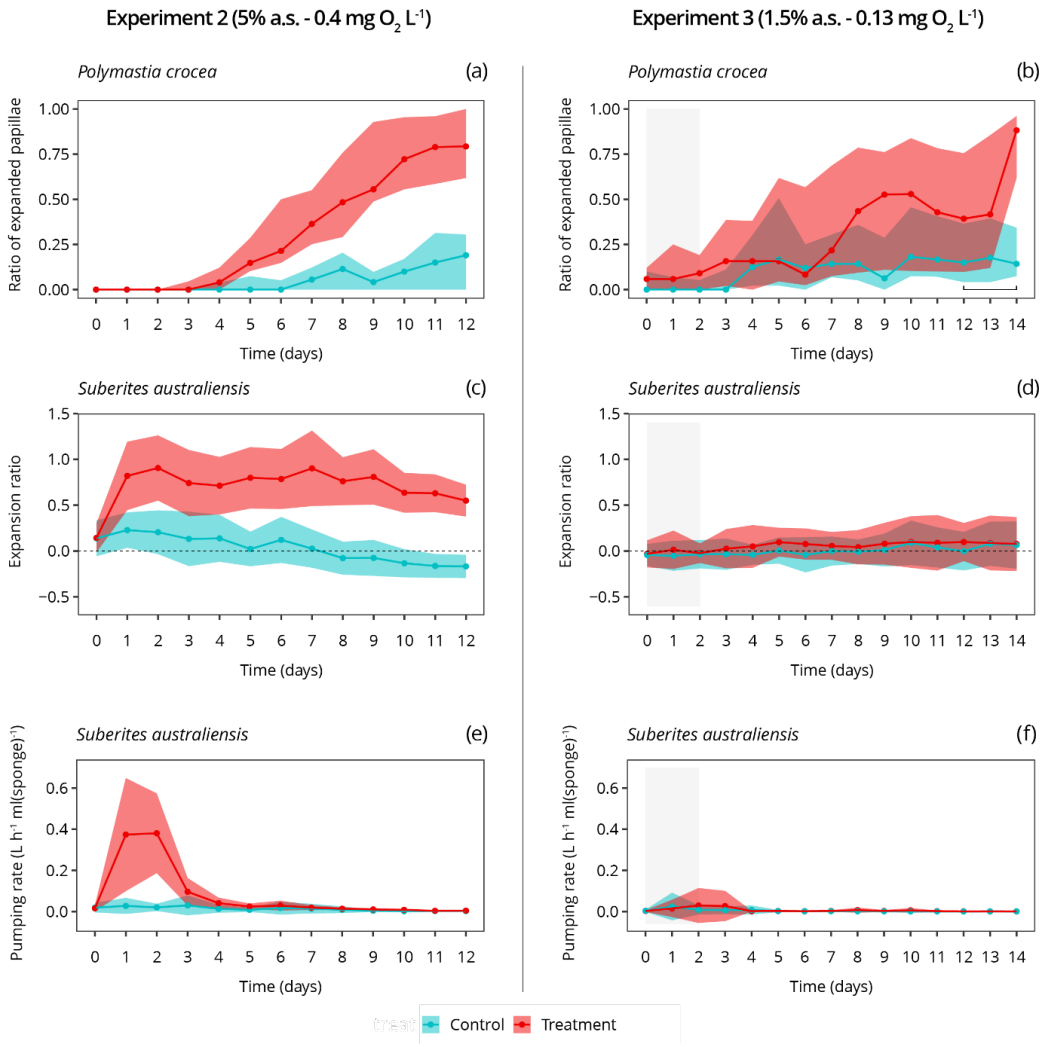

Figure 3.2. Contractile behaviour and pumping rate during experiments 2 and 3 (severe hypoxic conditions). Changes in the ratio of expanded papillae over time in *Polymastia crocea* in each treatment in experiments 2 (a) and 3 (b). Changes in the expansion ratio over time in *Suberites australiensis* in each treatment in experiments 2 (c) and 3 (d). Changes in the pumping rate over time (estimated from the osculum cross-sectional area) in *S. australiensis* in each treatment in experiments 2 (e) and 3 (f). In (a) and (b), points represent the median, while lower and upper edges of the ribbons represent the 75th and 25th percentile, respectively. In (c), (d), (e) and (f), points represent the means while lower and upper edges of the ribbon represent the standard deviation. Days of hypoxic acclimation (10% a.s.) are highlighted in grey. In (b), a black line is used to highlight days when sponges experienced mortality.

found significant expansion in sponges (+60%, $p < 0.0001$) between day 0 and 1. Sponges then remained expanded for the whole duration of the experiment, and the expansion ratio was significantly higher in the treatments compared to the controls from the first to the last day of the experiment ($p < 0.0003$) (Tab. S3.10; Fig. 3.2c, d).

3.3.2.4. Morphological modifications

During experiments 2 (5% a.s.) and 3 (1.5% a.s.), some *Polymastia crocea* and *Suberites australiensis* sponges exposed to hypoxic treatments underwent morphological modifications (Fig. 3.3; S3.12). In some *P. crocea*, the conical papillae showed a progressive elongation, flattening, and, in some cases, spiralization (Fig. S3.12a–f). This process occurred in both the 5% a.s. and 1.5% a.s. treatments, but morphological changes were more pronounced in the lower DO treatment (Fig. S3.12d-e). Exposed to the 1.5% a.s. treatment, some sponges developed papillae so slender that they could not sustain their weight (Fig. S3.12d-e). The development of these modified papillae was also associated with an apparent increase in the porosity of the sponge external surface (Fig. S3.12e). In the 5% a.s. treatment, 73% of the sponges developed modified papillae, starting from day 6. In the 1.5% a.s. treatment, 60% of sponges developed modified papillae, starting from day 2, from the beginning of the final treatment (day 4 considering hypoxic acclimation period) (Fig. S3.13). The median time of development of these morphological structures (considering only the sponges that developed them) was 7.2 ± 0.2 days in the 5% a.s. treatment and 4.6 ± 0.4 days in the 1.5% a.s. treatment (Fig. S3.14). Although not significant ($\chi^2 = 3.62$, $p = 0.057$), a relationship between modified papillae and survival was found. Among the *P. crocea* that survived the 1.5% a.s. treatment, six had developed modified papillae, while one had not. While among the sponges that died following the 1.5% a.s. treatment, three had developed modified papillae, while five had not.

In the the 5% a.s. treatment, 53% of *Suberites australiensis* developed a semi-transparent protruding membrane surrounding the oscula. This membrane progressively reduced the oscular-cross sectional area (Fig. 3.3; S3.12g–i). The median time it took for these protruding oscular membranes to become noticeable (considering only the sponges that developed them) was 5.1 ± 0.2 days (Fig. S3.14). By the end of the experiment, 53% of sponges had developed these structures (Fig. S3.13).

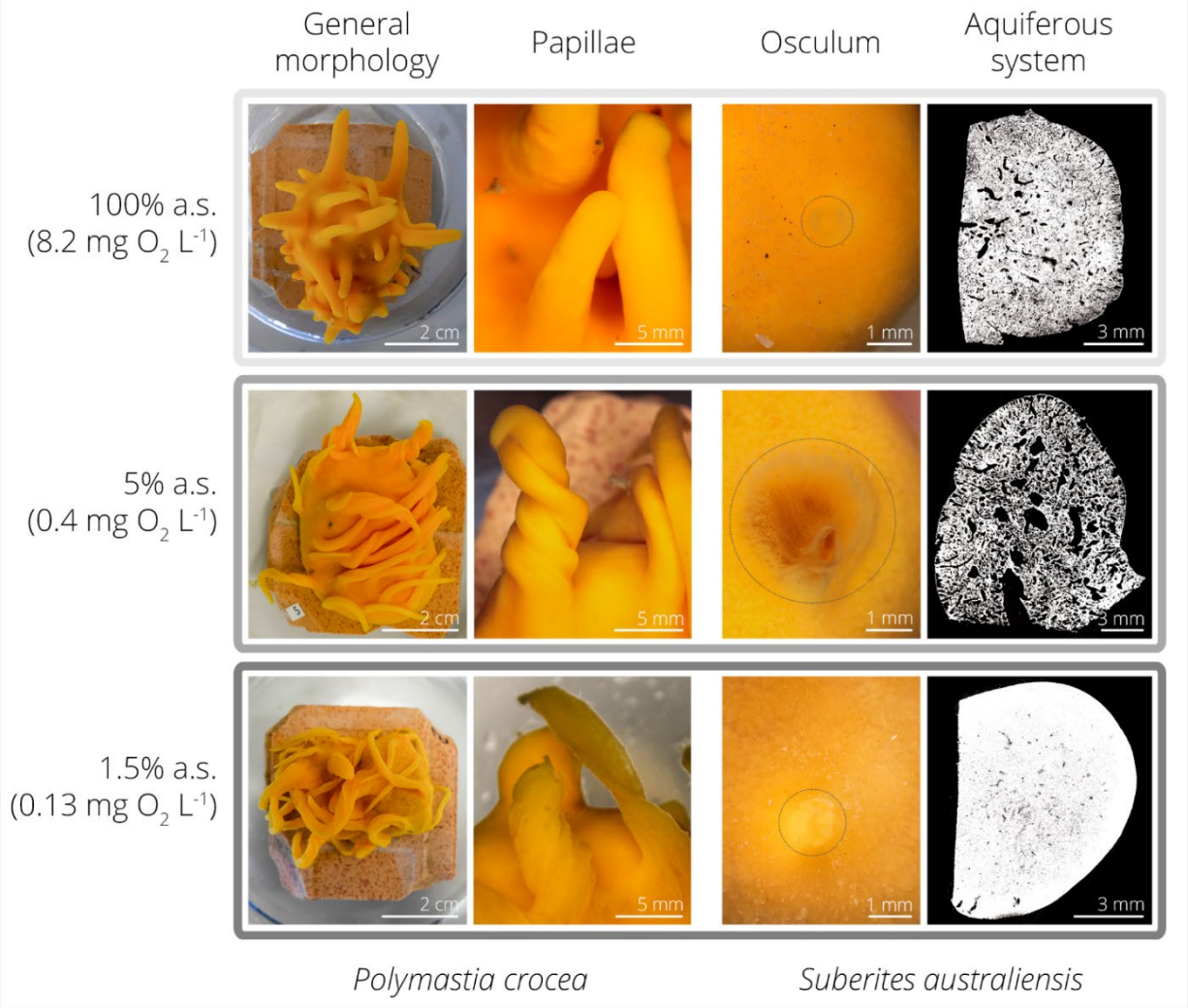

Figure 3.3. Examples of the morphological modifications reported in sponges exposed to low dissolved oxygen in the severe hypoxia treatments compared to the controls. From left to right: general external morphology, and details of papillae in *Polymastia crocea*; details of the osculum (evidenced with a dotted line), and transverse histological section (sponge tissue is in white and empty spaces representing the aquiferous system are in black) in *Suberites australiensis*. An extended version of this figure is found in Appendix B (Fig. S3.12).

3.3.2.5. Histology

Histological analyses indicated that hypoxia influences the percentage of the sponge body occupied by the aquiferous system in *Suberites australiensis*. At the end of experiment 2 (5%

a.s.), treatment sponges had a significantly higher percentage of aquiferous system (t = -9.82, p < 0.0001), compared to the controls (35.9 ± 7.1% vs 6.4 ± 1.8 %). No significant differences were found for experiment 3 (1.5% a.s.) (Fig. 3.3; S3.12j–m; S3.15).

3.3.2.6. Pumping rate

Oxygen concentration significantly affected the pumping rate of *Suberites australiensis* in both experiments 2 (5% a.s.) and 3 (1.5% a.s.) (Tab. S3.12–15). In experiment 2 (5% a.s.), there was significant interaction between treatment and time (p = 0.0001, linear mixed-effects model; Tab. S3.12). Pumping rate significantly increased from day 0 to 1 (p < 0.0001), remained stable from day 1 to 2, and then decreased from day 2 to 3 (p < 0.0001) and from day 3 to 4 (p = 0.005) (Tab. S3.12). Sponges from the 5% a.s. treatment had a significantly higher pumping rate than the control at day 1 (p = 0.007) and 2 (p = 0.002) (Tab. S3.12; Fig. 3.2e). Similar results were given by PERMANOVA (Tab. S3.13). For experiment 3 (1.5% a.s.), both the linear mixed-effects model and PERMANOVA revealed significant interaction between time and treatment (p = 0.049 and p = 0.002, respectively) on the pumping rate of *S. australiensis* (Tab. S3.14–15). However, differences were less marked compared to experiment 2 and pairwise comparisons

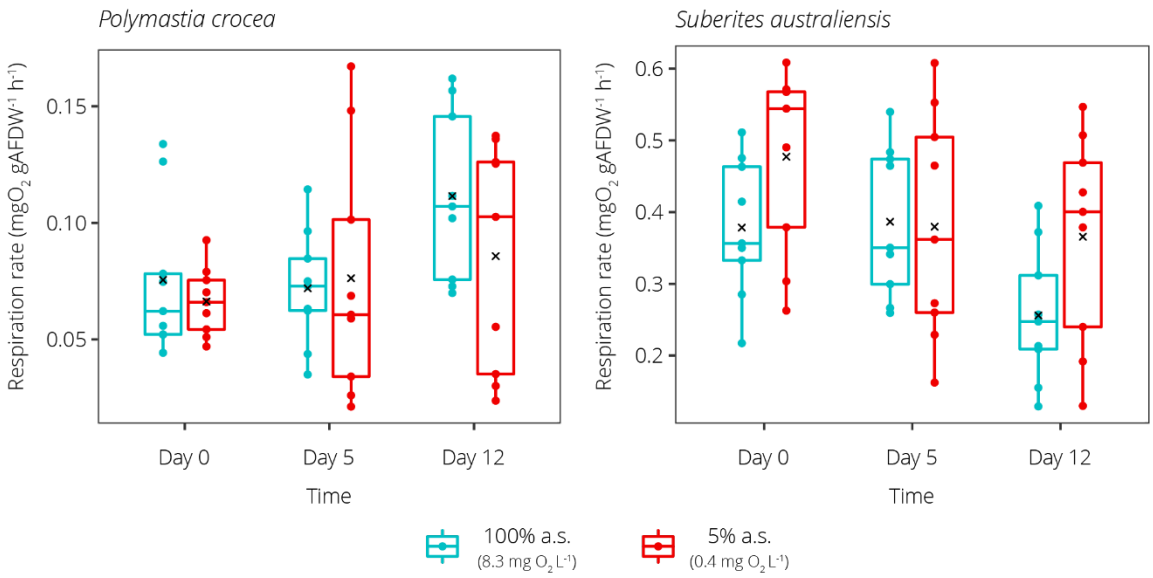

Figure 3.4. Respiration rates in *Polymastia crocea* and *Suberites australiensis* from experiment 2 (5% a.s.) measured at *T*0, *T*1/2 and *T-end*. Note: x-axis and y-axis scales differ between species. Horizontal bars inside the boxplots represent medians; the symbol × represents means. Lower and upper hinges of the boxplots correspond to the first and third quartiles, respectively. Points represent data points.

only revealed a slight decrease of pumping rate of treatment sponges between day 0 and 14 (p = 0.0002) (Tab. S3.14; Fig. 3.2f).

3.3.2.7. Respiration rate

In experiment 2 (5% a.s.), linear mixed-effects models revealed a significant effect of time on the respiration rate, for both *Polymastia crocea* and *Suberites australiensis* (Tab. S3.16–17; Fig. 3.4). In *P. crocea*, pairwise comparisons revealed a slightly higher respiration rate of the controls at day 12 compared to day 0 (p = 0.008) and day 5 (p = 0.004), but no differences between controls and treatments at any time. In *S. australiensis,* pairwise comparisons revealed a slightly lower respiration rate at day 12 compared to day 0 (p = 0.008) and day 5 (p = 0.005) in control sponges; while in treatment sponges, respiration rate was slightly lower at day 5 (p = 0.032) and 12 (p = 0.016) compared to day 0, but also in this case, there was no significant difference between treatments and controls at any time point.

3.4. Discussion

Hypoxia has become an increasingly common situation in the marine environment and will likely become wider spread in the future (Diaz and Rosenberg, 2011). Nevertheless, the direct effects of hypoxia on marine organisms are still very poorly studied (Vaquer-Sunyer and Duarte, 2008). I describe the first multi-species experiment from two oceans to test sponge tolerance, behaviour, and physiological responses to oxygen concentrations as low as 1.5% a.s. (0.13 mg O_2 L^{-1}) for up to 12 days. I found that the study sponge species were generally very tolerant to low DO irrespective of species or location. Only *Polymastia crocea* showed mortality in the lower DO treatment (0.13 mg O_2 L^{-1}, LT_{50} = 286 h). Furthermore, my results suggest that sponges can display species-specific acclimation, including physiological, morphological, and behavioural changes, in response to severe hypoxia that might help them survive periods of very low oxygen. This study also suggests that the same species can show different adaptive strategies for different degrees of hypoxia.

3.4.1. Sponge response to hypoxia

The results suggest that sub-lethal oxygen thresholds for sponges could be in the range of 6–20% a.s. (0.48–1.56 mg O_2 L^{-1}), while lethal thresholds are lower than 5% a.s. (0.4 mg O_2 L^{-1}). These pieces of evidence are consistent with Mills *et al.*, (2014) for *Halichondria panicea*, which showed a sub-lethal response starting from 17% air saturation. However, my results contrast with Mills *et al.*, (2018) studying *Tethya wilhelma*, which did not show any response down to 4% a.s. (0.27 mg O_2 L^{-1}). The very high tolerance of *T. wilhelma* could be explained by the extremely low metabolism of *Tethya* species generally (Leys and Kahn, 2018), and by their very small size (0.5–1 cm) (Sarà *et al.*, 2001). Of the two species I exposed to the lowest DO concentration (1.5% a.s., 0.13 mg O_2 L^{-1}), only *Polymastia crocea* showed mortality, while all the *Suberites australiensis* survived the 12 days of treatment conditions. This differential response could be due to the different habitats where these species are usually found. *Polymastia crocea* lives on rocky reefs, while *S. australiensis* lives on sediments in bays and semi-enclosed basins, where hypoxic events are more likely to occur (Diaz and Rosenberg, 2008; de Cook, 2010).

Some sponges can live in anoxic conditions for several months, such as the sponges of the family Raspailiidae found in the deeper cliffs of Lough Hyne (Bell and Barnes, 2000; McAllen *et al.*, 2009). Schuster *et al.*, (2021) suggested that this tolerance could be conferred by specific bacterial symbionts, which are able to carry out anaerobic metabolism. In addition, these sponges

living in anoxia are all thin crusts, with a very high surface-to-volume ratio, which could favour the release of metabolic waste (Levin *et al.*, 1991). Other examples of sponges living in very low oxygen conditions are the ones found at the edges of Oxygen Minimum Zones (OMZ) (Mosch *et al.*, 2012). These sponges can live with a consistent oxygen concentration as low as 0.13mg O_2 L^{-1} (Wishner *et al.*, 1995, Murty *et al.*, 2009). Sponges are not the only organisms able to live in OMZs. Many representatives of other phyla live in these extremely hypoxic conditions, where they benefit from the rich supply of organic matter (Levin, 2003). However, since OMZs have existed over long geological timescales, organisms have had the time to evolve specific adaptations to cope with permanent hypoxia (Levin, 2003). Therefore, these organisms cannot be used to generalize tolerance to periodic hypoxic events experienced by organisms usually living in fully oxygenated waters.

The degree of hypoxia tolerance in sponges could also be influenced by the abundance and diversity of sponge-associated microbial symbionts. Based on bacterial biomass, sponges are generally divided into "low microbial abundance" (LMA) or "high microbial abundance" (HMA) species (Hentschel *et al.*, 2003). Bacterial densities in HMA sponges are generally two to four orders of magnitude higher than in LMA sponges and can constitute up to 35% of the total sponge biomass (Vacelet, 1975; Hentschel *et al.*, 2006). Sponges with HMA tend to have a lower choanocyte chamber density, and a slower pumping rate compared LMA sponges (Lavy *et al.*, 2016), which means HMA species might have a lower ability to ventilate in low oxygen conditions. Furthermore, HMA species generally have a higher metabolic cost than LMA species, and therefore a higher oxygen requirement (Leys and Kahn, 2018). Although these differences suggest that LMA sponges might be better adapted to hypoxic conditions, HMA species have a higher diversity of microbial symbionts that could help them cope with low oxygen conditions (Hoffmann *et al.*, 2005, Lavy *et al.*, 2016). All the sponges for which responses to hypoxia has been investigated so far are LMA species (or are likely to be, based on known congenerics, see Kamke *et al.*, 2010; Mills *et al.*, 2014; Moitinho-Silva *et al.*, 2017). Therefore, future research is needed to investigate the response of HMA sponges to hypoxia and shed light on possible differences between LMA and HMA sponges and the mechanisms involved.

The ability of some organisms to tolerate hypoxia result from their physiological ability to lower metabolism and oxygen demand (McAllen *et al.*, 1999; Altieri, 2019). Instead, other species switch from aerobic to anaerobic metabolism or a combination of the two (Altieri and Diaz, 2019). My results suggest that three of the four study species (not *Suberites carnosus*) have

respiration rates at 5-6% a.s. that are comparable to sponges in normoxic conditions. This is consistent with what was found in *Geodia barretti* and *H. panicea*, suggesting that sponges have a common ability to uptake oxygen at very low concentrations in the surrounding environment (Leys and Kahn, 2018). In *Cliona celata*, hypoxic water initially resulted in a decrease in the respiration rate, which then increased back to pre-treatment levels after seven days of exposure. This suggests that the sponges gradually adjusted to hypoxic conditions. In *S. carnosus,* instead, the respiration rate remained stable after two days of exposure to low dissolved oxygen, but it more than halved after seven days. This response may allow *S. carnosus* to cope with long periods of hypoxia, in which sponges decrease their metabolism, as has been reported for other organisms (Hagerman, 1998; Mentel *et al.*, 2014). Although this study shows that sponges can perform aerobic metabolism when exposed to extremely low oxygen concentrations, the presence of anaerobic metabolism cannot be excluded and needs further investigation.

Sponge species exposed to the lowest DO concentrations (0.4 and 0.13 mg O_2 L^{-1}) also showed other phenotypic modifications that could represent adaptive strategies to cope with hypoxia. In *Suberites australiensis*, hypoxic water (0.4 mg O_2 L^{-1}) induced expansion of the sponge body and the aquiferous system that lasted for the duration of the experiment. This expansion was likely semi-permanent as it persisted after inducing the contraction and corresponded to a reorganization of the sponge aquiferous system at the histological level. These behavioural and morphological changes are likely beneficial for the sponge, as higher internal water flow corresponds to an increase in oxygen that can be taken up. The body expansion was accompanied by a marked increase in the pumping rate that then dropped after two days. The pumping rate increase could be a strategy to increase ventilation and oxygen availability, similarly to other animals when exposed to hypoxic waters (Hagerman, 1998). However, the successive decrease in pumping rate (after two days) and the gradual production of a membrane to close the oscula remains unclear but could represent a trade-off between increasing ventilation and keeping the energetic coast of pumping reasonable. In *S. australiensis*, body expansion is correlated with an increase in osculum area, and osculum area is the main determinant of pumping rate in this and many other species (Morganti *et al.*, 2021; Goldstein *et al.*, 2019). Perhaps the increase in pumping rate only represents a physiological consequence of the body expansion and is then quickly brought back to normal, decreasing the osculum size by producing an oscular membrane. These physiological and morphological changes of *S. australiensis* described above was not present on sponges exposed to more severe hypoxia (0.13 mg O_2 L^{-1}). This could mean that the same sponge species may display different adaptive strategies to cope with decreased oxygen depending on the oxygen concentration. At 0.4 mg L^{-1}, oxygen might

still be sufficient to support regular metabolism, but sponges may need to increase the amount of water flowing through their bodies to absorb the oxygen needed. However, 0.13 mg L^{-1} might be too low a DO concentration, and sponges might decrease their metabolism to cope with lack of oxygen, similarly to other metazoans (Hagerman 1998, Mentel *et al.*, 2014).

Polymastia crocea also showed a behavioural change in response to hypoxic conditions: hypoxic water at 0.4 mg L^{-1} induced the progressive expansion of sponge papillae (where inhalant and exhalant channels are found), that was significantly greater than in the control sponges. It is unlikely that the papillae expansion represents an increase in sponge filtering activity because the respiration rate was very similar in the treatments and the controls. Therefore, sponges might expand their papillae to increase the volume occupied by the aquiferous systems, as in the case of *Suberites australiensis*, but also to access more oxygenated water further from the bottom. A similar response occurred in sponges exposed to 0.13 mg L^{-1} but with much more variability across specimens, and the statistical test did not detect any change. Interestingly, sponges that survived after the 12-day treatment had a significantly higher ratio of expanded papillae than sponges that died, suggesting that expansion might help cope with severe hypoxic conditions.

Along with behavioural changes, *Polymastia* underwent morphological modifications that could help to tolerate low DO. Papillae become thinner and flattened, and some even spiralized. These modifications of the papillae could increase the surface-to-volume ratio and help oxygen diffusion (Levin *et al.*, 1991). The elongation of papillae, which accompanies the thinning, could be an evolutionary relic of a process that moved the inhalant pores of the papillae as far as possible from the surface. However, in the lowest DO treatment, papillae often lost their vertical orientation and laid horizontally on the sponge surface. I hypothesized that the new orientation of papillae was a consequence of their thinning process: probably papillae became so thin that they could not support their weight anymore. Interestingly, sponges that developed modified papillae showed less mortality than sponges that did not, although the evidence is not strong enough to claim this with confidence ($p = 0.057$). These structures may not only represent a stress response, but could provide an advantage to the sponge. Further research is needed on this topic needed to elucidate the function of these structures.

Despite the remarkable tolerance of sponges to hypoxia observed in laboratory conditions, field observations suggest that severe hypoxic/anoxic events can catastrophically affect sponge populations. Mass mortalities of sponges following hypoxic/anoxic events have been reported both in temperate and tropical ecosystems (Stachowitsch, 1984, Altieri *et al.*, 2017; Chu *et al.*,

2018; Johnson *et al.*, 2018; Kealoha *et al.*, 2020). For example, in a hypoxic/anoxic event in the Gulf of Trieste, all the sponges living in several hundred km^2 area died within 2-3 days (Stachowitsch, 1984). Some anemones survived up to a week, but virtually all macroscopic organisms were dead within two weeks from the onset. Altieri *et al.*, (2017) also reported widespread mortality of sponges and corals following a hypoxic event (~0.5 mg O_2 L^{-1}) that occurred in Bocas del Toro, Panama. Since this study focused on corals, it is unclear what proportion of the sponges were affected and if some species were more tolerant than others. These reports highlight that hypoxic events, in their most severe form, leave no survivors among macrofauna.

Furthermore, it is possible that in natural conditions, other factors combine with low dissolved oxygen. For example, a recent meta-analysis showed that in marine organisms, increased temperature reduces survival times under hypoxia by 74% on average and increased median lethal concentration by 16% on average (Vaquer-Sunyer and Duarte, 2011). Another meta-analysis showed that hydrogen sulphide (H_2S) also reduces survival time of marine organisms under hypoxia by an average of 30% (Vaquer-Sunyer and Duarte, 2010). Acidification was shown to have additive or synergistic negative effects combined with hypoxia (Gobler and Baumann, 2016; Steckbauer *et al.*, 2020). Since all these factors usually co-occur during hypoxic events, *in situ* sponge thresholds to hypoxia are likely to be lower than determined through single stressor laboratory experiments (Diaz and Rosenberg, 1995; Steckbauer *et al.*, 2020). Future experiments that evaluate the combined effect of these factors will be crucial to understand the full response of sponges to hypoxia in natural ecosystems.

Diel oxygen variation is another factor that could influence organism tolerance to hypoxia in natural conditions. In the photic zone of marine ecosystems, dissolved oxygen generally increases during the day because of photosynthesis and decreases at night because of aerobic respiration (Kroeker *et al.*, 2019). The amplitude of these diel fluctuations can sometimes lead to hypoxia or complete anoxia at night and supersaturation in peak sunny hours, or both (Diaz and Breitburg, 2009). Extreme oxygen dynamics have been reported from a wide variety of macro- and micro-habitats from both tropical and temperate ecosystems, such as intertidal reef platforms, tide pools, semi-enclosed basins, tropical lagoons, and the boundary layer around macroalgal canopies (Morris and Taylor, 1983, Frieder *et al.*, 2012, Cornwall *et al.*, 2013, Gruber *et al.*, 2017, Trowbridge *et al.*, 2017a, Hughes *et al.*, 2020). Diurnal fluctuations in oxygen can produce different responses from static exposure in laboratory experiments, which may either overestimate or underestimate the emergent effects of hypoxia in natural environments (Bumett

and Stickle, 2001). Therefore, future experiments will need to account for current and future temporal variability in oxygen concentration to accurately predict the emergent ecological effects of deoxygenation (Kroeker *et al.*, 2019).

3.4.2. Hypoxia Tolerance of sponges compared to other sessile organisms

Marine organisms have very variable tolerance to low dissolved oxygen, with lethal thresholds ranging from 8.6 mg O_2 L^{-1} for the first larval zoea stage of the crustacean *Cancer irroratus*, to resistance to complete anoxia as in the case of the sea anemone *Metridium senile* and the oyster *Crassostrea virginica* (Wahl 1984; Vaquer-Sunyer and Duarte, 2008). Sessile organisms are generally more tolerant than mobile ones, which is likely due to them not being able to escape hypoxic conditions (Altieri and Diaz, 2019). Therefore, sessile organisms that experience these conditions must have evolved other adaptive strategies to cope with reduced oxygen (Diaz and Rosenberg, 1995).

Here I provide new evidence to support the hypothesis that sponges are a group of sessile organisms that are tolerant to hypoxia and could be favoured in future deoxygenated oceans. Other phyla, such as cnidarians and molluscs, include very tolerant species that can cope with prolonged periods of anoxia (Fig. 3.5). This is not surprising since tolerance to severe hypoxia/anoxia is a widespread feature amongst animals, and many organisms independently evolved this feature to cope with local conditions (Hochachka and Lutz, 2001; Nilsson and Renshaw, 2004; Vaquer-Sunyer and Duarte, 2008). This ability is not restricted to invertebrates and includes higher vertebrates such as fish and reptiles (Milton and Prentice, 2007; Vornanen *et al.*, 2009).

What makes sponges unique as a phylum is their likely widespread tolerance to hypoxia. All the species investigated so far have been shown to cope with very low levels of dissolved oxygen. In contrast, other animal phyla have a much wider range of tolerances, with some species resistant to anoxia and others very sensitive to decreased oxygen (Fig. 3.5). For example, in sessile cnidarians, lethal hypoxia thresholds range between 0 and 4 mg O_2 L^{-1}, while sublethal ones are between 0.71 and 4.56 mg O_2 L^{-1} (Mangum, 1980; Dodds *et al.*, 2007). In sessile bivalves, lethal thresholds range between 0 and 2 mg O_2 L^{-1}, with the sub-lethal threshold being 3.1 mg O_2 L^{-1} for *Mytilus galloprovincialis* (de Zwaan *et al.*, 1991; Woo *et al.*, 2013). Sponges, instead, show much less variation with known lethal thresholds that are lower than 0.5 mg O_2 L^{-1}, and sublethal thresholds that range between 0.27 and 1.56 mg O_2 L^{-1} (Mills *et al.*, 2014; 2018) (Fig. 3.5). It is worth noting that lethal thresholds are highly dependent on the time of exposure.

In the studies I considered, these ranged from a few days to weeks. However, there were no noticeable differences in the experimental duration and the median lethal time for the different organisms. Therefore, I believe that differences in time of exposure do not represent a bias in my comparison. In contrast, sublethal responses (e.g., changes in respiration rate, behaviour, and feeding activity) usually have rapid time-to-onset, so they will likely be independent of exposure time. The high tolerance of sponges to hypoxia compared to other organisms can be explained by the evolutionary history of this group. Sponges are one of the most ancient groups of metazoans. They likely evolved before the Marinoan glaciation (657-645 million years ago), when oxygen was perhaps less than 10% of present atmospheric concentration (Love *et al.*, 2009; Maloof *et al.*, 2010; Brocks *et al.*, 2017; Whelan *et al.*, 2017; Cole *et al.*, 2020; Turner, 2021). Modern sponges might have retained an ancestral condition concerning oxygen requirements (Mills *et al.*, 2014; 2018). Therefore, it is possible that sponges unable to survive severe hypoxia today (e.g., *P. crocea*) have lost certain key ancestral adaptations to hypoxia, rather than hypoxia-tolerant lineages (e.g., *S. australiensis*) having evolved relatively new capacities for hypoxia tolerance (Müller *et al.*, 2012). Likewise, other animals which might have evolved in similar conditions, such as ctenophores, also show great resistance to hypoxia (Thuesen *et al.*, 2005). Therefore, I speculate that early aspects of sponges' long evolutionary history could give these organisms an adaptive advantage in future deoxygenated oceans, since they may have experienced similar conditions in long past geological eras.

3.5. Conclusions

Overall, sponges show high tolerance to low dissolved oxygen compared to all the other phyla of sessile marine organisms that have been studied. Species-specific phenotypic plasticity appears to help these organisms to overcome hypoxic events, and future research will need to elucidate the mechanisms behind these changes. This exceptional adaptive capacity of sponges could derive from their ancient evolutionary origin and could confer sponges a competitive advantage in future deoxygenated oceans over other organisms (Mills *et al.*, 2014; Schuster *et al.*, 2021).

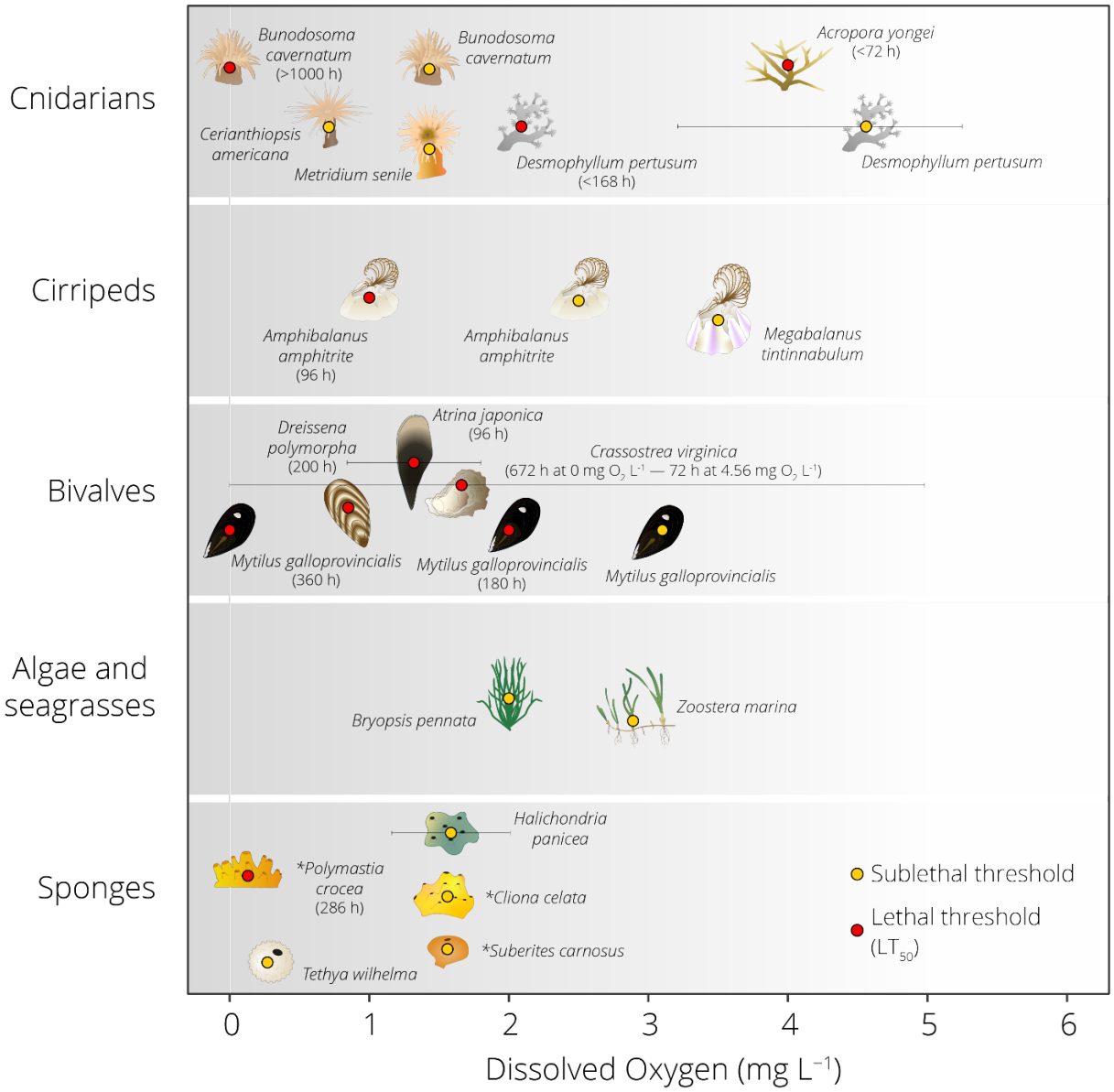

Figure 3.5. The tolerance of marine sessile organisms to hypoxia. Red dots indicate lethal thresholds, while yellow dots indicate sub-lethal thresholds. Organisms for which threshold values were found in the present study are labelled with an asterisk. For studies that report multiple values for the same species according to other abiotic conditions (i.e., temperature and salinity), I report a range where the dots represent the mean value, and the edges of the whiskers represent minimum and maximum values. For lethal thresholds, I report in bracket the median Lethal time (LT_{50}, hours) at that specific oxygen concentration (or at the extremes of the range). The symbol < was used when LT_{50} was not reported, but more than 50% of the organisms died after a certain amount of time; while > was used when LT_{50} was not reached by the end of the experiment. For *H. panicea*, Mills *et al.*, (2014) only report oxygen measurement as per cent air saturation without reporting temperature and salinity, so the actual oxygen concentration is unknown. We, therefore, estimated the oxygen content using the range of temperatures and

salinity found where these sponges were sampled (Salinity 8.9–29.5; Temperature: 5–25 °C; Thomassen and Riisgård, 1995) and I provide the mean and the range of possible values. List of references associated with each species: *A. yongei* (Haas *et al.*, 2014), *A. amphitrite* (Rao and Ganapati, 1968; Desai and Prakash, 2009), *A. japonica* (Nagasoe *et al.*, 2020), *B. pennata* (Haas *et al.*, 2014), *B. cavernatum* (Mangum, 1980; Ellington, 1982), *C. americana* (Vaquer-Sunyer and Duarte, 2008), *C. virginica* (Stickle *et al.*, 1989), *D. pertusum* (Dodds *et al.*, 2007; Lunden *et al.*, 2014), *D. polymorpha* (Johnson and McMahon, 1998), *H. panicea* (Mills *et al.*, 2014), *M. tintinnabulum* (Rao and Ganapati 1968), *M. senile* (Sassaman and Mangum 1972), *M. galloprovincialis* (De Zwaan *et al.*, 1991; Woo *et al.*, 2013), *T. wilhelma* (Mills *et al.*, 2018), *Z. marina* (Hughes *et al.*, 2020). Figure inspired by Hughes *et al.*, (2020).

4. Chapter 4 - Resilience to disturbance and interannual dynamics of a rocky temperate mesophotic ecosystem.

The new sponge recruits

Abstract

The mesophotic zone ("middle light") of temperate seas hosts rich and diverse habitats dominated by long-lived, slow-growing animals (e.g., sponges, cnidarians, bryozoans) and shade-adapted algae. Research and interest in mesophotic ecosystems have increased exponentially over the last decade, but we still know very little about the processes and dynamics of these ecosystems. This study aimed to investigate the resilience and temporal dynamics of shallow-water (~ 17 m) mesophotic communities at Lough Hyne (Ireland) following a severe sponge mass mortality that occurred between 2010 and 2015. I analysed the percentage cover of sessile organisms from two time series: 1994–1995 (pre-impact) and 2018–2021 (post-impact), at five sites experiencing a gradient of environmental conditions. Historical data were used to assess whether differences in temporal patterns between sites were exclusive to impacted communities or also occurred in the past. I found weak signs of recovery for some of the three-dimensional sponges and anemones that were highly affected by the disturbance, represented by a small increase in percentage cover. However, multivariate analyses did not detect any community or assemblage changes over time at the impacted sites following the disturbance event, suggesting an overall low resilience to disturbance. In general, temporal dynamics (turnover, diversity and percentage cover of benthic groups) were found to be different between: 1) sites experiencing very distinct environmental conditions; and 2) sites that shared similar conditions and communities. These findings suggest that small-scale variation in environmental conditions can affect the dynamics and recovery of mesophotic subtidal ecosystems. I propose that higher water flow rates facilitate the growth of sponges by decreasing the metabolic cost associated with water filtering and providing food. Given the limited recovery capacity (i.e., engineering resilience) of mesophotic ecosystems, their conservation needs to be prioritised. Furthermore, future management of mesophotic habitats will need to take into account abiotic factors (e.g., water flow) as these can radically affect the resilience of these fragile ecosystems.

4.1. Introduction

Temperate mesophotic ecosystems (TMEs) occur at the limit of light availability for photosynthesis, between the well-illuminated shallow waters and the dark deep sea (Cerrano *et al.*, 2019; Turner *et al.*, 2019). These ecosystems host exceptionally rich and diverse benthic communities, mainly dominated by sponges, cnidarians, bryozoans, and shade-adapted algae (Ballesteros, 2006; Bell *et al.*, *in review*). In deeper waters, environmental constraints (e.g., light, food, temperature, disturbance) favour the dominance of organisms with slower growth and longer lifespans, and organisms tend to form stable three-dimensional structures (Montero-Serra *et al.*, 2018; Rossi *et al.*, 2017). These biogenic habitats offer refuge and nursery grounds for a wide variety of organisms, enhancing the diversity and complexity of the system (Bruno and Bertness, 2001; Cerrano *et al.*, 2010; Verdura *et al.*, 2019). Therefore, mesophotic ecosystems provide important ecosystem services such as supporting fisheries (recreational and commercial), biodiscovery (e.g., pharmaceutical and genetic resources), and the diving industry (Goñi *et al.*, 2006; Chimienti *et al.*, 2017; Paoli *et al.*, 2017; Ingrosso *et al.*, 2018 Ferrigno *et al.*, 2018; Enrichetti *et al.*, 2019a; de Ville d'Avray *et al.*, 2019)

In recent decades, research effort in mesophotic ecosystems has increased considerably, mostly due to technological developments, particularly Remotely Operated Vehicles (ROVs), that have facilitated their exploration. Along with scientific data, legislative efforts by governments to protect TMEs have increased substantially: for example in Europe, important mesophotic habitats (e.g., coralligenous reefs, coral gardens and deep-sea sponge aggregations) have been formally given special protection under the EU Marine Strategy Framework Directive 2008/56/EC (OSPAR, 2008; UNEP-MAP-RAC/SPA, 2008). Despite recent research having provided a fair amount of information about TME structure (at least in some geographic areas), we still know very little about TME ecological processes such as community dynamics, tolerance to stressors, and resilience to impacts (Bell *et al.*, *in review*).

Among the most common habitat found in mesophotic zones, are the so-called sponge grounds or “sponge gardens” (Bo *et al.*, 2012; Idan *et al.*, 2018; Santín *et al.*, 2018; Soares *et al.*, 2019; Enrichetti *et al.*, 2020; Harris *et al.*, 2021). These habitats are dominated by upright sponge forms (e.g., arborescent, massive), which thrive at mesophotic depths, sheltered from the high energy of swell and storms (Bell and Barnes, 2000d; Maldonado *et al.*, 2017). Sponge aggregations play important roles in ecosystem function, such as providing habitat, affecting water flow, circulation, and nutrient cycling, and transferring matter and energy between the

water column and the benthos (Bell, 2008; Maldonado *et al.*, 2012). Despite their ecological relevance and likely extreme vulnerability due to the longevity of many sponge species, these systems remain largely understudied (Maldonado *et al.*, 2017). For example, we know virtually nothing about the dynamics and resilience of sponge grounds and other mesophotic habitats to disturbance.

Resilience is a key concept in ecology and conservation biology to understand and predict ecosystem responses to human and natural disturbance (Capdevila *et al.*, 2021). Resilience describes the capacity of an ecosystem to maintain its structure and function in response to an exogenous disturbance (Holling, 1973; Hodgson *et al.*, 2015). It is determined by the capacity to reduce the impact of a disturbance (ecological resilience or resistance) and the ability to recover from the impact of disturbance (engineering resilience or recovery capacity) (Holling, 1973; 1996; Pimm, 1984; Ingrisch and Bahn, 2018). The resilience of benthic communities to disturbance has been investigated in a wide range of marine habitats, from coral reefs to seagrass meadows and soft sediments (Sherman and Coull, 1980; Halford *et al.*, 2004; Unsworth *et al.*, 2015). However, these types of studies usually require *in situ* manipulation and repeated sampling over time, which can be difficult to perform in deep waters (Turner *et al.*, 2019). Furthermore, estimating patterns and recovery trajectories requires baseline data, which are extremely rare due to the challenges of studying deep- and cold-water habitats (Bianchi *et al.*, 2017). As a result, the knowledge about resilience in mesophotic animal-dominated communities mainly comes from studies on population dynamics and growth rates made of single structuring species, such as corals and sponges (Marschal *et al.*, 2004; Teixidó *et al.*, 2011; Rossi, 2013; Bramanti *et al.*, 2014; Hitt *et al.*, 2020). These previous studies found low dynamics, high longevity and persistence of most structuring species, suggesting a low resilience to disturbance (Teixidó *et al.*, 2011).

Lough Hyne Marine Nature Reserve is a fully marine semi-enclosed lough located in southwest Ireland (Lawson *et al.*, 2004). Lough Hyne has long been considered a natural laboratory because of its high biodiversity and predictable environmental gradients such as flow and sedimentation regimes (Kitching, 1987; Bell, 2007; Davenport *et al.*, 2021). Due to the particular environmental conditions, Lough Hyne hosts rich and abundant mesophotic communities in relatively shallow waters (Picton, 1990; Bell and Barnes, 2000a, b). Specifically, the high sedimentation and the low light penetration do not allow photophilic algae to grow deeper than 6–12 m. Furthermore, the sheltered conditions and the complete absence of oceanic swell allow the growth of delicate organisms more adapted to deeper, less turbulent waters.

Lough Hyne mesophotic communities are dominated by sponges (Picton, 1990; Bell, 2007). The same species and genera found at Lough Hyne can be found at greater depths in other mesophotic ecosystems in the North Atlantic and worldwide (Pansini and Sará, 1999; Cook, 2010; Goodwin and Picton, 2011; Enrichetti *et al.*, 2020; author's unpublished data). Unfortunately, major community changes have occurred at Lough Hyne in recent years, from the intertidal to the deeper areas (Chapter 2; Trowbridge *et al.*, 2013; Little *et al.*, 2018; McAllen *et al.*, 2021; Chapter 2). All the three-dimensional sponges have markedly declined, and even disappeared in some areas (Chapter 2). The cause of this sponge decrease is still unresolved, but it was likely the result of one or more disturbance events that occurred in pulses between 2010 and 2015 (Chapter 2).

This decline in the shallow water mesophotic communities at Lough Hyne provides an opportunity to gain insight into the dynamics, resilience, and recovery of temperate mesophotic communities. I analysed percentage cover of sessile organisms from two time series taken before (1994–1995) and after (2018–2021) the disturbance events at five sites inside the lough. I then investigated the dynamics and evaluated recovery of the benthic communities comparing past and present data. Finally, I discuss the possible influence of environmental factors on the dynamics observed and the potential implications for the conservation of temperate mesophotic ecosystems.

4.2 Materials and Methods

4.2.1. Area of Study

A detailed description of the study area is reported in Chapter 1, section 1.10. In recent years, Lough Hyne subtidal communities have undergone marked changes in response to a not-yet identified stressor(s) (Chapter 2, Micaroni *et al.*, 2021). The possible factors involved in these community changes include eutrophication, increased temperature, and the occurrence of a toxic event or a combination of these factors. It is worth noting that total nitrogen inside the lough increased from a maximum monthly concentration of 210 mg m^{-3} in the 1990s (Johnson *et al.*, 1995) to 720 mg m^{-3} in the late 2000s (Jessopp *et al.*, 2011).

Among the major changes reported, there was a general decrease in sponge cover with a marked decline in most three-dimensional forms at the internal sites of the lough, which virtually disappeared from the most internal sites. This decline was likely the result of one or more mass mortality events that occurred between 2010 and 2015 (Chapter 2). There was also a significant increase in ascidians, turf forming organisms and a decrease in macroalgae.

4.2.2. Study sites

This study focused on the rocky cliffs at five sites within Lough Hyne (Fig. 4. 1). Sites can be considered in three groups according to their biological communities: lough's entrance (Whirlpool Cliff), internal sites (Glannafeen, Labhra Cliff and Goleen), and innermost site (West Cliff).

The site at the entrance of the lough (Whirlpool Cliff) is subjected to strong flow conditions (up to 250 cm s^{-1} during inflow), and sediment accumulation on rocky surfaces is negligible (3 ± 0.2 mm) (Bell and Barnes, 2002; Fig. 4. 1). The deeper areas of Whirlpool Cliff are dominated by cnidarians (mostly jewel anemones and soft corals) and sponges.

The four internal sites (Glannafeen, Labhra Cliff, Goleen) share similar environmental conditions, which is reflected in the similar biological communities found at these sites (Picton, 1990; Bell and Barnes, 2000a, b, d). These sites experience low current flow (max 5–20 cm s^{-1} at 18 m) during the incoming tide, but little or no flow during the rest of the time (Bell and Barnes, 2002). At Glannafeen, the incoming current lasts slightly longer than at either Labhra Cliff or Goleen (Bell and Barnes, 2002). Sedimentation rates are high (18–25 g m^{-1} day^{-1}), and considerable sediment accumulation can be found on cliff surfaces (7–11 mm) (Bell and Turner,

2000; see Figure 4.1 for more details). Cliffs are dominated by sponges and turf forming organisms (Chapter 2). Of these sites, Glannafeen was the least impacted during the 2010–2015 changes, while Goleen was the most affected. All the arborescent and papillate sponges, which once dominated the cliffs, had disappeared at the latter site.

The innermost site (West Cliff) is subjected to similar conditions to the internal sites, with a slightly higher sedimentation rate (27–34 g m^{-1} day^{-1}), and weaker currents (~ 15 cm s^{-1}, during incoming spring tide, but only for ~ 15 min) (Bell and Barnes, 2002). Before the 2010-2015 change, this site hosted similar communities and sponge assemblages to the internal sites. For example, the sponge morphological assemblage at West Cliff was > 85% similar to Goleen, Labhra Cliff and Glannafeen, but < 45% similar to Whirlpool Cliff (Bell and Barnes, 2000d). However, West Cliff is the site whose community has changed the most across all the sites in

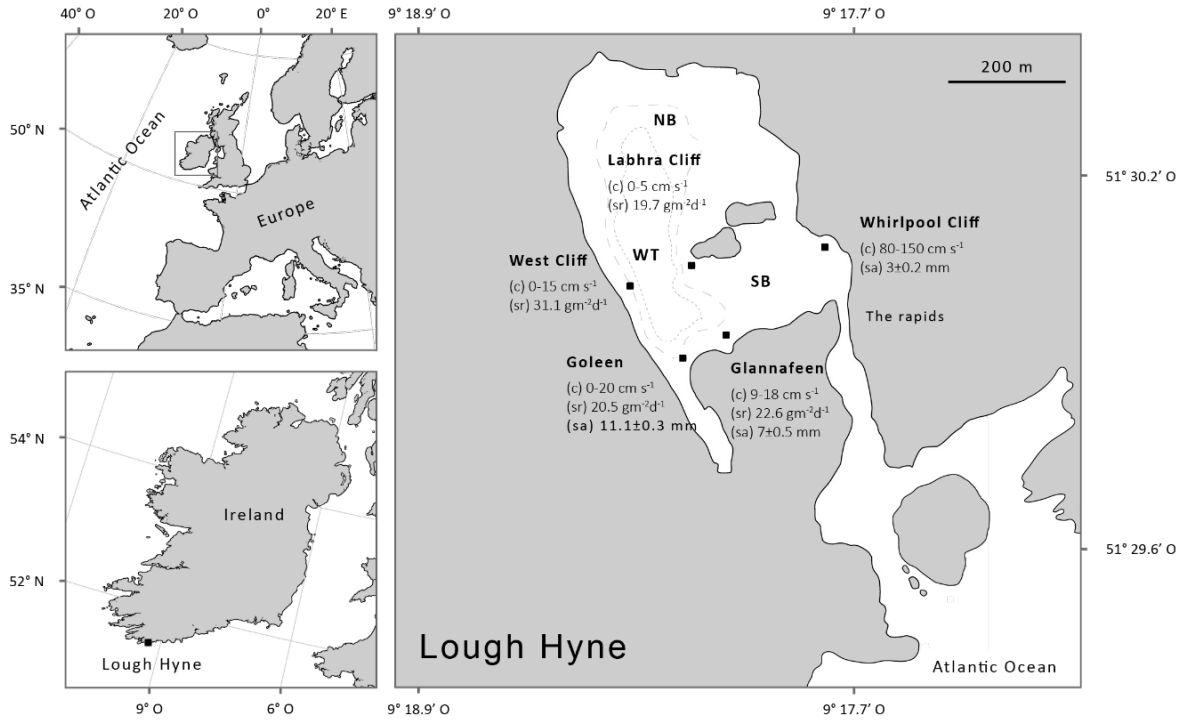

Figure 4.1. Lough Hyne map showing its position in the North-East Atlantic (top left corner) and Ireland (bottom left corner). NB, North Basin; SB, South Basin; WT, Western Trough. For each site, current speed range between neap and spring tide at 18 m (c, from Bell and Barnes, 2002), mean sedimentation rate at 18 m (sr, from Bell and Barnes, 2000d) and accumulated sediment on surfaces (sa, from Bell and Turner, 2000) are shown. Inside Lough Hyne, the 25 and 35 m bathymetric contours around the Western Trough are indicated by the short-dashed and dotted line, respectively (from Sullivan *et al.*, 2013).

Lough Hyne. It now hosts different communities compared to the internal sites with fewer sponges and more ephemeral organisms, such as ascidians and hydroids (Micaroni *et al.*, 2021).

4.2.3. Sampling design

In order to investigate recovery and dynamics of benthic sessile communities on the subtidal cliffs at Lough Hyne, in 2018, I established five permanent replicate quadrats (0.25 m^2) at each of the five sites described above (17–18 m). Photos of 0.065 m^2 sub-quadrats were taken to provide a higher resolution of the benthic organisms (i.e., four images per quadrat). Photographs were taken twice a year (only once in 2020) at 5–7 time points between June 2018 and June 2021 (36 months, see Table S4.1 for a scheme of study design). Photos from 2018 to 2019 were taken using a Sony RX100 Mk1 (20.2 MP), while photos from 2020 to 2021 were taken using a SeaLife Micro 2.0 (16 MP). Both cameras were equipped with 6000–12000 lumens video lights.

In addition to these newly collected photoquadrats, I analysed historical photographs of permanent quadrats established at two internal sites (Glannafeen and Labhra Cliff) in 1994 at 16–17 m of depth. Photos (0.065 m^2) of five replicate quadrats (0.25 m^2) were collected at 4 data points (April 1994 – August 1995, 16 months). Photos were taken with a Nikon F3 (35 mm) with underwater strobes.

4.2.4. Image analysis

For each quadrat, three out of four randomly chosen sub-quadrats were analysed (corresponding to an area of 0.1875 m^2). All the photoquadrats were analysed using the area/length analysis tool in Coral Point Count with Excel extensions (CPCe; Kohler and Gill, 2006) and ImageJ (US National Institutes of Health, Bethesda, Md, USA). Every organism was manually outlined using a freehand drawing tool to measure the planar area occupied in the photo. Organisms were identified to the lowest possible taxonomic level with the help of additional close-up pictures and voucher specimens. Due to indistinguishable external morphology, some species were combined into OTUs that included multiple species. OTUs are generally effective for identifying patterns of distribution of benthic invertebrates (Brind'Amour *et al.*, 2014), and marine sponges more specifically (Strano *et al.*, 2020). Bare substrate was also quantified from the photographs. The category 'Undetermined' was used for the substrate that was visible in the photographs, but that was impossible to identify, such as shadows, overexposed areas or unidentified organisms. This category only represented ~0.5% of the substrate on average.

Taxa/OTUs were collapsed into the following benthic categories to facilitate univariate analyses: algae, animal turf (i.e., turf-forming hydroids and bryozoans), anthozoans, ascidians, barnacles, lophophorates (including bryozoans and phoronids), polychaetes, and sponges. Separately, sponges were collapsed into the following morphological categories: encrusting Raspailiidae, encrusting non-Raspailiidae, erect, globular, massive, papillate, pedunculate, repent, and "other". I distinguished encrusting Raspailiidae from other encrusting sponges because these showed very different dynamics (the former are slow growing, while the latter are usually fast growing).

4.2.5. Statistical analysis

All the statistical data analyses were performed in R version 3.1.3 (R Core Team, 2013). All the multiple comparisons were corrected using the Benjamini-Hochberg Procedure (Benjamini and Hochberg, 1995). In the text, *p*-values are reported uncorrected, while in Appendix C, *p*-values are reported both corrected and uncorrected. Statistical significance was set to $p < 0.05$ for all analyses. All the results of all the statistical tests are reported in Appendix C.

Because some time points and replicates were missing for some sites (due to Covid-19 related disruptions), I could not perform analyses using all the sites, time points and replicates. To overcome the problem, I subsetted the main dataset into four balanced datasets, each analysed independently (see also Table S4.2 for a scheme of the subsets):

Comparison across all sites. This dataset included four time points (June 2018 – November 2019, 17 months), collected at all five sites. I used this dataset to compare present (2018–2019) temporal dynamics between all sites.

2.5-year comparison. This dataset included six time points (June 2018 – March 2021, 32 months), collected at all sites except West Cliff. This dataset was used to validate patterns observed from the analysis of the first two datasets, but over a longer period of time.

3-year full comparison. This dataset included seven time points (June 2018 – June 2021, 36 months) collected at two internal sites (Goleen and Labhra Cliff). This dataset was used to further validate patterns observed from the analysis of the first two datasets over a longer period of time.

Present-past comparison. This dataset included four time points from the pre-disturbance (April 1994 – August 1995, 16 months) and post-disturbance (June 2018 – November 2019, 17 months) time series collected at two internal sites (Glannafeen and Labhra Cliff). This dataset was used to compare present (2018-2021) and past (1994-1995) community dynamics.

4.2.5.1 Multivariate analyses and metrics

Changes in community and assemblage structure across sites, historical periods, and over time were examined with unconstrained ordination methods (R package *vegan*, Oksanen *et al.*, 2007). Only living organisms were included in the multivariate analysis, while bare space and "undetermined" substrate were excluded. At the entrance site (Whirlpool Cliff), ascidians were only found in one-third of the photoquadrats (< 0.1% cover on average), so I excluded this site from the multivariate analyses of the ascidian assemblages.

Community and assemblage structure was visualised with non-metric Multidimensional Scaling (nMDS) in two dimensions, based on a Bray-Curtis similarity matrix. The amount of variation explained by time and space and historical periods was then quantified with permutational multivariate analysis of variance (PERMANOVA, Anderson, 2001) based on Bray-Curtis dissimilarities. For these analyses, the percentage cover of the different taxa was log (x + 1) transformed to reduce the influence of the most abundant and rare groups.

After the PERMANOVA, I checked the nature of temporal changes with the function *rate_change_interval* implemented in the R package *codyn* (Hallett *et al.*, 2016). This statistical tool can be used to assess rates and patterns of variability in communities (Collins *et al.*, 2000). Changes in community composition are described by Euclidean distances calculated on pairwise communities across the entire time series. These distance values are then regressed against the time lag interval. The slope of this relationship indicates the rate and direction of the changes (Hallett *et al.*, 2016). Trends were tested using linear mixed-effects models (*lmer*, R package *lme4*; Bates *et al.*, 2015) using quadrat as a random factor and site, historical period, and time lag as fixed factors. Fixed-effect terms were tested using *anova* (R package *lmerTest*, Kuznetsova *et al.*, 2017). *Post hoc* comparisons were computed on estimated marginal means using the functions *emtrends* and *emmeans* included in the R package *emmeans* (Lenth, 2021).

The degree of temporal variation in community and assemblage composition at each site and period was assessed by calculating the turnover rate of the community, which is a measure of the rate of change in taxonomic composition over time (Diamond, 1969, Buckley *et al.*, 2019). Temporal turnover was calculated using the function *turnover* implemented in the R package *codyn* as follow: total turnover = species gained + species lost / total species observed in both time points. Turnover was averaged over all the time points. Differences in turnover between sites, historical periods and biological communities were evaluated using Kruskal-Wallis rank

sum tests with Dunn *post hoc* tests or two-way non-parametric ANOVAs (*raov*, R package *Rfit*; Kloke and McKean, 2012) with Wilcoxon signed-rank tests as *post hoc* comparisons.

Changes in taxon richness, diversity, and evenness over time for each site and period were assessed using linear mixed-effects models. Species richness indicates the number of taxa found in each sample. Species diversity was expressed as the Shannon diversity index (H), and evenness with the Simpson's diversity index (Williams, 1964). The Shannon–Wiener index is strongly influenced by species richness and rare species, while the Simpson index gives more weight to evenness and common species (DeJong, 1975).

4.2.5.2 Univariate analysis on single benthic groups and sponge morphologies

Temporal dynamics of percentage cover of individual taxa between sites and over time were analysed using linear mixed-effects models with normally distributed errors and random intercepts (*lme*, R package *nlme*; Pinheiro *et al.*, 2021). Site, time and historical period (for the past and present comparison) were considered fixed effects, while quadrat was considered a random effect to account for quadrat-related variance. In the models, I also included: 1) a continuous autocorrelation function to account for the temporal structure in the data, with correlation strength declining for time points further apart; 2) a constant variance-covariance structure (*varIdent*) to allow different variances for each quadrat. Fixed-effect terms were tested using the function *Anova* (R package *car*; Fox *et al.*, 2012); while *post hoc* comparisons were computed on estimated marginal means using the functions *emmeans* and *emtrends* (R package *emmeans*). The goodness of fit, normality and homoscedasticity of the errors were checked for all models by inspecting the normalised residuals and the quantile-quantile plots.

4.3. Results

4.3.1. General description of communities and assemblages

Across all historical periods, sites, and time points, I found 71 taxa/OTUs, which were collapsed into eight different groups (see Materials and methods). Sponges were the group with the most taxa/OTUs (40), followed by ascidians (14) and anthozoans (5) (Tab. S4.3). The benthic groups with the highest percentage cover in 2018–2021 across all sites and time points were animal turf (34 ± 15%), algae (22 ± 21%), sponges (21 ± 8%), anthozoans (7.8 ± 10%), ascidians (5.4 ± 7.7%), and polychaetes (3.2 ± 4.9%) (Fig. 4. 2A). Bare space accounted for a considerable portion of the substrate only at two internal sites (Goleen and Glannafeen, 13.7% and 12.4% on average, respectively). Bare space was negligible at the other sites (< 1%) (Fig. 4. 2a). The OTUs/taxa with the highest percentage cover across all time points and sites were animal turf (34 ± 15%), turf red algae (16 ± 21%), the jewel anemone *Corynactis viridis* (7.1 ± 10.8%), the sponge *Eurypon* orange (5.6 ± 6.6%), encrusting non-calcified red algae (4.2 ± 7.4%), and the sponge *Iophon* sp. (3 ± 6.6%). Regarding sponge morphologies, encrusting Raspailiidae had the highest cover (11 ± 10%), followed by encrusting non-Raspailiidae (7.5 ± 7.6%) and repent forms (1.3 ± 3.2%) (Fig. 4. 2b).

The overall benthic community, and sponge and ascidian assemblages all differed between sites (p = 0.0001) (Fig. 4. 3a–c, 4; Tab S3–4). However, the factor site explained more of the variance in the overall benthic community and sponge assemblage (78% and 73%, respectively), compared to the ascidian assemblage (25%) (Tab S4–6). Each site differed from all other sites for the overall benthic community (p = 0.0001), sponge assemblage (p = 0.0001), and ascidian assemblage (p = 0.02–0.0002) composition (Fig. 4. 3a–c, 4; Tab S4). The three internal sites were more similar to each other than the innermost site and particularly the site at the entrance (Fig. 4. 3a–c, 4). The internal sites also had a higher overall taxa/OTUs richness (47–53) than the innermost site (33), and the entrance site (12).

Overall benthic communities, and sponge and ascidian assemblages also differed between historical periods (p = 0.0001) (Tab. S4.7). However, the historical period explained a higher proportion of variance at Labhra Cliff compared to Glannafeen for the overall benthic

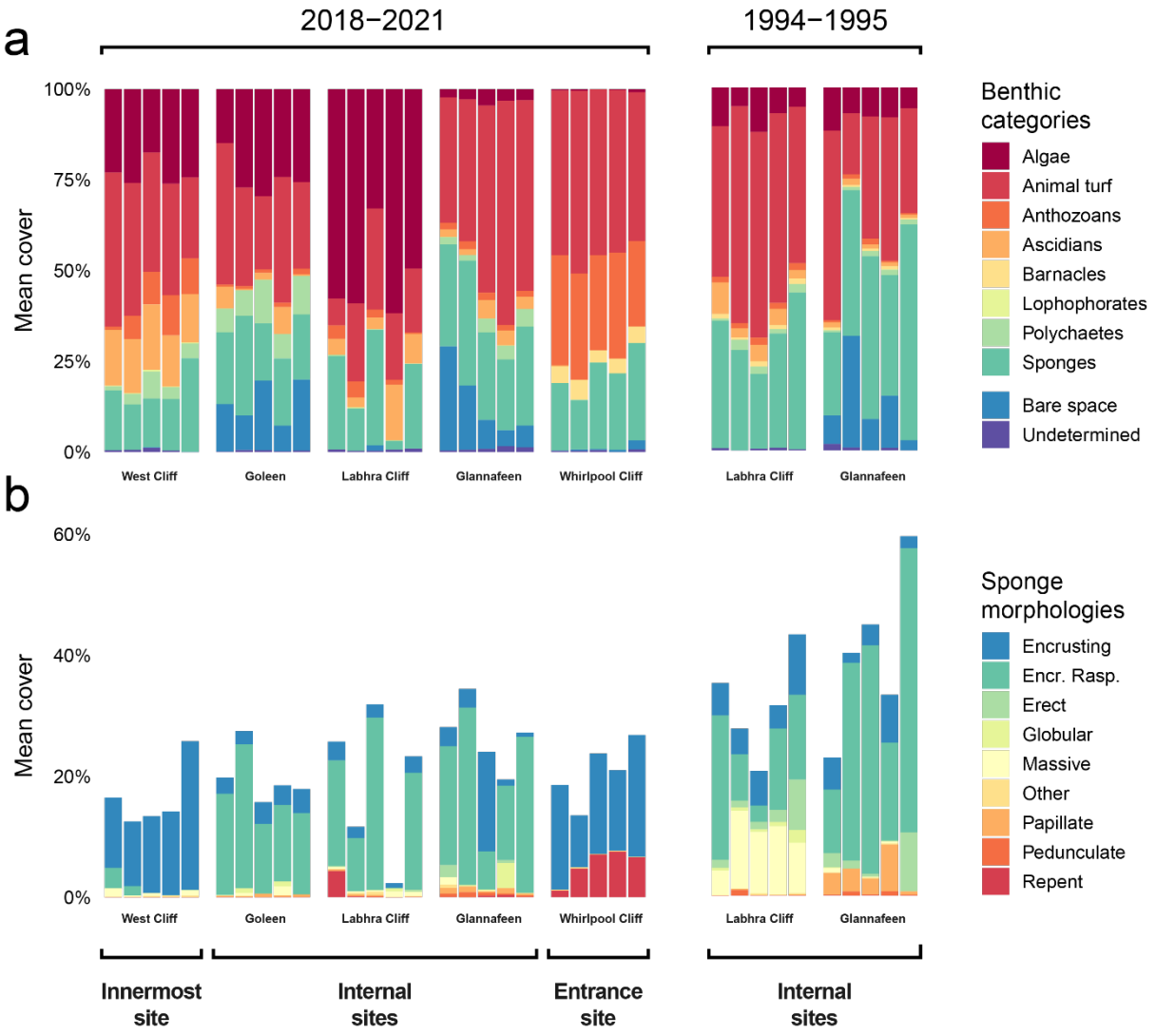

Figure 4.2. Percentage cover of benthic organisms and bare space (a) and sponge morphologies (b) at each permanent quadrat averaged across all time points, for the period 2018–2021 and 1994-1995. Encr. Rasp.: Encrusting Raspaiilidae. Note the different y-axis scales.

community (44% *vs* 24%), sponge assemblage (28% *vs* 18%), and ascidian assemblage (18% *vs* 12%).

4.3.2. Temporal dynamics of communities and assemblages

In 2018–2021, over 17 months, benthic communities and ascidian assemblages changed significantly over time, but the changes were site-specific (interaction between site and time; $p = 0.04$ and $p = 0.0003$, respectively). PERMANOVAs for only internal sites found a significant effect of time for the overall benthic community ($p = 0.004$) and ascidian assemblage ($p =$

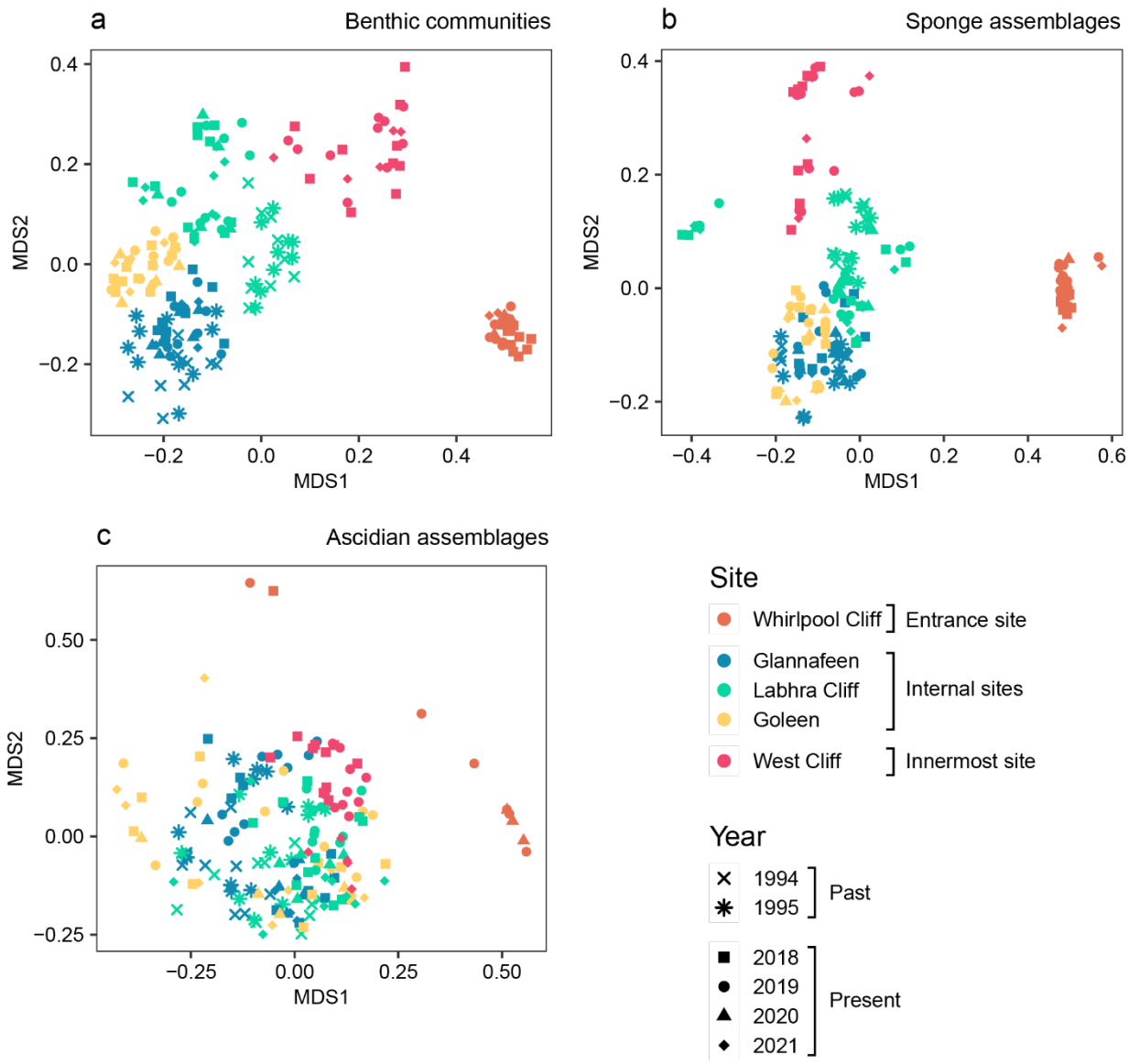

Figure 4.3. Non-metric multidimensional scaling (nMDS) plot for benthic communities (a), sponge assemblages (b) and ascidian assemblages (c) for the period 1995–1995 and 2018–2021. Samples correspond to quadrats at each time point.

0.0001). However, one-way PERMANOVAs made at each site revealed that the overall benthic community only changed over time at the entrance site (p = 0.0001) and the innermost site (p = 0.007), but not at the internal sites. Sponge assemblages only changed at the entrance site (p = 0.006), while ascidian assemblages changed at all sites (p = 0.01–0.0003), except Goleen (Tab. S4.4).

Over the longer time frame (32–36 months), observed trends were generally consistent with the 17-month analysis for sponge assemblages, but differed for the overall benthic community

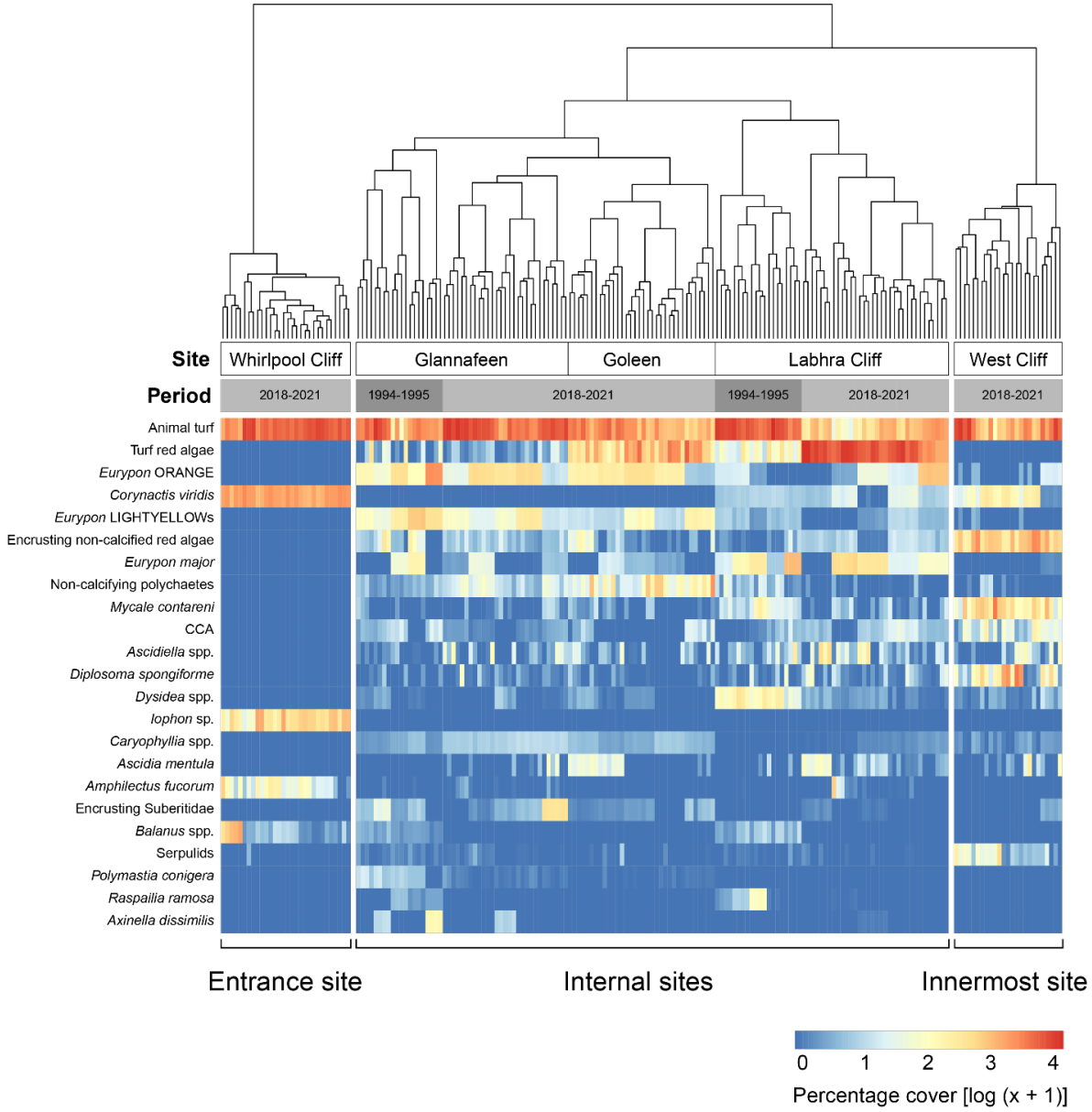

Figure 4.4. Heat map of the abundance of benthic taxa/OTUs that contribute the most to variability between sites and historical periods at each sample (each quadrat at each time point). Abundance is log (x + 1) transformed. Dendrogram of the cluster analysis (Bray Curtis dissimilarity) of samples, using the benthic taxa/OTUs as variables, is reported on the top. Samples are annotated per historical period and site. The three main clusters are reported as separate clusters in the heatmap.

(no effect of time was found at the internal sites) and ascidian assemblage (no effect of time was found at any site) (Tab S5–6). In 1994–1995, over 16 months, no significant changes over time were found for the overall benthic communities or sponge assemblages at the two internal sites

investigated (Glannafeen and Labhra Cliff). Ascidian assemblages instead changed significantly over time (p = 0.0001). When comparing 1994–1995 and 2018–2019, for the overall benthic communities, most of the variance was explained by the factor site (32–35%) and historical period (9–11%), while time accounted for less than 2%; in contrast, time accounted for 11% of the variation in the ascidian assemblage (Tab. S4.7).

4.3.3. Rates and patterns of variability in overall benthic communities and assemblages.

The analysis of the overall benthic community and sponge/ascidian assemblage variation over time (2018–2021, 17 months) revealed a significant positive trend (i.e., directional change) only at the entrance site for both the overall benthic community (p = 0.0003) and sponge assemblage (p = 0.007) (i.e., the communities are increasingly dissimilar over time). This positive trend means that the temporal changes detected by the PERMANOVA do not represent fluctuations or stochastic variations, but a gradual transition to a new community/assemblage. A negative trend was found at the innermost site for sponge assemblage (p = 0.009) (i.e., the communities

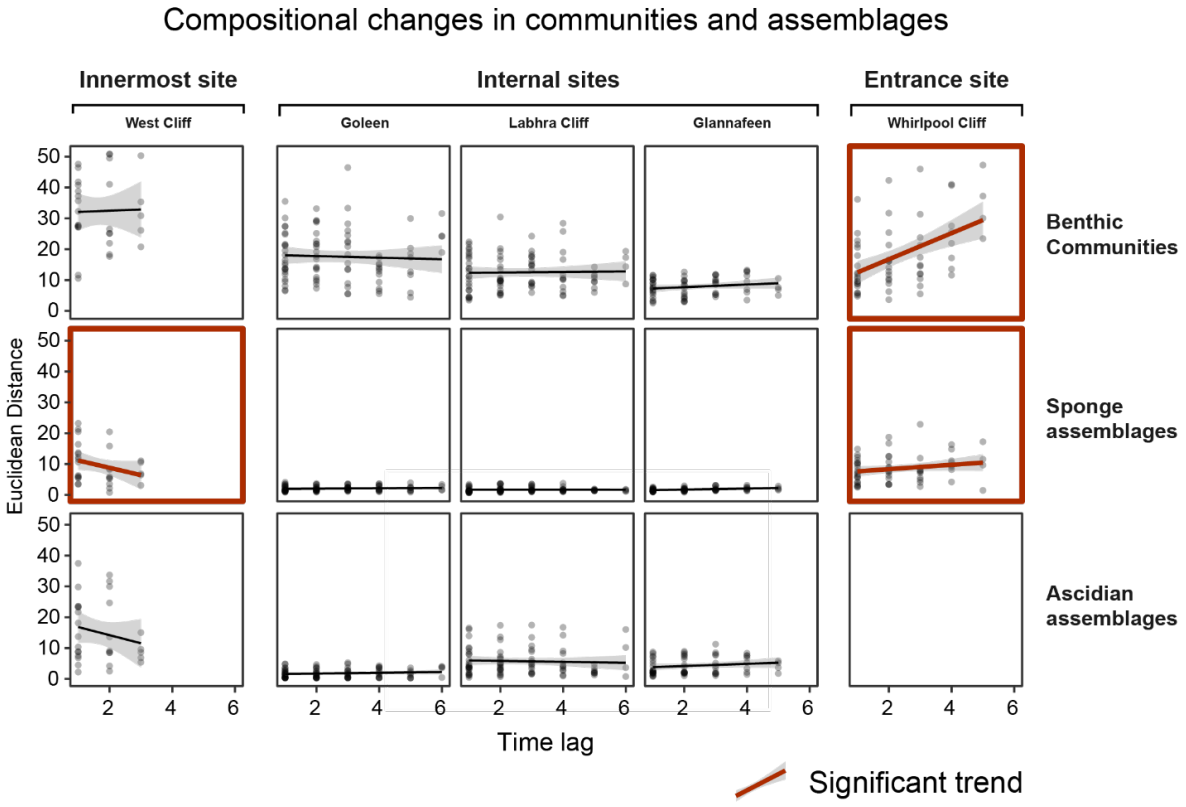

Figure 4.5. Compositional changes in benthic communities, and sponge and ascidian assemblages at each site in 2018–2021 described by Euclidean distances calculated on pairwise communities across the entire time series. These distance values are then regressed against the time lag interval. Significant trends (p < 0.05) are highlighted in red.

are increasingly similar over time) (Tab. S4.8; Fig. 4. 5). Trends were also consistent if the analyses were performed over a longer time frame (32-36 months) (Tab. S4.9–10). No significant trend was found for the 1994–1995 period (Tab. S4.11; Fig. 4. 5).

The rate change analysis also revealed that compositional differences across time (represented by the Euclidean distance) were highly variable across sites. In general, the innermost and entrance sites had the highest variability (Tab. S4.8; Fig. 4. 5).

4.3.4. Community and assemblage turnover

Overall, ascidian assemblages (site average: 33–61%) had the highest compositional turnover followed by the overall benthic communities (15–26%) and sponge assemblages (7–22%), irrespective of historical period and site investigated (multiple comparisons, $p < 0.02$) (Tab. S4.12; Fig. 4. 6).

Between 2018–2021, over 17 months, compositional turnover of the overall benthic communities differed significantly across sites ($p = 0.006$), while there were no significant differences for the sponge and ascidian assemblages. The innermost site had a higher overall benthic community turnover than all the internal sites ($p = 0.0003–0.04$), except the entrance site (Tab. S4.13; Fig. 4. 6).

Over the longer time scale (32–36 months), differences in turnover across sites were consistent with previous results for the overall benthic communities and sponge assemblages,

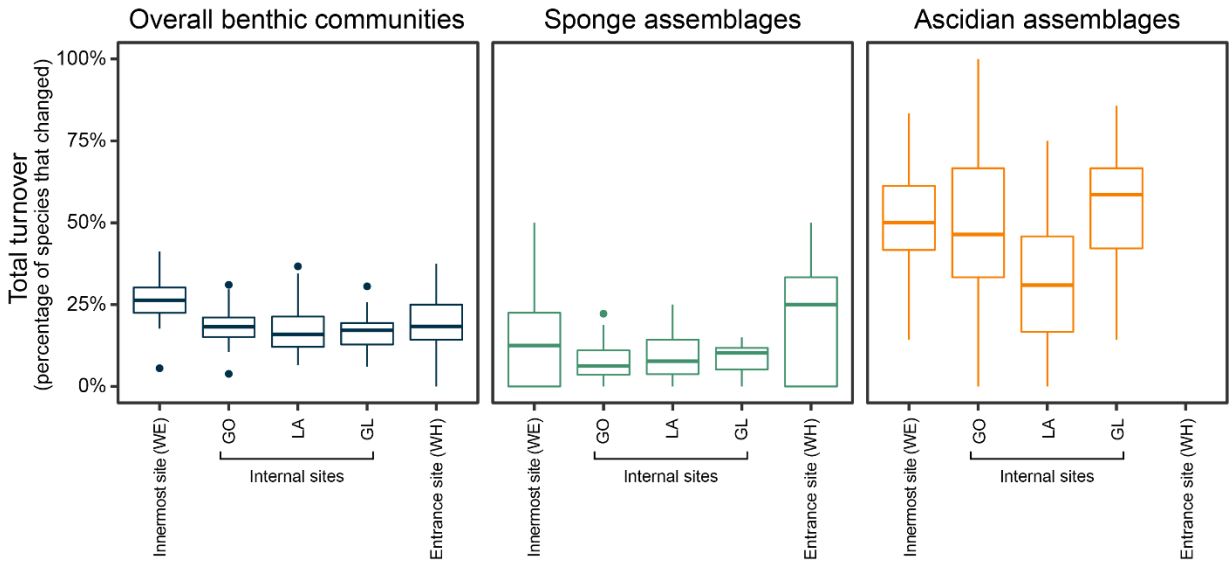

Figure 4.6. Compositional turnover over time for the overall benthic communities, and sponge and ascidian assemblages at each site in 2018–2021.

but not for ascidian assemblages. Pairwise comparisons found a higher ascidian assemblage turnover at Glannafeen than Labhra Cliff, which was not detected over the first 17 months (p = 0.002) (2.5-years comparison, June 2018 – March 2021; Tab. S4.14–15; Fig. 4. 7). In 1994–1995, I found significant differences in turnover of the overall benthic communities between the two internal sites (Tab. S4.16).

4.3.5. Variation in taxa diversity over time

There were significant temporal trends in taxa diversity at most sites, but trends differed substantially according to diversity index used, site, historical period and timeframe investigated. Between 2018–2021 (over 17 months), taxa richness and Shannon and Simpson diversity indices changed significantly over time at the entrance, innermost and some internal sites. At the internal sites, temporal trends differed between sites for all three indices: taxa richness increased at all sites but Glannafeen ($p < 0.02$); Shannon index increased only at Labhra Cliff ($p < 0.0001$). Simpson diversity increased at Labhra Cliff ($p = 0.002$) but decreased at Glannafeen ($p = 0.0005$). At the internal sites, all three indices increased significantly ($p < 0.0001$). At the entrance site, taxa richness increased while Shannon and Simpson's indices decreased ($p < 0.0001$) (Tab. S4.17; Fig. 4. 8).

Over the longer time frame (32-36 months, 2018–2021), I only found a negative trend in taxa richness at Goleen ($p = 0.03$), while no significant trend was found at the other internal sites (Tab. S4.18–19; Fig. 4. 8). Between 1994–1995, all three diversity indices showed different trends at the two internal sites ($p < 0.005$). There were also significant interactions between historical periods, sites, and time for all three indices ($p < 0.0001$), meaning that temporal changes varied between the different sites at different historical periods (Tab. S4.20).

4.3.6. Temporal changes in percentage cover of main benthic groups

Temporal dynamics of all the main benthic organisms differed substantially between the entrance, innermost and internal sites. I also found different trends between the internal sites, but

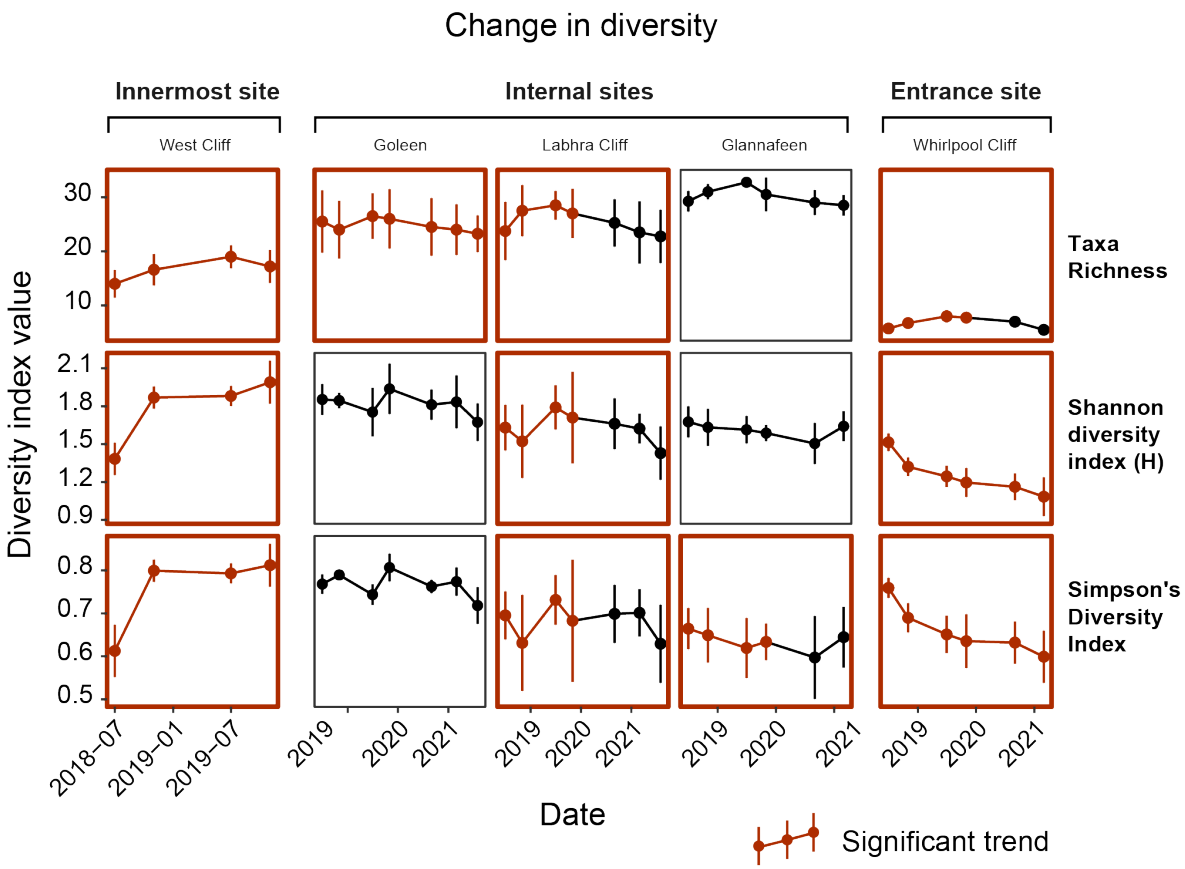

Figure 4.7. Change over time in taxa diversity per sample (Taxa richness, Shannon Diversity Index H, and Simpson's Diversity Index) at each site. Significant trends ($p < 0.05$) are highlighted in red; when only part of the trend is highlighted in red, the trend is significant only when analysed on a subset of data. Note the different axis scales.

only for sponges (in both historical periods), animal turf (in 1994–1995), and polychaetes (in 2018–2021) (Tab. S4.21–24: Fig. 4. 8).

In the 2018–2019 period, sponge coverage increased significantly at two internal sites (Glannafeen, $p = 0.004$; and Labhra Cliff, $p < 0.0001$). Animal turf decreased at the innermost site $p = 0.005$), while it increased at the entrance site ($p < 0.0001$). Anthozoans and ascidians significantly increased but only at the innermost site ($p = 0.0004$ and $p = 0.0003$, respectively). Barnacles have declined at the entrance site, where their average cover dropped from 21 ± 5 % in June 2018 to 1.5 ± 0.8% in November 2018, and have never recovered. Polychaetes showed a significant trend only at Goleen, where they increased from 6 ± 3% in June 2018 to 21 ± 6%

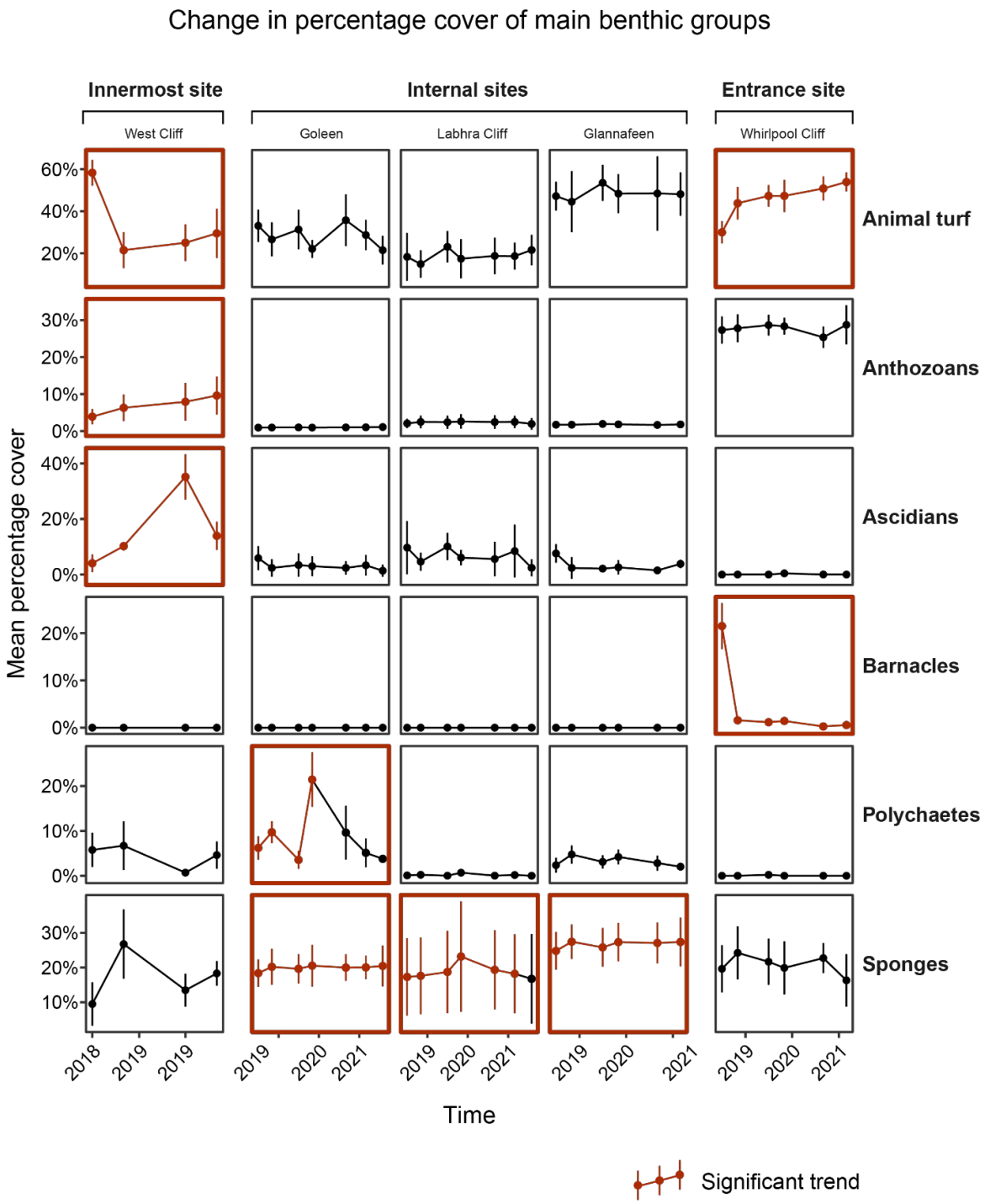

Figure 4.8. Change over time in percentage cover of main benthic groups at each site. Significant trends ($p < 0.05$) are highlighted in red; when only part of the trend is highlighted in red, the trend is significant only when analysed on a subset of data. Note the different axis scales.

in November 2019 ($p < 0.0001$) (Tab. S4.21, Fig. 4. 8). While at the other internal sites, polychaetes did not show any trend and never exceeded 4.7 ± 2%

Over the longer time scale (32-36 months, 2018–2021), most trends were consistent, with a few exceptions. Sponges showed a significant increase at Goleen (internal site, $p = 0.015$), which was not detected in the first 17 months. Over 32 months, sponges were increasing at a significantly higher rate at Glannafeen than Labhra Cliff ($p = 0.001$). Polychaetes declined after November 2019, so they did not change significantly over the longer time scale (Tab. S4.22–23; Fig. 4. 8). Different temporal variations within internal sites were also found between 1994–1995, for sponges ($p < 0.0001$) and turf-forming animals ($p < 0.0001$).

4.3.7. Temporal changes in percentage cover of the main sponge morphologies

As for the main benthic groups, temporal dynamics of sponge morphologies differed substantially between all sites and also between internal sites. The innermost site did not show any increase for any sponge morphology, while the entrance site only showed a temporal increase in encrusting sponges between 2018 and 2019 ($p < 0.0001$).

With respect to the internal sites, all of them showed some increase in sponges, but morphologies and trends differed between sites. Glannafeen was the site experiencing the highest growth rate, with most three-dimensional morphologies and encrusting raspailids, showing significant positive trends. Erect sponges increased +0.08% year^{-1} ($p = 0.0002$), papillate +0.24% year^{-1} ($p < 0.0001$), pedunculate +0.21% year^{-1} ($p = 0.004$), and encrusting raspailids sponges +0.41% year^{-1} ($p = 0.001$). Pedunculate sponge cover at Glannafeen is now comparable to pre-impact cover. At Labhra Cliff, I detected increases, but only in erect (+0.06% year^{-1}, $p = 0.0001$) and encrusting raspailids sponges (+0.22% year^{-1}, $p = 0.001$). At Goleen, I only detected an increase in encrusting raspailids (+0.36% year^{-1}, $p = 0.02$). No significant changes were found in massive sponges at any site.

Different trends at different internal sites were also found in 1994–1995 for encrusting non-Raspailiidae (only decreasing at Labhra Cliff, $p = 0.0001$), papillate (only decreasing at Glannafeen, $p = 0.046$), and erect sponges (only decreasing at Labhra Cliff, $p = 0.02$).

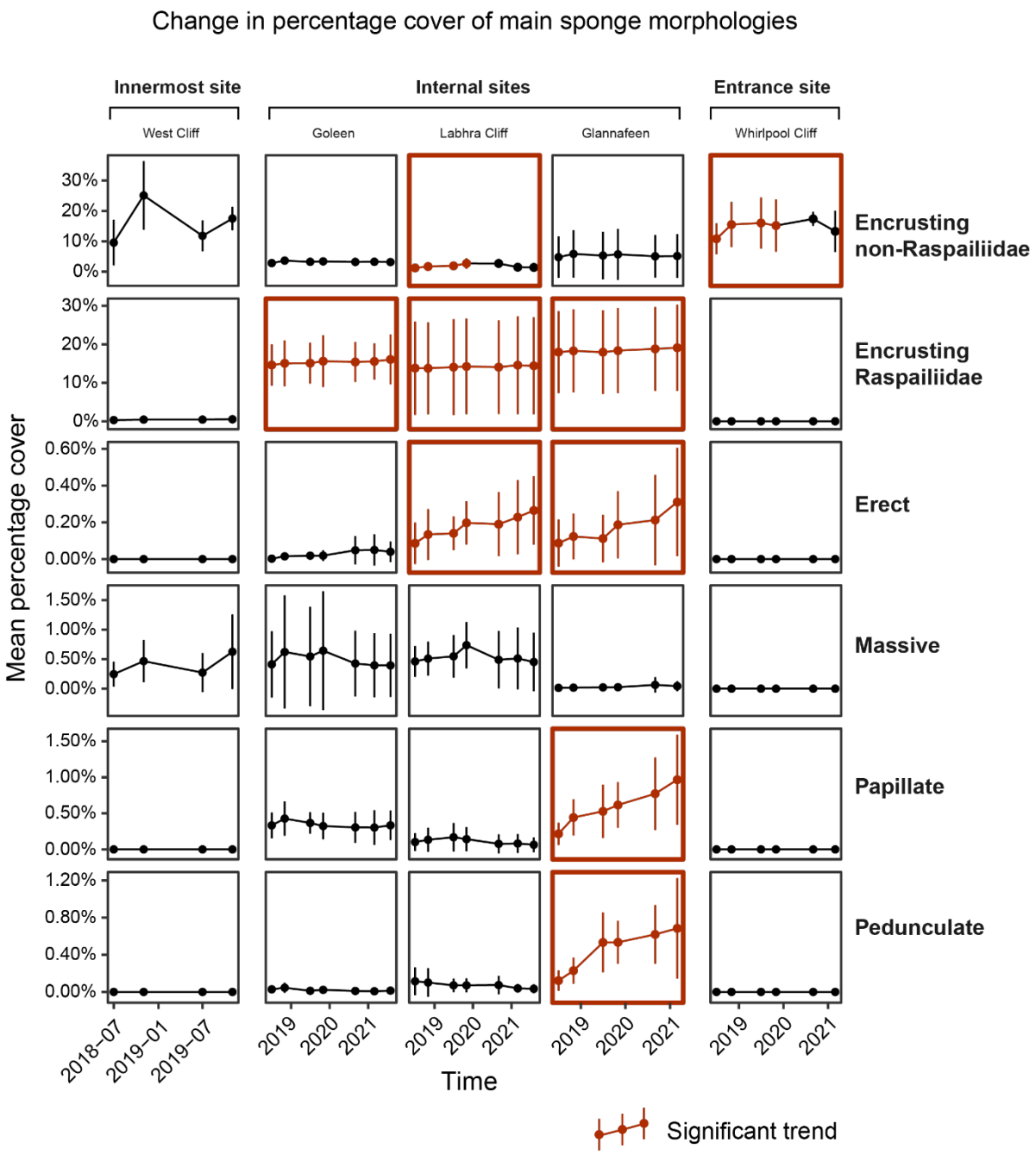

Figure 4.9. Change over time in percentage cover of main sponge morphologies at each site. Significant trends ($p < 0.05$) are highlighted in red; when only part of the trend is highlighted in red, trend is significant only when analysed on a subset of data. Note the different axis scales.

4.4. Discussion

Recent research has,highlighted the economic and ecological importance of temperate mesophotic ecosystems (TMEs) and their vulnerability to impacts (Chapter 2; Micaroni *et al.*, 2021; Cerrano *et al.*, 2019; Turner *et al.*, 2019; Bell *et al.*, *in review*). Yet, we know very little about TMEs resilience to disturbance, limiting our ability to manage and conserve these ecosystems properly.

The widespread community changes that occurred at Lough Hyne between 2010 and 2015, gave the rare opportunity to investigate how mesophotic circalittoral communities might recover after a mass mortality event. I found that mesophotic sessile communities and sponge assemblages at Lough Hyne show little variation over time, both before and after disturbance. Importantly, regardless of the historical period investigated, I found marked differences in temporal dynamics between sites sharing similar communities and comparable environmental conditions. Impacted sponge populations seem to be slowly recovering only in areas experiencing slightly higher water flow. These findings suggest that small differences in environmental conditions can strongly affect the dynamics and recovery of temperate mesophotic communities.

4.4.1. General temporal dynamics of mesophotic subtidal ecosystems

Our past and present time series indicate that mesophotic ecosystems are characterised by very little compositional turnover and temporal fluctuations. This was especially seen in the internal sites, experiencing more stable conditions, and hosting typical mesophotic species (Bell and Barnes, 2002). Low dynamism of TMEs have been already suggested by previous studies, since these are mainly inhabited by long-lived and slow-growing species, but it has never been studied in detail (Benedetti *et al.*, 2016; Bramanti *et al.*, 2017).

Sponges and ascidians were the most speciose and dominant groups identified amongst the benthic communities. Of these, the sponge assemblages showed the lowest degree of dynamism, with very low compositional turnover rates (7–10% in the internal sites, over 6 months). Most taxa showed very little change over time (time explained only ~ 1% of the sponge assemblage variation in the internal sites; 6-month time lags). One explanation of this low temporal variation is that most mesophotic sponges are *K*-strategists, which is likely the result of the constant environmental conditions in which these have evolved (Rossi *et al.*, 2017).

In contrast, the ascidian assemblages were highly dynamic, with very high compositional turnover (29–53%), and high temporal assemblage variation. Most of the species I found were highly dynamic seasonal species (Mastrototaro *et al.*, 2008; Aldred and Clare, 2014). During my study, only specimens from one species (i.e., *Ascidia mentula*) were found to live longer than one year. Interestingly, ascidians were more abundant and showed different and more extreme dynamics at the innermost site. At this site, ascidian cover increased from 4.1 ± 3.2% to 35 ± 8.2% in just 12 months, decreasing to 14 ± 5% four months later. This large fluctuation may be due to ascidians thriving in more sheltered conditions (Svane, 1983; Mastrototaro *et al.*, 2008). Alternatively, this could be due to the large decrease in *K*-selected species (i.e., sponges and anthozoans) at this site, which, if present, might prevent substrate colonisation by producing antifouling compounds (Satheesh *et al.*, 2016).

I also reported an overall lough-wide decrease in barnacles that was not detected during previous investigations (Micaroni *et al.*, 2021, Chapter 2). Firstly, I found that barnacles were not present in the internal sites in 2018–2021, while they occupied 0.7–1.2% of the substrate in 1994–1995. These might have also died due to the 2010–2015 disturbance event(s), since empty plates are still present on the cliffs. Secondly, I observed a die-off of barnacles at the entrance site, which decimated their population. Barnacle coverage changed from 21% in June 2018 to 1.5% in November 2018 and did not recover in the study period. These barnacles belonged to the genus *Balanus* and were presumably the same species as at the internal sites. The mass mortality observed could also be related to the 2018 heatwave, one of the most severe in the last 40 years (Undorf *et al.*, 2018, see Fig. S2.5). A barnacle die-off following a heatwave has been reported by Chan (2007) from the intertidal zone of Hong Kong. However, nearly nothing is known about the ecology of barnacles in the subtidal habitat, so the mortality could also be related to natural population fluctuations.

I found no evidence of any directional change in the communities of the internal sites, meaning that the little temporal variation detected by some of the PERMANOVAs only represented community fluctuations. In contrast, I found positive directional changes at the entrance of the lough for both the overall benthic community and the sponge assemblage, which means that the community and sponge assemblage are gradually changing over time towards a different state. These changes resulted from the barnacle mortality and the colonisation of the available substrate by other organisms such as turf-forming organisms, and two opportunistic sponges: *Iophon* sp. and *Amphilectus fucorum*. In contrast, I found a negative trend in the sponge assemblages at the innermost site (i.e., the communities are becoming increasingly similar over

time). Negative trends are usually due to cyclical dynamics such as seasonality (Collins *et al.*, 2000). Unfortunately, due to logistical constraints on the sampling design, seasonality was beyond the scope of this work, but it needs to be addressed in future studies. I noticed seasonal patterns in several groups (i.e., ascidians, algae, polychaetes, turf-forming animals and bryozoans), which might account for some of the community intra-annual variability.

I also found temporal variation in taxa diversity at most sites. At the innermost and internal sites, these differences mostly result from the proliferation of ascidians and other ephemeral organisms in summer 2019, which were scarce in 2018. However, the spread of these organisms was not even across the internal sites, resulting in significantly different trends between these sites. In most cases, trends then were not significant when analysed over a longer time frame, indicating that diversity was constant in the internal part of the lough. At the entrance site, the barnacle mass mortality led to a temporary increase in richness in 2018–2019 and a persistent decrease in diversity and evenness (Simpson's index).

The general pattern emerging from these observations is that temporal dynamics differ between sites and that these differences are more pronounced between sites experiencing the most different environmental conditions. Specifically, the internal innermost and entrance sites, show very different temporal dynamics. Furthermore, I found significant differences in temporal dynamics between the internal sites from most metrics and variables investigated (i.e., taxa turnover, diversity, evenness and percentage cover of benthic groups and sponge morphologies). These sites share very similar communities with most species in common, and they are exposed to similar environmental conditions. Different dynamics between internal sites were also found in 1994–1995, when nutrient levels in the area were still low, and mesophotic communities were healthy (Johnson *et al.*, 1995). Therefore, I speculate that these variations in temporal dynamics are due to small variations in environmental conditions such as water flow and sedimentation regimes (Bell and Barnes, 2000a, b, d; Bell *et al.*, 2015a). The two main abiotic gradients found at Lough Hyne are flow rate and sedimentation, which are known to influence sponge assemblage structure (Bell and Barnes, 2000a, b, d). Therefore, it is possible that these also affect the dynamics of both sponges and other benthic organisms.

4.4.2. Resilience of mesophotic subtidal ecosystems to disturbance

Our analysis of the benthic communities at Lough Hyne shows a distinct separation between pre- and post-impacted communities even in the late stages of my monitoring (i.e., 2021), after 6–11 years from the disturbance event(s). Furthermore, multivariate analyses (PERMANOVA

and *rate change*) suggest no positive directional change in community or assemblage at any of the impacted sites. This means that the recovery of benthic communities and sponge assemblages is occurring too slowly to be detected with these statistical tools, suggesting a low resilience to disturbance. This is consistent with many studies from other ecosystems reporting decades-long recovery times to disturbance events (Stevely *et al.*, 2011; Blasnig *et al.*, 2013; Konar, 2013; Di Camillo and Cerrano, 2015; Kahn *et al.*, 2016; Morrison *et al.*, 2020). However, several other studies found that sponges are relatively resistant to disturbance and impacts than other organisms (Norström *et al.*, 2009; Luter *et al.*, 2011; Kelmo *et al.*, 2014; Bell *et al.*, 2018). Therefore, sponges may generally have low engineering resilience (recovery capacity) but high ecological resilience (resistance to disturbance; *sensu* Holling, 1996).

In contrast to multivariate analyses, I did find signs of recovery for some sponges and anthozoans looking at changes in percentage cover over time for individual OTUs. This discrepancy could be due to the higher statistical power of linear mixed models than multivariate methods, which could detect weak positive trends. However, as for other temporal dynamics, rate of recovery differs substantially between sites. Only one site (Glannafeen) is experiencing a slow but steady recovery of most three-dimensional sponges lost during the 2010–2015 mass mortality event. In contrast, the other sites are experiencing only partial or no recovery. The innermost site, which before the impacts used to host very similar communities to the internal sites, has shown no sign of sponge recovery. However, I found a steady increase in anthozoans (i.e., the jewel anemones *Corynactis viridis*). This is consistent with findings from the shallow Mediterranean Sea, where cnidarians showed higher recolonisation rates than sponges after a mass mortality event (Di Camillo and Cerrano, 2015).

As for other dynamics, I believe sponge recovery is affected by small variations in environmental conditions. In the case of sponge recovery at Lough Hyne, I believe the major driver may be water flow, while sedimentation might play a minor role. I found a 'recovery gradient' that correlates with the flow gradient. The highest recovery occurred where water flow was slightly higher (Glannafeen), while slow or no recovery occurred at the innermost site experiencing the weakest currents (Bell and Barnes 2000d).

It is known that sponges can exploit ambient currents to reduce the high energetic cost of filtration rate (Vogel *et al.*, 1977; Ludeman *et al.*, 2017). Sponges experiencing faster water currents up to a certain velocity could have benefit from more saved energy to invest in growth, thus translating to more rapid population recovery. Higher water flow could also mean increased water exchange, and therefore possibly increased food availability, while low flow areas could

see local depletion of food (Wildish and Kristmanson, 1979; Frechette *et al.*, 1989). The great influence of ambient current on sponge dynamics can also be seen at the highest-energy site (entrance site). There, sponge diversity is at the lowest, because most sponge forms are delicate and cannot withstand strong currents (Bell and Barnes, 2000d). However, the few sponges adapted to these conditions are highly dynamic and have the fastest growth rates (e.g., *Amphilectus fucorum* and *Iophon* sp.). The different flow regimes might explain higher recovery rates at Labhra Cliff than Goleen and the innermost site (West Cliff). These sites experience comparable currents at incoming tide when currents are faster, but only last 1–2 hours. Differently, Labhra Cliff experiences faster water flow at outgoing tide, when currents are slower but last 5–6 hours (Bassindale *et al.*, 1957). A weak but sustained water flow might be more important than faster currents for a short time.

Sedimentation is likely another important factor shaping sponge assemblages at Lough Hyne (Bell and Barnes, 2000d). Many temperate sponges possess adaptations to cope with high sedimentation (Bell *et al.*, 2015a). These could give them a competitive advantage over organisms that are instead smothered by sediment (Bell and Barnes, 2000d). Therefore, sedimentation could have a role in the recovery of sponges, releasing them from spatial competition. But given the presence of a large portion of bare space at Goleen (14 ± 7% on average), it is unlikely that spatial competition is limiting sponge recovery. Furthermore, sedimentation could be detrimental for sponge recruits because of smothering (Maldonado *et al.*, 2008). This could explain why the site with the highest sedimentation rate (the innermost one) experienced no recovery.

Population recovery from impacts strongly relies on larval supply and recruitment (Whitlatch *et al.*, 1998; Mumby and Steneck, 2008; Connolly and Baird, 2010; Gladstone-Gallagher *et al.*, 2017). In general, sponge populations recover relatively quicker from disturbances if part of the population remains and can provide future recruits (Blasnig *et al.*, 2013; Gochfeld *et al.*, 2020). In this case, from a qualitative analysis of the photoquadrats, it seems that between-site differences in recovery are more related to slower growth and higher mortality. However, sponges that survived the mass mortality could play an important role in the recovery of the populations at Lough Hyne, and should this be a focus of future research.

From the current information, I estimate that the complete recovery of sponge assemblages at Lough Hyne will probably be in the order of decades. At the current growth rate, papillate sponges will reach their pre-impact cover at Glannafeen in 5-8 years, while erect sponges will take longer (18–30 years, at both Glannafeen and Labhra Cliff). However, the absence of

recovery at the most internal sites 6–10 years after the disturbance event(s) suggests that whole-lough recovery could take even longer. In this context, continuing the subtidal monitoring at Lough Hyne will allow the modelling of population dynamics and recovery, which will provide more accurate estimates.

4.4.3. Implications for the management and conservation of TMEs

My study highlights the low resilience of temperate mesophotic habitats to disturbance. In particular, sponges and anthozoans showed the highest degree of stability and the lowest recovery rates. Sponges and anthozoans represent the main components and ecosystem engineers of most temperate mesophotic ecosystems worldwide (Cerrano *et al.*, 2019; Rossi *et al.*, 2017; Bell *et al.*, *in review*). Any decline in these habitat-former species can affect important ecosystem functions (e.g., nutrient cycling, bentho-pelagic coupling, habitat provisioning) for decades, as recovery times are very slow (Bell *et al.*, 2008; Maldonado *et al.*, 2012). This will result in detrimental effects on related ecosystem services (Ballesteros, 2006; Jaspars *et al.*, 2016; Gómez-Gras *et al.*, 2021). Therefore, the conservation of these ecosystems needs to be supported and prioritised.

I also showed that the dynamics and recovery of most temperate mesophotic organisms could be very sensitive to small variations in environmental conditions. Variation in abiotic factors could have major implications for the management of these habitats. Indeed, these findings raise caution about generalising dynamics of TME organisms and communities from single-location studies which don't consider environmental variability. In addition, ecosystem models that support marine ecosystem-based management need to account for this variability in parameters like the growth rate of ecosystems components.

5. Chapter 5 – General discussion

A survivor Polymastia sp. at Whirlpool Cliff

5.1. Thesis overview

This thesis investigates causes, effects, and resilience of temperate mesophotic ecosystems (TMEs) to disturbance using an Irish sea lough as a model system. I firstly analysed 30 years (1990–2019) of scientific surveys and opportunistic observations at Lough Hye to investigate the long-term variability and stability of TMEs. I then identified all the possible factors involved in the biological community changes observed, exploring possible relationships with environmental variables. I then used the information obtained to select key stressors (i.e., oxygen depletion) to formally test proximate causes of the change in laboratory conditions. Finally, I analysed the dynamics and resilience of mesophotic communities to the disturbance pulse that likely caused the community changes observed at Lough Hyne.

The main findings were that TMEs at Lough Hyne are vulnerable ecosystems that can undergo dramatic changes as a result of stress events. All the three-dimensional, long-lived forms that give complexity to the subtidal ecosystems seem the most vulnerable. Differently, encrusting, and ephemeral organisms were the least affected, and they seem to have proven robust over the long term. I also found that oxygen depletion alone is unlikely to be the main cause of the community changes I observed at Lough Hyne. In laboratory conditions, sponges were able to withstand prolonged periods in very low oxygen concentrations (down to 1.5% air saturation), proving to be the most tolerant phylum (from the ones we have information on) to hypoxia. Finally, I found that mesophotic communities have a relatively low resilience in terms of recovery capacity, which is likely the result of the life-history traits of the main components of these ecosystems. Despite that, I found that some of the organisms affected by the disturbance events at Lough Hyne are slowly recovering. Still, recovery times will be in the order of decades in the absence of any further future disturbance.

The results of my thesis strongly suggest that TMEs are vulnerable ecosystems with low resilience to impacts, so conservation actions aimed to preserve this important natural capital need to be prioritised. Here, I will integrate my findings with existing knowledge to outline a framework for managing and conserving mesophotic ecosystems at Lough Hyne and worldwide (Figure 5.1). Finally, I will discuss the possible future of Lough Hyne subtidal habitats providing suggestions for forthcoming research and management actions.

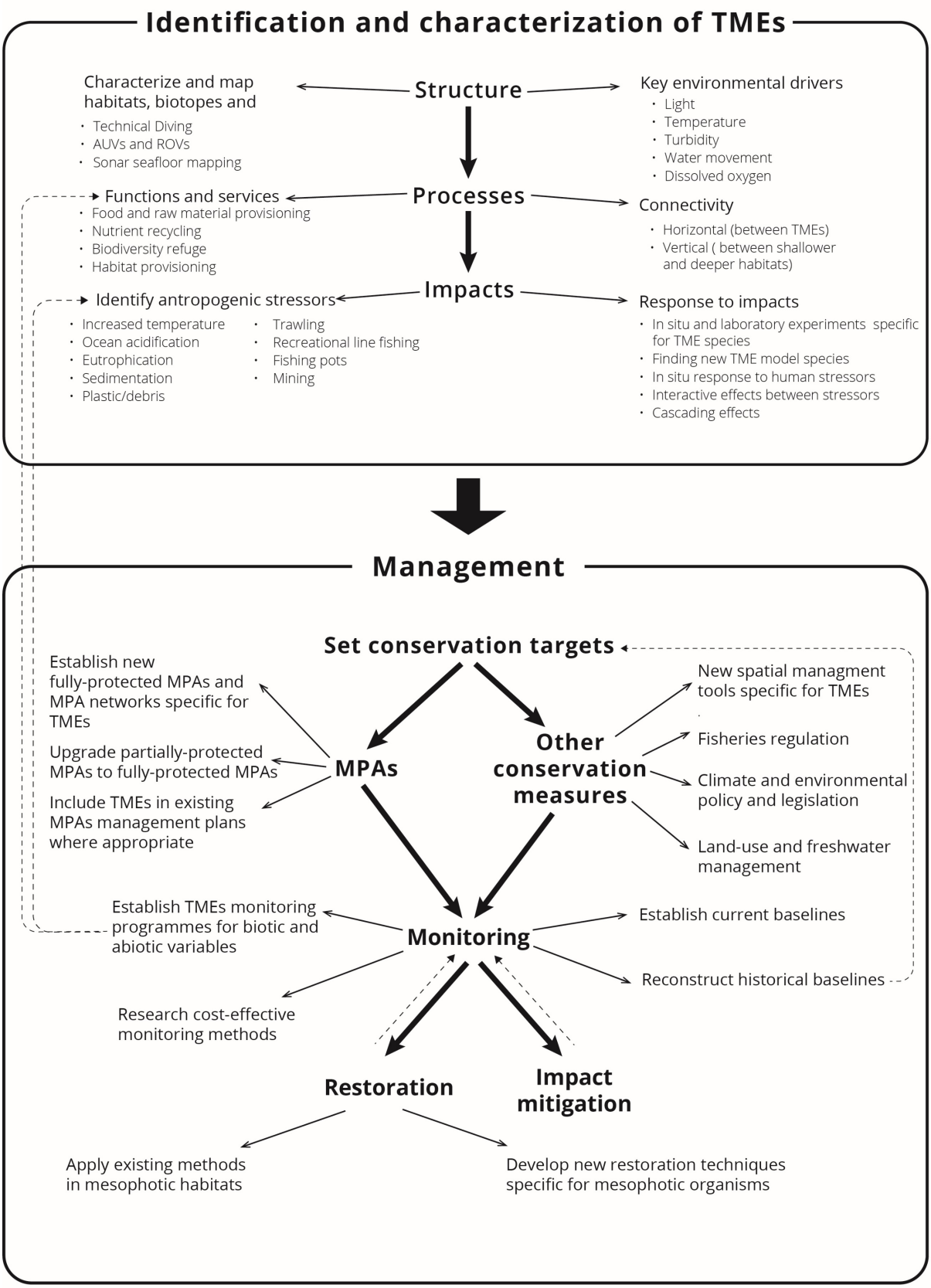

Figure 5.1. Decision-making framework for the management and the conservation of temperate mesophotic ecosystems. Dashed lines indicate feedback loops. Made by the author for Bell et al. (*in review*)

5.2. Management of TMEs

5.2.1. Identification and characterisation of TMEs

The first step we need to take to manage and conserve mesophotic ecosystems appropriately should be to identify sites of interest (including exploration of unstudied areas), characterise the ecosystem structure (i.e., habitats, biotopes, and species), and understand the environmental drivers of abundance, diversity, and species distribution patterns (Giangrande, 2003; Costello, 2009). Lough Hyne represents an exception, because several previous studies have qualitatively and quantitatively investigated mesophotic habitat composition and some of the processes involved in shaping their communities (Maggs *et al.*, 1983; see Picton, 1990; Bell and Turner, 2000; Maughan and Barnes, 2000; Maughan, 2001; Bell, 2007 and references therein), while for the rest of the world, our knowledge of TMEs is still inadequate. Recent research has provided very basic knowledge on TME structure (even if most of the studies only provide qualitative data), but information about processes is still very scant and only comes from a few geographical areas (Giraldo-Ospina *et al.*, 2020; Gómez-Gras *et al.*, 2021; Bell *et al.*, *in review*). As a result, we still know very little about TME functioning, provisioning of ecosystem services, and responses to human and natural disturbance (Bianchi *et al.*, 2017; Cerrano *et al.*, 2019; Turner *et al.*, 2019).

Lists of temperate mesophotic habitats and biotopes are only available for a few areas (Connor, 2004; EEA, 2019; Lucieer *et al.*, 2009), while very little is known for the rest of the world. Even in very well-known areas, the increasing interest in TMEs leads to the regular discovery of new habitats and biotopes (Idan *et al.*, 2018; Corriero *et al.*, 2019; Cardone *et al.*, 2020). TMEs need to be explored and mapped. Understanding the spatial distribution of TMEs will provide a baseline information against which future changes can be recognised and set the spatial framework for ecosystem-based management (Costello, 2009; Baker and Harris, 2020). In the case of Lough Hyne, habitats, biotopes, and environmental drivers have already been characterised and mapped in detail. Without this information, the recognition and the accurate description of the changes would not have been possible (Chapter 2). However, the presence of several undescribed species prevented the comparison between past and present diversity in detail. Some of these species might have disappeared without being ever described (for example, species of the family Polymastidae), highlighting the importance of taxonomy in biodiversity monitoring and conservation (Chapter 2; Giangrande, 2003).

Next, we need to understand which environmental drivers shape mesophotic communities and assemblages. Mesophotic ecosystems lie in the transition zone between shallow and deep waters. Mesophotic area is characterised by several environmental gradients, which are relatively constant worldwide (e.g., light, temperature, nutrient and food availability, water energy; Bell *et al.*, *in review*). The structure of the resulting communities is probably driven by the complex interaction of these gradients and other local abiotic factors such as currents, sedimentation, type of substrate, etc. (Bell and Barnes, 2000b, c, d; Cerrano *et al.*, 2019; Canessa *et al.*, 2020; Chimienti *et al.*, 2020). Furthermore, as shown in Chapter 4, even small variations in environmental conditions can radically affect the dynamics and resilience of mesophotic ecosystems (Chapter 4). For future research, importance needs to be given to water flow and food availability and composition, since mesophotic reefs are mainly dominated by suspension-feeding animals (Rossi *et al.*, 2017). Currents are an important driver for many filter feeders such as gorgonians (Leversee, 1976; Mortensen *et al.*, 2005), corals (Chimienti *et al.*, 2020), bryozoans (Winston *et al.*, 1979), barnacles (Smith, 1946) and sponges (Bell and Barnes, 2000b, c, d). This study suggests that laminar flow rate is a key factor in promoting higher growth rates and recovery from disturbance for impacted sponge assemblages (Chapter 4). A higher sponge growth rate in higher water flow was already observed in previous studies, so it might represent a general rule (Wilkinson and Vacelet, 1979). Along with current, we also need to understand the spatio-temporal variability of food (particularly seston and dissolved organic matter), and its influence on mesophotic organism dynamics (Rossi *et al.*, 2019). A better knowledge of environmental drivers influencing TMEs will improve the management and conservation of these ecosystems, for example for predicting the location of habitats of special interest, and particularly vulnerable communities.

We also need a better understanding of the processes underlying TMEs (i.e., dynamics, functions, services and connectivity) to manage and conserve these ecosystems effectively. Ecological processes within mesophotic ecosystems have been poorly investigated mainly due to the technical and logistical difficulties in performing experiments and repeating sampling at depths below 30 meters (Turner *et al.*, 2019). The limited available information suggests that TMEs provide important services, including supporting commercial fisheries (e.g., rock lobster fisheries, Steneck and Wilson 2001), providing raw materials (e.g., pharmaceuticals, Aiello *et al.*, 2005; genetic resources, Arrieta *et al.*, 2010), waste bioremediation (de Ville d'Avray *et al.*, 2019), and a range of cultural and recreational values (e.g. scuba diving, Rodrigues *et al.*, 2016; angling, Tonin, 2018). However, much more research is needed to understand, quantify, and evaluate TME function and the services they provide. The knowledge derived will make

decision-makers and the general public more aware of the value of these ecosystems. For now, we can only speculate on TME processes using data available for organisms of the same groups in different ecosystems or from shallower waters. However, since environmental conditions of mesophotic ecosystems are relatively unique, the conclusions derived from these assumptions could be inaccurate (Bell *et al.*, *in review*).

Understanding connectivity and recruitment will also be very important for TME conservation, particularly regarding designing MPA networks and determining ecosystem resilience (Palumbi, 2003). For example, the recovery observed on the mesophotic cliffs of Lough Hyne could be mainly due to recruit supply from populations having survived in less impacted areas of the lough (Chapter 4). Larvae are unlikely to come from outside the lough, since sponges mainly have a short pelagic larval duration (from a few hours to a few weeks) and limited dispersal (Maldonado, 2006; Shanks, 2009; Bell *et al.*, 2014; Riesgo *et al.*, 2016; Griffiths *et al.*, 2020). Furthermore, Lough Hyne is a small basin, and the periodic flow of the water likely provides good mixing of larvae in the area. This means that if mass mortalities of sponges were to occur at larger spatial scales, recovery times could be even longer than the few decades assumed for Lough Hyne. In such a scenario, the low connectivity and slow growth rates of mesophotic sponges could act synergistically, drastically limiting population resilience and recovery. In addition to horizontal connectivity, we need to understand the vertical connectivity between TMEs with shallower habitats to evaluate the possibility of TMEs acting as refugia for shallower species, as suggested for tropical MCEs ('deep reef refugia' hypothesis, Bongaerts *et al.*, 2010).

My and other recent research have highlighted that mesophotic ecosystems are not immune to human-derived and natural disturbances. Importantly, TMEs are threatened by the combined effect of climate change and a wide range of other anthropogenic stressors characteristic of both shallow (e.g., artisanal and recreational fishing, eutrophication, pollution, land-derived sediment) and deep waters (e.g. mechanical disturbance and increased sedimentation caused by bottom trawling, hypoxia, hydrocarbon extraction and seabed mining) (Gennaro and Piazzi, 2011; Cerrano *et al.*, 2013; Bo *et al.*, 2014; Rossi *et al.*, 2017, Ferrigno *et al.*, 2018; Marzloff *et al.*, 2018; Enrichetti *et al.*, 2019a; Turner *et al.*, 2019; Betti *et al.*, 2020). As for other ecosystem processes, the ecological resilience (resistance) of TME organisms to human impacts is mainly inferred from phylogenetically related organisms living in shallower waters or from tropical ecosystems. Given that environmental conditions in mesophotic habitats are much more stable than shallow-water ecosystems, and very different from tropical waters, these assumptions are

likely to be inadequate (Bell *et al.*, *in review*). For example, sponges are relatively resilient (both in terms of resistance and recovery) to disturbance and impacts in shallow tropical waters (Kelmo *et al.*, 2014; Bell *et al.*, 2013; 2018). In some cases, sponges were found even to thrive following important disturbance events such as heatwaves and hurricanes, replacing corals as the dominant benthic organisms (Norström *et al.*, 2009; Luter *et al.*, 2011; Kelmo *et al.*, 2014; Bell *et al.*, 2018). In contrast, my and other studies suggest that temperate sponges from deeper waters are particularly vulnerable to impacts and have low resilience capacity (Chapter 2 and 4; Garrabou *et al.*, 2009; Stevely *et al.*, 2011; Di Camillo and Cerrano, 2015; Kahn *et al.*, 2016).

My second chapter contrasts with the finding of the temperate sponges being vulnerable and having low resilience to stressors. Indeed, I found that sponges are the phylum with the highest overall tolerance to deoxygenation. This exceptional adaptive capacity could represent an ancestral character derived from the ancient evolutionary origins of sponges. Temperate sponges may be relatively tolerant to some stressors such as hypoxia, sedimentation, and acidification while being sensitive to others (e.g., increased temperature) (Bell *et al.*, 2015a, b; Bates and Bell, 2018; Cummings *et al.*, 2020; Idan *et al.*, 2020; Garrabou *et al.*, 2009). In any case, human impacts are probably one of the least studied aspects of TME ecology, and further research is needed to elucidate the spatial and temporal extent of stressors and how mesophotic ecosystems, communities and populations respond to their influence. Major importance needs to be given to habitat-forming organisms such as sponges, cnidarians, and bryozoans, because any change in their abundance could have major consequences for the ecosystems they support (Vergés *et al.*, 2019; Woodhead *et al.*, 2019; Piazzi *et al.*, 2021). This knowledge will be critical for the elaboration of effective measures of protection.

Mesophotic ecosystem research has been limited by the available technology, as these ecosystems are usually out of range of conventional scientific diving (Pyle *et al.*, 2019). Indeed, the all-year accessibility of Lough Hyne's mesophotic communities, and their occurrence within the limits of recreational diving (12–30 m) represent a rare opportunity to study mesophotic systems. However, the rapid technological developments of the last decades have led to the development of a wide range of tools to facilitate the exploration of the deeper areas of the ocean. Remotely operated vehicles (ROVs) and autonomous underwater vehicles (AUVs), together with advanced acoustic and optical imaging techniques, have been already successfully used for the characterisation and mapping of TMEs (Williams *et al.*, 2010; Zapata-Ramírez *et al.*, 2013; Armstrong *et al.*, 2019). These tools only need to be used on a broader spatial scale to investigate

poorly studied areas and adapted to perform manipulative and more complex experiments to investigate ecosystem processes.

In general, our knowledge of TME processes and impacts is still very basic and localised to specific geographic locations (mainly the Mediterranean Sea), while not much is known about the rest of the world. This lack of information limits our understanding of both the reasons for and the consequences of the changes at Lough Hyne, hindering our ability to communicate to decision-makers the benefits of possible conservation measures (Chapter 2).

5.2.2 Management of TMEs

Understanding the ecological structure of TMEs and the effects of anthropogenic impacts will support appropriate and effective management. Such management should aim to preserve these ecosystems while maximising the ecosystem services they can provide. To achieve this, it will be important to define conservation targets, which will be different for TMEs compared to shallower water ecosystems. Marine ecosystems have all been profoundly modified by human activities and returning them to pristine conditions might be impossible (Dayton *et al.*, 1998). Therefore, new targets need to be established that consider the human presence in these ecosystems (i.e., industrial and artisanal fisheries, recreational activities such as boating, angling and scuba diving, the presence of urban centres, etc.) and so an acceptable level of disturbance (Borja *et al.*, 2012).

Marine protected areas (MPAs) are one of the most important management tools for conserving and restoring marine biodiversity and ocean productivity (Kelleher, 1999). MPA management plans rarely account for TMEs, and often, as in the case of Lough Hyne, protection only results from shallow MPA designation extending into deeper waters (Kitching, 1987; Turner *et al.*, 2019). Therefore, existing MPAs must integrate TMEs in their management and monitoring, adopting specific measures to protect them. Furthermore, since TMEs also occur offshore, new MPAs and MPA networks should be designed to protect the wide range of TME habitats located far from the coast. The effectiveness of MPA networks in protecting habitat, species and genetic diversity at a large scale will be a function of the knowledge on the habitat types together with their spatial distribution and connectivity (Lourie and Vincent, 2004).

To determine if management measures are effective, we need to investigate habitat, community, and species dynamics. Successful management can only be achieved through fit-for-purpose monitoring (Borja *et al.*, 2016). To date, TMEs are monitored in only a few regions of the world (particularly in the Mediterranean Sea and Australia), while very little is known

about the rest of the world. TMEs should be included in current MPA monitoring programmes, and new TME monitoring schemes should be established to monitor particularly rich and vulnerable habitats and communities. The absence of regular monitoring of Lough Hyne's TMEs resulted in almost a decade between the occurrence of the change and its formal recognition, which has significantly reduced the chances of identifying the drivers (Chapter 2). Current baselines need to be established, against which potential changes are measured and evaluated in relation to natural variation in the system (Borja *et al.*, 2012). Furthermore, historical baselines need to be reconstructed, to assess if changes have already occurred and to help set future targets.

Quantitative data for TMEs are rarely available, so it is often necessary to use other approaches. Published and unpublished historical material including photos, videos, historical descriptions from any possible sources and the knowledge of local fishermen, dive clubs, and naturalists (traditional ecological knowledge) can, in some circumstances, provide useful information to reconstruct earlier conditions (Drew, 2005; Ferretti *et al.*, 2015; Thurstan *et al.*, 2017). In my case, historical information was critical for reconstructing the historical baseline and evaluating the long-time dynamics of Lough Hyne's TMEs communities (Chapter 2). In addition, the ecological knowledge of local experts helped in the reconstruction of events (Chapter 2).

Monitoring needs to have the appropriate temporal and spatial scale while being cost-effective, as budget is often a major constraint (Patricio *et al.*, 2016). As previously discussed, the depth of the mesophotic zone poses major challenges in the study of TMEs, which requires the development of new more efficient and economic monitoring techniques. New approaches, such as the use of autonomous underwater vehicles (AUVs), automatic classification systems based on machine learning, environmental DNA (eDNA), and metabarcoding have the potential to enormously increase the spatial and temporal scales of monitoring, while reducing the depth-related issues and minimising the costs (Thomsen and Willerslev, 2015; Danovaro *et al.*, 2016; Wangensteen and Turon, 2017; Armstrong *et al.*, 2019). In particular, the AUV ability to revisit benthic sites and image the same location on the seafloor will be particularly useful for low dynamics ecosystems such as TMEs (Williams *et al.*, 2012). These technologies are already available for a wide range of applications and, with further development, could be integrated into current marine monitoring programmes and include TMEs.

The achievement of targets and the evaluation of the ecological status needs to be evaluated through specific indicators and indices (Borja *et al.*, 2013). Regarding TMEs, there is a need for the development of indicators for evaluating the health status, since the small number of indices

available are specific for coralligenous reefs and other Mediterranean habitats (CAI, Deter *et al.*, 2012; ESCA, Cecchi *et al.*, 2014; COARSE, Gatti *et al.*, 2015; CBQI, Ferrigno *et al.*, 2017; INDEX-COR, Sartoretto *et al.*, 2017; MACS, Enrichetti *et al.*, 2019b). In my case, I focused on sponge assemblages since these dominated the mesophotic cliffs of Lough Hyne, and other studies suggest that sponges are good indicators of environmental stress levels (Carballo *et al.*, 1996; Mary George *et al.*, 2018). The low temporal variability of sponges found at Lough Hyne suggests that sponges could be used as indicators also in TMEs (Chapter 4). Finally, it is critically important to integrate the monitoring of biological variables with abiotic variables. Otherwise, it is very difficult to explain the assemblage dynamics and identify possible causes of change. The limited monitoring of abiotic variables at Lough Hyne has prevented the accurate identification of the drivers of the change (Chapter 2).

5.3. Future of Lough Hyne

Lough Hyne is globally-recognised biodiversity hotspot, which has been extensively studied since the 18th century. However, several major changes have occurred during the last few decades and its biodiversity is now under threat. Overall, this thesis added an important piece of knowledge to the study of Lough Hyne, providing evidence for ecological changes in the deeper mesophotic reefs and important information on community dynamics.

From the knowledge I gathered, a few possible future scenarios can be considered. In the best case, the disturbance events that caused the sponge die-off represented stochastic events, or the causative factor(s) are no longer present. Hence, the disturbance will not occur again in the future. Sponge populations will continue to recover, and eventually, in a few decades (probably more for the inner areas), the mesophotic communities will come back to a pre-impact state. However, if the causative factor(s) are still present, future disturbance events may reoccur, causing new mass mortalities. If the disturbance is of the same magnitude as previous events, populations of sensitive organisms will persist in certain areas of the lough, providing recruits for other sites. In this scenario, communities will remain in a perpetual transient state, until the causative factors are removed. In the worst-case scenario, the causative factors will not only remain, but will interact synergistically with other climate-change derived factors such as warming, acidification, and deoxygenation. In this case, disturbance events could become more severe and gradually affect bigger portions of the lough. Sponge and other organism populations will persist until there are not enough specimens of a remnant population to support recovery. Under this scenario, eventually the Lough Hyne sponge-dominated communities will face a

permanent regime shift towards assemblages dominated by ephemeral organisms such as ascidians and turf.

Unfortunately, I could not determine with certainty any causal processes responsible for the changes that occurred at the mesophotic cliffs of Lough Hyne. I could not find any evidence of extreme temperature or precipitation events, or changes in any other environmental variables (See Chapter 2 and Table 2.1 in particular). The only factor that has certainly changed is nitrogen, which has increased three-fold in the last 25 years. Therefore, I believe eutrophication is a likely contributor to the changes. It could be possible that eutrophication might have triggered a toxic event in conjunction with other environmental factors. Anoxic, acidic, and H_2S-rich water might have spread from the deeper waters of the lough to the shallow areas, as a result of a storm (Chapter 2). My experiments on the tolerance of sponges to hypoxia suggest that hypoxia alone was not the cause of the sponge mortality (Chapter 3). I suggest future research to focus on other eutrophication-related stressors (e.g., hydrogen sulphide, toxins produced by phytoplankton and by the decomposition of ephemeral algae) and the interactive effect of hypoxia with hydrogen sulphide and temperature.

Tolerance experiments on TME organisms will surely help understand the cause of the change at Lough Hyne and will provide valuable information for the management of TMEs globally. However, laboratory experiments are resource-consuming and, alone, are unlikely to provide conclusive evidence of the driver. For this reason, I would like to stress the benefit of continuing the biological monitoring and implementing a sound monitoring of environmental variables such as temperature, oxygen, H_2S, nutrients, and food (seston and dissolved organic carbon). In case of new disturbance events, the monitoring will guarantee its early detection, and a better understanding of the abiotic factors involved.

Future research will also need to address possible consequences of the changes occurred. Sponges pump a considerable amount of water (up to 72,000 times their body per day, Koopmans *et al.*, 2010). Given the low water exchange of Lough Hyne with the open coast (complete water replacement every ~41 days, Johnson *et al.*, 1995), sponges might have/had a considerable effect on the quality and quantity of seston and dissolved organic matter in the water column (Peterson *et al.*, 2006). Future feeding experiments coupled with statistical modelling will be able to elucidate this aspect.

Finally, it will be useful to find methods to improve and speed up community recovery. Active restoration in TMEs has been only investigated on octocorals and mainly in the Mediterranean

Sea (e.g., Linares *et al.*, 2008), although ongoing projects are testing restoration protocols for other mesophotic organisms such as macroalgae, sponges and bryozoans (e.g., MERCES project, http://www. merces-project.eu). In the case of sponges, the only example of temperate sponge restoration published so far involved only one species (*Spongia officinalis*) (Baldacconi *et al.*, 2010). Lough Hyne could represent an ideal site to experiment with new restoration techniques specifically designed for mesophotic organisms that could be applied elsewhere when needed. In addition, since sponges were mostly unaffected in certain areas of the lough, it might be helpful to place artificial substrate that will increase the substrate availability for their growth. The new sponges that will grow on these structures will contribute to maintaining a large genetic pool and could be transplanted in future restoration actions.

5.4. Concluding remarks

Despite temperate mesophotic ecosystems (TMEs) being important, we still know little about their distribution, ecology, and response to impacts (Cerrano *et al.*, 2019; Bell *et al.*, *in review*). In this thesis, I show that TMEs are vulnerable ecosystems. I also show that despite sponges being resistant to certain stressors, mesophotic sponge assemblages appear less resilient, particularly in regard to recovery capacity. For these reasons, the study and protection of TMEs need to be prioritised by institutions and environmental management agencies. Overall, my thesis not only improved our understanding of the change that occurred at Lough Hyne, but also contributed to the knowledge of mesophotic ecosystems in general, supporting their management and conservation.

References

Aiello, A., D'Esposito, M., Fattorusso, E., Menna, M., Müller, W. E., Perović-Ottstadt, S., Tsuruta, H., Gulder, T.A., & Bringmann, G. (2005). Daminin, a bioactive pyrrole alkaloid from the Mediterranean sponge *Axinella damicornis*. Tetrahedron, 61(30), 7266-7270.

Aldred, N., & Clare, A. S. (2014). Mini-review: impact and dynamics of surface fouling by solitary and compound ascidians. Biofouling, 30(3), 259-270.

Altieri, A. H., & Diaz, R. J. (2019). Dead zones: oxygen depletion in coastal ecosystems. In: C. Sheppard (Ed) World Seas: An Environmental Evaluation. Academic Press, pp. 453–473.

Altieri, A. H., & Gedan, K. B. (2015). Climate change and dead zones. Global Change Biology, 21(4), 1395–1406.

Altieri, A. H., Harrison, S. B., Seemann, J., Collin, R., Diaz, R. J., & Knowlton, N. (2017). Tropical dead zones and mass mortalities on coral reefs. Proceedings of the National Academy of Sciences, 114(14), 3660–3665.

Anderson, D. M., Glibert, P. M., & Burkholder, J. M. (2002). Harmful algal blooms and eutrophication: nutrient sources, composition, and consequences. Estuaries, 25(4), 704-726.

Anderson, M. J. (2001). A new method for non-parametric multivariate analysis of variance. Austral Ecology, 26(1), 32–46.

Anderson, M. J. (2014). Permutational multivariate analysis of variance (PERMANOVA). Wiley statsref: statistics reference online, 1–15.

Anderson, M. J., Gorley, R. N. & Clarke, K. R. (2008). PERMANOVA+ for PRIMER: Guide to software and statistical methods. PRIMER-E, Plymouth, UK.

Angiolillo, M., di Lorenzo, B., Farcomeni, A., Bo, M., Bavestrello, G., Santangelo, G., Cau, A., & Canese, S. (2015). Distribution and assessment of marine debris in the deep Tyrrhenian Sea (NW Mediterranean Sea, Italy). Marine Pollution Bulletin, 92(1-2), 149-159.

Armstrong, R. A., Pizarro, O., & Roman, C. (2019). Underwater robotic technology for imaging mesophotic coral ecosystems. In: Y. Loya, K. A. Puglise, T. Bridge (Eds) Mesophotic Coral Ecosystems. Springer, Cham, Switzerland, pp. 973-988.

Arrieta, J. M., Arnaud-Haond, S., & Duarte, C. M. (2010). What lies underneath: conserving the oceans' genetic resources. Proceedings of the National Academy of Sciences, 107(43), 18318-18324.

Ayling, A. L. (1980). Patterns of sexuality, asexual reproduction and recruitment in some subtidal marine Demospongiae. The Biological Bulletin, 158(3), 271-282.

Ayling, A. L. (1983). Factors affecting the spatial distributions of thinly encrusting sponges from temperate waters. Oecologia, 60(3), 412–418.

Baker, E. K., & Harris, P. T. (2020). Habitat mapping and marine management. In: P. Harris, E. Baker (eds) Seafloor geomorphology as benthic habitat. GeoHab Atlas of Seafloor Geomorphic Features and Benthic Habitats. Elsevier, pp. 17-33.

Bakran-Petricioli, T., Vacelet, J., Zibrowius, H., Petricioli, D., Chevaldonné, P., & Raa, T. (2007). New data on the distribution of the 'deep-sea'sponges *Asbestopluma hypogea* and Oopsacas minuta in the Mediterranean Sea. Marine Ecology, 28, 10-23.

Baldacconi, R., & Corriero, G. (2009). Effects of the spread of the alga *Caulerpa racemosa* var. *cylindracea* on the sponge assemblage from coralligenous concretions of the Apulian coast (Ionian Sea, Italy). Marine Ecology, 30(3), 337-345.

Baldacconi, R., Cardone, F., Longo, C., Mercurio, M., Marzano, C. N., Gaino, E., & Corriero, G. (2010). Transplantation of *Spongia officinalis* L. (Porifera, Demospongiae): a technical approach for restocking this endangered species. Marine Ecology, 31(2), 309-317.

Ballesteros, E. (2006). Mediterranean coralligenous assemblages: A synthesis of present knowledge. Oceanography and Marine Biology, 44, 123-195.

Barbier, E. B., Hacker, S. D., Kennedy, C., Koch, E. W., Stier, A. C., & Silliman, B. R. (2011). The value of estuarine and coastal ecosystem services. Ecological monographs, 81(2), 169-193.

Barrett, N. S., & Edgar, G. J. (2010). Distribution of benthic communities in the fjord-like Bathurst Channel ecosystem, south-western Tasmania, a globally anomalous estuarine protected area. Aquatic Conservation: Marine and Freshwater Ecosystems, 20(4), 397-406.

Barrett, N. S., Oh, E., Meyer, L., Jones, D., & Edgar, G. J. (2010). A biological monitoring survey of reef biota within Bathurst Channel, Southwest Tasmania. Institute of Marine and Antarctic Studies, Hobart, Tasmania.

Bassindale, R., Davenport, E., Ebling, F. J., Kitching, J. A., Sleigh, M. A., & Sloane, J. F. (1957). The ecology of the Lough Ine Rapids with special reference to water currents: VI. Effects of the Rapids on the hydrography of the South Basin. The Journal of Ecology, 879-900.

Bates, D., Maechler, M., Bolker, B., & Walker, S. (2015). Fitting Linear Mixed-Effects Models Using lme4. Journal of Statistical Software, 67(1), 1–48.

Bates, T. E., & Bell, J. J. (2018). Responses of two temperate sponge species to ocean acidification. New Zealand Journal of Marine and Freshwater Research, 52(2), 247-263.

Battaglini, E., Plonka, B., & Merla, A. (2008). Europe and Central Asia Region. World Bank Environment Matters. Available at: http://go.worldbank.org/83RJ1ZP660: 32-34.

Bax, N., Williamson, A., Aguero, M., Gonzalez, E., Geeves, W. (2003). Marine invasive alien species: a threat to global biodiversity. Marine Policy, 27(4), 313-323.

Beaumont, N. J., Austen, M. C., Atkins, J. P., Burdon, D., Degraer, S., Dentinho, T. P., Derous, S., Holm, P., Horton, T., Van Ierland, E., & Marboe, A. H. (2007). Identification, definition and quantification of goods and services provided by marine biodiversity: implications for the ecosystem approach. Marine Pollution Bulletin, 54(3), 253-265.

Beepat, S. S., Davy, S. K., Woods, L., & Bell, J. J. (2020). Short-term responses of tropical lagoon sponges to elevated temperature and nitrate. Marine Environmental Research, 157, 104922.

Bell, J. J. (2002). The Sponge Community in a Semi-Submerged Temperate Sea Cave: Density, Diversity and Richness. Marine Ecology, 23(4), 297-311.

Bell, J. J. (2004). Evidence for morphology-induced sediment settlement prevention on the tubular sponge Haliclona urceolus. Marine Biology, 146(1), 29-38.

Bell, J. J. (2007). The ecology of sponges in Lough Hyne Marine Nature Reserve (south-west Ireland): past, present and future perspectives. Journal of the Marine Biological Association of the United Kingdom, 87(6), 1655-1668.

Bell, J. J. (2008). The functional roles of marine sponges. Estuarine, Coastal and Shelf Science, 79(3), 341–353.

Bell, J. J., & Barnes, D. K. (2000a). A sponge diversity centre within a marine ‘island’. Hydrobiologia 440, 55–64.

Bell, J. J., & Barnes, D. K. (2000b). The distribution and prevalence of sponges in relation to environmental gradients within a temperate sea lough: inclined cliff surfaces. Diversity and Distributions, 6(6), 305-323.

Bell, J. J., & Barnes, D. K. (2000c). The distribution and prevalence of sponges in relation to environmental gradients within a temperate sea lough: vertical cliff surfaces. Diversity and Distributions, 6(6), 283–303.

Bell, J. J., & Barnes, D. K. (2000d). The influences of bathymetry and flow regime upon the morphology of sublittoral sponge communities. Journal of the Marine Biological Association of the United Kingdom, 80(4), 707-718.

Bell, J. J., & Barnes, D. K. (2001). Sponge morphological diversity: a qualitative predictor of species diversity? Aquatic Conservation: Marine and Freshwater Ecosystems, 11(2), 109-121.

Bell, J. J., & Barnes, D. K. (2002). The relationship between sedimentation, flow rates, depth and time at Lough Hyne Marine Nature Reserve. The Irish Naturalists' Journal, 106-116.

Bell, J. J., & Barnes, D. K. A. (2003). Effect of disturbance on assemblages: an example using Porifera. The Biological Bulletin, 205(2), 144-159.

Bell, J. J., & Turner, J. R. (2000). Factors influencing the density and morphometrics of the cup coral *Caryophyllia smithii* in Lough Hyne. Journal of the Marine Biological Association of the United Kingdom, 80(3), 437-441.

Bell, J. J., Bennett, H. M., Rovellini, A., & Webster, N. S. (2018). Sponges to Be Winners under Near-Future Climate Scenarios. Bioscience, 68(12), 955-968.

Bell, J. J., Davy, S. K., Jones, T., Taylor, M. W., & Webster, N. S. (2013). Could some coral reefs become sponge reefs as our climate changes? Global Change Biology, 19(9), 2613-2624.

Bell, J. J., McGrath, E., Biggerstaff, A., Bates, T., Bennett, H., Marlow, J., & Shaffer, M. (2015a). Sediment impacts on marine sponges. Marine Pollution Bulletin, 94(1-2), 5-13.

Bell, J. J., McGrath, E., Biggerstaff, A., Bates, T., Cárdenas, C. A., & Bennett, H. (2015b). Global conservation status of sponges. Conservation Biology, 29(1), 42-53.

Bell, J. J., McGrath, E., Kandler, N. M., Marlow, J., Beepat, S. S., Bachtiar, R., Shaffer, M. R., Mortimer, C., Micaroni, V., Mobilia, V., Rovellini, A., Harris, B., Farnham, E., Strano, F., & Carballo, J. L. (2020). Interocean patterns in shallow water sponge assemblage structure and function. Biological Reviews, 95(6), 1720–1758.

Bell, J. J., Micaroni, V., Harris, B., Strano, F., Broadribb, M., & Rogers, A. (in review). Global status, impacts and management of rocky Temperate Mesophotic Ecosystems (TMEs). Conservation Biology.

Bell, J. J., Rovellini, A., Davy, S. K., Taylor, M. W., Fulton, E. A., Dunn, M. R., Bennett, H.M., Kandler, N.M., Luter, H.M., & Webster, N. S. (2018). Climate change alterations to ecosystem dominance: how might sponge-dominated reefs function? Ecology, 99(9), 1920-1931.

Bell, J. J., Smith, D., Hannan, D., Haris, A., Jompa, J., & Thomas, L. (2014). Resilience to disturbance despite limited dispersal and self-recruitment in tropical barrel sponges: implications for conservation and management. PLoS One, 9(3), e91635.

Bell, J.J., & Smith, D. (2004). Ecology of sponge assemblages (Porifera) in the Wakatobi region, south-east Sulawesi, Indonesia: richness and abundance. Journal of the Marine Biological Association of the United Kingdom, 84, 581-591

Bendtsen, J., & Hansen, J. L. (2013). Effects of global warming on hypoxia in the Baltic Sea–North Sea transition zone. Ecological Modelling, 264, 17-26.

Benedetti, M. C., Priori, C., Erra, F., & Santangelo, G. (2016). Growth patterns in mesophotic octocorals: timing the branching process in the highly-valuable Mediterranean *Corallium rubrum*. Estuarine, Coastal and Shelf Science, 171, 106-110.

Benjamini, Y., & Hochberg, Y. (1995). Controlling the false discovery rate: a practical and powerful approach to multiple testing. Journal of the Royal Statistical Society: Series B (Methodological), 57(1), 289-300.

Bennett, H. M., Altenrath, C., Woods, L., Davy, S. K., Webster, N. S., & Bell, J. J. (2017). Interactive effects of temperature and pCO 2 on sponges: from the cradle to the grave. Global Change Biology, 23(5), 2031-2046.

Berrill, N. J. (1951). Regeneration and budding in tunicates. Biological Reviews, 26(4), 456-475.

Betti, F., Bavestrello, G., Bo, M., Ravanetti, G., Enrichetti, F., Coppari, M., Cappanera, V., Venturini, S., & Cattaneo-Vietti, R. (2020). Evidences of fishing impact on the coastal gorgonian forests inside the Portofino MPA (NW Mediterranean Sea). Ocean & Coastal Management, 187, 105105.

Beuck, L., Freiwald, A., & Taviani, M. (2010). Spatiotemporal bioerosion patterns in deep-water scleractinians from off Santa Maria di Leuca (Apulia, Ionian Sea). Deep Sea Research Part II: Topical Studies in Oceanography, 57(5-6), 458-470.

Bianchi, C. N., Morri, C., Lasagna, R., Montefalcone, M., Gatti, G., Parravicini, V., & Rovere, A. (2016). Resilience of the marine animal forest. In: S. Rossi, L. Bramanti, A. Gori, C. Orejas (Eds) Marine animal forests: the ecology of benthic biodiversity hotspots. Springer, Cham, Switzerland, pp. 1241-1270.

Bijma, J., Pörtner, H. O., Yesson, C., & Rogers, A. D. (2013). Climate change and the oceans–What does the future hold? Marine Pollution Bulletin, 74(2), 495–505.

Blasnig, M., Riedel, B., Schiemer, L., Zuschin, M., & Stachowitsch, M. (2013). Short-term post-mortality scavenging and longer term recovery after anoxia in the northern Adriatic Sea. Biogeosciences, 10(11), 7647-7659.

Bo, M., Bava, S., Canese, S., Angiolillo, M., Cattaneo-Vietti, R., & Bavestrello, G. (2014). Fishing impact on deep Mediterranean rocky habitats as revealed by ROV investigation. Biological Conservation, 171, 167-176.

Bo, M., Bertolino, M., Bavestrello, G., Canese, S., Giusti, M., Angiolillo, M., Pansini, M., & Taviani, M. (2012). Role of deep sponge grounds in the Mediterranean Sea: a case study in southern Italy. Hydrobiologia, 687(1), 163-177.

Boesch, D. F., Brinsfield, R. B., & Magnien, R. E. (2001). Chesapeake Bay eutrophication. Journal of Environmental Quality, 30(2), 303-320.

Bongaerts, P., Perez-Rosales, G., Radice, V. Z., Eyal, G., Gori, A., Gress, E., Hammerman, N. M., Hernandez-Agreda, A., Laverick, J., Muir, P., Pinheiro, H., Pyle, R. L., Rocha, L., Turner, J. A., & Booker, R. (2019). Mesophotic.org: a repository for scientific information on mesophotic ecosystems. Database 2019, baz140.

Bongaerts, P., Ridgway, T., Sampayo, E. M., & Hoegh-Guldberg, O. (2010). Assessing the 'deep reef refugia' hypothesis: focus on Caribbean reefs. Coral Reefs, 29(2), 309-327.

Borja, A. (2014). Grand challenges in marine ecosystems ecology. Frontiers in Marine Science, 1, 1.

Borja, Á., Dauer, D. M., & Grémare, A. (2012). The importance of setting targets and reference conditions in assessing marine ecosystem quality. Ecological Indicators, 12(1), 1-7.

Borja, A., Elliott, M., Andersen, J. H., Cardoso, A. C., Carstensen, J., Ferreira, J. G., Heiskanen, A.S., Marques, J.C., Neto, J.M., Teixeira, H., & Uusitalo, L. (2013). Good environmental status of marine ecosystems: what is it and how do we know when we have attained it? Marine Pollution Bulletin, 76(1-2), 16-27.

Borja, A., Elliott, M., Snelgrove, P. V., Austen, M. C., Berg, T., Cochrane, S., Carstensen, J., Danovaro, R., Greenstreet, S., Heiskanen, A.S., & Lynam, C. P. (2016). Bridging the gap between policy and science in assessing the health status of marine ecosystems. Frontiers in Marine Science, 3, 175.

Boström, C., Bonsdorff, E., Kangas, P., & Norkko, A. (2002). Long-term changes of a brackish-water eelgrass (*Zostera marina* L.) community indicate effects of coastal eutrophication. Estuarine, Coastal and Shelf Science, 55(5), 795-804.

Bradstock, M., & Gordon, D. P. (1983). Coral-like bryozoan growths in Tasman Bay, and their protection to conserve commercial fish stocks. New Zealand Journal of Marine and Freshwater Research, 17(2), 159-163.

Bramanti, L., Benedetti, M. C., Cupido, R., Cocito, S., Priori, C., Erra, F., Erra, F., Iannelli, M., & Santangelo, G. (2017). Demography of animal forests: The example of Mediterranean gorgonians. In: S. Rossi, L. Bramanti, A. Gori, C. Orejas (Eds) Marine animal forests: the ecology of benthic biodiversity hotspots. Springer, Cham, Switzerland, pp. 529-548.

Bramanti, L., Vielmini, I., Rossi, S., Tsounis, G., Iannelli, M., Cattaneo-Vietti, R., Priori, C., & Santangelo, G. (2014). Demographic parameters of two populations of red coral (*Corallium rubrum* L. 1758) in the North Western Mediterranean. Marine Biology, 161(5), 1015-1026.

Brantley, S. E., Molinski, T. F., Preston, C. M., & DeLong, E. F. (1995). Brominated acetylenic fatty acids from *Xestospongia* sp., a marine spongebacteria association. Tetrahedron, 51(28), 7667-7672.

Breitburg, D. L. (1990). Near-shore hypoxia in the Chesapeake Bay: patterns and relationships among physical factors. Estuarine, Coastal and Shelf Science, 30(6), 593–609.

Bridge, T. C., Done, T. J., Friedman, A., Beaman, R. J., Williams, S. B., Pizarro, O., & Webster, J. M. (2011). Variability in mesophotic coral reef communities along the Great Barrier Reef, Australia. Marine Ecology Progress Series, 428, 63-75.

Brind'Amour, A., Laffargue, P., Morin, J., Vaz, S., Foveau, A., & Le Bris, H. (2014). Morphospecies and taxonomic sufficiency of benthic megafauna in scientific bottom trawl surveys. Continental Shelf Research, 72, 1-9.

Brocks, J. J., Jarrett, A. J., Sirantoine, E., Hallmann, C., Hoshino, Y., & Liyanage, T. (2017). The rise of algae in Cryogenian oceans and the emergence of animals. Nature, 548(7669), 578-581.

Brooks, M. E., Kristensen, K., Van Benthem, K. J., Magnusson, A., Berg, C. W., Nielsen, A., Skaug, H. J., Machler, M. & Bolker, B.M. (2017). glmmTMB balances speed and flexibility among packages for zero-inflated generalized linear mixed modeling. The R Journal, 9(2), 378–400.

Bruno, J. F., & Bertness, M. D. (2001). Habitat modification and facilitation in benthic marine communities. In: M. D. Bertness, S. D. Gaines, M. E. Hay (Eds) Marine Community Ecology. Sinauer Associates, Inc., Sunderland, Massachusetts, pp. 201-218

Brusca, R. C., Moore, W., & Schuster, M. (2016). Invertebrates. Massachusetts, Sinauer Associated. Inc, Publishers.

Buckley, H. L., Day, N. J., Case, B. S., Lear, G., & Ellison, A. M. (2019). Multivariate methods for testing hypotheses of temporal community dynamics. bioRxiv, 362822.

Bumett, L. E., & Stickle, W. B. (2001). Physiological responses to hypoxia. In: N. N. Rabalais, R. E. Turner (Eds). Coastal and Estuarine Studies, Volume 58. Coastal hypoxia: consequences for living resources and ecosystems. AGU Publications, pp. 101–114.

Canessa, M., Bavestrello, G., Bo, M., Trainito, E., Panzalis, P., Navone, A., Caragnano, A., Betti, F., & Cattaneo-Vietti, R. (2020). Coralligenous assemblages differ between limestone and granite: a case study at the Tavolara-Punta Coda Cavallo Marine Protected Area (NE Sardinia, Mediterranean Sea). Regional Studies in Marine Science, 35, 101159.

Capdevila, P., Stott, I., Oliveras Menor, I., Stouffer, D. B., Raimundo, R. L., White, H., Barbour, M., & Salguero-Gómez, R. (2021). Reconciling resilience across ecological systems, species and subdisciplines. Journal of Ecology, 109, 3102–3113

Caputi, L., Crocetta, F., Toscano, F., Sordino, P., & Cirino, P. (2015). Long-term demographic and reproductive trends in *Cliona intestinalis* sp. A. Marine Ecology, 36(1), 118-128.

Carballo, J. L. (2006). Effect of natural sedimentation on the structure of tropical rocky sponge assemblages. Ecoscience, 13(1), 119-130.

Carballo, J. L., & Bell, J. J. (2017). Climate Change, Ocean Acidification and Sponges: Impacts Across Multiple Levels of Organization. Springer.

Carballo, J. L., & Naranjo, S. (2002). Environmental assessment of a large industrial marine complex based on a community of benthic filter-feeders. Marine Pollution Bulletin, 44(7), 605-610.

Carballo, J. L., Naranjo, S. A., & García-Gómez, J. C. (1996). Use of marine sponges as stress indicators in marine ecosystems at Algeciras Bay (southern Iberian Peninsula). Marine Ecology Progress Series, 135, 109-122.

Cardone, F., Corriero, G., Longo, C., Mercurio, M., Tarantini, S. O., Gravina, M. F., Lisco, S., Moretti, M., De Giosa, F., Giangrande, A., & Marzano, C. N. (2020). Massive bioconstructions built by *Neopycnodonte cochlear* (Mollusca, Bivalvia) in a mesophotic environment in the central Mediterranean Sea. Scientific Reports, 10(1), 1-16.

Carlton, J. T. (1989). Man's role in changing the face of the ocean: biological invasions and implications for conservation of near-shore environments. Conservation Biology, 3(3), 265-273.

Cecchi, E., Gennaro, P., Piazzi, L., Ricevuto, E., & Serena, F. (2014). Development of a new biotic index for ecological status assessment of Italian coastal waters based on coralligenous macroalgal assemblages. European Journal of Phycology, 49(3), 298-312.

Cerrano, C., Bastari, A., Calcinai, B., Di Camillo, C., Pica, D., Puce, S., Valisano, L., & Torsani, F. (2019). Temperate mesophotic ecosystems: gaps and perspectives of an emerging conservation challenge for the Mediterranean Sea. The European Zoological Journal, 86(1), 370-388.

Cerrano, C., Bavestrello, G., Bianchi, C. N., Calcinai, B., Cattaneo-Vietti, R., Morri, C., & Sarà, M. (2001). The role of sponge bioerosion in Mediterranean coralligenous accretion. In: Mediterranean Ecosystems. Springer, Milano, pp. 235-240.

Cerrano, C., Bavestrello, G., Bianchi, C. N., Cattaneo-Vietti, R., Bava, S., Morganti, C., Morri, C., Picco, P., Sara, G., Schiaparelli, S. and Siccardi, A., & Sponga, F. (2000). A catastrophic mass-mortality episode of gorgonians and other organisms in the Ligurian Sea (North-western Mediterranean), summer 1999. Ecology Letters, 3(4), 284-293.

Cerrano, C., Calcinai, B., Di Camillo, C. G., Valisano, L., & Bavestrello, G. (2007). How and why do sponges incorporate foreign material? Strategies in Porifera. Porifera Research: Biodiversity, Innovation and Sustainability. Série Livros, 28, 239-246.

Cerrano, C., Cardini, U., Bianchelli, S., Corinaldesi, C., Pusceddu, A., & Danovaro, R. (2013). Red coral extinction risk enhanced by ocean acidification. Scientific Reports, 3(1), 1-7.

Cerrano, C., Danovaro, R., Gambi, C., Pusceddu, A., Riva, A., & Schiaparelli, S. (2010). Gold coral (*Savalia savaglia*) and gorgonian forests enhance benthic biodiversity and ecosystem functioning in the mesophotic zone. Biodiversity and Conservation, 19(1), 153-167.

Chan, B. K. (2007). Ecology and biodiversity of rocky intertidal barnacles along a latitudinal gradient; Japan, Taiwan and Hong Kong. Publications of the Seto Marine Biological Laboratory. Special Publication Series., 8, 1-10.

Chan, H. Y., Xu, W. Z., Shin, P. K. S., & Cheung, S. G. (2008). Prolonged exposure to low dissolved oxygen affects early development and swimming behaviour in the gastropod *Nassarius festivus* (Nassariidae). Marine Biology, 153(4), 735-743.

Cheung, W. W., Lam, V. W., Sarmiento, J. L., Kearney, K., Watson, R., & Pauly, D. (2009). Projecting global marine biodiversity impacts under climate change scenarios. Fish and Fisheries, 10(3), 235-251.

Chimienti, G., De Padova, D., Mossa, M., & Mastrototaro, F. (2020). A mesophotic black coral forest in the Adriatic Sea. Scientific Reports, 10(1), 1-15.

Chimienti, G., Stithou, M., Mura, I. D., Mastrototaro, F., D'Onghia, G., Tursi, A., Izzi, C., & Fraschetti, S. (2017). An explorative assessment of the importance of Mediterranean Coralligenous habitat to local economy: The case of recreational diving. Journal of Environmental Accounting and Management, 5(4), 315-325.

Chu, J. W., Curkan, C., & Tunnicliffe, V. (2018). Drivers of temporal beta diversity of a benthic community in a seasonally hypoxic fjord. Royal Society Open Science, 5(4), 172284.

Clarke, K. R., & Gorley, R. N. (2015). Getting started with PRIMER v7. PRIMER-E, Plymouth, UK.

Cloern, J. E., Foster, S. Q., & Kleckner, A. E. (2014). Phytoplankton primary production in the world's estuarine-coastal ecosystems. Biogeosciences, 11(9), 2477-2501.

Cocito, S. (2004). Bioconstruction and biodiversity: their mutual influence. Scientia Marina, 68(S1), 137-144.

Cockcroft, A. C. (2001). *Jasus lalandii* 'walkouts' or mass strandings in South Africa during the 1990s: an overview. Marine and Freshwater Research, 52(8), 1085-1093.

Cole, D. B., Mills, D. B., Erwin, D. H., Sperling, E. A., Porter, S. M., Reinhard, C. T., & Planavsky, N. J. (2020). On the co-evolution of surface oxygen levels and animals. Geobiology, 18(3), 260–281.

Cole, M., Lindeque, P., Halsband, C., & Galloway, T. S. (2011). Microplastics as contaminants in the marine environment: a review. Marine Pollution Bulletin, 62(12), 2588-2597.

Colella, M. A., Ruzicka, R. R., Kidney, J. A., Morrison, J. M., & Brinkhuis, V. B. (2012). Cold-water event of January 2010 results in catastrophic benthic mortality on patch reefs in the Florida Keys. Coral reefs, 31(2), 621-632.

Collins, S. L., Micheli, F., & Hartt, L. (2000). A method to determine rates and patterns of variability in ecological communities. Oikos, 91(2), 285-293.

Colman, A. S. (2015). Sponge symbionts and the marine P cycle. Proceedings of the National Academy of Sciences, 112(14), 4191-4192.

Coma, R., Ribes, M., Serrano, E., Jiménez, E., Salat, J., & Pascual, J. (2009). Global warming-enhanced stratification and mass mortality events in the Mediterranean. Proceedings of the National Academy of Sciences, 106(15), 6176-6181.

Connolly, S. R., & Baird, A. H. (2010). Estimating dispersal potential for marine larvae: dynamic models applied to scleractinian corals. Ecology, 91(12), 3572-3583.

Connor, D.W., J.H. Allen, N. Golding, K.L. Howell, L.M. Lieberknecht, K.O. Northen and J.B. Reker (2004) The Marine Habitat Classification for Britain and Ireland Version 04.05 ISBN 1 861 07561 8. In: JNCC (2015) The Marine Habitat Classification for Britain and Ireland Version 15.03.

Cook, S. D. C. (2010). New Zealand coastal marine invertebrates. Canterbury University Press.

Coppari, M., Zanella, C., & Rossi, S. (2019). The importance of coastal gorgonians in the blue carbon budget. Scientific Reports, 9(1), 1-12.

Cornwall, C. E., Hepburn, C. D., Pilditch, C. A., & Hurd, C. L. (2013). Concentration boundary layers around complex assemblages of macroalgae: Implications for the effects of ocean acidification on understory coralline algae. Limnology and Oceanography, 58(1), 121–130.

Corriero, G., Pierri, C., Mercurio, M., Marzano, C. N., Tarantini, S. O., Gravina, M. F., Lisco, S., Moretti, M., De Giosa, F., Valenzano, E., & Giangrande, A. (2019). A Mediterranean mesophotic coral reef built by non-symbiotic scleractinians. Scientific Reports, 9(1), 1-17.

Costanza, R., d'Arge, R., De Groot, R., Farber, S., Grasso, M., Hannon, B., Limburg, K., Naeem, S., O'neill, R.V., Paruelo, J., & Raskin, R. G. (1997). The value of the world's ecosystem services and natural capital. Nature, 387(6630), 253.

Costanza, R., De Groot, R., Sutton, P., Van der Ploeg, S., Anderson, S. J., Kubiszewski, I., Farber, S., & Turner, R. K. (2014). Changes in the global value of ecosystem services. Global Environmental Change, 26, 152-158.

Costello, M. J. (2009). Distinguishing marine habitat classification concepts for ecological data management. Marine Ecology Progress Series, 397, 253-268.

Costello, M.J., & Emblow, C.S. (1997) Marine areas of nature conservation importance in Ireland. BioMarLife project.

Crain, C. M., Halpern, B. S., Beck, M. W., & Kappel, C. V. (2009). Understanding and managing human threats to the coastal marine environment. Annals of the New York Academy of Sciences, 1162(1), 39-62.

Cummings, V. J., Beaumont, J., Mobilia, V., Bell, J. J., Tracey, D., Clark, M. R., & Barr, N. (2020). Responses of a common New Zealand coastal sponge to elevated suspended sediments: Indications of resilience. Marine Environmental Research, 155, 104886.

Danovaro, R., Carugati, L., Berzano, M., Cahill, A. E., Carvalho, S., Chenuil, A., Corinaldesi, C., Cristina, S., David, R., Dell'Anno, A., & Dzhembekova, N. (2016). Implementing and innovating marine monitoring approaches for assessing marine environmental status. Frontiers in Marine Science, 3, 213.

Davenport, J., Jessopp, M., Harman, L., Micaroni, V., & McAllen, R. (2021). Diurnal and nocturnal scavenger communities differ at two shallow-water depths in an Irish marine lough. Estuarine, Coastal and Shelf Science, 262, 107580.

Davidson, K., Gowen, R. J., Harrison, P. J., Fleming, L. E., Hoagland, P., & Moschonas, G. (2014). Anthropogenic nutrients and harmful algae in coastal waters. Journal of Environmental Management, 146, 206-216.

Dayton, P. K., Robilliard, G. A., Paine, R. T., & Dayton, L. B. (1974). Biological accommodation in the benthic community at McMurdo Sound, Antarctica. Ecological Monographs, 44(1), 105-128.

Dayton, P. K., Tegner, M. J., Edwards, P. B., & Riser, K. L. (1998). Sliding baselines, ghosts, and reduced expectations in kelp forest communities. Ecological Applications, 8(2), 309-322.

de Caralt, S., & Cebrian, E. (2013). Impact of an invasive alga (*Womersleyella setacea*) on sponge assemblages: compromising the viability of future populations. Biological Invasions, 15(7), 1591-1600.

de Goeij, J. M., van den Berg, H., van Oostveen, M. M., Epping, E. H., & Van Duyl, F. C. (2008). Major bulk dissolved organic carbon (DOC) removal by encrusting coral reef cavity sponges. Marine Ecology Progress Series, 357, 139-151.

De Groot, R. S., Blignaut, J., Van Der Ploeg, S., Aronson, J., Elmqvist, T., & Farley, J. (2013). Benefits of investing in ecosystem restoration. Conservation Biology, 27(6), 1286-1293.

De Groot, R., Brander, L., Van Der Ploeg, S., Costanza, R., Bernard, F., Braat, L., Christie, M., Crossman, N., Ghermandi, A., Hein, L., & Hussain, S. (2012). Global estimates of the value of ecosystems and their services in monetary units. Ecosystem Services, 1(1), 50-61.

de Ville d'Avray, L. T., Ami, D., Chenuil, A., David, R., & Féral, J. P. (2019). Application of the ecosystem service concept at a small-scale: The cases of coralligenous habitats in the North-western Mediterranean Sea. Marine Pollution Bulletin, 138, 160-170.

De Zwaan, A., Cortesi, P., Van den Thillart, G., Roos, J., & Storey, K. B. (1991). Differential sensitivities to hypoxia by two anoxia-tolerant marine molluscs: a biochemical analysis. Marine Biology, 111(3), 343–351.

DeJong, T. M. (1975). A comparison of three diversity indices based on their components of richness and evenness. Oikos, 222-227.

Desai, D. V., & Prakash, S. (2009). Physiological responses to hypoxia and anoxia in *Balanus amphitrite* (Cirripedia: Thoracica). Marine Ecology Progress Series, 390, 157–166.

Deter, J., Descamp, P., Ballesta, L., Boissery, P., & Holon, F. (2012). A preliminary study toward an index based on coralligenous assemblages for the ecological status assessment of Mediterranean French coastal waters. Ecological Indicators, 20, 345-352.

Di Camillo, C. G., & Cerrano, C. (2015). Mass mortality events in the NW Adriatic Sea: phase shift from slow-to fast-growing organisms. PloS One, 10(5), e0126689.

Di Camillo, C. G., Ponti, M., Bavestrello, G., Krzelj, M., & Cerrano, C. (2018). Building a baseline for habitat-forming corals by a multi-source approach, including Web Ecological Knowledge. Biodiversity and Conservation, 27(5), 1257-1276.

Diamond, J. M. (1969). Avifaunal equilibria and species turnover rates on the Channel Islands of California. Proceedings of the National Academy of Sciences, 64(1), 57-63.

Diaz, R. J., & Breitburg, D. L. (2009). The hypoxic environment. In: J. G. Richards, A. P. Farrell, C. J. Brauner (Eds) Fish physiology, Volume 27. Academic Press. pp. 1–23.

Diaz, R. J., & Rosenberg, R. (1995). Marine benthic hypoxia: a review of its ecological effects and the behavioural responses of benthic macrofauna. Oceanography and Marine Biology. An annual review, 33, 245–03.

Diaz, R. J., & Rosenberg, R. (2008). Spreading dead zones and consequences for marine ecosystems. Science, 321(5891), 926–929.

Diaz, R. J., & Rosenberg, R. (2011). Introduction to environmental and economic consequences of hypoxia. International Journal of Water Resources Development, 27(1), 71–82.

Dodds, L. A., Roberts, J. M., Taylor, A. C., & Marubini, F. (2007). Metabolic tolerance of the cold-water coral *Lophelia pertusa* (Scleractinia) to temperature and dissolved oxygen change. Journal of Experimental Marine Biology and Ecology, 349(2), 205–214.

Doney, S. C. (2010). The growing human footprint on coastal and open-ocean biogeochemistry. Science, 328(5985), 1512–1516.

Drew, J. A. (2005). Use of traditional ecological knowledge in marine conservation. Conservation Biology, 19(4), 1286-1293.

Dulvy, N.K., Sadovy, Y., & Reynolds, J.D. (2003). Extinction vulnerability in marine populations. Fish 4, 25–64.

EEA, European Environmental Agency (2019) EUNIS habitat classification. https://www.eea.europa.eu/data-and-maps/data/eunis-habitat-classification

Ellington, W. R. (1982). Metabolic responses of the sea anemone *Bunodosoma cavernata* (Bosc) to declining oxygen tensions and anoxia. Physiological Zoology, 55(3), 240–249.

Elton, C. S. (1958). The ecology of invasions by animals and plants. University of Chicago Press.

Enrichetti, F., Bava, S., Bavestrello, G., Betti, F., Lanteri, L., & Bo, M. (2019a). Artisanal fishing impact on deep coralligenous animal forests: a Mediterranean case study of marine vulnerability. Ocean & Coastal Management, 177, 112-126.

Enrichetti, F., Bavestrello, G., Betti, F., Coppari, M., Toma, M., Pronzato, R., Canese, S., Bertolino, M., Costa, G., Pansini, & Bo, M. (2020). Keratose-dominated sponge grounds from temperate mesophotic ecosystems (NW Mediterranean Sea). Marine Ecology, 41(6), e12620.

Enrichetti, F., Bo, M., Morri, C., Montefalcone, M., Toma, M., Bavestrello, G., Tunesi, L., Canese, S., Giusti, M., Salvati, E., & Bertolotto, R. M. (2019b). Assessing the environmental status of temperate mesophotic reefs: A new, integrated methodological approach. Ecological Indicators, 102, 218-229.

Ereskovsky, A. V. (2010). The comparative embryology of sponges. Springer Science & Business Media.

Eriksson, B. K., & Johansson, G. (2005). Effects of sedimentation on macroalgae: species-specific responses are related to reproductive traits. Oecologia, 143(3), 438-448.

Estes, J. A., Duggins, D. O., & Rathbun, G. B. (1989). The ecology of extinctions in kelp forest communities. Conservation Biology, 3(3), 252-264.

Faganeli, J., Avčin, A., Fanuko, N., Malej, A., Turk, V., Tušnik, P., Vrišer, B., & Vukovič, A. (1985). Bottom layer anoxia in the central part of the Gulf of Trieste in the late summer of 1983. Marine Pollution Bulletin, 16(2), 75-78.

Ferretti, F., Crowder, L. B., Micheli, F., Blight, L. K. (2015). Using Disparate Datasets to Reconstruct Historical Baselines of Animal Populations, in: J. N. Kittinger, L. McClenachan, K. B. Gedan, L.K. Blight (Eds) Marine historical ecology in conservation: Applying the past to manage for the future. University of California Press, Berkeley, California.

Ferrigno, F., Appolloni, L., Russo, G. F., & Sandulli, R. (2018). Impact of fishing activities on different coralligenous assemblages of Gulf of Naples (Italy). Journal of the Marine Biological Association of the United Kingdom, 98(1), 41-50.

Ferrigno, F., Russo, G. F., & Sandulli, R. (2017). Coralligenous Bioconstructions Quality Index (CBQI): a synthetic indicator to assess the status of different types of coralligenous habitats. Ecological Indicators, 82, 271-279.

Filbee-Dexter, K., & Wernberg, T. (2018). Rise of turfs: a new battlefront for globally declining kelp forests. Bioscience, 68(2), 64-76.

Folke, C., Carpenter, S., Walker, B., Scheffer, M., Elmqvist, T., Gunderson, L., & Holling, C. S. (2004). Regime shifts, resilience, and biodiversity in ecosystem management. Annual Review of Ecology, Evolution, and Systematics, 35, 557-581.

Foote, K. J., Joy, M. K., & Death, R. G. (2015). New Zealand dairy farming: milking our environment for all its worth. Environmental Management, 56(3), 709-720.

Försterra, G., Häussermann, V., & Laudien, J. (2017). Animal Forests in the Chilean fjords: discoveries, perspectives and threats in shallow and deep waters. In: S. Rossi, L. Bramanti, A. Gori, C. Orejas (Eds) Marine animal forests: the ecology of benthic biodiversity hotspots. Springer, Cham, Switzerland, pp. 277-314.

Försterra, G., Häussermann, V., Laudien, J., Jantzen, C., Sellanes, J., & Muñoz, P. (2014). Mass die-off of the cold-water coral *Desmophyllum dianthus* in the Chilean Patagonian fjord region. Bulletin of Marine Science, 90(3), 895-899.

Fowler, S., & Laffoley, D. (1993). Stability in Mediterranean-Atlantic sessile epifaunal communities at the northern limits of their range. Journal of Experimental Marine Biology and Ecology, 172(1-2), 109 ( )5(1)TBogy, 173 (ne)-1Tj□

Frieder, C. A., Nam, S. H., Martz, T. R., & Levin, L. A. (2012). High temporal and spatial variability of dissolved oxygen and pH in a nearshore California kelp forest. Biogeosciences, 9(10), 3917–3930.

Gaino, E., Pronzato, R., Corriero, G., & Buffa, P. (1992). Mortality of commercial sponges: incidence in two Mediterranean areas. Italian Journal of Zoology, 59(1), 79-85.

Gallagher, M. C., Culloty, S. C., Davenport, J., Harman, L., Jessopp, M. J., Kerrigan, C., Murray, C., O'Riordan, R.M., & McAllen, R. (2017). Short-term losses and long-term gains: The non-native species *Austrominius modestus* in Lough Hyne Marine Nature Reserve. Estuarine, Coastal and Shelf Science, 191, 96-105.

Gamenick, I., Jahn, A., Vopel, K., & Giere, O. (1996). Hypoxia and sulphide as structuring factors in a macrozoobenthic community on the Baltic Sea shore: colonisation studies and tolerance experiments. Marine Ecology Progress Series, 144, 73-85.

Garrabou, J., Coma, R., Bensoussan, N., Bally, M., Chevaldonné, P., Cigliano, M., Diaz, D., Harmelin, J. G., Gambi, M. C., Kersting, D. K., Ledoux, J. B., Lejeusne, C., Linares, C., Marschal, C., Pérez, T., Ribes, M., Romano, J. C., Serrano, E., Teixido, N., Torrents, O., Zabala, M., Zuberer, F., & Cerrano, C. (2009). Mass mortality in Northwestern Mediterranean rocky benthic communities: effects of the 2003 heat wave. Global Change Biology, 15(5), 1090-1103.

Garrabou, J., Sala, E., Arcas, A., & Zabala, M. (1998). The impact of diving on rocky sublittoral communities: a case study of a bryozoan population. Conservation Biology, 12(2), 302-312.

Gatti, G., Bianchi, C. N., Morri, C., Montefalcone, M., & Sartoretto, S. (2015). Coralligenous reefs state along anthropized coasts: application and validation of the COARSE index, based on a rapid visual assessment (RVA) approach. Ecological Indicators, 52, 567-576.

Gazave, E., Lapébie, P., Ereskovsky, A. V., Vacelet, J., Renard, E., Cárdenas, P., & Borchiellini, C. (2011). No longer Demospongiae: Homoscleromorpha formal nomination as a fourth class of Porifera. In: M. Maldonado, X. Turon, M. Becerro, M. J. Uriz (Eds) Ancient Animals, New Challenges. Springer, Dordrecht, pp. 3-10.

Gennaro, P., & Piazzi, L. (2011). Synergism between two anthropic impacts: *Caulerpa racemosa* var. *cylindracea* invasion and seawater nutrient enrichment. Marine Ecology Progress Series, 427, 59-70.

Gerrodette, T., & Flechsig, A. O. (1979). Sediment-induced reduction in the pumping rate of the tropical sponge *Verongia lacunosa*. Marine Biology, 55(2), 103-110.

Giangrande, A. (2003). Biodiversity, conservation, and the 'Taxonomic impediment'. Aquatic Conservation: Marine and Freshwater Ecosystems, 13(5), 451-459.

Giraldo-Ospina, A., Kendrick, G. A., & Hovey, R. K. (2020). Depth moderates loss of marine foundation species after an extreme marine heatwave: could deep temperate reefs act as a refuge? Proceedings of the Royal Society B, 287(1928), 20200709.

Gladstone-Gallagher, R. V., Pilditch, C. A., Stephenson, F., & Thrush, S. F. (2019). Linking traits across ecological scales determines functional resilience. Trends in Ecology & Evolution, 34(12), 1080-1091.

Glynn, P. W., & Manzello, D. P. (2015). Bioerosion and coral reef growth: a dynamic balance. In: C. Birkeland (Ed) Coral reefs in the Anthropocene, Springer, Dordrecht, pp. 67-97.

Gobler, C. J., & Baumann, H. (2016). Hypoxia and acidification in ocean ecosystems: coupled dynamics and effects on marine life. Biology Letters, 12(5), 20150976.

Gochfeld, D. J., Olson, J. B., Chaves-Fonnegra, A., Smith, T. B., Ennis, R. S., & Brandt, M. E. (2020). Impacts of hurricanes Irma and Maria on coral reef sponge communities in St. Thomas, US Virgin Islands. Estuaries and Coasts, 1-13.

Goldstein, J., Riisgård, H. U., & Larsen, P. S. (2019). Exhalant jet speed of single-osculum explants of the demosponge *Halichondria panicea* and basic properties of the sponge-pump. Journal of Experimental Marine Biology and Ecology, 511, 82–90.

Gómez-Gras, D., Linares, C., Dornelas, M., Madin, J. S., Brambilla, V., Ledoux, J. B., López-Sendino, P., Bensoussan, N., & Garrabou, J. (2021). Climate change transforms the functional identity of Mediterranean coralligenous assemblages. Ecology Letters, 24(5), 1038-1051.

Goñi, R., Quetglas, A., & Reñones, O. (2006). Spillover of spiny lobsters Palinurus elephas from a marine reserve to an adjoining fishery. Marine Ecology Progress Series, 308, 207-219.

Goodwin, C. E., Strain, E. M., Edwards, H., Bennett, S. C., Breen, J. P., & Picton, B. E. (2013). Effects of two decades of rising sea surface temperatures on sublittoral macrobenthos communities in Northern Ireland, UK. Marine Environmental Research, 85, 34-44.

Goodwin, C., & Picton, B. (2011). Sponge Biodiversity of the United Kingdom. National Museums Northern Ireland.

Goodwin, C., Rodolfo-Metalpa, R., Picton, B., & Hall-Spencer, J. M. (2014). Effects of ocean acidification on sponge communities. Marine Ecology, 35, 41-49.

Gori, A., Bavestrello, G., Grinyó, J., Dominguez-Carrió, C., Ambroso, S., & Bo, M. (2017). Animal forests in deep coastal bottoms and continental shelf of the Mediterranean Sea. In: S. Rossi, L. Bramanti, A. Gori, C. Orejas (Eds) Marine animal forests: the ecology of benthic biodiversity hotspots. Springer, Cham, Switzerland, pp. 207-234.

Gorr, T. A., Wichmann, D., Hu, J., Hermes-Lima, M., Welker, A. F., Terwilliger, N., Wren, J.F., Viney, M., Morris, S., Nilsson, G.E. and Deten, A., & Deten, A. (2010). Hypoxia tolerance in animals: biology and application. Physiological and Biochemical Zoology, 83(5), 733-752.

Grall, J., & Chauvaud, L. (2002). Marine eutrophication and benthos: the need for new approaches and concepts. Global Change Biology, 8(9), 813-830.

Granek, E. F., Polasky, S., Kappel, C. V., Reed, D. J., Stoms, D. M., Koch, E. W., Kennedy, C.J., Cramer, L.A., Hacker, S.D., Barbier, E.B., & Aswani, S. (2010). Ecosystem services as a common language for coastal ecosystem-based management. Conservation Biology, 24(1), 207-216.

Gray, J. S. (1997). Marine biodiversity: patterns, threats and conservation needs. Biodiversity & Conservation, 6(1), 153-175.

Gray, J. S., Wu, R. S. S., & Or, Y. Y. (2002). Effects of hypoxia and organic enrichment on the coastal marine environment. Marine Ecology Progress Series, 238, 249-279.

Griffiths, S. M., Taylor-Cox, E. D., Behringer, D. C., Butler, M. J., & Preziosi, R. F. (2020). Using genetics to inform restoration and predict resilience in declining populations of a keystone marine sponge. Biodiversity and Conservation, 29(4), 1383-1410.

Gruber, R. K., Lowe, R. J., & Falter, J. L. (2017). Metabolism of a tide-dominated reef platform subject to extreme diel temperature and oxygen variations. Limnology and Oceanography, 62(4), 1701–1717.

Gunda, V. G., & Janapala, V. R. (2009). Effects of dissolved oxygen levels on survival and growth in vitro of *Haliclona pigmentifera* (Demospongiae). Cell and Tissue Research, 337(3), 527-535.

Guppy, M., & Withers, P. (1999). Metabolic depression in animals: physiological perspectives and biochemical generalizations. Biological Reviews, 74(1), 1-40.

Haas, A. F., Smith, J. E., Thompson, M., & Deheyn, D. D. (2014). Effects of reduced dissolved oxygen concentrations on physiology and fluorescence of hermatypic corals and benthic algae. PeerJ, 2, e235.

Hagerman, L. (1998). Physiological flexibility; a necessity for life in anoxic and sulphidic habitats. Hydrobiologia, 375, 241–254.

Halford, A., Cheal, A. J., Ryan, D., & Williams, D. M. (2004). Resilience to large-scale disturbance in coral and fish assemblages on the Great Barrier Reef. Ecology, 85(7), 1892-1905.

Hallett, L. M., Jones, S. K., MacDonald, A. A. M., Jones, M. B., Flynn, D. F., Ripplinger, J., Slaughter, P., Gries, C., & Collins, S. L. (2016). *codyn*: An r package of community dynamics metrics. Methods in Ecology and Evolution, 7(10), 1146-1151.

Halpern, B. S., Selkoe, K. A., Micheli, F., & Kappel, C. V. (2007). Evaluating and ranking the vulnerability of global marine ecosystems to anthropogenic threats. Conservation Biology, 21(5), 1301-1315.

Harris, B., Davy, S. K., & Bell, J. J. (2021). Benthic community composition of temperate mesophotic ecosystems (TMEs) in New Zealand: sponge domination and contribution to habitat complexity. Marine Ecology Progress Series, 671, 21-43.

Häussermann, V., Försterra, G., Melzer, R. R., & Meyer, R. (2013). Gradual changes of benthic biodiversity in Comau fjord, Chilean Patagonia–lateral observations over a decade of taxonomic research. Spixiana, 36(2), 161-171.

Heip, C. (1995). Eutrophication and zoobenthos dynamics. Ophelia, 41(1), 113-136.

Heip, C., Hummel, H., Van Avesaath, P., Appeltans, W., Arvanitidis, C., Aspden, R., Austen, M., Boero, F., Bouma, T.J., Boxshall, C., & Buchholz, F. (2009). Marine biodiversity and ecosystem functioning. Printbase, Dublin, Ireland.

Hentschel, U., Fieseler, L., Wehrl, M., Gernert, C., Steinert, M., Hacker, J., & Horn, M. (2003). Microbial diversity of marine sponges. In: W. E. G. Müller (Ed) Progress in Molecular and Subcellular Biology. Sponges (Porifera). Springer, pp 59–88.

Hentschel, U., Usher, K. M., & Taylor, M. W. (2006). Marine sponges as microbial fermenters. FEMS microbiology ecology, 55(2), 167–177.

Hervé, M. (2021). *RVAideMemoire*: testing and plotting procedures for biostatistics. R package version 0.9-79. https://cran.r-project.org/web/packages/RVAideMemoire/index.html

Heyns, E. R., Bernard, A. T. F., Richoux, N. B., & Götz, A. (2016). Depth-related distribution patterns of subtidal macrobenthos in a well-established marine protected area. Marine Biology, 163(2), 39.

Hickman, C. P., Roberts, L. S., Larson, A., Ober, W. C., & Garrison, C. (2001). Integrated principles of zoology (Vol. 15). New York: McGraw-Hill.

Hill, M. S. (1996). Symbiotic zooxanthellae enhance boring and growth rates of the tropical sponge *Anthosigmella varians* forma *varians*. Marine Biology, 125(4), 649-654.

Hiscock, K. (2014). Marine biodiversity conservation: A practical approach. Routledge, Abingdon.

Hiscock, K., (1983). Water movement. In: R.C. Earll, D.G. Erwin (Eds) Sublittoral Ecology: The Ecology of the Shallow Sublittoral Benthos. Clarendon Press, Oxford, United Kingdom, pp. 58–96.

Hitt, N. T., Sinclair, D. J., Fallon, S. J., Neil, H. L., Tracey, D. M., Komugabe-Dixson, A., & Marriott, P. (2020). Growth and longevity of New Zealand black corals. Deep Sea Research Part I: Oceanographic Research Papers, 162, 103298.

Hobday, A.J., Alexander, L.V., Perkins, S.E., Smale, D.A., Straub, S.C., Oliver, E.C., Benthuysen, J.A., Burrows, M.T., Donat, M.G., Feng, M., Holbrook, N.J., Moore, P.J., Scannell, H.A., Gupta, A.S., & Wernberg, T. (2016). A hierarchical approach to defining marine heatwaves. Progress in Oceanography, 141, 227-238.

Hobday, A.J., Oliver, E.C., Gupta, A.S., Benthuysen, J.A., Burrows, M.T., Donat, M.G., Holbrook, N.J., Moore, P.J., Thomsen, M.S., Wernberg, T., & Smale, D.A. (2018). Categorizing and naming marine heatwaves. Oceanography, 31(2), 162-173.

Hochachka, P. W., & Lutz, P. L. (2001). Mechanism, origin, and evolution of anoxia tolerance in animals. Comparative Biochemistry and Physiology Part B: Biochemistry and Molecular Biology, 130(4), 435–459.

Hodgson, D., McDonald, J. L., & Hosken, D. J. (2015). What do you mean, 'resilient'? Trends in Ecology & Evolution, 30(9), 503-506.

Hoegh-Guldberg, O., & Bruno, J. F. (2010). The impact of climate change on the world's marine ecosystems. Science, 328(5985), 1523-1528.

Hoffmann, F., Larsen, O., Thiel, V., Rapp, H. T., Pape, T., Michaelis, W., & Reitner, J. (2005). An anaerobic world in sponges. Geomicrobiology Journal, 22(1–2), 1–10.

Holling, C. S. (1973). Resilience and stability of ecological systems. Annual Review of Ecology and Systematics, 4(1), 1-23.

Holling, C. S. (1996). Engineering resilience versus ecological resilience. Engineering within ecological constraints, 31(1996), 32.

Hong, J.S., 1983. (1983). Impact of the Pollution on the Benthic Community Environmental impact of the pollution on the benthic coralligenous community in the Gulf of Fos, northwestern Mediterranean. Korean Journal of Fisheries and Aquatic Sciences, 16(3), 273-290.

Hooper, J. N., & Van Soest, R. W. (2002). Systema Porifera. A guide to the classification of sponges. Springer, Boston, MA.

Howarth, R. W., & Marino, R. (2006). Nitrogen as the limiting nutrient for eutrophication in coastal marine ecosystems: evolving views over three decades. Limnology and Oceanography, 51(1part2), 364-376.

Howarth, R. W., Anderson, D., Cloern, J., Elfring, C., Hopkinson, C., Lapointe, B., Malone, T., Marcus, N., McGlathery, K., Sharpley, A.N., & Walker, D. (2000). Nutrient pollution of coastal rivers, bays and seas, Issues in Ecology, 7.

Huey, R. B., & Ward, P. D. (2005). Hypoxia, global warming, and terrestrial Late Permian extinctions. Science, 308(5720), 398-401.

Hughes, D. J., Alderdice, R., Cooney, C., Kühl, M., Pernice, M., Voolstra, C. R., & Suggett, D. J. (2020). Coral reef survival under accelerating ocean deoxygenation. Nature Climate Change, 10(4), 296–307.

Hughes, T. P., Baird, A. H., Bellwood, D. R., Card, M., Connolly, S. R., Folke, C., Grosberg, R., Hoegh-Guldberg, O., Jackson, J.B., Kleypas, J., & Lough, J. M. (2003). Climate change, human impacts, and the resilience of coral reefs. Science, 301(5635), 929-933.

Hughes, T. P., Bellwood, D. R., Folke, C., Steneck, R. S., & Wilson, J. (2005). New paradigms for supporting the resilience of marine ecosystems. Trends in ecology & evolution, 20(7), 380-386.

Idan, T., Goren, L., Shefer, S., & Ilan, M. (2020). Sponges in a changing climate: Survival of Agelas oroides in a warming Mediterranean Sea. Frontiers in Marine Science, 603593

Idan, T., Shefer, S., Feldstein, T., Yahel, R., Huchon, D., & Ilan, M. (2018). Shedding light on an East-Mediterranean mesophotic sponge ground community and the regional sponge fauna. Mediterranean Marine Science, 19(1), 84-106.

Ingleby, B., & Huddleston, M. (2007). Quality control of ocean temperature and salinity profiles—Historical and real-time data. Journal of Marine Systems, 65(1-4), 158-175.

Inglehart, R. (1995). Public support for environmental protection: Objective problems and subjective values in 43 societies. PS: Political Science & Politics, 28(1), 57-72.

Ingrisch, J., & Bahn, M. (2018). Towards a comparable quantification of resilience. Trends in Ecology & Evolution, 33(4), 251-259.

Ingrosso, G., Abbiati, M., Badalamenti, F., Bavestrello, G., Belmonte, G., Cannas, R., Benedetti-Cecchi, L., Bertolino, M., Bevilacqua, S., Bianchi, C.N. and Bo, M. & Boero, F. (2018). Mediterranean bioconstructions along the Italian coast. Advances in Marine Biology, 79, 61-136.

IPCC (2014) Climate Change 2014: Synthesis Report. Contribution of Working Groups I, II and III to the Fifth Assessment Report of the Intergovernmental Panel on Climate Change [Core Writing Team, R.K. Pachauri and L.A. Meyer (eds.)]. IPCC, Geneva, Switzerland.

IPCC (2021). Summary for Policymakers. In: V. Masson-Delmotte, P. Zhai, A. Pirani, S. L. Connors, C. Péan, S. Berger, N. Caud, Y. Chen, L. Goldfarb, M. I. Gomis, M. Huang, K. Leitzell, E. Lonnoy, J.B.R. Matthews, T. K. Maycock, T. Waterfield, O. Yelekçi, R. Yu & B. Zhou (Eds) Climate Change 2021: The Physical Science Basis. Contribution of Working Group I to the Sixth Assessment Report of the Intergovernmental Panel on Climate Change. Cambridge University Press.

Islam, M. S., & Tanaka, M. (2004). Impacts of pollution on coastal and marine ecosystems including coastal and marine fisheries and approach for management: a review and synthesis. Marine Pollution Bulletin, 48(7-8), 624-649.

Jackson, J. B., Kirby, M. X., Berger, W. H., Bjorndal, K. A., Botsford, L. W., Bourque, B. J., Bradbury, R.H., Cooke, R., Erlandson, J., Estes, J.A., & Hughes, T. P. (2001). Historical overfishing and the recent collapse of coastal ecosystems. Science, 293(5530), 629-637.

Jankowski, J. A., Malcherek, A., & Zielke, W. (1996). Numerical modeling of suspended sediment due to deep-sea mining. Journal of Geophysical Research: Oceans, 101(C2), 3545-3560.

Jaspars, M., De Pascale, D., Andersen, J. H., Reyes, F., Crawford, A. D., & Ianora, A. (2016). The marine biodiscovery pipeline and ocean medicines of tomorrow. Journal of the Marine Biological Association of the United Kingdom, 96(1), 151-158.

Jessopp, M., McAllen, R., O'Halloran, J., & Kelly, T. (2011). Nutrient and Ecosystem Dynamics in Ireland's only marine nature reserve (NEIDIN). Final report for the STRIVE-Funded Project: 2007-FS-B-4–M5 66.

Johnson, K. A. (2002). A review of national and international literature on the effects of fishing on benthic habitats. Silver Springs, MD: US Department of Commerce, National Oceanic and Atmospheric Administration, National Marine Fisheries Service.

Johnson, M. D., Rodriguez, L. M., & Altieri, A. H. (2018). Shallow-water hypoxia and mass mortality on a Caribbean coral reef. Bulletin of Marine Science, 94(1), 143–144.

Johnson, M. P., Costello, M. J., & O'Donnell, D. (1995). The nutrient economy of a marine inlet: Lough Hyne, south west Ireland. Ophelia 41, 137–151.

Johnson, P. D., & McMahon, R. F. (1998). Effects of temperature and chronic hypoxia on survivorship of the zebra mussel (*Dreissena polymorpha*) and Asian clam (*Corbicula fluminea*). Canadian Journal of Fisheries and Aquatic Sciences, 55(7), 1564–1572.

Jones, J. B. (1992). Environmental impact of trawling on the seabed: a review. New Zealand Journal of Marine and Freshwater Research, 26(1), 59-67.

Jørgensen, B. B. (1980). Seasonal oxygen depletion in the bottom waters of a Danish fjord and its effect on the benthic community. Oikos, 68-76.

Jurgens, L. J., Rogers-Bennett, L., Raimondi, P. T., Schiebelhut, L. M., Dawson, M. N., Grosberg, R. K., & Gaylord, B. (2015). Patterns of mass mortality among rocky shore invertebrates across 100 km of northeastern Pacific coastline. PLoS One 10, e0126280.

Justić, D. (1987). Long-term eutrophication of the northern Adriatic Sea. Marine Pollution Bulletin, 18(6), 281-284.

Justić, D. (1991). Hypoxic conditions in the northern Adriatic Sea: historical development and ecological significance. Geological Society, London, Special Publications, 58(1), 95-105.

Kaelin WG, & Ratcliffe PJ. (2008). Oxygen sensing by metazoans: the central role of the HIF hydroxylase pathway. Molecular Cell 30:393–402.

Kahn, A. S., Vehring, L. J., Brown, R. R., & Leys, S. P. (2016). Dynamic change, recruitment and resilience in reef-forming glass sponges. Journal of the Marine Biological Association of the United Kingdom, 96(2), 429-436.

Kamke, J., Taylor, M. W., & Schmitt, S. (2010). Activity profiles for marine sponge-associated bacteria obtained by 16S rRNA vs 16S rRNA gene comparisons. The ISME Journal, 4(4), 498–508.

Kealoha, A. K., Doyle, S. M., Shamberger, K. E., Sylvan, J. B., Hetland, R. D., & Di Marco, S. F. (2020). Localized hypoxia may have caused coral reef mortality at the Flower Garden Banks. Coral Reefs, 39(1), 119–132.

Keeling, R. F., Körtzinger, A., & Gruber, N. (2010). Ocean deoxygenation in a warming world. Annual Review of Marine Science, 2, 199–229.

Kelleher, G. (1999). Guidelines for marine protected areas. IUCN, Gland, Switzerland and Cambridge, UK.

Kelmo, F., Bell, J. J., Moraes, S. S., Gomes, R. D. C. T., Mariano-Neto, E., & Attrill, M. J. (2014). Differential responses of emergent intertidal coral reef fauna to a large-scale El-Niño Southern oscillation event: sponge and coral resilience. PloS One, 9(3), e93209.

Kemp, W. M., Boynton, W. R., Adolf, J. E., Boesch, D. F., Boicourt, W. C., Brush, G., Cornwell, J.C., Fisher, T.R., Glibert, P.M., Hagy, J.D., & Harding, L. W. (2005). Eutrophication of Chesapeake Bay: historical trends and ecological interactions. Marine Ecology Progress Series, 303, 1-29.

Kennish, M. J. (2017). Practical handbook of estuarine and marine pollution. CRC press.

Kitching, J. A. (1987). Ecological studies at Lough Hyne. Advances in Ecological Research, 17, 115-186.

Kitching, J. A., Ebling, F. J., Gamble, J. C., Hoare, R., McLeod, A. A. Q. R., & Norton, T. A. (1976). The Ecology of Lough Ine. The Journal of Animal Ecology, 731-758.

Kloke, J. D., & McKean, J. W. (2012). Rfit: rank-based estimation for linear models. R J., 4(2), 57.

Kohler, K. E., & Gill, S. M. (2006). Coral Point Count with Excel extensions (CPCe): A Visual Basic program for the determination of coral and substrate coverage using random point count methodology. Computers & Geosciences, 32(9), 1259-1269.

Konar, B. (2013). Lack of recovery from disturbance in high-arctic boulder communities. Polar Biology, 36(8), 1205-1214.

Koopmans, M., Martens, D., & Wijffels, R. H. (2010). Growth efficiency and carbon balance for the sponge *Haliclona oculata*. Marine Biotechnology, 12(3), 340-349.

Krautter, M., Conway, K. W., Barrie, J. V., & Neuweiler, M. (2001). Discovery of a "living dinosaur": globally unique modern hexactinellid sponge reefs off British Columbia, Canada. Facies, 44(1), 265-282.

Kroeker, K. J., Bell, L. E., Donham, E. M., Hoshijima, U., Lummis, S., Toy, J. A., & Willis-Norton, E. (2020). Ecological change in dynamic environments: Accounting for temporal environmental variability in studies of ocean change biology. Global change biology, 26(1), 54–67.

Kummu, M., De Moel, H., Salvucci, G., Viviroli, D., Ward, P. J., & Varis, O. (2016). Over the hills and further away from coast: global geospatial patterns of human and environment over the 20th–21st centuries. Environmental Research Letters, 11(3), 034010.

Kuznetsova, A., Brockhoff, P. B., & Christensen, R. H. (2017). lmerTest package: tests in linear mixed effects models. Journal of Statistical Software, 82(13), 1–26.

Lakens, D. (2013). Calculating and reporting effect sizes to facilitate cumulative science: a practical primer for t-tests and ANOVAs. Frontiers in Psychology, 4, 863.

Lavy, A., Keren, R., Yahel, G., & Ilan, M. (2016). Intermittent hypoxia and prolonged suboxia measured in situ in a marine sponge. Frontiers in Marine Science, 3, 263.

Lawson, J., Davenport, J., & Whitaker, A. (2004). Barnacle distribution in Lough Hyne Marine Nature Reserve: a new baseline and an account of invasion by the introduced Australasian species Elminius modestus Darwin. Estuarine, Coastal and Shelf Science, 60(4), 729-735.

Lazzari, P., Solidoro, C., Salon, S., & Bolzon, G. (2016). Spatial variability of phosphate and nitrate in the Mediterranean Sea: A modeling approach. Deep Sea Research Part I: Oceanographic Research Papers, 108, 39-52.

Lee, Y. K., Lee, J. H., & Lee, H. K. (2001). Microbial symbiosis in marine sponges. Journal of Microbiology, 39(4), 254-264.

Lenth, R. (2021). *emmeans*: estimated marginal means, aka least-squares means. R package version 1.6.0. https://CRAN.R-project.org/package=emmeans

Leversee, G. J. (1976). Flow and feeding in fan-shaped colonies of the gorgonian coral, *Leptogorgia*. The Biological Bulletin, 151(2), 344-356.

Levin, L. A. (2003). Oxygen minimum zone benthos: adaptation and community response to hypoxia. Oceanography and Marine Biology: An Annual Review. 41, 1–45.

Levin, L. A., & Breitburg, D. L. (2015). Linking coasts and seas to address ocean deoxygenation. Nature Climate Change, 5(5), 401–403.

Levin, L. A., Ekau, W., Gooday, A. J., Jorissen, F., Middelburg, J. J., Naqvi, S. W. A., Neira, C., Rabalais, N. N. & Zhang, J. (2009). Effects of natural and human-induced hypoxia on coastal benthos. Biogeosciences, 6(10), 2063–2098.

Levin, L. A., Huggett, C. L., & Wishner, K. F. (1991). Control of deep-sea benthic community structure by oxygen and organic-matter gradients in the eastern Pacific Ocean. Journal of Marine Research, 49(4), 763–800.

Leys, S. P., & Kahn, A. S. (2018). Oxygen and the energetic requirements of the first multicellular animals. Integrative and Comparative Biology, 58(4), 666–676.

Leys, S. P., Wilson, K., Holeton, C., Reiswig, H. M., Austin, W. C., & Tunnicliffe, V. (2004). Patterns of glass sponge (Porifera, Hexactinellida) distribution in coastal waters of British Columbia, Canada. Marine Ecology Progress Series, 283, 133-149.

Li, T., & Brouwer, M. (2007). Hypoxia-inducible factor, gsHIF, of the grass shrimp *Palaemonetes pugio*: molecular characterization and response to hypoxia. Comparative Biochemistry and Physiology Part B: Biochemistry and Molecular Biology, 147(1), 11-19.

Li, Z., Wang, Y., Li, J., Liu, F., He, L., He, Y., & Wang, S. (2016). Metagenomic analysis of genes encoding nutrient cycling pathways in the microbiota of deep-sea and shallow-water sponges. Marine Biotechnology, 18(6), 659-671.

Limburg, K. E., Breitburg, D., & Levin, L. A. (2017). Ocean deoxygenation-a climate-related problem. Frontiers in Ecology and the Environment, 15(9), 479–479.

Linares, C., Coma, R., & Zabala, M. (2008). Restoration of threatened red gorgonian populations: an experimental and modelling approach. Biological Conservation, 141(2), 427-437.

Little, C., Trowbridge, C. D., Pilling, G. M., Cottrell, D. M., Plowman, C. Q., Stirling, P., Morritt, D., & Williams, G. A. (2018). Long-term fluctuations in epibiotic bryozoan and hydroid abundances in an Irish sea lough. Estuarine, Coastal and Shelf Science, 210, 142-152.

Little, C., Trowbridge, C. D., Pilling, G. M., Williams, G. A., Morritt, D., & Stirling, P. (2020). Long-term variation of trochid populations in an Irish sea lough. Journal of Molluscan Studies, 86(2), 83-95.

Llanso, R. J. (1992). Effects of hypoxia on estuarine benthos: the lower Rappahannock River (Chesapeake Bay), a case study. Estuarine, Coastal and Shelf Science, 35(5), 491-515.

Llanso, R. J., & Diaz, R. J. (1994). Tolerance to low dissolved oxygen by the tubicolous polychaete Loimia medusa. Journal of the Marine Biological Association of the United Kingdom, 74(1), 143-148.

Lotze, H. K., Coll, M., Magera, A. M., Ward-Paige, C., & Airoldi, L. (2011). Recovery of marine animal populations and ecosystems. Trends in Ecology & Evolution, 26(11), 595-605.

Lotze, H. K., Lenihan, H. S., Bourque, B. J., Bradbury, R. H., Cooke, R. G., Kay, M. C., Kidwell, S.M., Kirby, M.X., Peterson, C.H., & Jackson, J. B. (2006). Depletion, degradation, and recovery potential of estuaries and coastal seas. Science, 312(5781), 1806-1809.

Lourie, S. A., & Vincent, A. C. (2004). Using biogeography to help set priorities in marine conservation. Conservation Biology, 18(4), 1004-1020.

Love, G.D., Grosjean, E., Stalvies, C., Fike, D.A., Grotzinger, J.P., Bradley, A.S., Kelly, A.E., Bhatia, M., Meredith, W., Snape, C.E. and Bowring, S.A., Condon, D. J., & Summons, R. E. (2009). Fossil steroids record the appearance of Demospongiae during the Cryogenian period. Nature, 457(7230), 718–721.

Lucieer, V., Lawler, M., Pender, A., & Morffew, M. (2009). Seamap Tasmania–Mapping the Gaps. Marine Research Laboratories—Tasmanian Aquaculture and Fisheries Institute. Univ. of Tasmania, Tasmania.

Ludeman, D. A., Reidenbach, M. A., & Leys, S. P. (2017). The energetic cost of filtration by demosponges and their behavioural response to ambient currents. Journal of Experimental Biology, 220(6), 995-1007.

Lunden, J. J., McNicholl, C. G., Sears, C. R., Morrison, C. L., & Cordes, E. E. (2014). Acute survivorship of the deep-sea coral *Lophelia pertusa* from the Gulf of Mexico under acidification, warming, and deoxygenation. Frontiers in Marine Science, 1, 78.

Luter, H. M., Gibb, K., & Webster, N. S. (2014). Eutrophication has no short-term effect on the *Cymbastela stipitata* holobiont. Frontiers in Microbiology, 5, 216.

Luter, H. M., Whalan, S., & Webster, N. S. (2011). The marine sponge *Ianthella basta* can recover from stress-induced tissue regression. In: M. Maldonado, X. Turon, M. Becerro, M. J. Uriz (Eds) Ancient animals, new challenges. Springer, Dordrecht, pp. 227-235

Luther, G. W., Ma, S., Trouwborst, R., Glazer, B., Blickley, M., Scarborough, R. W., & Mensinger, M. G. (2004). The roles of anoxia, H2S, and storm events in fish kills of dead-end canals of Delaware inland bays. Estuaries, 27(3), 551-560.

Lynch, S. A., Darmody, G., O'Dwyer, K., Gallagher, M. C., Nolan, S., McAllen, R., & Culloty, S. C. (2016). Biology of the invasive ascidian *Ascidiella aspersa* in its native habitat: Reproductive patterns and parasite load. Estuarine, Coastal and Shelf Science, 181, 249-255.

Lyons, D. A., Arvanitidis, C., Blight, A. J., Chatzinikolaou, E., Guy-Haim, T., Kotta, J., Orav-Kotta, H., Queirós, A.M., Rilov, G., Somerfield, P.J., & Crowe, T. P. (2014). Macroalgal blooms alter community structure and primary productivity in marine ecosystems. Global Change Biology, 20(9), 2712-2724.

MAE (Millennium Ecosystem Assessment) (2005) Ecosystems and human wellbeing: Synthesis. Washington, DC: Island Press.

Maggs, C. A., Freamhainn, M. T., & Guiry, M. D. (1983). A study of the marine algae of subtidal cliffs in Lough Hyne (Ine), Co. Cork. In: Proceedings of the Royal Irish Academy. Section B: Biological, Geological, and Chemical Science. Royal Irish Academy, pp. 251-266

Malakoff, D. (1998). Death by suffocation in the Gulf of Mexico. Science

Maldonado, M. (2006). The ecology of the sponge larva. Canadian Journal of Zoology, 84(2), 175-194.

Maldonado, M., Aguilar, R., Bannister, R. J., Bell, J. J., Conway, K. W., Dayton, P. K., Díaz, C., Gutt, J., Kelly, M., Kenchington, E. and Leys, S., & Young, C. M. (2017). Sponge grounds as key marine habitats: a synthetic review of types, structure, functional roles, and conservation concerns. In: S. Rossi, L. Bramanti, A. Gori, C. Orejas (Eds) Marine animal forests: the ecology of benthic biodiversity hotspots. Springer, Cham, Switzerland, pp. 145-184.

Maldonado, M., Giraud, K., & Carmona, C. (2008). Effects of sediment on the survival of asexually produced sponge recruits. Marine Biology, 154(4), 631-641.

Maldonado, M., Ribes, M., & van Duyl, F. C. (2012). Nutrient fluxes through sponges: biology, budgets, and ecological implications. Advances in Marine Biology, 62, 113-182.

Maloof, A. C., Rose, C. V., Beach, R., Samuels, B. M., Calmet, C. C., Erwin, D. H., Poirier, G. R., Yao, N., & Simons, F.J. (2010). Possible animal-body fossils in pre-Marinoan limestones from South Australia. Nature Geoscience, 3(9), 653–659.

Manconi, R., & Pronzato, R. (2007). Gemmules as a key structure for the adaptive radiation of freshwater sponges: a morphofunctional and biogeographical study. Porifera research: biodiversity, innovation and sustainability. Série Livros, 28, 61-77.

Mangum, D. C. (1980). Sea anemone neuromuscular responses in anaerobic conditions. Science, 208(4448), 1177–1178.

Marschal, C., Garrabou, J., Harmelin, J. G., & Pichon, M. (2004). A new method for measuring growth and age in the precious red coral *Corallium rubrum* (L.). Coral reefs, 23(3), 423-432.

Marshall, A. J., Parker, T. J., Haswell, W. A., & Williams, W. D. (1972). A Text-book of Zoology: Invertebrates (Vol. 1). Elsevier Publishing Company.

Martínez, M. L., Intralawan, A., Vázquez, G., Pérez-Maqueo, O., Sutton, P., & Landgrave, R. (2007). The coasts of our world: Ecological, economic and social importance. Ecological Economics, 63(2-3), 254-272.

Mary George, A., Brodie, J., Daniell, J., Capper, A., & Jonker, M. (2018). Can sponge morphologies act as environmental proxies to biophysical factors in the Great Barrier Reef, Australia? Ecological Indicators, 93, 1152-1162.

Marzloff, M. P., Oliver, E. C., Barrett, N. S., Holbrook, N. J., James, L., Wotherspoon, S. J., & Johnson, C. R. (2018). Differential vulnerability to climate change yields novel deep-reef communities. Nature Climate Change, 8(10), 873-878.

Mastrototaro, F., D'onghia, G., & Tursi, A. (2008). Spatial and seasonal distribution of ascidians in a semi-enclosed basin of the Mediterranean Sea. Journal of the Marine Biological Association of the United Kingdom, 88(5), 1053-1061.

Matear, R. J., & Hirst, A. C. (2003). Long-term changes in dissolved oxygen concentrations in the ocean caused by protracted global warming. Global Biogeochemical Cycles, 17(4).

Maughan, B. C. (2001). The effects of sedimentation and light on recruitment and development of a temperate, subtidal, epifaunal community. Journal of Experimental Marine Biology and Ecology, 256(1), 59-71.

Maughan, B. C., & Barnes, D. K. (2000). Epilithic boulder communities of Lough Hyne, Ireland: the influences of water movement and sediment. Journal of the Marine Biological Association of the United Kingdom, 80(5), 767-776.

McAllen, R., Bell, J., Davenport, J., Little, C., Micaroni, V., Nunn, J., Strano, F., & Trowbridge, C. D. (2021). Lough Hyne: Europe's First Statutory Marine Reserve—A Biodiversity Hotspot. In: Reference Module in Earth Systems and Environmental Sciences. Elsevier

McAllen, R., Davenport, J., Bredendieck, K., & Dunne, D. (2009). Seasonal structuring of a benthic community exposed to regular hypoxic events. Journal of Experimental Marine Biology and Ecology, 368(1), 67–74.

McAllen, R., Taylor, A. C., & Davenport, J. (1999). The effects of temperature and oxygen partial pressure on the rate of oxygen consumption of the high-shore rock pool copepod *Tigriopus brevicornis*. Comparative Biochemistry and Physiology Part A: Molecular & Integrative Physiology, 123(2), 195–202.

McCarthy, M., Bane, V., García-Altares, M., van Pelt, F. N., Furey, A., & O'Halloran, J. (2015). Assessment of emerging biotoxins (pinnatoxin G and spirolides) at Europe's first marine reserve: Lough Hyne. Toxicon, 108, 202-209.

McCarthy, M., van Pelt, F. N., Bane, V., O'halloran, J., & Furey, A. (2014). Application of passive (SPATT) and active sampling methods in the profiling and monitoring of marine biotoxins. Toxicon, 89, 77-86.

Mentel, M., Röttger, M., Leys, S., Tielens, A. G., & Martin, W. F. (2014). Of early animals, anaerobic mitochondria, and a modern sponge. Bioessays, 36(10), 924–932.

Meybeck, M., & Vörösmarty, C. (1999). Global transfer of carbon by rivers. Global Change Newsletter, 37, 18-19.

Micaroni, V., McAllen, R., Turner, J., Strano, F., Morrow, C., Picton, B., Harman, L., & Bell, J. J. (2021). Vulnerability of Temperate Mesophotic Ecosystems (TMEs) to environmental impacts: Rapid ecosystem changes at Lough Hyne Marine Nature Reserve, Ireland. Science of The Total Environment, 789, 147708.

Miller, S. A., & Harley, J. P. (2011). Zoology. New York.

Mills, D. B., Francis, W. R., Vargas, S., Larsen, M., Elemans, C. P., Canfield, D. E., & Wörheide, G. (2018). The last common ancestor of animals lacked the HIF pathway and respired in low-oxygen environments. Elife, 7, e31176.

Mills, D. B., Ward, L. M., Jones, C., Sweeten, B., Forth, M., Treusch, A. H., & Canfield, D. E. (2014). Oxygen requirements of the earliest animals. Proceedings of the National Academy of Sciences, 111(11), 4168–4172.

Milton, S. L., & Prentice, H. M. (2007). Beyond anoxia: the physiology of metabolic downregulation and recovery in the anoxia-tolerant turtle. Comparative Biochemistry and Physiology Part A: Molecular and Integrative Physiology, 147(2), 277–290.

Moitinho-Silva, L., Steinert, G., Nielsen, S., Hardoim, C. C., Wu, Y. C., McCormack, G. P., López-Legentil, S., Marchant, R., Webster, N., Thomas, T., & Hentschel, U. (2017). Predicting the HMA-LMA status in marine sponges by machine learning. Frontiers in Microbiology, 8, 752.

Montero-Serra, I., Linares, C., Doak, D. F., Ledoux, J. B., & Garrabou, J. (2018). Strong linkages between depth, longevity and demographic stability across marine sessile species. Proceedings of the Royal Society B: Biological Sciences, 285(1873), 20172688.

Morganti, T. M., Ribes, M., Moskovich, R., Weisz, J. B., Yahel, G., & Coma, R. (2021). In situ Pumping Rate of 20 Marine Demosponges Is a Function of Osculum Area. Frontiers in Marine Science, 8, 583188.

Morris, S., & Taylor, A. C. (1983). Diurnal and seasonal variation in physico-chemical conditions within intertidal rock pools. Estuarine, Coastal and Shelf Science, 17, 339–355.

Morrison, K. M., Meyer, H. K., Roberts, E. M., Rapp, H. T., Colaço, A., & Pham, C. K. (2020). The First Cut Is the Deepest: Trawl Effects on a Deep-Sea Sponge Ground Are Pronounced Four Years on. Frontiers in Marine Science, 7, 1059.

Morrow, C., & Cárdenas, P. (2015). Proposal for a revised classification of the Demospongiae (Porifera). Frontiers in Zoology, 12(1), 7.

Morrow, K. M., Bourne, D. G., Humphrey, C., Botté, E. S., Laffy, P., Zaneveld, J., Uthicke, S., Fabricius, K.E., & Webster, N. S. (2015). Natural volcanic CO_2 seeps reveal future trajectories for host–microbial associations in corals and sponges. The ISME journal, 9(4), 894.

Mortensen, P. B., & Buhl-Mortensen, L. (2005). Morphology and growth of the deep-water gorgonians *Primnoa resedaeformis* and *Paragorgia arborea*. Marine Biology, 147(3), 775-788.

Mosch, T., Sommer, S., Dengler, M., Noffke, A., Bohlen, L., Pfannkuche, O., Liebetrau, V. & Wallmann, K. (2012). Factors influencing the distribution of epibenthic megafauna across the Peruvian oxygen minimum zone. Deep Sea Research Part I: Oceanographic Research Papers, 68, 123–135.

Moss, B., Kosten, S., Meerhoff, M., Battarbee, R. W., Jeppesen, E., Mazzeo, N., Havens, K., Lacerot, G., Liu, Z., De Meester, L., & Paerl, H. (2011). Allied attack: climate change and eutrophication. Inland Waters, 1(2), 101-105.

Müller, M., Mentel, M., van Hellemond, J. J., Henze, K., Woehle, C., Gould, S. B., Yu, R.Y., van der Giezen, M., Tielens, A.G., & Martin, W. F. (2012). Biochemistry and evolution of anaerobic energy metabolism in eukaryotes. Microbiology and Molecular Biology Reviews, 76(2), 444–495.

Mumby, P. J., & Steneck, R. S. (2008). Coral reef management and conservation in light of rapidly evolving ecological paradigms. Trends in Ecology & Evolution, 23(10), 555-563.

Murty, S. J., Bett, B. J., & Gooday, A. J. (2009). Megafaunal responses to strong oxygen gradients on the Pakistan margin of the Arabian Sea. Deep Sea Research Part II: Topical Studies in Oceanography, 56(6-7), 472–487.

Myers, A.A., Little, C., Costello, M.J., & Partridge, J.C. (1991) The ecology of Lough Hyne. Proceedings of a conference 4–5 September, 1990. Royal Irish Academy, Dublin.

Nabil, S., & Cosson, J. (1996). Seasonal variations in sterol composition of *Delesseria sanguinea* (Ceramiales, Rhodophyta). Hydrobiologia, 326(1), 511-514.

Nagasoe, S., Tokunaga, T., Yurimoto, T., & Matsuyama, Y. (2020). Survival and behavior patterns associated with hypoxia at different life stages of the pen shell *Atrina* cf. *japonica.* Aquatic Toxicology, 227, 105610.

Naranjo, S. A., Carballo, J. L., & Garcia-Gomez, J. C. (1996). Effects of environmental stress on ascidian populations in Algeciras Bay (southern Spain). Possible marine bioindicators? Marine Ecology Progress Series, 144, 119-131.

Nelson, T. A., Lee, D. J., & Smith, B. C. (2003). Are "green tides" harmful algal blooms? Toxic properties of water-soluble extracts from two bloom-forming macroalgae, *Ulva fenestrata* and *Ulvaria obscura* (Ulvophyceae). Journal of Phycology, 39(5), 874-879.

Neumann, B., Vafeidis, A. T., Zimmermann, J., & Nicholls, R. J. (2015). Future coastal population growth and exposure to sea-level rise and coastal flooding-a global assessment. PloS One, 10(3), e0118571.

Nezlin, N. P., Kamer, K., Hyde, J., & Stein, E. D. (2009). Dissolved oxygen dynamics in a eutrophic estuary, Upper Newport Bay, California. Estuarine, Coastal and Shelf Science, 82(1), 139–151.

Nilsson, G. E., & Renshaw, G. M. (2004). Hypoxic survival strategies in two fishes: extreme anoxia tolerance in the North European crucian carp and natural hypoxic preconditioning in a coral-reef shark. Journal of Experimental Biology, 207(18), 3131–3139.

Nixon, S. W. (1995). Coastal marine eutrophication: a definition, social causes, and future concerns. Ophelia, 41(1), 199–219.

Norström, A. V., Nyström, M., Lokrantz, J., & Folke, C. (2009). Alternative states on coral reefs: beyond coral–macroalgal phase shifts. Marine Ecology Progress Series, 376, 295-306.

NPWS (National Parks and Wildlife Service) (2014) Conservation Objectives: Lough Hyne Nature Reserve and Environs SAC 000097. Version 1. National Parks and Wildlife Service, Department of Arts, Heritage and the Gaeltacht.

NRC (National Research Council) (1995). Priorities for coastal ecosystem science. National Academies Press.

O'neil, J. M., Davis, T. W., Burford, M. A., & Gobler, C. J. (2012). The rise of harmful cyanobacteria blooms: the potential roles of eutrophication and climate change. Harmful Algae, 14, 313-334.

O'Brien, J. M., & Scheibling, R. E. (2018). Turf wars: competition between foundation and turf-forming species on temperate and tropical reefs and its role in regime shifts. Marine Ecology Progress Series, 590, 1-17.

Occhipinti-Ambrogi, A., & Savini, D. (2003). Biological invasions as a component of global change in stressed marine ecosystems. Marine Pollution Bulletin, 46(5), 542-551.

Oenema, O., Liu, Q., & Wang, J. (2018). Agricolture. In: M. Salomon, T. Markus (Eds) Handbook on Marine Environment Protection. Springer, Cham, pp. 429-445.

Officer, C. B., Biggs, R. B., Taft, J. L., Cronin, L. E., Tyler, M. A., & Boynton, W. R. (1984). Chesapeake Bay anoxia: origin, development, and significance. Science, 223(4631), 22-27.

Oksanen, J., Kindt, R., Legendre, P., O'Hara, B., Stevens, M. H. H., Oksanen, M. J., & Suggests, M. A. S. S. (2007). The *vegan* package. Community ecology package, 10(631-637), 719.

Osinga, R., Tramper, J., & Wijffels, R. H. (1999). Cultivation of marine sponges. Marine Biotechnology, 1(6), 509–532.

OSPAR Commission (2008). OSPAR list of threatened and/or declining species and habitats. OSPAR Commission, London, United Kingdom.

Paerl, H. W., Valdes, L. M., Joyner, A. R., Piehler, M. F., & Lebo, M. E. (2004). Solving problems resulting from solutions: evolution of a dual nutrient management strategy for the eutrophying Neuse River Estuary, North Carolina. Environmental Science & Technology, 38(11), 3068-3073.

Palumbi, S. R. (1984). Tactics of acclimation: morphological changes of sponges in an unpredictable environment. Science 225, 1478–1480.

Palumbi, S. R. (2003). Population genetics, demographic connectivity, and the design of marine reserves. Ecological Applications, 13, 146-158.

Pansini, M., & Sará, M. (1999). Taxonomical and biogeographical notes on the sponges of the Strait of Magellan. Scientia Marina, 63(S1), 203-208.

Paoli, C., Montefalcone, M., Morri, C., Vasallo, P., & Bianchi, C.N. (2017). Ecosystem functions and services of the marine animal forests. In: S. Rossi, L. Bramanti, A. Gori, C. Orejas (Eds) Marine animal forests: the ecology of benthic biodiversity hotspots. Springer, Cham, Switzerland, pp. 1271-1312.

Patrício, J., Little, S., Mazik, K., Papadopoulou, K. N., Smith, C. J., Teixeira, H., Hoffmann, H., Uyarra, M.C., Solaun, O., Zenetos, A. and Kaboglu, G., & Elliott, M. (2016). European marine biodiversity monitoring networks: strengths, weaknesses, opportunities and threats. Frontiers in Marine Science, 3, 161.

PCE (Parliamentary Commissioner for the Environment) (2013). Water quality in New Zealand: land use and nutrient pollution. Wellington: Parliamentary Commissioner for the Environment

Perea-Blazquez, A., Davy, S. K., & Bell, J. J. (2012). Estimates of particulate organic carbon flowing from the pelagic environment to the benthos through sponge assemblages. PLoS One, 7(1), e29569.

Perkins, N. R., Foster, S. D., Hill, N. A., Marzloff, M. P., & Barrett, N. S. (2017). Temporal and spatial variability in the cover of deep reef species: Implications for monitoring. Ecological Indicators, 77, 337-347.

Perkins, N. R., Hosack, G. R., Foster, S. D., Monk, J., & Barrett, N. S. (2020). Monitoring the resilience of a no-take marine reserve to a range extending species using benthic imagery. PloS One, 15(8), e0237257.

Petersen, J. K. (2007). Ascidian suspension feeding. Journal of Experimental Marine Biology and Ecology, 342(1), 127-137.

Peterson, B. J., Chester, C. M., Jochem, F. J., & Fourqurean, J. W. (2006). Potential role of sponge communities in controlling phytoplankton blooms in Florida Bay. Marine Ecology Progress Series, 328, 93-103.

Piazzi, L., Atzori, F., Cadoni, N., Cinti, M. F., Frau, F., Pansini, A., Pinna, F., Stipcich, P. & Ceccherelli, G. (2021). Animal Forest Mortality: Following the Consequences of a Gorgonian Coral Loss on a Mediterranean Coralligenous Assemblage. Diversity, 13(3), 133.

Piazzi, L., Gennaro, P., & Balata, D. (2011). Effects of nutrient enrichment on macroalgal coralligenous assemblages. Marine Pollution Bulletin, 62(8), 1830-1835.

Piazzi, L., Gennaro, P., & Balata, D. (2012). Threats to macroalgal coralligenous assemblages in the Mediterranean Sea. Marine Pollution Bulletin, 64(12), 2623-2629.

Piazzi, L., Kaleb, S., Ceccherelli, G., Montefalcone, M., & Falace, A. (2019). Deep coralligenous outcrops of the Apulian continental shelf: biodiversity and spatial variability of sediment-regulated assemblages. Continental Shelf Research, 172, 50-56.

Picton, B.E. (1990). The sessile fauna of sublittoral cliffs, in: The ecology of Lough Hyne: proceedings of a conference: 1990 Sep 4–5. Royal Irish Academy, Dublin, Ireland.

Pile, A. J., Patterson, M. R., & Witman, J. D. (1996). In situ grazing on plankton< 10 μm by the boreal sponge *Mycale lingua*. Marine Ecology Progress Series, 95-102.

Pimm, S. L. (1984). The complexity and stability of ecosystems. Nature, 307(5949), 321-326.

Pinheiro, J., Bates, D., DebRoy, S., Sarkar, D., & R Core Team (2021). *nlme*: Linear and Nonlinear Mixed Effects Models. R package version 3.1-152. https://CRAN.R-project.org/package=nlme.

Pita, L., Rix, L., Slaby, B. M., Franke, A., & Hentschel, U. (2018). The sponge holobiont in a changing ocean: from microbes to ecosystems. Microbiome, 6(1), 46.

Pizarro, O., Williams, S. B., Jakuba, M. V., Johnson-Roberson, M., Mahon, I., Bryson, M., Steinberg, D., Friedman, A., Dansereau, D., Nourani-Vatani, N., Bongiorno, Bewley, M., Bender, A., Ashan, N., & Douillard, B. (2013). Benthic monitoring with robotic platforms—the experience of Australia. Underwater Technology Symposium (UT), 2013 IEEE International: 1–10.

Plowman, C. Q., Trowbridge, C. D., Davenport, J., Little, C., Harman, L., & McAllen, R. (2020). Stressed from above and stressed from below: dissolved oxygen fluctuations in Lough Hyne, a semi-enclosed marine lake. ICES Journal of Marine Science, 77(6), 2106-2117.

Poloczanska, E. S., Brown, C. J., Sydeman, W. J., Kiessling, W., Schoeman, D. S., Moore, P. J., Brander, K., Bruno, J.F., Buckley, L.B., Burrows, M.T., & Duarte, C. M. (2013). Global imprint of climate change on marine life. Nature Climate Change, 3(10), 919.

Porte, C., Janer, G., Lorusso, L. C., Ortiz-Zarragoitia, M., Cajaraville, M. P., Fossi, M. C., & Canesi, L. (2006). Endocrine disruptors in marine organisms: approaches and perspectives. Comparative Biochemistry and Physiology Part C: Toxicology & Pharmacology, 143(3), 303-315.

Pörtner, H. O., & Grieshaber, M. K. (1993). Critical PO2 (s) in oxyconforming and oxyregulating animals gas exchange, metabolic rate and the mode of energy production. In The vertebrate gas transport cascade adaptations to environment and mode of life (JEPW Bicudo, ed) CRC Press, Boca Raton FL (pp. 330-357).

Pörtner, H. O., Langenbuch, M., & Michaelidis, B. (2005). Synergistic effects of temperature extremes, hypoxia, and increases in CO2 on marine animals: From Earth history to global change. Journal of Geophysical Research: Oceans, 110(C9).

Pronzato, R., & Manconi, R. (2008). Mediterranean commercial sponges: over 5000 years of natural history and cultural heritage. Marine Ecology, 29(2), 146-166.

Pyle, R. L. (2019). Advanced technical diving. In: Y. Loya, K. A. Puglise, T. Bridge (Eds) Mesophotic Coral Ecosystems. Springer, Cham, Switzerland, pp. 959-972.

R Core Team (2013). R: A language and environment for statistical computing.

Rabalais N. N., & Turner R. E., (2001). Coastal Hypoxia: Consequences for Living Resources. American Geophysical Union.

Rabalais, N. N., Turner, R. E., & Wiseman Jr, W. J. (2002). Gulf of Mexico hypoxia, aka "The dead zone". Annual Review of Ecology and Systematics, 33(1), 235-263.

Rabalais, N. N., Turner, R. E., Diaz, R. J., & Justić, D. (2009). Global change and eutrophication of coastal waters. ICES Journal of Marine Science, 66(7), 1528-1537.

Rabotyagov, S. S., Kling, C. L., Gassman, P. W., Rabalais, N. N., & Turner, R. E. (2012). The economics of dead zones: linking externalities from the land to their consequences in the sea. Iowa State University Center for Agricultural and Rural Development (CARD) Working Papers. Paper 547. Iowa State University, Ames.

Rae, M., Folch, H., Moniz, M. B., Wolff, C. W., McCormack, G. P., Rindi, F., & Johnson, M. P. (2013). Marine bioactivity in Irish waters. Phytochemistry Reviews, 12(3), 555-565.

Ramsby, B. D., Heishman, J., Hoogenboom, M. O., Whalan, S., & Webster, N. S. (2020). Dissolved inorganic nutrient enrichment does not affect sponge growth or condition. Marine Ecology Progress Series, 634, 77-88.

Rao, D. P., & Ganapati, P. N. (1968). Respiration as a function of oxygen concentration in intertidal barnacles. Marine Biology, 1(4), 309–310.

Raupach, M. R., & Canadell, J. G. (2010). Carbon and the Anthropocene. Current Opinion in Environmental Sustainability, 2(4), 210–218.

Ray, D. K., Mueller, N. D., West, P. C., & Foley, J. A. (2013). Yield trends are insufficient to double global crop production by 2050. PloS One, 8(6), e66428.

Reiswig, H. M. (1971). Particle feeding in natural populations of three marine demosponges. The Biological Bulletin, 141(3), 568-591.

Reynolds, L. K., Waycott, M., McGlathery, K. J., & Orth, R. J. (2016). Ecosystem services returned through seagrass restoration. Restoration Ecology, 24(5), 583-588.

Reynolds, R. W., Smith, T. M., Liu, C., Chelton, D. B., Casey, K. S., & Schlax, M. G. (2007). Daily high-resolution-blended analyses for sea surface temperature. Journal of Climate, 20(22), 5473-5496.

Ribes, M., Coma, R., & Gili, J. M. (1999). Natural diet and grazing rate of the temperate sponge *Dysidea avara* (Demospongiae, Dendroceratida) throughout an annual cycle. Marine Ecology Progress Series, 179-190.

Riesgo, A., Pérez-Portela, R., Pita, L., Blasco, G., Erwin, P. M., & López-Legentil, S. (2016). Population structure and connectivity in the Mediterranean sponge *Ircinia fasciculata* are affected by mass mortalities and hybridisation. Heredity, 117(6), 427-439.

Riisgård, H. U., & Larsen, P. S. (2000). Comparative ecophysiology of active zoobenthic filter feeding, essence of current knowledge. Journal of Sea Research, 44(3-4), 169-193.

Riisgård, H. U., Thomassen, S., Jakobsen, H., Weeks, J. M., & Larsen, P. S. (1993). Suspension feeding in marine sponges *Halichondria panicea* and *Haliclona urceolus*: effects of temperature on filtration rate and energy cost of pumping. Marine Ecology Progress Series, 177-188.

Roberts, D. E., Smith, A., Ajani, P., & Davis, A. R. (1998). Rapid changes in encrusting marine assemblages exposed to anthropogenic point-source pollution: a 'Beyond BACI' approach. Marine Ecology Progress Series, 163, 213-224.

Robinson, C. (2019). Microbial respiration, the engine of ocean deoxygenation. Frontiers in Marine Science, 5, 533.

Rodrigues, L. C., van den Bergh, J. C., Loureiro, M. L., Nunes, P. A., & Rossi, S. (2016). The cost of Mediterranean Sea warming and acidification: a choice experiment among scuba divers at Medes Islands, Spain. Environmental and Resource Economics, 63(2), 289-311.

Rosenberg, R., Hellman, B., & Johansson, B. (1991). Hypoxic tolerance of marine benthic fauna. Marine ecology progress series. Oldendorf, 79(1), 127-131.

Rossi, S. (2013). The destruction of the 'animal forests' in the oceans: towards an over-simplification of the benthic ecosystems. Ocean & Coastal Management, 84, 77-85.

Rossi, S., Bramanti, L., Gori, A., & Orejas, C. (2017). Marine animal forest: the ecology of benthic biodiversity hotspots. Springer, Cham, Switzerland.

Rossi, S., Isla, E., Bosch-Belmar, M., Galli, G., Gori, A., Gristina, M., Ingrosso, G., Milisenda, G., Piraino, S., Rizzo, L. Schubert, N., & Ziveri, P. (2019). Changes of energy fluxes in marine animal forests of the Anthropocene: factors shaping the future seascape. ICES Journal of Marine Science, 76(7), 2008-2019.

Ruiz, G. M., Carlton, J. T., Grosholz, E. D., & Hines, A. H. (1997). Global invasions of marine and estuarine habitats by non-indigenous species: mechanisms, extent, and consequences. American Zoologist, 37(6), 621-632.

Ruxton, G. D. (2006). The unequal variance t-test is an underused alternative to Student's t-test and the Mann–Whitney U test. Behavioral Ecology, 17(4), 688-690.

Salvaterra, T., Green, D. S., Crowe, T. P., & O'Gorman, E. J. (2013). Impacts of the invasive alga *Sargassum muticum* on ecosystem functioning and food web structure. Biological Invasions, 15(11), 2563-2576.

Sampaio, E., Santos, C., Rosa, I. C., Ferreira, V., Pörtner, H. O., Duarte, C. M., Levin, L. A. & Rosa, R. (2021). Impacts of hypoxic events surpass those of future ocean warming and acidification. Nature Ecology and Evolution, 5(3), 311–321.

Santín, A., Grinyó, J., Ambroso, S., Uriz, M. J., Gori, A., Dominguez-Carrió, C., & Gili, J. M. (2018). Sponge assemblages on the deep Mediterranean continental shelf and slope (Menorca Channel, Western Mediterranean Sea). Deep Sea Research Part I: Oceanographic Research Papers, 131, 75-86.

Sarà, M., Sarà, A., Nickel, M., & Brümmer, F. (2001). Three New Species of *Tethya* (Porifera: Demospongiae) From German Aquaria. Stuttgarter Beiträge zur Naturkunde 631, 1–15.

Sartoretto, S., Schohn, T., Bianchi, C. N., Morri, C., Garrabou, J., Ballesteros, E., Ruitton, S., Verlaque, M., Daniel, B., Charbonnel, E., & Blouet, S. (2017). An integrated method to evaluate and monitor the conservation state of coralligenous habitats: The INDEX-COR approach. Marine Pollution Bulletin, 120(1-2), 222-231.

Sassaman, C., & Mangum, C. P. (1972). Adaptations to environmental oxygen levels in infaunal and epifaunal sea anemones. The Biological Bulletin, 143(3), 657–678.

Satheesh, S., Ba-akdah, M. A., & Al-Sofyani, A. A. (2016). Natural antifouling compound production by microbes associated with marine macroorganisms—A review. Electronic Journal of Biotechnology, 21, 26-35.

Scheffer, M., Bascompte, J., Brock, W. A., Brovkin, V., Carpenter, S. R., Dakos, V., Held, H., Van Nes, E.H., Rietkerk, M., & Sugihara, G. (2009). Early-warning signals for critical transitions. Nature, 461(7260), 53-59.

Scheffer, M., Carpenter, S., & de Young, B. (2005). Cascading effects of overfishing marine systems. Trends in Ecology & Evolution, 20(11), 579-581.

Schiel, D. R., & Hickford, M. J. H. (2001). Biological structure of nearshore rocky subtidal habitats in southern New Zealand. Department of Conservation, Science for Conservation 182

Schindler, D. W., & Vallentyne, J. R. (2008). The algal bowl: overfertilization of the world's freshwaters and estuaries. Edmonton: University of Alberta Press.

Schlegel, R. W., Oliver, E. C., Wernberg, T., & Smit, A. J. (2017). Nearshore and offshore co-occurrence of marine heatwaves and cold-spells. Progress in Oceanography, 151, 189-205.

Schmitt, S., Tsai, P., Bell, J., Fromont, J., Ilan, M., Lindquist, N., Perez, T., Rodrigo, A., Schupp, P.J., Vacelet, J., & Webster, N. (2012). Assessing the complex sponge microbiota: core, variable and species-specific bacterial communities in marine sponges. The ISME Journal, 6(3), 564.

Schönberg, C. H. L. (2016). Happy relationships between marine sponges and sediments–a review and some observations from Australia. Journal of the Marine Biological Association of the United Kingdom, 96(2), 493-514.

Schuster, A., Strehlow, B. W., Eckford-Soper, L., McAllen, R., & Canfield, D. E. (2021). Effects of Seasonal Anoxia on the Microbial Community Structure in Demosponges in a Marine Lake in Lough Hyne, Ireland. Msphere, 6(1), e00991-20.

Seibel, B. A. (2011). Critical oxygen levels and metabolic suppression in oceanic oxygen minimum zones. Journal of Experimental Biology, 214(2), 326–336.

Semenza, G. L. (2007). Life with oxygen. Science, 318(5847), 62–64.

Sempere-Valverde, J., Ostalé-Valriberas, E., Maestre, M., Aranda, R. G., Bazairi, H., & Espinosa, F. (2021). Impacts of the non-indigenous seaweed *Rugulopteryx okamurae* on a Mediterranean coralligenous community (Strait of Gibraltar): The role of long-term monitoring. Ecological Indicators, 121, 107135.

Shanks, A. L. (2009). Pelagic larval duration and dispersal distance revisited. The Biological Bulletin, 216(3), 373-385.

Sherman, K. M., & Coull, B. C. (1980). The response of meiofauna to sediment disturbance. Journal of Experimental Marine Biology and Ecology, 46(1), 59-71.

Simpson, T. L., & Fell, P. E. (1974). Dormancy among the Porifera: gemmule formation and germination in fresh-water and marine sponges. Transactions of the American Microscopical Society, 544-577.

Sivaramakrishnan, V. R. (1951, December). Studies on early development and regeneration in some Indian marine sponges. Proceedings of the Indian Academy of Sciences-Section B, 34, 273-310.

Smith, F. W. (1946). Effect of water currents upon the attachment and growth of barnacles. The Biological Bulletin, 90(1), 51-70.

Smith, V. H., & Schindler, D. W. (2009). Eutrophication science: where do we go from here? Trends in Ecology & Evolution, 24(4), 201-207.

Smith, V. H., Joye, S. B., & Howarth, R. W. (2006). Eutrophication of freshwater and marine ecosystems. Limnology and Oceanography, 51, 351–355.

Smith, V. H., Tilman, G. D., & Nekola, J. C. (1999). Eutrophication: impacts of excess nutrient inputs on freshwater, marine, and terrestrial ecosystems. Environmental Pollution, 100(1-3), 179-196.

Snelder, T. H., Larned, S. T., & McDowell, R. W. (2018). Anthropogenic increases of catchment nitrogen and phosphorus loads in New Zealand. New Zealand Journal of Marine and Freshwater Research, 52(3), 336-361.

Soares, M. D. O., Tavares, T. C. L., & Carneiro, P. B. D. M. (2019). Mesophotic ecosystems: Distribution, impacts and conservation in the South Atlantic. Diversity and Distributions, 25(2), 255-268.

Stachowitsch, M. (1984). Mass mortality in the Gulf of Trieste: the course of community destruction. Marine Ecology, 5(3), 243–264.

Stachowitsch, M. (1991). Anoxia in the Northern Adriatic Sea: rapid death, slow recovery. Geological Society, London, Special Publications, 58(1), 119-129.

Steckbauer, A., Klein, S. G., & Duarte, C. M. (2020). Additive impacts of deoxygenation and acidification threaten marine biota. Global Change Biology, 26(10), 5602–5612.

Steneck, R. S., & Wilson, C. J. (2001). Large-scale and long-term, spatial and temporal patterns in demography and landings of the American lobster, *Homarus americanus*, in Maine. Marine and Freshwater Research, 52(8), 1303-1319.

Stevely, J. M., Sweat, D. E., Bert, T. M., Sim-Smith, C., & Kelly, M. (2011). Sponge mortality at Marathon and Long Key, Florida: patterns of species response and population recovery. Proceedings of the 63rd Gulf and Caribbean Fisheries Institute November 1 - 5, 2010 San Juan, Puerto Rico.

Stickle, W. B., Kapper, M. A., Liu, L. L., Gnaiger, E., & Wang, S. Y. (1989). Metabolic adaptations of several species of crustaceans and molluscs to hypoxia: tolerance and microcalorimetric studies. The Biological Bulletin, 177(2), 303–312.

Strain, E. M., Thomson, R. J., Micheli, F., Mancuso, F. P., & Airoldi, L. (2014). Identifying the interacting roles of stressors in driving the global loss of canopy-forming to mat-forming algae in marine ecosystems. Global Change Biology, 20(11), 3300-3312.

Strano, F., Micaroni, V., Costa, G., Bertocci, I., & Bertolino, M. (2020). Shallow-water sponge grounds along the Apulian coast (central Mediterranean Sea). Marine Biodiversity, 50(1), 1-12.

Strano, F., Micaroni, V., Davy, S. K., Maldonado, M., & Bell, J. J. (2021). Reproduction and early life stages of the poecilosclerid sponge *Crella incrustans.* Invertebrate Biology, e12335.

Strehlow, B. W., Pineda, M. C., Duckworth, A., Kendrick, G. A., Renton, M., Wahab, M. A. A., Webster, N.S., & Clode, P. L. (2017). Sediment tolerance mechanisms identified in sponges using advanced imaging techniques. PeerJ, 5, e3904.

Strunz, S. (2012). Is conceptual vagueness an asset? Arguments from philosophy of science applied to the concept of resilience. Ecological Economics, 76, 112-118.

Stuart, V., & Klumpp, D. W. (1984). Evidence for food-resource partitioning by kelp-bed filter feeders. Marine Ecology Progress Series. 16(1), 27-37.

Sukhotin, A., & Berger, V. (2013). Long-term monitoring studies as a powerful tool in marine ecosystem research. Hydrobiologia, 706(1), 1-9.

Sullivan, D. O., & Emmerson, M. (2011). Marine reserve designation, trophic cascades and altered community dynamics. Marine Ecology Progress Series, 440, 115-125.

Sullivan, T., & Regan, F. (2013). Challenges and opportunities associated with monitoring marine anoxic zones with autonomous sensors _an irish perspective. In: Martech 2013 - 5th International Workshop on Marine Technology. SARTI.

Sullivan, T., Broszeit, S., O'Sullivan, K. P., McAllen, R., Davenport, J., & Regan, F. (2013). High resolution monitoring of episodic stratification events in an enclosed marine system. Estuarine, Coastal and Shelf Science, 123, 26-33.

Svane, I. (1983). Ascidian reproductive patterns related to long-term population dynamics. Sarsia, 68(4), 249-255.

Swezey, D. S., Bean, J. R., Ninokawa, A. T., Hill, T. M., Gaylord, B., & Sanford, E. (2017). Interactive effects of temperature, food and skeletal mineralogy mediate biological responses to ocean acidification in a widely distributed bryozoan. Proceedings of the Royal Society B: Biological Sciences, 284(1853), 20162349.

Tanaka, T., & Rassoulzadegan, F. (2002). Full-depth profile (0–2000 m) of bacteria, heterotrophic nanoflagellates and ciliates in the NW Mediterranean Sea: vertical partitioning of microbial trophic structures. Deep Sea Research Part II: Topical Studies in Oceanography, 49(11), 2093-2107.

Teixidó, N., Garrabou, J., & Harmelin, J. G. (2011). Low dynamics, high longevity and persistence of sessile structural species dwelling on Mediterranean coralligenous outcrops. PloS One, 6(8), e23744.

Therneau, T. (2021). A Package for Survival Analysis in R. R package version 3.2-10. https://CRAN.R-project.org/package=survival.

Thomsen, P. F., & Willerslev, E. (2015). Environmental DNA–An emerging tool in conservation for monitoring past and present biodiversity. Biological Conservation, 183, 4-18.

Thuesen, E. V., Rutherford Jr, L. D., & Brommer, P. L. (2005). The role of aerobic metabolism and intragel oxygen in hypoxia tolerance of three ctenophores: *Pleurobrachia bachei, Bolinopsis infundibulum* and *Mnemiopsis leidyi.* Journal of the Marine Biological Association of the United Kingdom, 85(3), 627.

Thurstan, R. H., Pandolfi, J. M., & zu Ermgassen, P. S. (2017). Animal forests through time: historical data to understand present changes in marine ecosystems. In: S. Rossi, L. Bramanti, A. Gori, C. Orejas (Eds) Marine animal forests: the ecology of benthic biodiversity hotspots. Springer, Cham, Switzerland, pp. 947-964.

Tilman, D., & Downing, J. A. (1994). Biodiversity and stability in grasslands. Nature, 367(6461), 363-365.

Tilman, D., Balzer, C., Hill, J., & Befort, B. L. (2011). Global food demand and the sustainable intensification of agriculture. Proceedings of the National Academy of Sciences, 108(50), 20260-20264.

Tonin, S. (2018). Economic value of marine biodiversity improvement in coralligenous habitats. Ecological Indicators, 85, 1121-1132.

Topçu, N. E., Turgay, E., Yardımcı, R. E., Topaloğlu, B., Yüksek, A., Steinum, T. M., Karataş, S., & Öztürk, B. (2019). Impact of excessive sedimentation caused by anthropogenic activities on benthic suspension feeders in the Sea of Marmara. Journal of the Marine Biological Association of the United Kingdom, 99(5), 1075-1086.

Trowbridge, C. D., Davenport, J., Cottrell, D. M., Harman, L., Plowman, C. Q., Little, C., & McAllen, R. (2017a). Extreme oxygen dynamics in shallow water of a fully marine Irish sea lough. Regional Studies in Marine Science, 11, 9–16.

Trowbridge, C. D., Davenport, J., Plowman, C. Q., Harman, L., & McAllen, R. (2017b). Marine aloricate ciliate red tides in a temperate Irish sea lough. Marine Biodiversity, 47(3), 869-878.

Trowbridge, C. D., Little, C., Dlouhy-Massengale, B., Stirling, P., & Pilling, G. M. (2013). Changes in brown seaweed distributions in Lough Hyne, SW Ireland: a long-term perspective. Botanica Marina, 56(4), 323-338.

Trowbridge, C. D., Little, C., Pilling, G. M., Stirling, P., & Miles, A. (2011). Decadal-scale changes in the shallow subtidal benthos of an Irish marine reserve. Botanica Marina, 54, 497–506.

Trowbridge, C. D., Little, C., Plowman, C. Q., Ferrenburg, L. S., Resk, H. M., Stirling, P., Davenport, J., & McAllen, R. (2018). Recent changes in shallow subtidal fauna with new invertebrate records in Europe's first marine reserve, Lough Hyne. In: Biology and Environment: Proceedings of the Royal Irish Academy, Vol. 118, No. 1. Royal Irish Academy, pp. 29-44

Tseng, L. C., Dahms, H. U., Hsu, N. J., & Hwang, J. S. (2011). Effects of sedimentation on the gorgonian *Subergorgia suberosa* (Pallas, 1766). Marine Biology, 158(6), 1301-1310.

Turner, E. C. (2021). Possible poriferan body fossils in early Neoproterozoic microbial reefs. Nature, 596, 87–91.

Turner, J. A., Andradi-Brown, D. A., Gori, A., Bongaerts, P., Burdett, H. L., Ferrier-Pagès, C., Voolstra, C. R., Weinstein, D. K., Bridge, T. C. L., Costantini, F., Gress, E., Laverick, J., Loya, Y., Goodbody-Gringley, G., Rossi, S., Taylor, M. L., Viladrich, N., Voss, J. D., Williams, J., Woodall, L. C., & Eyal, G. (2019). Key questions for research and conservation of mesophotic coral ecosystems and temperate mesophotic ecosystems. In: Y. Loya, K. A. Puglise, T. Bridge (Eds) Mesophotic Coral Ecosystems. Springer, Cham, Switzerland, pp. 989–1003.

UN (United Nations, Department of Economic and Social Affairs, Population Division) (2015). World Population Prospects: The 2015 Revision, Key Findings and Advance Tables. Working Paper No. ESA/P/WP.241.

Undorf, S., Allen, K., Hagg, J., Li, S., Lott, F. C., Metzger, M. J., Sparrow, S.N., & Tett, S. F. B. (2020). Learning from the 2018 heatwave in the context of climate change: are high-temperature extremes important for adaptation in Scotland? Environmental Research Letters, 15(3), 034051.

UNEP (United Nations Environment Programme) (1992). The world environment 1972–1992: Two decades of challenge. Chapman & Hall, New York

UNEP-MAP-RAC/SPA (2008). Action plan for the conservation of the coralligenous and other calcareous bio-concretions in the Mediterranean Sea. UNEPMAP RACSPA publications, Tunis, Tunisia.

Unsworth, R. K., Collier, C. J., Waycott, M., Mckenzie, L. J., & Cullen-Unsworth, L. C. (2015). A framework for the resilience of seagrass ecosystems. Marine Pollution Bulletin, 100(1), 34-46.

Usher, K. M. (2008). The ecology and phylogeny of cyanobacterial symbionts in sponges. Marine Ecology, 29(2), 178-192.

Vaalgamaa, S. (2004). The effect of urbanisation on Laajalahti Bay, Helsinki City, as reflected by sediment geochemistry. Marine Pollution Bulletin, 48(7-8), 650-662.

Vacelet, J. (1975). Étude en microscopie électronique de l'association entre bactéries et spongiaires du genre *Verongia* (Dictyoceratida). Journal de Microscopie et de Biologie Cellulaire 23, 271–288.

Van Soest, R. W., Boury-Esnault, N., Vacelet, J., Dohrmann, M., Erpenbeck, D., De Voogd, N. J., Santodomingo, N., Vanhoorne, B., Kelly, M., & Hooper, J. N. (2012). Global diversity of sponges (Porifera). PLoS One, 7(4), e35105.

Van Soest, R.W., Hajdu, E. (2002). Family Esperiopsidae Hentschel, 1923. In: R.W. Van Soest, J. Hooper (Eds) Systema Porifera. Springer, Boston, Massachusetts, pp. 656–664.

van Van Beusekom, J. E. (2018). Eutrophication. In: M. Salomon, T. Markus (Eds) Handbook on Marine Environment Protection. Springer, Cham, pp. 429-445.

Vaquer-Sunyer, R., & Duarte, C. M. (2008). Thresholds of hypoxia for marine biodiversity. Proceedings of the National Academy of Sciences, 105(40), 15452–15457.

Vaquer-Sunyer, R., & Duarte, C. M. (2010). Sulfide exposure accelerates hypoxia-driven mortality. Limnology and Oceanography, 55(3), 1075–1082.

Vaquer-Sunyer, R., & Duarte, C. M. (2011). Temperature effects on oxygen thresholds for hypoxia in marine benthic organisms. Global Change Biology, 17(5), 1788–1797.

Verdura, J., Linares, C., Ballesteros, E., Coma, R., Uriz, M. J., Bensoussan, N., & Cebrian, E. (2019). Biodiversity loss in a Mediterranean ecosystem due to an extreme warming event unveils the role of an engineering gorgonian species. Scientific Reports, 9(1), 1-11.

Vergés, A., McCosker, E., Mayer-Pinto, M., Coleman, M. A., Wernberg, T., Ainsworth, T., & Steinberg, P. D. (2019). Tropicalisation of temperate reefs: implications for ecosystem functions and management actions. Functional Ecology, 33(6), 1000–1013.

Vicente, V. P. (1989). Regional commercial sponge extinctions in the West Indies: are recent climatic changes responsible? Marine Ecology, 10(2), 179-191.

Vogel, S. (1977). Current-induced flow through living sponges in nature. Proceedings of the National Academy of Sciences, 74(5), 2069-2071.

Vornanen, M., Stecyk, J. A., & Nilsson, G. E. (2009). The anoxia-tolerant crucian carp (*Carassius carassius* L.). In: J. Richards, A. Farrell, C. Brauner (Eds) Fish Physiology: Hypoxia, Volume 27. Academic Press, pp. 397–441

Voultsiadou-Koukoura, H. E., Koukouras, A., & Eleftheriou, A. (1987). Macrofauna associated with the sponge *Verongia aerophoba* in the North Aegean Sea. Estuarine, Coastal and Shelf Science, 24(2), 265-278.

Wall, C. C., Rodgers, B. S., Gobler, C. J., & Peterson, B. J. (2012). Responses of loggerhead sponges *Spechiospongia vesparium* during harmful cyanobacterial blooms in a sub-tropical lagoon. Marine Ecology Progress Series, 451, 31-43.

Wangensteen, O. S., & Turon, X. (2017). Metabarcoding techniques for assessing biodiversity of marine animal forests. In: S. Rossi, L. Bramanti, A. Gori, C. Orejas (Eds) Marine animal forests: the ecology of benthic biodiversity hotspots. Springer, Cham, Switzerland, pp. 445-503.

Wassenberg, T. J., Dews, G., & Cook, S. D. (2002). The impact of fish trawls on megabenthos (sponges) on the north-west shelf of Australia. Fisheries Research, 58(2), 141-151.

Webster, N. S. (2007). Sponge disease: a global threat? Environmental Microbiology, 9(6), 1363-1375.

Webster, N. S., & Taylor, M. W. (2012). Marine sponges and their microbial symbionts: love and other relationships. Environmental Microbiology, 14(2), 335-346.

Whelan, N. V., Kocot, K. M., Moroz, T. P., Mukherjee, K., Williams, P., Paulay, G., Moroz, L. L. & Halanych, K. M. (2017). Ctenophore relationships and their placement as the sister group to all other animals. Nature Ecology & Evolution, 1(11), 1737–1746.

Whitlatch, R. B., Lohrer, A. M., Thrush, S. F., Pridmore, R. D., Hewitt, J. E., Cummings, V. J., & Zajac, R. N. (1998). Scale-dependent benthic recolonization dynamics: life stage-based dispersal and demographic consequences. Hydrobiologia, (375-376), 217-226.

Wildish, D. J., & Kristmanson, D. D. (1979). Tidal energy and sublittoral macrobenthic animals in estuaries. Journal of the Fisheries Board of Canada, 36(10), 1197-1206.

Wildish, D. J., & Kristmanson, D. D. (2005). Benthic suspension feeders and flow. Cambridge University Press.

Wilkinson, C. R., & Vacelet, J. (1979). Transplantation of marine sponges to different conditions of light and current. Journal of Experimental Marine Biology and Ecology, 37(1), 91-104.

Williams, C. B. (1964). Patterns in the balance of nature and related problems of quantitative ecology. Academic Press.

Williams, J., Jordan, A., Harasti, D., Davies, P., & Ingleton, T. (2019). Taking a deeper look: Quantifying the differences in fish assemblages between shallow and mesophotic temperate rocky reefs. PloS one, 14(3), e0206778.

Williams, S. B., Pizarro, O. R., Jakuba, M. V., Johnson, C. R., Barrett, N. S., Babcock, R. C., Kendrick, G.A., Steinberg, P.D., Heyward, A.J., Doherty, P.J. and Mahon, I., & Friedman, A. (2012). Monitoring of benthic reference sites: using an autonomous underwater vehicle. IEEE Robotics & Automation Magazine, 19(1), 73-84.

Williams, S. B., Pizarro, O., Jakuba, M., & Barrett, N. (2010). AUV benthic habitat mapping in south eastern Tasmania. In: A. Howard, K. Iagnemma, A. Kelly (Eds) Field and Service Robotics. Springer, Berlin, Heidelberg, pp. 275–284.

Wilson, K. (1984). A bibliography of Lough Hyne (Ine) 1687-1982. Journal of Life Sciences Royal Dublin Society, 5(1), 1-11.

Wilson, K., & Picton, B. E. (1983). A list of the Opisthobranchia: Mollusca of Lough Hyne Nature Reserve, Co. Cork, with notes on distribution and nomenclature. The Irish Naturalists' Journal, 69-72.

Winston, J. E., Larwood, G. P., & Abbott, M. B. (1979). Current-related morphology and behaviour in some Pacific coast bryozoans. Advances in Bryozoology, 13, 247-268.

Wishner, K. F., Ashjian, C. J., Gelfman, C., Gowing, M. M., Kann, L., Levin, L. A., Mullineaux, L. S. & Saltzman, J. (1995). Pelagic and benthic ecology of the lower interface of the Eastern Tropical Pacific oxygen minimum zone. Deep Sea Research Part I: Oceanographic Research Papers, 42(1), 93–115.

Wisshak, M., Schönberg, C. H., Form, A., & Freiwald, A. (2012). Ocean acidification accelerates reef bioerosion. PloS One, 7(9), e45124.

Woo, S., Denis, V., Won, H., Shin, K., Lee, G., Lee, T. K., & Yum, S. (2013). Expressions of oxidative stress-related genes and antioxidant enzyme activities in *Mytilus galloprovincialis* (Bivalvia, Mollusca) exposed to hypoxia. Zoological Studies, 52(1), 1–8.

Woodhead, A. J., Hicks, C. C., Norström, A. V., Williams, G. J., & Graham, N. A. (2019). Coral reef ecosystem services in the Anthropocene. Functional Ecology, 33(6), 1023–1034.

Worm, B., & Lotze, H. K. (2006). Effects of eutrophication, grazing, and algal blooms on rocky shores. Limnology andO, 51, 569-579.

Worm, B., Barbier, E. B., Beaumont, N., Duffy, J. E., Folke, C., Halpern, B. S., Jackson, J.B., Lotze, H.K., Micheli, F., Palumbi, S.R., & Sala, E. (2006). Impacts of biodiversity loss on ocean ecosystem services. Science, 314(5800), 787-790.

Wu, R. S. (2002). Hypoxia: from molecular responses to ecosystem responses. Marine pollution bulletin, 45(1-12), 35-45.

Wulff, J. L. (1991). Asexual fragmentation, genotype success, and population dynamics of erect branching sponges. Journal of Experimental Marine Biology and Ecology, 149(2), 227-247.

Wulff, J. L. (2006). Ecological interactions of marine sponges. Canadian Journal of Zoology, 84(2), 146–166.

Yahel, G., Marie, D., & Genin, A. (2005). InEx—a direct in situ method to measure filtration rates, nutrition, and metabolism of active suspension feeders. Limnology and Oceanography: Methods, 3(2), 46–58.

Yahel, G., Sharp, J. H., Marie, D., Häse, C., & Genin, A. (2003). In situ feeding and element removal in the symbiont-bearing sponge *Theonella swinhoei*: Bulk DOC is the major source for carbon. Limnology and Oceanography, 48(1), 141-149.

Yıldız, T., & Karakulak, F. S. (2016). Types and extent of fishing gear losses and their causes in the artisanal fisheries of Istanbul, Turkey. Journal of Applied Ichthyology, 32(3), 432-438.

Zaitsev, Y. P. (1992). Recent changes in the trophic structure of the Black Sea. Fisheries Oceanography, 1(2), 180-189.

Zapata-Ramírez, P. A., Scaradozzi, D., Sorbi, L., Palma, M., Pantaleo, U., Ponti, M., & Cerrano, C. (2013). Innovative study methods for the Mediterranean coralligenous habitats. Advances in Oceanography and Limnology, 4(2), 102-119.

Appendix A - Changes in the subtidal benthic communities of Lough Hyne

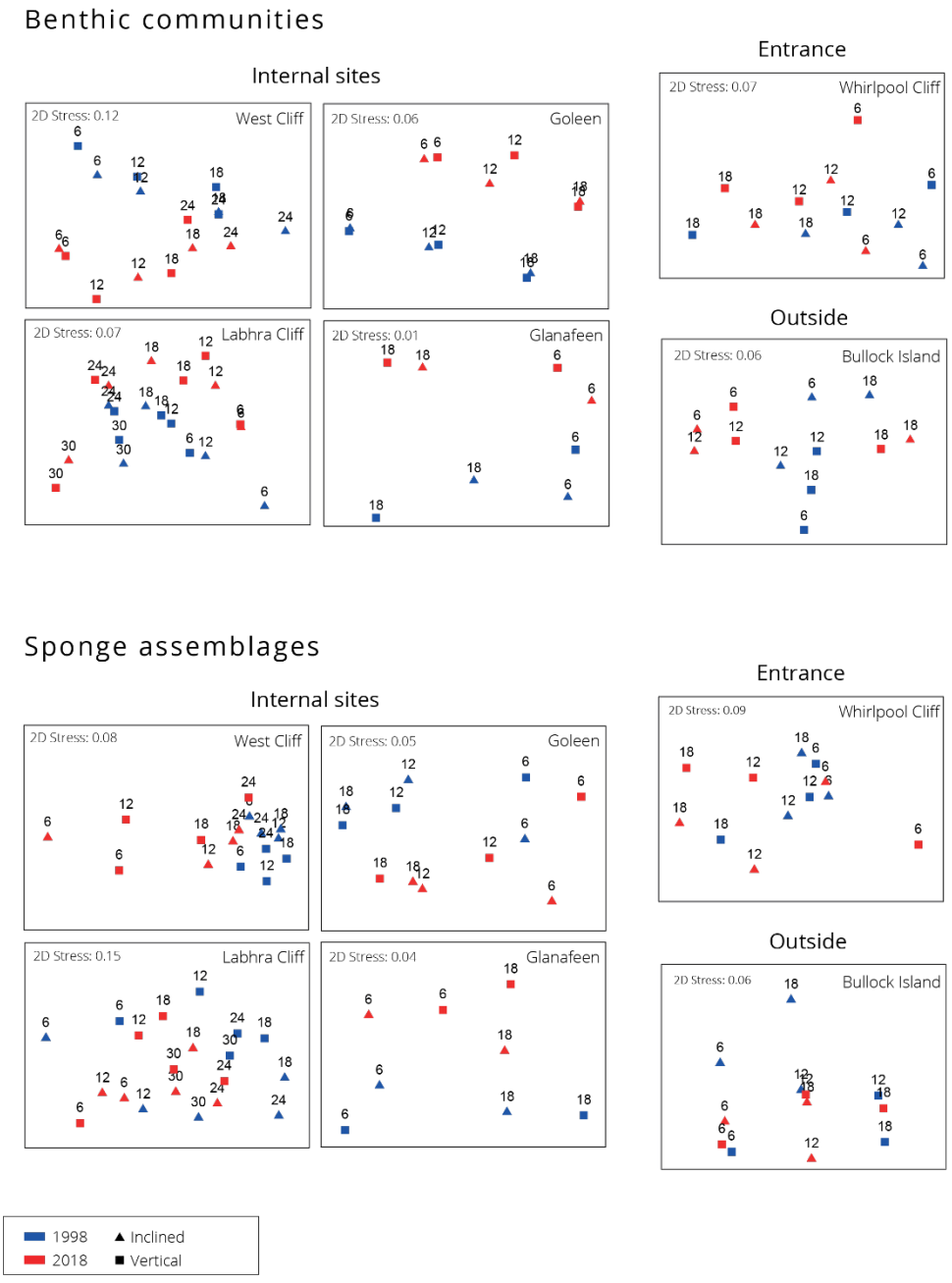

Figure S2.1. Non-metric multidimensional scaling (nMDS) of centroids of benthic communities and sponge assemblages for each combination of depth and inclination for each site at Lough Hyne. Data are untransformed, and analyses were carried out on Bray-Curtis dissimilarities. Depth is reported above each data point. Data from inclined surfaces are reported as triangles, data from vertical surfaces are reported as squares.

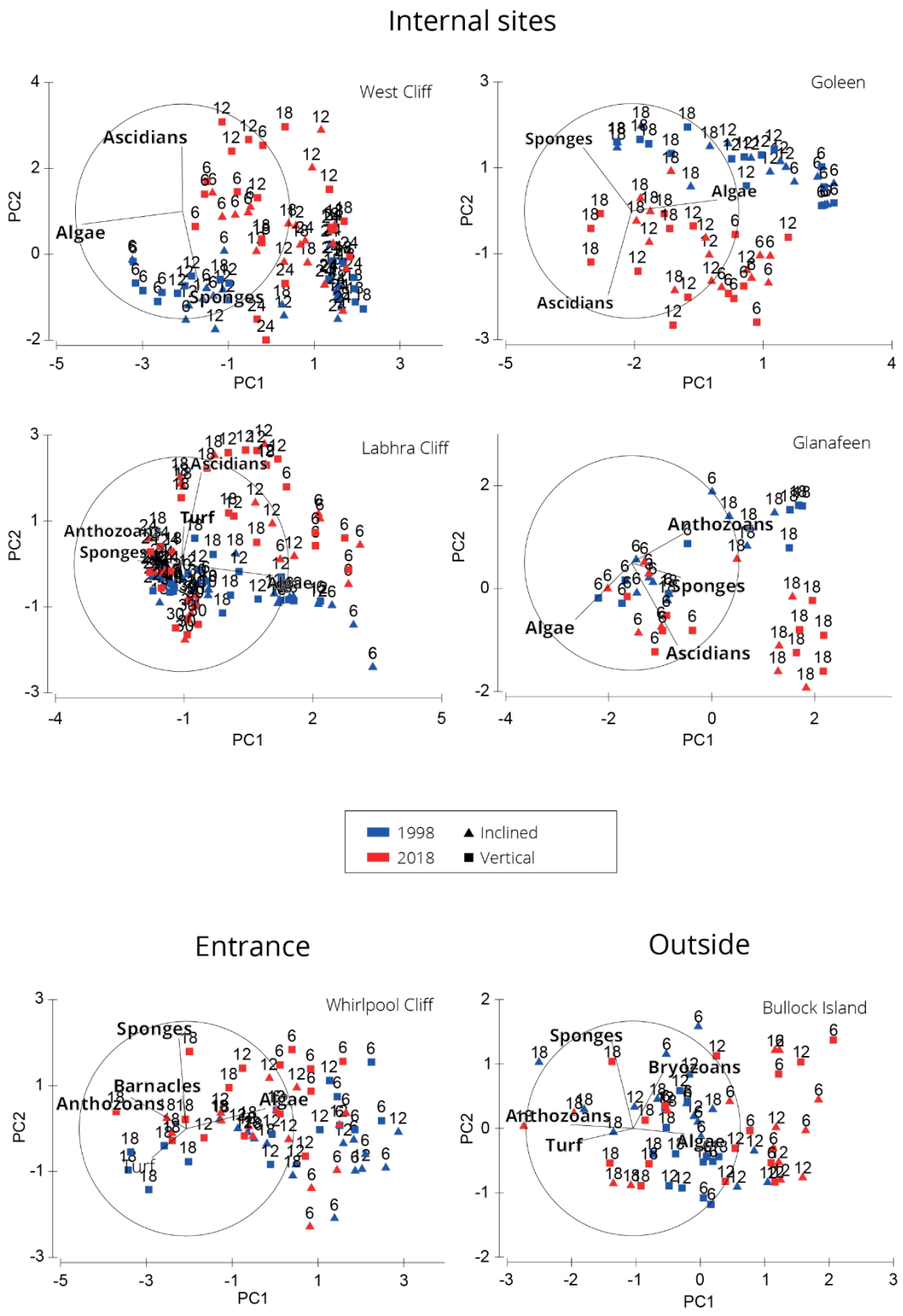

Figure S2.2. Principal Component Analysis (PCA) of benthic communities for each combination of depth and inclination, for each site at Lough Hyne. Data are log+1 transformed. Depth is reported above each data point. Data from inclined surfaces are reported as triangles, data from vertical surfaces are reported as squares.

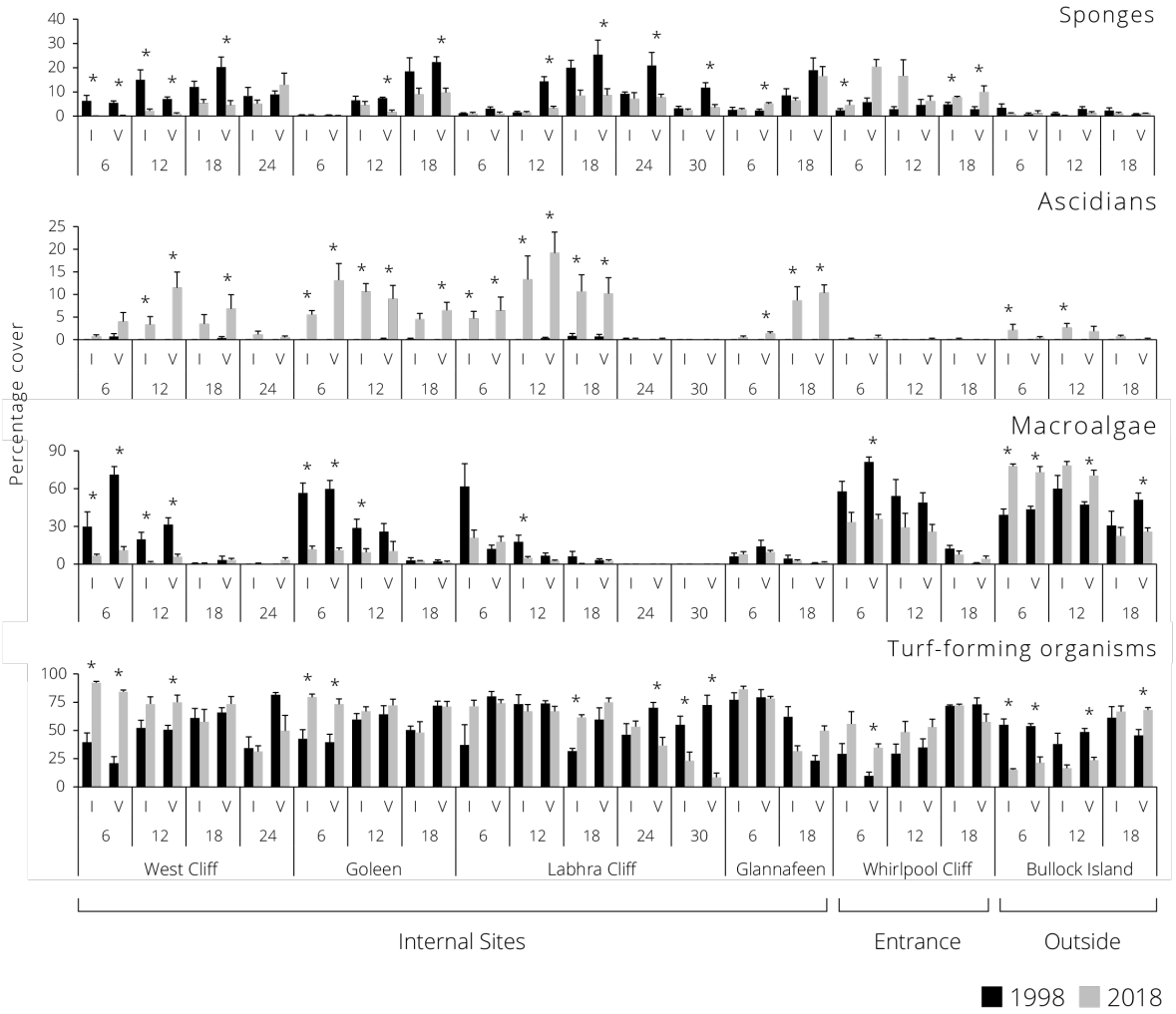

Figure S2.3. Mean percentage cover of main benthic organisms at each site, depth and inclination in 1998 and 2018. (I) Inclined surfaces. (V) Vertical surfaces. Sites are ordered from the innermost one (left) to the outer one (right). Error bars indicate standard errors (n = 5). Note the different scales. * indicates significant difference ($p < 0.05$) between 1998 and 2018.

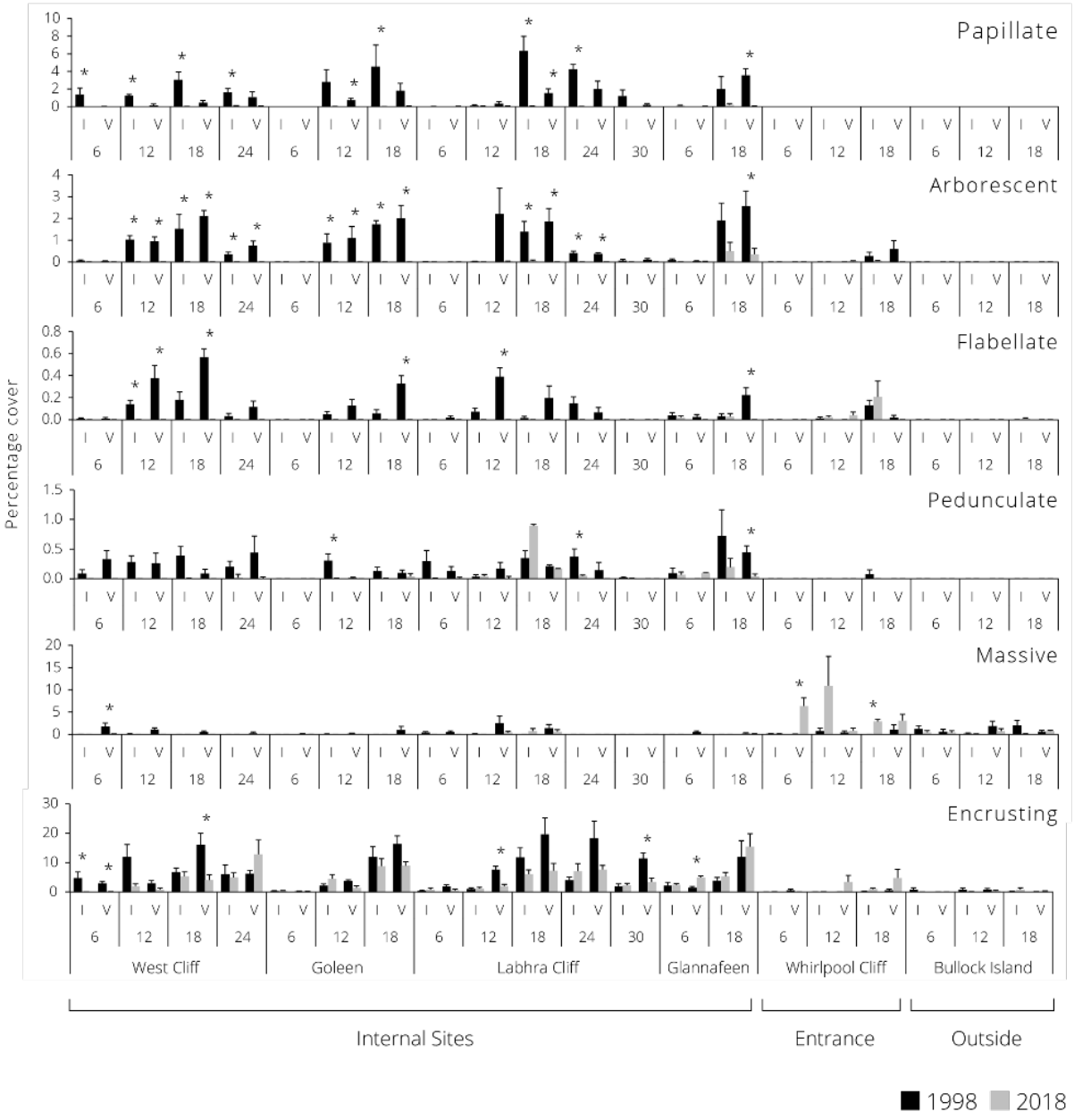

Figure S2.4. Mean percentage cover of main sponge morphological types at each site, depth and inclination in 1998 and 2018. (I) Inclined surfaces. (V) Vertical surfaces. Sites are ordered from the innermost one (left) to the outer one (right). Error bars indicate standard errors (n = 5). Note the different scales. * indicates significant difference ($p < 0.05$) between 1998 and 2018.

Figure S2.5. Heatwaves and cold spells occurred in the area of study. Graphical visualisation of SST heatwaves (a) and cold spells (b) occurred between October 2010 and August 2015. (c) Heatwave and cold spell cumulative intensity between 1982 and 2019. Graphical visualisation of air temperature heatwaves (d) and cold spells (d) occurred between October 2010 and August 2015. (f) Cumulative intensity of air temperature heatwaves and cold spells between 1982 and 2019. Note the different scales. In (d) and (e), the estimated time frame of the change (10/2010 - 08/2015) is highlighted in grey. SST Data Copyright: NOAA's Optimum Interpolation Sea Surface Temperature (OISST) version 2. Air Temperature Data Copyright: Met Éireann. Source www.met.ie. This data is published under a Creative Commons Attribution 4.0 International (CC BY 4.0). Met Éireann does not accept any liability whatsoever for any error or omission in the data, their availability, or any loss or damage arising from their use.

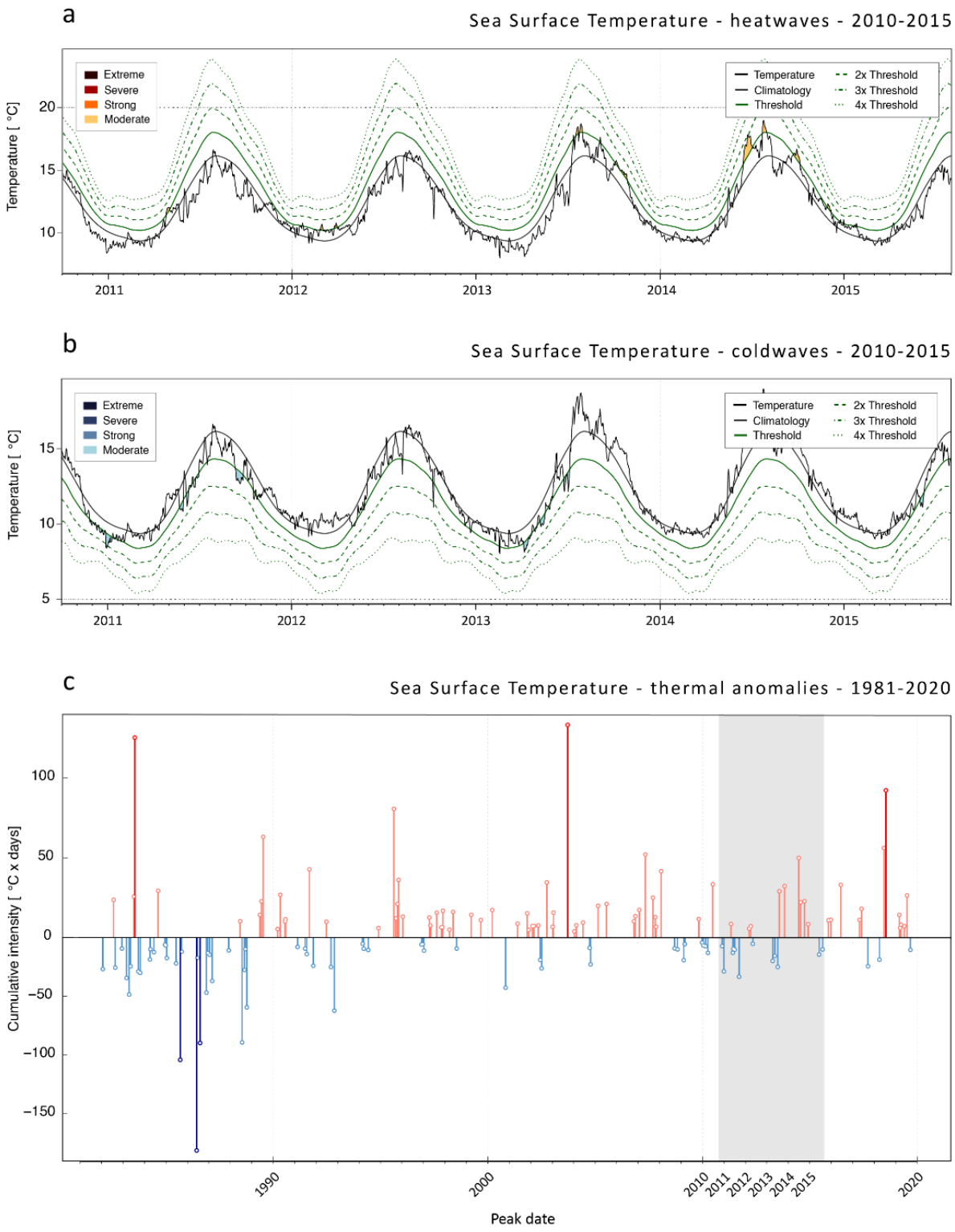
a
Sea Surface Temperature - heatwaves - 2010-2015
Extreme
Severe
Strong
Moderate
Temperature
Climatology
Threshold
2x Threshold
3x Threshold
4x Threshold
Temperature [°C]
20
15
10
2011
2012
2013
2014
2015
b
Sea Surface Temperature - coldwaves - 2010-2015
Extreme
Severe
Strong
Moderate
Temperature
Climatology
Threshold
2x Threshold
3x Threshold
4x Threshold
Temperature [°C]
15
10
5
2011
2012
2013
2014
2015
c
Sea Surface Temperature - thermal anomalies - 1981-2020
Cumulative intensity [°C x days]
100
50
0
−50
−100
−150
1990
2000
2010
2011
2012
2013
2014
2015
2020
Peak date

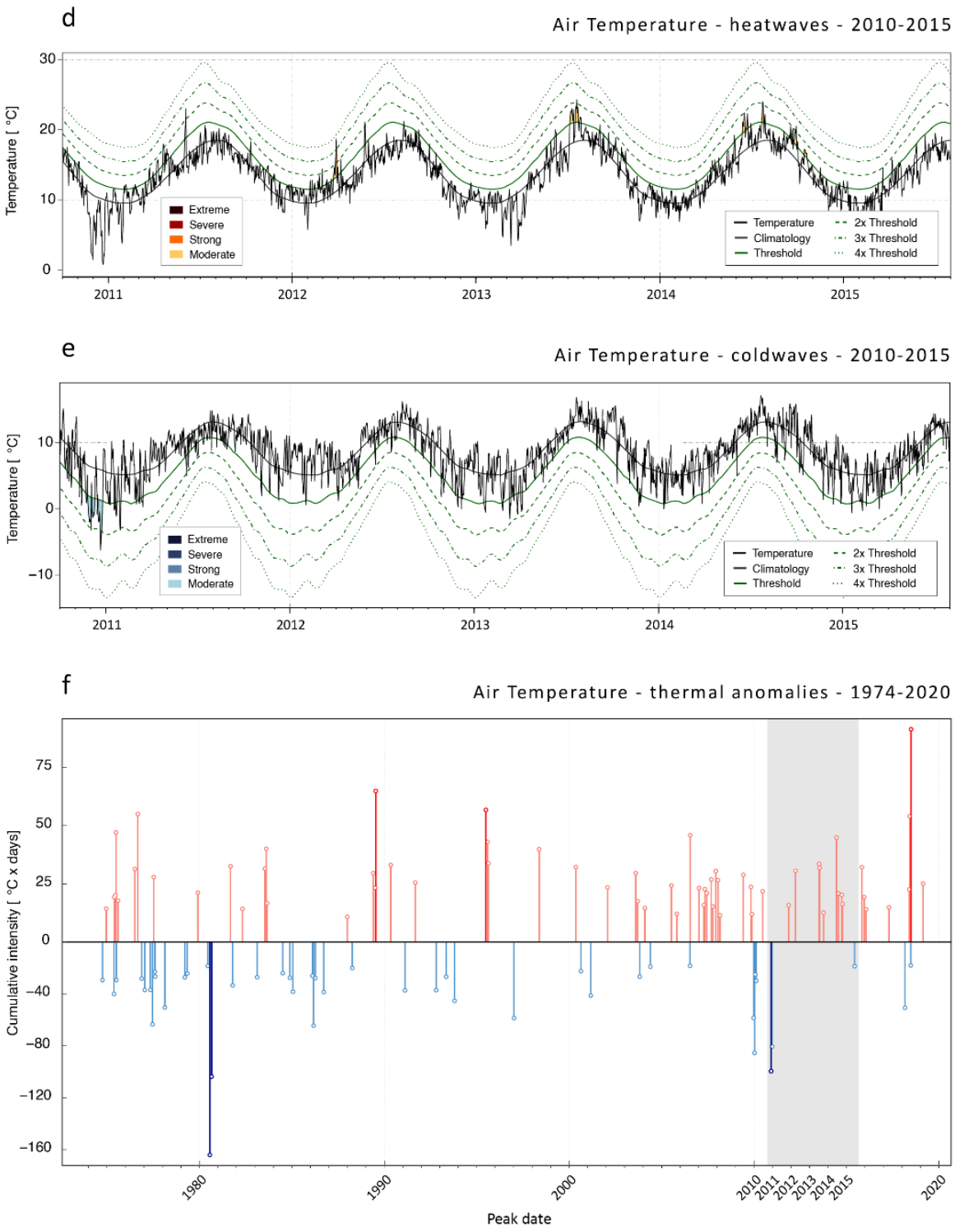
d
Air Temperature - heatwaves - 2010-2015
Temperature [°C]
30
20
10
0
2011
2012
2013
2014
2015
Extreme
Severe
Strong
Moderate
Temperature
Climatology
Threshold
2x Threshold
3x Threshold
4x Threshold
e
Air Temperature - coldwaves - 2010-2015
Temperature [°C]
10
0
−10
2011
2012
2013
2014
2015
Extreme
Severe
Strong
Moderate
Temperature
Climatology
Threshold
2x Threshold
3x Threshold
4x Threshold
f
Air Temperature - thermal anomalies - 1974-2020
Cumulative intensity [°C x days]
75
50
25
0
−40
−80
−120
−160
1980
1990
2000
2010
2011
2012
2013
2014
2015
2020
Peak date

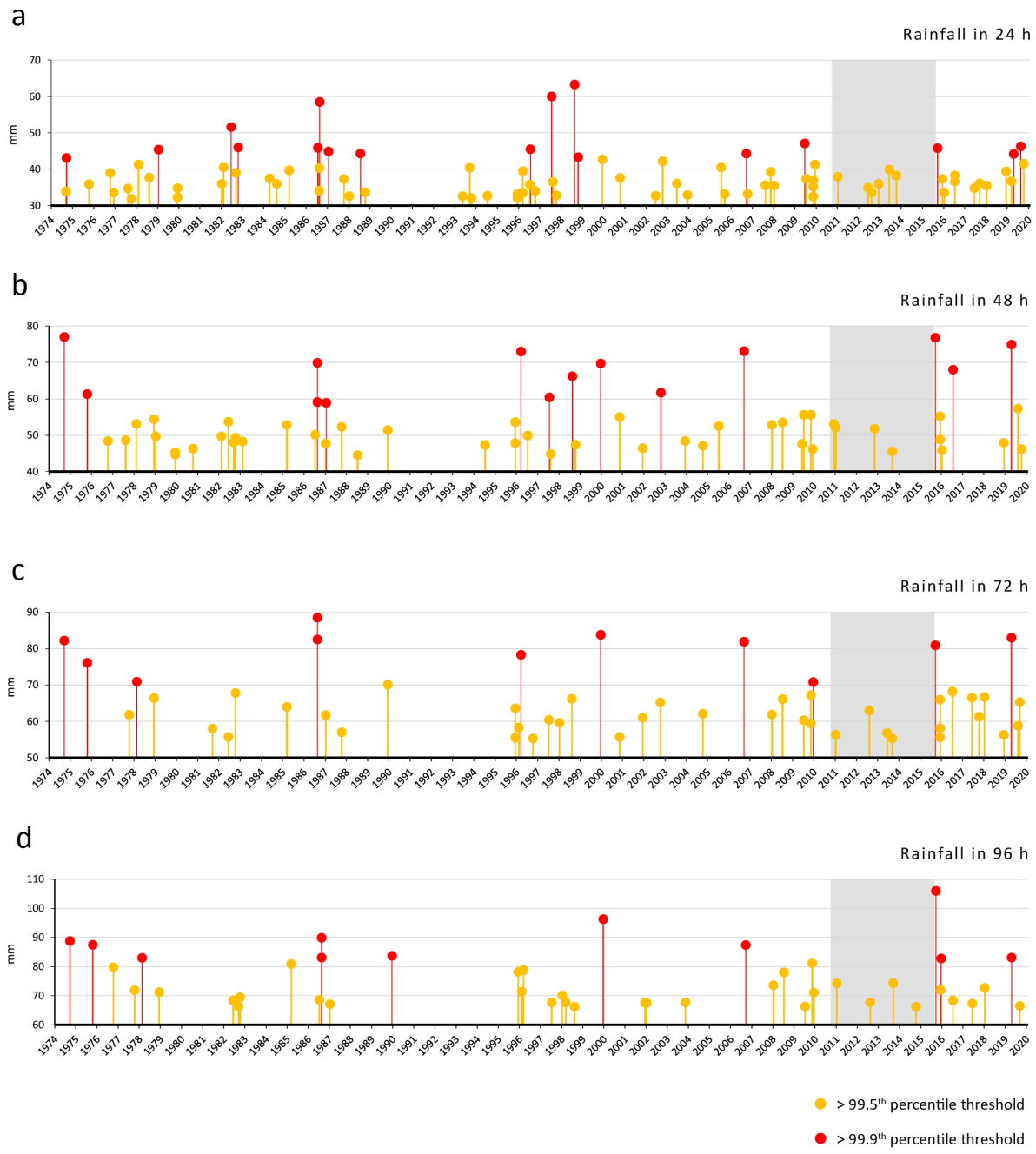

Figure S2.6. Extreme precipitation events at the Sherkin Island weather station (3402) between July 1974 and December 2019. Events of 24 h (a), 48 h (b), 72 h (c) and 96 h (d) in which total amount of rainfall exceeded the 99.5th percentile threshold (yellow dots) and 99.9th percentile threshold (red dots). The estimated time frame of the change (10/2010 - 08/2015) is highlighted in grey. Data Copyright: Met Éireann. Source www.met.ie. This data is published under a Creative Commons Attribution 4.0 International (CC BY 4.0). Met Éireann does not accept any liability whatsoever for any error or omission in the data, their availability, or any loss or damage arising from their use.

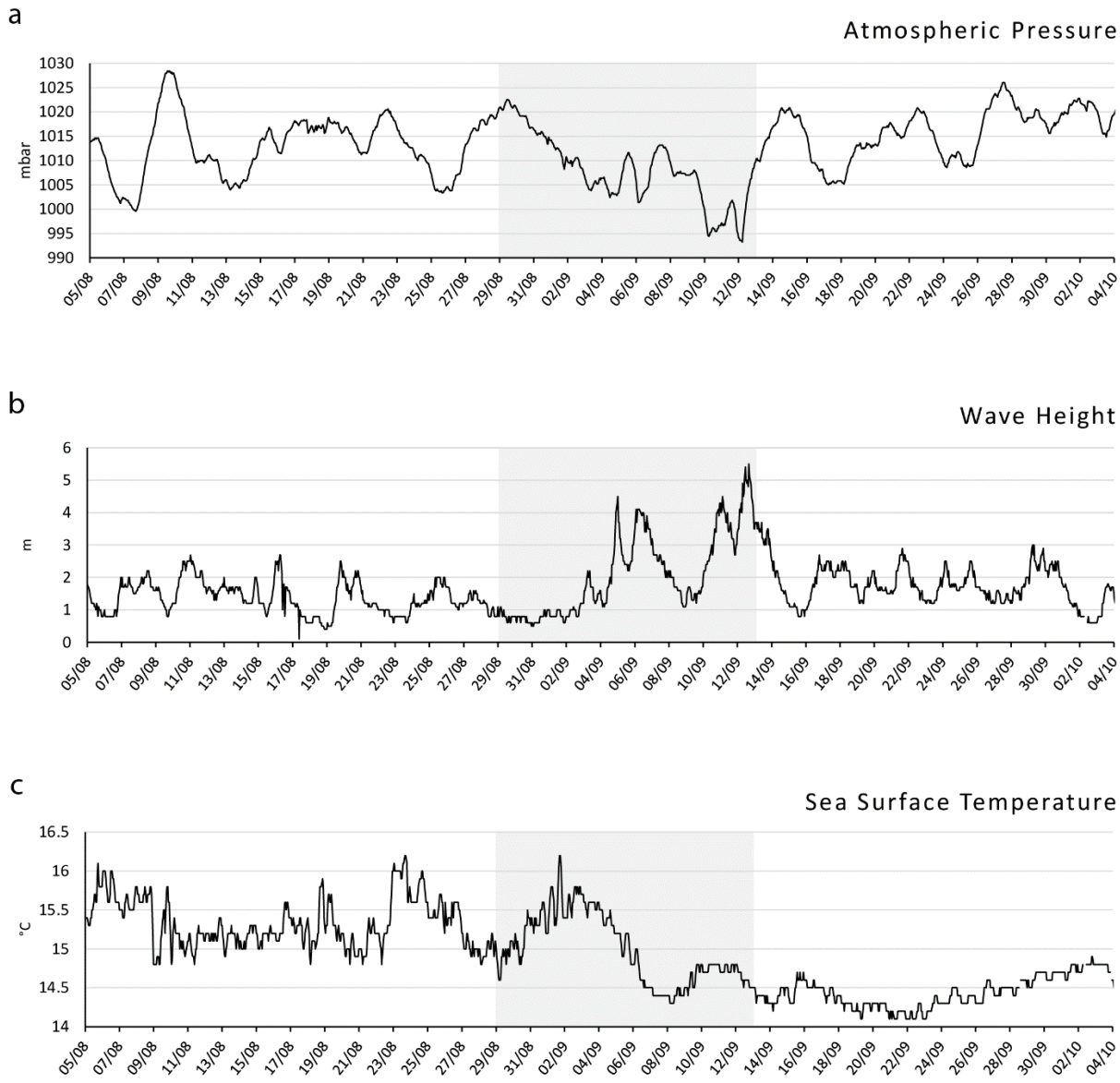

Figure S2.7. Effects of the Hurricane Katia (2011) on atmospheric pressure (a), wave height (b) and sea surface temperature (c) at the M5 buoy (51° 41' 25.5" N, 6° 42' 15.6" W) of the Irish Marine Data Buoy Observation Network. The period of the storm (29/08/2011 - 13/09/2011) is highlighted in grey. Data Copyright: Marine Institute. Source www.marine.ie. This data is published under a Creative Commons Attribution 4.0 International (CC BY 4.0). Marine Institute does not accept any liability whatsoever for any error or omission in the data, their availability, or for any loss or damage arising from their use.

Table S2.1. OTUs/taxa found during this study, with the correspondent morphological type and the sponge species/genera associated.

OTU/taxon	Morphological type	Species associated
Amphilectus fucorum	Repent	*Amphilectus fucorum* (Esper, 1794)
Aplysilla rosea	Encrusting	*Aplysilla rosea* (Barrois, 1876)
Aplysilla sulfurea	Encrusting	*Aplysilla sulfurea* Schulze, 1878
Axinella damicornis	Flabellate	*Axinella damicornis* (Esper, 1794)
Axinella dissimilis	Arborescent	*Axinella dissimilis* (Bowerbank, 1866)
Cliona celata	Massive	*Cliona celata* Grant, 1826
Dysidea spp.	Massive	*Dysidea fragilis* (Montagu, 1814)
		Dysidea pallescens (Schmidt, 1862)
Encrusting Orange Sponges (EOS)	Encrusting	*Antho involvens* (Schmidt, 1864)
		Eurypon spp. Gray, 1867
		Hymeraphia stellifera Bowerbank, 1864
Encrusting Red Sponges (ERS)	Encrusting	*Eurypon major* Sarà & Siribelli, 1960
		Eurypon spp. Gray, 1867
Encrusting Yellow Sponges (EYS)	Encrusting	*Encrusting Suberitidae* Schmidt, 1870
		Eurypon spp. Gray, 1867
		Halicnemia gallica (Topsent, 1893)
		Myxilla incrustans (Johnston, 1842)
		Paratimea loennbergi (Alander, 1942)
		Protosuberites incrustans (Hansen, 1885)
		Pseudosuberites sulphureus (Bowerbank, 1866)
		Unknown Tethyidae
Haliclona fistulosa	Other	*Haliclona fistulosa* (Bowerbank, 1866)
Haliclona spp.	Other	*Haliclona cinerea* (Grant, 1826)
		Haliclona simulans (Johnston, 1842)
		Haliclona spp. Grant, 1841
		Haliclona viscosa (Topsent, 1888)
Haliclona urceolus	Tubular	*Haliclona urceolus* (Rathke & Vahl, 1806)
Hymeniacidon perlevis	Massive	*Hymeniacidon perlevis* (Montagu, 1814)
Iophon hyndmani	Encrusting	*Iophon hyndmani* (Bowerbank, 1858)
Pachymatisma johnstonia	Massive	*Pachymatisma johnstonia* (Bowerbank in Johnston, 1842)
Polymastiidae	Papillate	*Polymastia boletiformis* (Lamarck, 1815)
		Polymastia spp. Bowerbank, 1862
		Sphaerotylus renoufi Plotkin, Morrow, Gerasimova & Rapp, 2017
		Sphaerotylus sp. Topsent, 1898
Raspailia ramosa	Arborescent	*Raspailia ramosa* (Montagu, 1814)
Stelligera rigida	Flabellate	*Stelligera rigida* (Montagu, 1814)
Suberites spp.	Pedunculate	*Suberites carnosus* (Johnston, 1842)
		Suberites ficus (Johnston, 1842)
Tethya aurantium	Globular	*Tethya aurantium* (Pallas, 1766)

OTU/species		Species associated
Yellow Arborescent Sponges (YAS)	Arborescent	*Raspailia hispida* (Montagu, 1814)
		Stelligera stuposa (Ellis & Solander, 1786)
Yellow-Brown Cushions (YBC)	Massive	*Biemna variantia* (Bowerbank, 1858)
		Halichondria bowerbanki Burton, 1930
		Halichondria panicea (Pallas, 1766)
		Hymeniacidon kitchingi (Burton, 1935)
		Mycale contarenii (Lieberkühn, 1859)
		Mycale macilenta (Bowerbank, 1866)

Table S2.2. Three-way PERMANOVAs testing differences in overall benthic community and sponge assemblage composition at Lough Hyne in 1998 and 2018, between sites (SI), depths (DE) and inclination (IN), and their interactions. Percentage of variance explained by each factor or combination of factors (SS_i/SS_{tot}) is indicated as "% Var". Significant p-values are given in bold.

Benthic communities

1998						2018					
Source	df	% Var	MS	Pseudo-*F*	*p*	Source	df	% Var	MS	Pseudo-*F*	*p*
SI	5	30.4%	4253	23.19	**0.0001**	SI	5	16.3%	2184	13.32	**0.0001**
DE	1	28.6%	20009	14.39	**0.0003**	DE	1	34.7%	23219	13.99	**0.0038**
IN	1	1.0%	672	1.22	0.3499	IN	1	0.2%	136	0.14	0.9201
SIxDE	5	9.9%	1390	7.58	**0.0001**	SIxDE	5	12.4%	1662	10.14	**0.0001**
SIxIN	5	3.9%	551	3.00	**0.0002**	SIxIN	5	7.4%	991	6.04	**0.0001**
DExIN	1	0.3%	243	2.73	0.0772	DExIN	1	0.6%	376	0.64	0.5399
SIxDExIN	5	0.6%	89	0.48	0.9466	SIxDExIN	5	4.4%	588	3.58	**0.0005**
Res	96	25.2%	183			Res	94	23.0%	164		

Sponge assemblages

1998						2018					
Source	df	% Var	MS	Pseudo-*F*	*p*	Source	df	% Var	MS	Pseudo-*F*	*p*
SI	5	29.0%	25195	14.06	**0.0001**	SI	5	32.3%	28716	17.44	**0.0001**
DE	1	7.6%	32856	3.12	**0.0318**	DE	1	7.4%	33023	2.64	**0.0268**
IN	1	1.8%	8035	1.93	0.111	IN	1	0.8%	3378	0.88	0.5541
SIxDE	5	12.1%	10544	5.88	**0.0001**	SIxDE	5	14.1%	12515	7.60	**0.0001**
SIxIN	5	4.8%	4170	2.33	**0.0001**	SIxIN	5	4.3%	3837	2.33	**0.0002**
DExIN	1	0.5%	1981	0.49	0.8293	DExIN	1	0.6%	2596	0.59	0.7898
SIxDExIN	5	4.7%	4051	2.26	**0.0001**	SIxDExIN	5	4.9%	4365	2.65	**0.0001**
Res	96	39.6%	1792			Res	96	35.6%	1647		

Table S2.3. Four-way PERMANOVA main tests and pairwise comparisons testing differences in benthic community composition and sponge assemblages between years (YE), depths (DE) and inclinations (IN) and their interactions at each site at Lough Hyne. The percentage of variance explained by each factor or combination of factors (SS_i/SS_{tot}) is indicated as "% Var". Significant *p*-values are given in bold.

Four-way PERMANOVA

	Benthic communities					Sponge assemblages				
Source	df	% Var	MS	Pseudo-F	p	df	% Var	MS	Pseudo-F	p
YE	1	8.5%	12804	7.01	**0.0014***	1	1.7%	15502	1.86	0.1434
SI	5	15.5%	4640	2.54	**0.0393***	5	25.5%	45577	5.47	**0.0053***
DE	1	28.9%	43249	20.60	**0.0001***	1	5.5%	49439	1.65	0.1245
IN	1	0.5%	788	1.49	0.2389	1	1.0%	9139	1.74	0.1235
YExSI	5	6.1%	1827	10.51	**0.0001***	5	4.7%	8334	4.85	**0.0001***
YExDE	1	0.0%	12	0.01	0.9864	1	1.8%	16439	2.75	**0.0338***
YExIN	1	0.0%	14	0.02	0.9933	1	0.3%	2275	0.71	0.6058
SIxDE	5	7.1%	2132	2.34	0.0719	5	9.5%	17077	2.85	**0.0022***
SIxIN	5	3.1%	931	1.50	0.2115	5	2.7%	4808	1.50	0.1677
DExIN	1	0.4%	562	0.93	0.5452	1	0.4%	3188	1.18	0.3231
YExSIxDE	5	3.0%	911	5.24	**0.0001***	5	3.3%	5982	3.48	**0.0001***
YExSIxIN	5	2.1%	619	3.56	**0.0003***	5	1.8%	3199	1.86	**0.0008***
YExDExIN	1	0.0%	58	0.89	0.4503	1	0.2%	1390	0.36	0.954
SIxDExIN	5	2.1%	616	9.46	**0.0002***	5	2.5%	4560	1.18	0.309
YExSIxDExIN	5	0.2%	65	0.37	0.9786	5	2.2%	3856	2.24	**0.0001***
Res	190	22.0%	174			192	36.9%	1719		

PERMANOVA Pairwise comparisons - Benthic communities

		Internal Sites				**Entrance**	**Outside**
		West Cliff	Goleen	Labhra Cliff	Glannafeen	Whirlpool Cliff	Bullock Island
6 m	Inclined	**0.0078*** (t=3.36)	**0.0058*** (t=5.5)	**0.0169*** (t=2.67)	0.0981 (t=1.46)	0.1383 (t=1.45)	**0.0091*** (t=3.15)
	Vertical	**0.0077*** (t=4.82)	**0.0083*** (t=4.54)	**0.0082*** (t=2.48)	**0.0075*** (t=2.32)	**0.0082*** (t=3.8)	**0.0087*** (t=2.61)
12m	Inclined	**0.0069*** (t=3.14)	**0.0082*** (t=3.84)	**0.0086*** (t=3.11)		0.0465 (t=1.98)	**0.0156*** (t=2.04)
	Vertical	**0.0079*** (t=4.09)	**0.0079*** (t=2.96)	**0.0056*** (t=4)		0.23 (t=1.26)	**0.0082*** (t=2.17)
18m	Inclined	0.2634 (t=1.26)	**0.0101*** (t=2.86)	**0.0088*** (t=2.64)	**0.0226*** (t=2.17)	0.0855 (t=1.84)	0.1983 (t=1.25)
	Vertical	**0.0258*** (t=1.96)	**0.007*** (t=3.71)	**0.0081*** (t=2.08)	**0.0081*** (t=3.64)	0.039 (t=1.79)	**0.0091*** (t=3.07)
24m	Inclined	0.4297 (t=1.01)		0.0882 (t=1.44)			
	Vertical	0.1668 (t=1.38)		**0.0074*** (t=2.55)			
30m	Inclined			**0.0169*** (t=2.54)			
	Vertical			**0.0084*** (t=3.13)			

PERMANOVA Pairwise comparisons - Sponge Assemblages

		Internal Sites				**Entrance**	**Outside**
		West Cliff	Goleen	Labhra Cliff	Glannafeen	Whirlpool Cliff	Bullock Island
6 m	Inclined	**0.0003*** (t=3.94)	0.3494 (t=1.06)	0.0637 (t=1.56)	0.1353 (t=1.28)	0.6761 (t=0.62)	0.2711 (t=1.09)
	Vertical	**0.0082*** (t=2.45)	0.2859 (t=1.13)	**0.0163*** (t=1.73)	**0.0086*** (t=1.94)	**0.0082*** (t=2.82)	0.8143 (t=0.57)
12m	Inclined	**0.0073*** (t=2.03)	**0.0165*** (t=2.2)	**0.0244*** (t=1.53)		0.1433 (t=1.45)	0.323 (t=1.1)
	Vertical	**0.0087*** (t=2.88)	**0.0069*** (t=1.93)	**0.0094*** (t=1.83)		0.0625 (t=1.36)	0.0538 (t=1.4)
18m	Inclined	**0.0069*** (t=2.88)	**0.009*** (t=2.85)	**0.0102*** (t=3.03)	0.0556 (t=1.56)	**0.0067*** (t=3.69)	0.0417 (t=1.54)
	Vertical	**0.0166*** (t=1.98)	**0.0073*** (t=2.56)	**0.006*** (t=2.84)	**0.0085*** (t=2.55)	0.0831 (t=1.42)	0.1828 (t=1.28)
24m	Inclined	0.0336 (t=1.89)		**0.0089*** (t=3.47)			
	Vertical	**0.0072*** (t=2.84)		**0.0163*** (t=2.56)			
30m	Inclined			0.0538 (t=1.42)			
	Vertical			**0.0166*** (t=2.33)			

Table S2.4. Three-way PERMANOVAs on each individual site, testing differences in sponge assemblages and benthic communities at Lough Hyne. WE West Cliff, GO Goleen, LA Labhra Cliff, GL Glannafeen, WH Whirlpool Cliff, BU Bullock Island. Percentage of variance explained by each factor or combination of factors (SSi/SStot) is indicated as "% Var". Significant p-values are given in bold.

Three-way PERMANOVA - Benthic communities

	WE (Internal)					GO (Internal)					LA (Internal)				
Source	df	% Var	MS	Pseudo-*F*	*p*	df	% Var	MS	Pseudo-*F*	*p*	df	% Var	MS	Pseudo-*F*	*p*
YE	1	14.0%	7494	28.05	**0.0001**	1	32.9%	10756	76.23	**0.0001**	1	8.0%	5800	27.88	**0.0001**
DE	3	34.0%	6061	3.48	**0.0426**	2	41.5%	6791	46.83	**0.0033**	4	51.2%	9242	5.20	**0.0021**
IN	1	5.1%	2726	15.29	**0.0222**	1	2.7%	894	83.21	**0.0036**	1	1.7%	1207	0.80	0.5538
YExDE	3	9.8%	1742	6.52	**0.0001**	2	0.9%	145	1.03	0.3958	4	9.9%	1779	8.55	**0.0001**
YExIN	1	0.3%	178	0.67	0.6052	1	0.0%	11	0.08	0.9236	1	2.1%	1513	7.27	**0.0001**
DExIN	3	4.4%	784	13.88	**0.0006**	2	1.0%	165	3.45	0.1198	4	2.9%	522	2.44	0.0593
YExDExIN	3	0.3%	57	0.21	0.9880	2	0.3%	48	0.34	0.8748	4	1.2%	214	1.03	0.4327
Res	64	32.0%	267			48	20.7%	141			80	23.1%	208		

	GL (Internal)					WH (Entrance)					BU (Outside)				
Source	df	% Var	MS	Pseudo-*F*	*p*	df	% Var	MS	Pseudo-*F*	*p*	df	% Var	MS	Pseudo-*F*	*p*
YE	1	13.6%	2433	13.06	**0.0001**	1	8.6%	2182	13.50	**0.0002**	1	13.2%	2115	16.26	**0.0001**
DE	1	39.4%	7057	8.78	0.0500	2	38.9%	4925	11.43	**0.0154**	2	27.4%	2193	2.63	0.1508
IN	1	3.4%	606	1.45	0.3705	1	8.8%	2224	3.90	0.1580	1	1.7%	269	0.66	0.6056
YExDE	1	4.5%	804	4.32	**0.0104**	2	3.4%	431	2.67	**0.0380**	2	10.4%	835	6.42	**0.0001**
YExIN	1	2.3%	419	2.25	0.0934	1	2.3%	571	3.53	**0.0353**	1	2.5%	408	3.14	**0.0344**
DExIN	1	2.0%	358	1.51	0.3957	2	5.3%	677	2.52	0.1975	2	4.5%	360	3.36	0.1121
YExDExIN	1	1.3%	237	1.28	0.2740	2	2.1%	268	1.66	0.1546	2	1.3%	107	0.82	0.5492
Res	30	31.2%	186			48	30.6%	162			48	39.0%	130		

Three-way PERMANOVA - Sponge assemblages

	WE (Internal)					GO (Internal)					LA (Internal)				
Source	df	% Var	MS	Pseudo-*F*	*p*	df	% Var	MS	Pseudo-*F*	*p*	df	% Var	MS	Pseudo-*F*	*p*
YE	1	14.8%	33400	22.32	**0.0001**	1	8.4%	14861	8.01	**0.0001**	1	7.1%	18710	11.56	**0.0001**
DE	3	12.8%	9615	1.02	0.4338	2	24.3%	21500	5.88	**0.0008**	4	18.2%	11943	1.70	0.1127
IN	1	2.9%	6639	0.76	0.6327	1	2.4%	4308	0.97	0.5196	1	4.3%	11271	2.63	0.0956
YExDE	3	12.5%	9387	6.27	**0.0001**	2	4.1%	3658	1.97	**0.0240**	4	10.7%	7043	4.35	**0.0001**
YExIN	1	3.9%	8714	5.82	**0.0002**	1	2.5%	4443	2.39	**0.0242**	1	1.6%	4285	2.65	**0.0070**
DExIN	3	6.3%	4777	1.45	0.2153	2	4.6%	4108	1.37	0.3246	4	4.1%	2690	0.92	0.5802
YExDExIN	3	4.4%	3287	2.20	**0.0047**	2	3.4%	2990	1.61	0.0741	4	4.5%	2917	1.80	**0.0056**
Res	64	42.4%	1496			48	50.3%	1856			80	49.4%	1619		

	GL (Internal)					WH (Entrance)					BU (Outside)				
Source	df	% Var	MS	Pseudo-*F*	*p*	df	% Var	MS	Pseudo-*F*	*p*	df	% Var	MS	Pseudo-*F*	*p*
YE	1	9.0%	6421	5.29	**0.0001**	1	7.2%	9410	6.55	**0.0001**	1	2.6%	5424	1.96	0.0651
DE	1	18.6%	13300	2.44	0.1567	2	15.5%	10154	3.04	0.0500	2	14.9%	15777	3.60	**0.0174**
IN	1	4.1%	2944	2.47	0.1560	1	4.3%	5615	1.90	0.2473	1	3.7%	7888	1.85	0.2305
YExDE	1	7.6%	5455	4.50	**0.0002**	2	5.1%	3337	2.32	**0.0140**	2	4.1%	4379	1.59	0.0879
YExIN	1	1.7%	1191	0.98	0.4418	1	2.3%	2948	2.05	0.0702	1	2.0%	4257	1.54	0.1509
DExIN	1	1.4%	995	0.41	0.8214	2	6.4%	4204	0.97	0.5109	2	7.3%	7752	2.94	**0.0372**
YExDExIN	1	3.4%	2407	1.98	0.0665	2	6.6%	4312	3.00	**0.0023**	2	2.5%	2641	0.96	0.4888
Res	32	54.3%	1213			48	52.7%	1437			48	62.7%	2761		

Table S2.5. Pairwise *t*-tests (unequal variance *t*-test on ranked data) comparing percentage cover of the benthic organisms that changed the most between 1998 and 2018 for each combination of site, depth and inclination at Lough Hyne. The values are *p*-values, while *t*-values are indicated in brackets (n = 5). Significant *p*-values after Benjamini-Hochberg procedure are indicated in bold with an asterisk.

Sponges

		West Cliff	Goleen	Labhra Cliff	Glanafeen	Whirlpool Cliff	Bullock Island
6m	Inclined	0.0004*	0.732	0.777	0.2	0.631	0.122
	Vertical	0.0008*	1	0.072	0.016*	0.0011*	1
12m	Inclined	0.001*	0.275	0.924		0.037	0.122
	Vertical	0.001*	0.001*	0.001*		0.126	0.192
18m	Inclined	0.071	0.122	0.037	0.631	0.005*	0.631
	Vertical	0.005*	0.001*	0.005*	0.774	0.005*	0.138
24m	Inclined	0.924		0.283			
	Vertical	0.924		0.005*			
30m	Inclined			0.379			
	Vertical			0.005*			

Ascidians

		West Cliff	Goleen	Labhra Cliff	Glanafeen	Whirlpool Cliff	Bullock Island
6m	Inclined	0.178	0.002*	0.002*	0.181	0.374	0.023*
	Vertical	0.072	0.002*	0.002*	0.022*	0.374	0.374
12m	Inclined	0.023*	0.002*	0.002*			0.023*
	Vertical	0.002*	0.001*	0.001*		0.374	0.077
18m	Inclined	0.077	0.03	0.015*	0.002*	0.374	0.077
	Vertical	0.003*	0.002*	0.004*	0.002*		0.374
24m	Inclined	0.181		0.892			
	Vertical	0.181		0.374			
30m	Inclined						
	Vertical						

Table S2.5. (Continued)

Macroalgae

		West Cliff	Goleen	Labhra Cliff	Glanafeen	Whirlpool Cliff	Bullock Island
6m	Inclined	0.005*	0.001*	0.121	0.629	0.072	0.001*
	Vertical	0.001*	0.001*	0.278	0.777	0.001*	0.001*
12m	Inclined	0.005*	0.016*	0.016*		0.275	0.278
	Vertical	0.001*	0.078	0.08		0.037	0.001*
18m	Inclined	0.441	0.635	0.248	0.704	0.19	0.773
	Vertical	0.244	0.549	0.848	0.361	0.081	0.001*
24m	Inclined	0.181					
	Vertical	0.077					
30m	Inclined						
	Vertical						

Turf-forming organisms

		West Cliff	Goleen	Labhra Cliff	Glanafeen	Whirlpool Cliff	Bullock Island
6m	Inclined	0.001*	0.001*	0.384	0.278	0.122	0.001*
	Vertical	0.001*	0.002*	0.276	0.637	0.001*	0.001*
12m	Inclined	0.072	0.631	0.498		0.378	0.071
	Vertical	0.005*	0.321	0.198		0.071	0.001*
18m	Inclined	0.631	0.777	0.001*	0.016*	0.699	0.924
	Vertical	0.499	1	0.189	0.005*	0.077	0.001*
24m	Inclined	0.924		0.28			
	Vertical	0.138		0.005*			
30m	Inclined			0.016*			
	Vertical			0.001*			

Table S2.6. Pairwise *t*-tests (unequal variance *t*-test on ranked data) comparing percentage cover of the main sponge morphological types between 1998 and 2018 for each combination of site, depth and inclination at Lough Hyne. The values are *p*-values, while *t*-values are shown in brackets (n = 5). Significant *p*-values after Benjamini-Hochberg procedure are indicated in bold with an asterisk.

Papillate							
		West Cliff	**Goleen**	**Labhra Cliff**	**Glanafeen**	**Whirlpool Cliff**	**Bullock Island**
6m	Inclined	0.001*		0.374	0.073		
	Vertical	0.374		0.374	0.073		
12m	Inclined	0.001*	0.033	0.936			
	Vertical	0.374	0.019*	0.549			
18m	Inclined	0.0004*	0.0004*	0.001*	0.47		
	Vertical	0.073	0.101	0.001*	0.001*		
24m	Inclined	0.005*		0.0004*			
	Vertical	0.315		0.073			
30m	Inclined			0.073			
	Vertical			0.179			

Arborescent							
		West Cliff	**Goleen**	**Labhra Cliff**	**Glanafeen**	**Whirlpool Cliff**	**Bullock Island**
6m	Inclined	0.179		0.374	0.179		
	Vertical	0.179			0.366		
12m	Inclined	0.001*	0.001*	0.374			
	Vertical	0.001*	0.019*	0.033		0.374	
18m	Inclined	0.019*	0.001*	0.0004*	0.058	0.769	
	Vertical	0.001*	0.001*	0.001*	0.001*	0.179	
24m	Inclined	0.001*		0.001*			
	Vertical	0.001*		0.001*			
30m	Inclined			0.374			
	Vertical			0.179			

Flabellate							
		West Cliff	**Goleen**	**Labhra Cliff**	**Glanafeen**	**Whirlpool Cliff**	**Bullock Island**
6m	Inclined	0.374			0.549		
	Vertical	0.374		0.374	0.374		
12m	Inclined	0.001*	0.073	0.073		0.654	
	Vertical	0.001*	0.073	0.001*		0.179	
18m	Inclined	0.073	0.179	0.374	0.654	0.716	0.374
	Vertical	0.001*	0.001*	0.073	0.001*	0.374	
24m	Inclined	0.179		0.019			
	Vertical	0.019		0.179			
30m	Inclined						
	Vertical						

Table S2.6. (Continued)

Pedunculate

		West Cliff	Goleen	Labhra Cliff	Glanafeen	Whirlpool Cliff	Bullock Island
6m	Inclined	0.179		0.073	0.176		
	Vertical	0.073		0.167	0.179		
12m	Inclined	0.019	0.001*	0.936			
	Vertical	0.179	0.374	0.073			
18m	Inclined	0.019	0.073	0.182	0.734	0.374	
	Vertical	0.179	0.288	0.187	0.001*		
24m	Inclined	0.167		0.002*			
	Vertical	0.019		0.179			
30m	Inclined			0.936			
	Vertical						

Massive

		West Cliff	Goleen	Labhra Cliff	Glanafeen	Whirlpool Cliff	Bullock Island
6m	Inclined	0.374		0.073		0.606	0.209
	Vertical	0.004*	0.221	0.019	0.073	0.0004*	0.549
12m	Inclined	0.374	0.179	0.179		0.283	0.176
	Vertical	0.019	0.073	0.209		0.732	0.078
18m	Inclined			0.073		0.001*	0.315
	Vertical	0.019	0.073	0.276	0.883	0.081	0.28
24m	Inclined						
	Vertical	0.374					
30m	Inclined						
	Vertical						

Globular

		West Cliff	Goleen	Labhra Cliff	Glanafeen	Whirlpool Cliff	Bullock Island
6m	Inclined			0.374	0.374	0.654	
	Vertical	0.073		0.654	0.374	0.374	
12m	Inclined	0.936		0.179		0.158	
	Vertical	0.019	0.366	0.501		0.654	0.936
18m	Inclined		0.374	0.549	0.374	0.002	
	Vertical	0.705	0.221	0.937	0.374	0.654	0.374
24m	Inclined						
	Vertical	0.374					
30m	Inclined						
	Vertical						

Table S2.6. (Continued)

Encrusting							
		West Cliff	**Goleen**	**Labhra Cliff**	**Glanafeen**	**Whirlpool Cliff**	**Bullock Island**
6m	Inclined	0.0004*	0.606	0.095	0.2	0.374	0.073
	Vertical	0.001*	0.466	0.078	0.001*	0.179	0
12m	Inclined	0.039	0.276	0.924		0.122	0.101
	Vertical	0.071	0.039	0.001*		0.033	0.458
18m	Inclined	0.499	0.774	0.19	0.497	0.056	0.715
	Vertical	0.005*	0.037	0.122	0.498	0.033	0.289
24m	Inclined	0.777		0.378			
	Vertical	0.192		0.072			
30m	Inclined			0.856			
	Vertical			0.005*			

Table S2.7. Presence/absence matrix of the sponge species found at Lough Hyne in 1998 and 2019. Data are given for the individual sites and for the all the sites inside the lough combined. Legend to morphology: **AR** arborescent, **EN** encrusting, **FL** flabellate, **G** globular, **MA** massive, **O** other, **PA** papillate, **PE** pedunculate, **RE** repent, **TU** tubular. * indicates taxa found only in 1998, † indicates taxa found only in 2019.

Species	West Cliff		Goleen		Labhra Cliff		Glanafeen		Whirlpool Cliff	
	2000	2019	2000	2019	2000	2019	2000	2019	2000	2019
Amphilectus fucorum		x				x		x	x	x
*Antho involvens**	x									
Aplysilla rosea			x		x	x				x
Aplysilla sulfurea	x	x	x	x	x	x			x	x
Axinella damicornis	x		x	x	x	x	x	x		x
Axinella dissimilis	x		x		x	x	x	x	x	x
Biemna variantia	x				x	x	x	x		
Ciocalypta penicillus†								x		
Clathrina coriacea	x	x	x		x		x		x	
Cliona celata	x		x		x	x	x	x	x	x
Dysidea fragilis	x	x	x	x	x	x	x	x	x	x
Dysidea pallescens	x				x			x		x
Encrusting Suberitidae	x	x	x	x	x	x	x	x	x	x
Eurypon major	x	x	x	x	x	x	x	x		x
Eurypon spp.	x	x	x	x	x	x	x	x	x	x
Halichondria bowerbanki	x		x	x	x	x	x	x	x	x
Halichondria panicea			x				x		x	x
Haliclona spp.	x	x	x	x	x	x	x	x	x	x
Haliclona urceolus	x	x	x	x	x	x	x			
Halicnemia patera	x		x		x	x	x	x		
Halisarca sp.					x	x	x	x		x
*Hemimycale columella**									x	
Homaxinella subdola†	x		x			x		x		
Hymedesmia coriacea†				x						x
*Hymedesmia paupertas**	x		x		x		x			
Hymeniacidon kitchingi	x		x	x	x		x	x	x	
Hymeniacidon perlevis	x		x	x	x	x	x	x	x	x
Hymeraphia stellifera	x	x	x	x	x	x	x	x	x	x
Iophon hyndmani		x		x			x	x	x	x
*Leuconia nivea**									x	
*Leucosolenia complicata**							x		x	
Mycale contarenii	x	x	x	x	x		x		x	x
Mycale macilenta	x			x			x			
Mycale rotalis	x	x	x	x		x	x		x	x
*Myxilla fimbriata**									x	
Myxilla incrustans†								x		x
Myxilla rosacea	x		x	x		x	x	x		x
Pachymatisma johnstonia		x	x	x					x	x
Paratimea constellata	x		x	x	x	x	x	x	x	x
Phakellia sp.*	x		x		x					
*Phorbas dives**									x	
*Phorbas fictitius**									x	
Plakortis simplex	x				x			x	x	
Polymastia spp.	x	x	x	x	x	x	x	x		x

Table A2.7. (Continued)

Species	West Cliff		Goleen		Labhra Cliff		Glanafeen		Whirlpool Cliff	
	2000	2019	2000	2019	2000	2019	2000	2019	2000	2019
Raspaciona aculeata†						x		x		
*Raspailia hispida**	x		x		x		x			
Raspailia ramosa	x		x		x	x	x	x	x	x
Stelligera rigida	x		x	x	x	x	x	x	x	x
Stelligera stuposa	x		x		x	x	x	x	x	x
Suberites carnosus	x	x	x	x	x	x	x	x	x	x
Suberites ficus	x	x			x	x	x	x		
Sycon ciliatum	x	x	x	x	x	x	x		x	x
Tethya aurantium	x	x	x	x	x	x	x	x	x	x
Unknown Thetyidae†								x		
TOTAL NUMBER OF SPECIES	37	19	34	25	34	31	35	33	32	32

Appendix B - Adaptive strategies of sponges to deoxygenated oceans

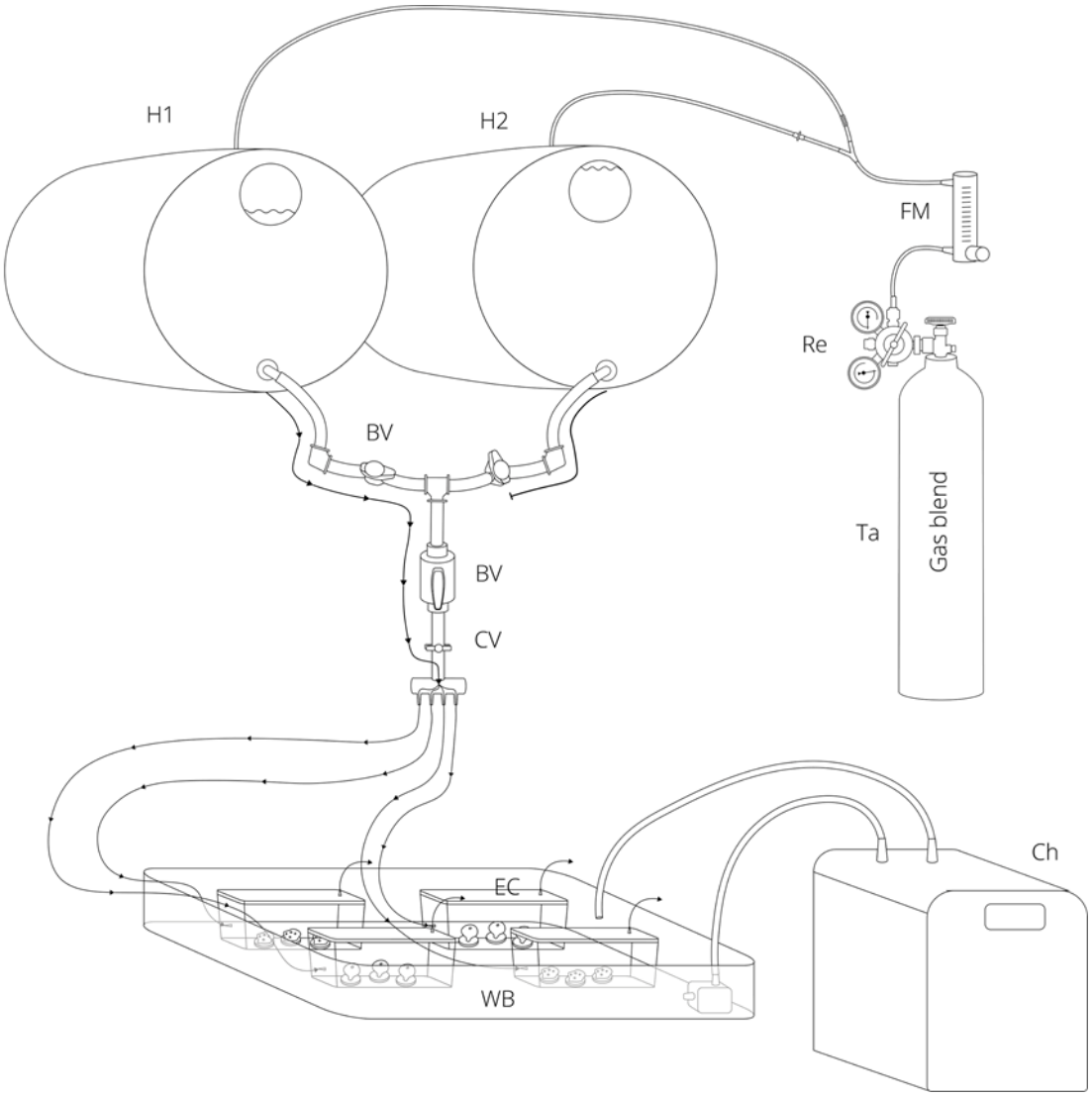

Figure S3.1. Scheme of a flow-through experimental module used in experiment 1 (moderate hypoxia). The whole setup consisted of eight of these units (two per treatment), each independent of the other and randomly distributed inside the laboratory. For each unit, water was treated in two replicate header tanks (**H1** and **H2**). Each header tank system consisted of two 60L drums (Food Grade HDPE), one for delivering water to the system (**H1**) and the other for conditioning new water (**H2**). The header tank delivering water was switched every 12 h, allowing a continuous flow without any interruption. Water was treated by bubbling specific hypoxic gas

blends (Ta), whose flow was controlled using a single-stage gas regulator (**Re**) and a gas flow meter (**FM**). Treated seawater flowed from the header tank to two replicate experimental chambers for each species (**EC**, Clip Fresh 2.3L containers, Food-Grade BPA-free Polypropylene) through food-grade vinyl tubing. One-way valves were placed at each experimental chamber's outlet to stabilize the water flow and avoid air coming back into the chambers. Header tanks were laid horizontally and placed ~1.2 m higher than the experimental chambers to reduce changes in flow rate caused by hydrostatic pressure changes at different water levels in the header tank. Water flow to each chamber was checked daily and finely tuned through a combination of clamp (**CV**) and ball valves (**BV**) positioned at different levels of the system. The temperature was kept constant using a water bath (**WB**) controlled by an aquarium chiller (**Ch**).

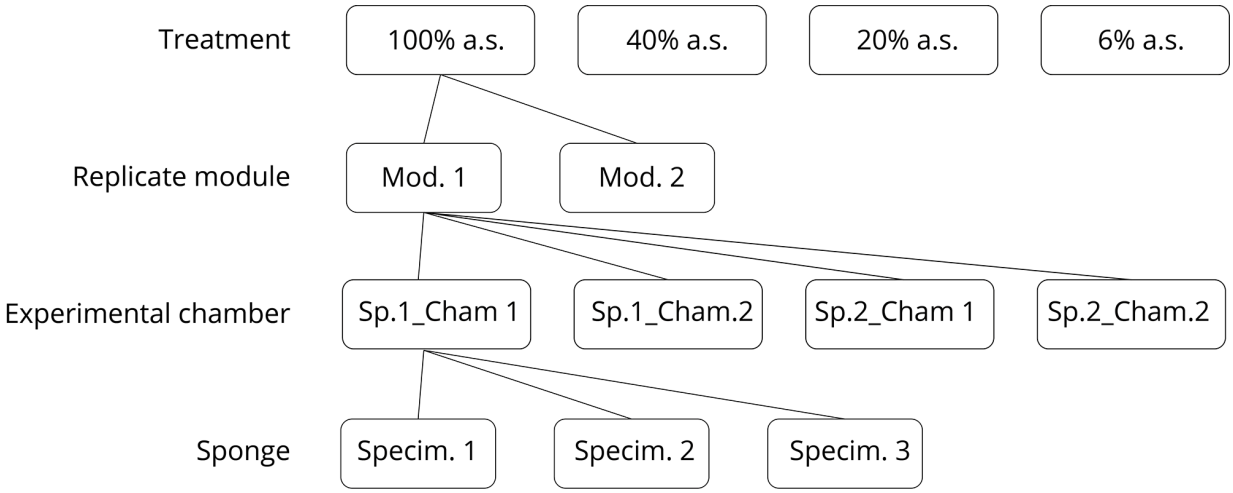

Figure S3.2. Diagram of the experimental design of experiment 1 (moderate hypoxia). There were four treatments in total, three hypoxic and one normoxic one. Each treatment was replicated in two independent replicate modules. Each replicate module had a total of four experimental chambers, two for each sponge species. Each experimental chamber contained three sponge specimens belonging to the same species.

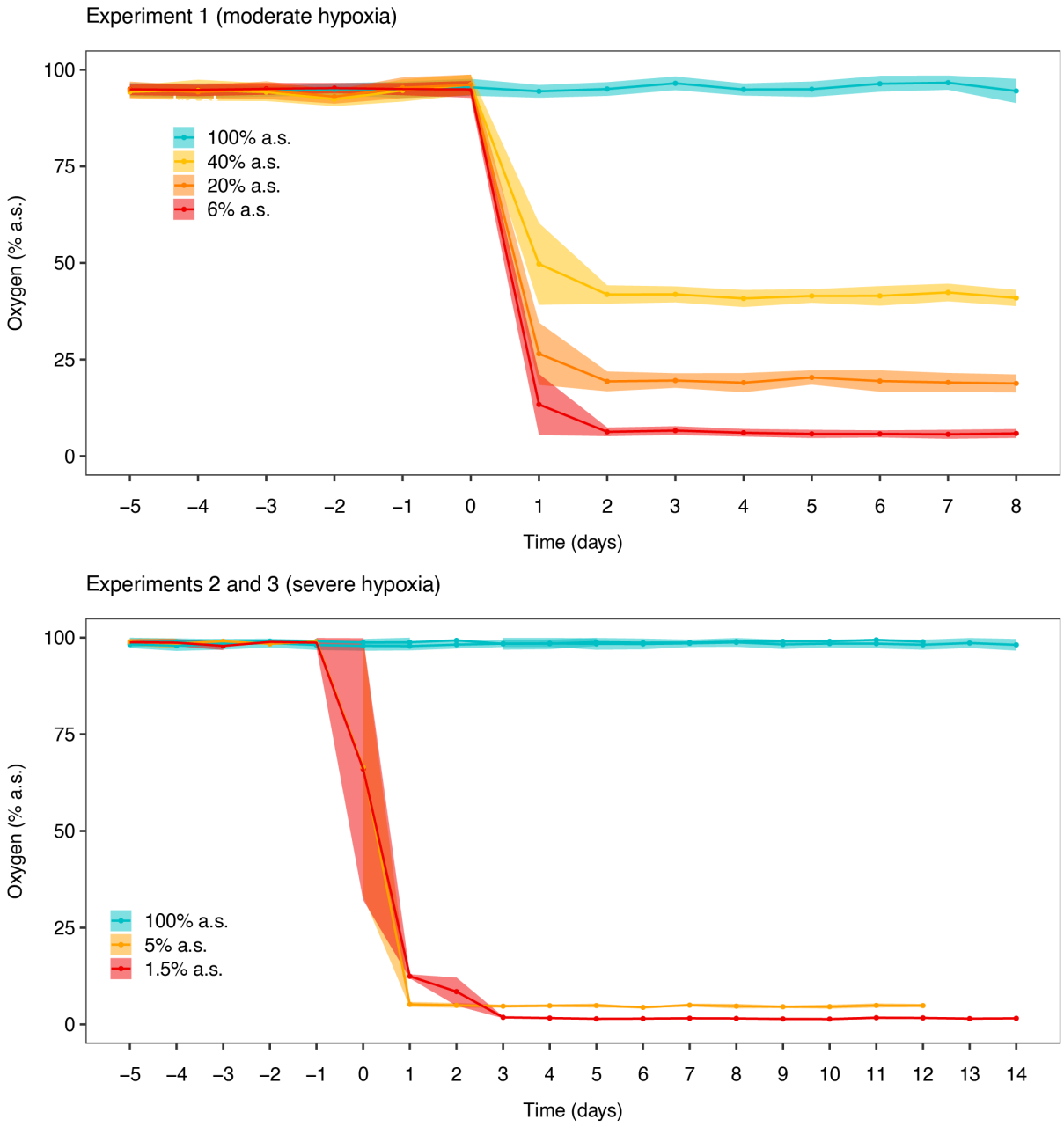

Figure S3.3. Mean daily oxygen concentration (% air saturation) in the experimental chambers with standard deviation for experiment 1 (moderate hypoxia), and experiments 2 and 3 (severe hypoxia)

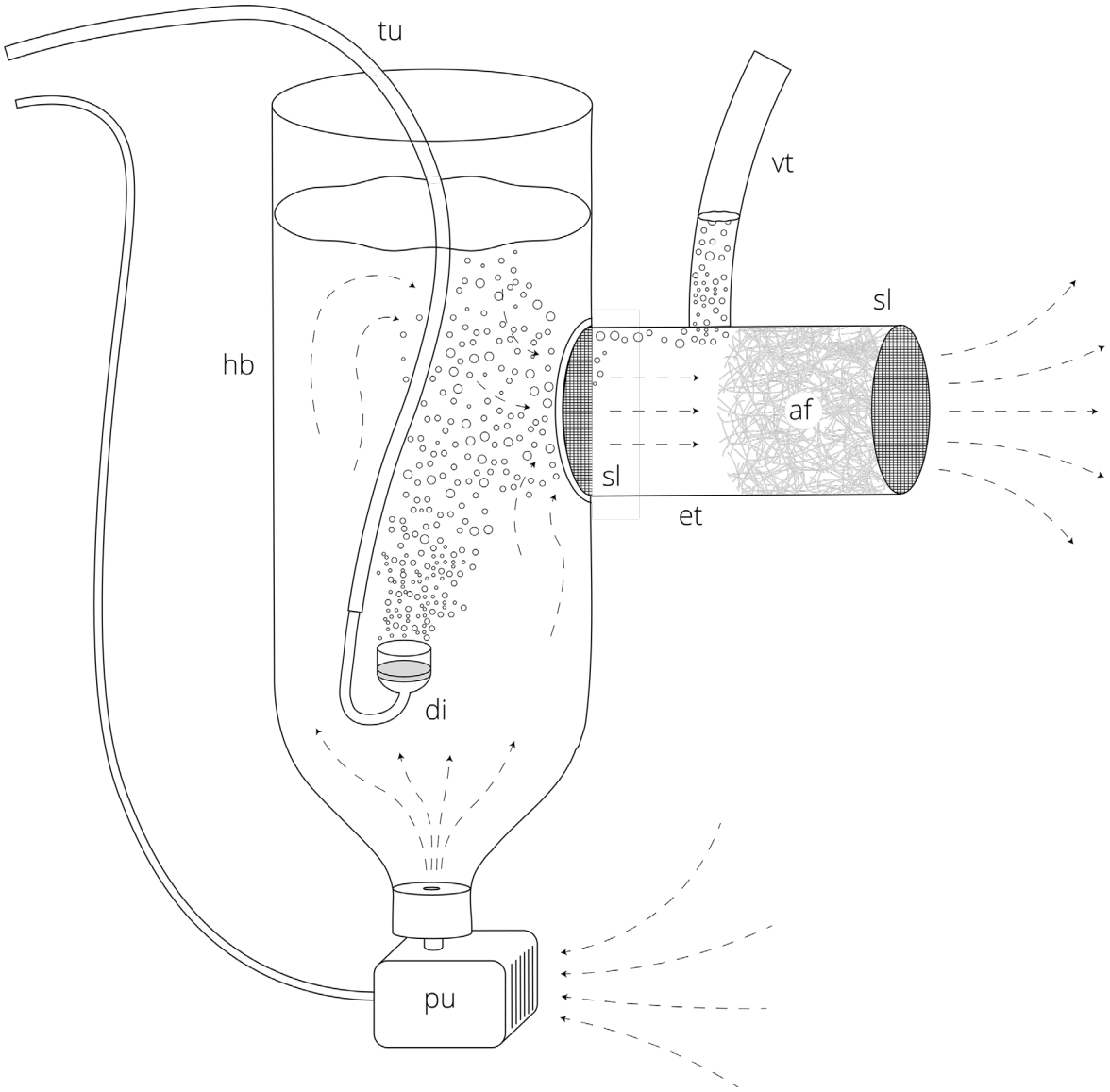

Figure S3.4. Debubbler device used in experiments 2 and 3 (severe hypoxia). The main body of the debubbler device was composed of an HDPE bottle (**hb**, 1 L), cut at the base, placed upside down. To isolate it from the experimental chamber, this was fixed to the side of the chamber and had the open extremity 30 mm over the water level. Air/Gas blend was delivered through food-grade vinyl tubing (**tu**) and bubbled inside the debubbler using a glass-ceramic gas diffuser (**di**). Water was pumped into the de-bubbler device from the bottleneck using a 3 W pump (**pu**), and expelled from an exhalant tube (**et**, vinyl, 40 mm ⌀, 80 mm long) attached on the side of the bottle. The exhalant tube had a scourer sponge layer at the base (**sl**, 3M™ Scotch-Brite®) and polyester aquarium filter material (**af**, ZooBest Filterwool) at the extremity to filter the bubbles from the water. The air trapped by the filtering material was then expelled from a vent tube (**vt**) that connected the exhalant tube to the air gap on the top of the chamber. Dashed lines indicate the water flow.

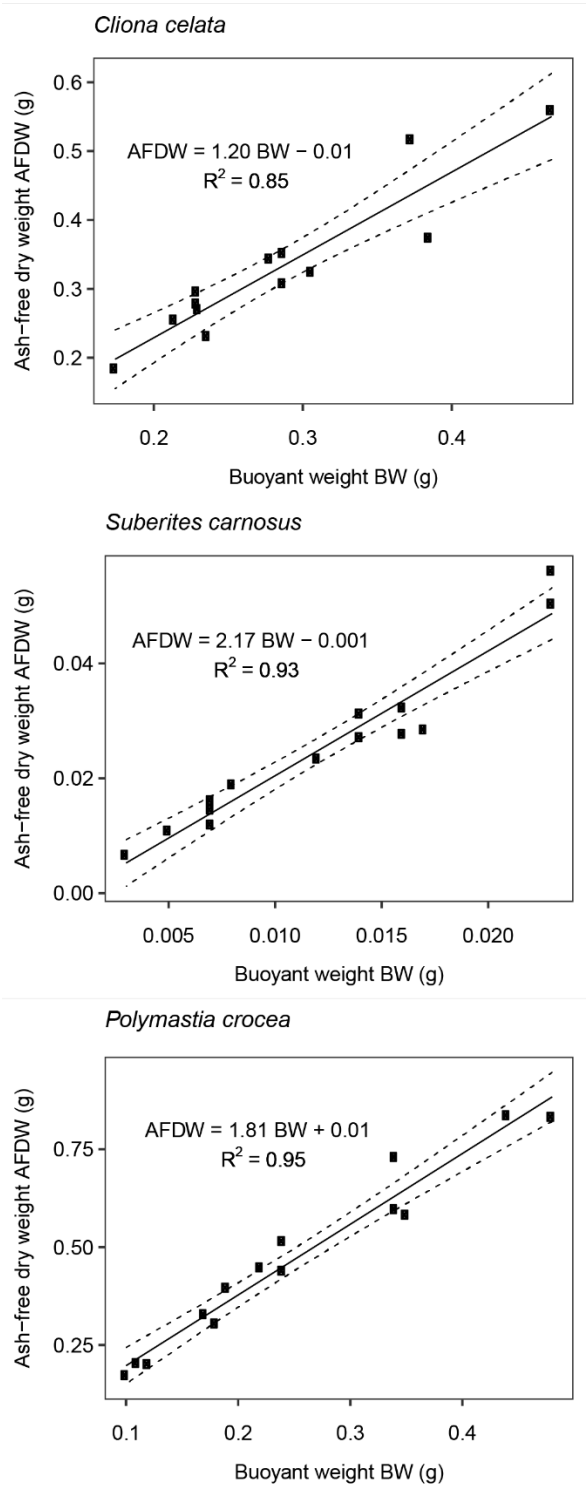

Figure S3.5. Ash-free dry weight as a function of buoyant weight for *Cliona celata*, *Suberites carnosus* and *Polymastia crocea*. Solid lines indicate the linear regression, while the dashed lines indicate the 95% confidence interval. Conversion ratios were calculated by first measuring the buoyant weight of 14 sponges of each species. The sponges were dried for 72 h in an oven at 60 °C, weighed and then ashed at 500 °C for five hours to determine their *AFDW*.

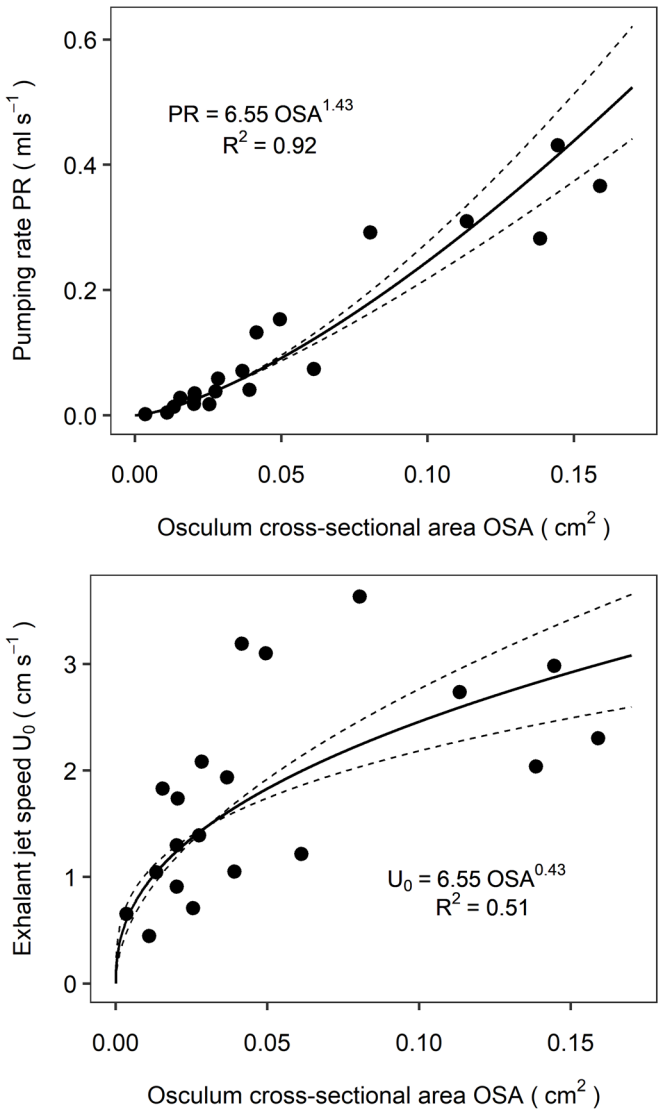

Figure S3.6. Pumping rate (PR) and Exhalant jet speed (U_0) as functions of Osculum cross-sectional area (OSA) in *Suberites australiensis*. Solid lines indicate the regression, while the dashed lines indicate the 95% confidence interval.

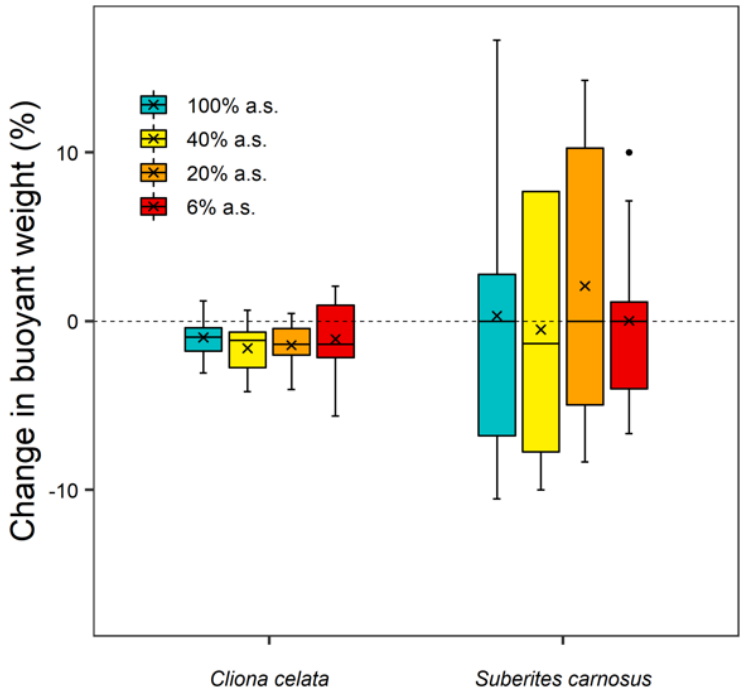

Figure S3.7. Change in buoyant weight relative to the initial weight between *T*0 and *T-end* in *Cliona celata* and *Suberites carnosus* from experiment 1 (moderate hypoxia). The oxygen concentration of the different treatments is expressed as % air saturation (% a.s.). Horizontal bars inside the boxplots represent medians; the symbol × represents means. The lower and upper hinges of the boxplots correspond to the first and third quartiles, respectively. Lower and upper whiskers represent the smallest and largest values, respectively. Single dots represent outliers.

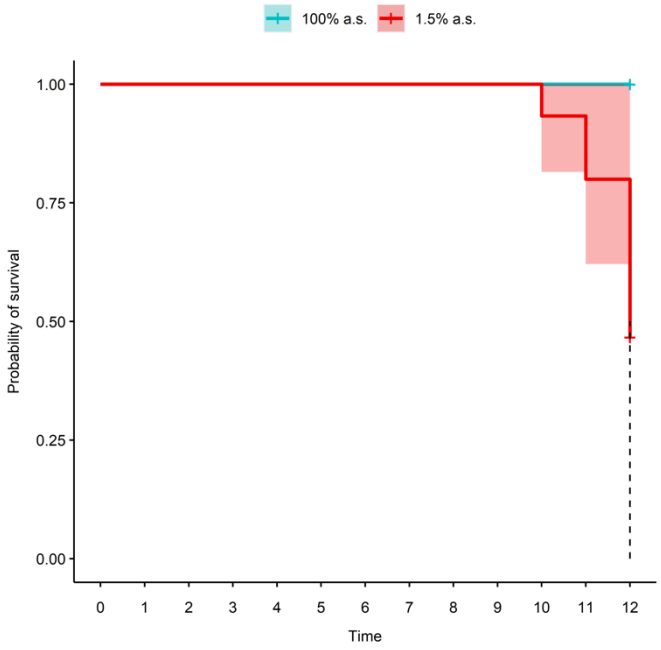

Figure S3.8. Kaplan-Meier Curve for hypoxia survival in *Polymastia crocea* from experiment 3 (1.5% a.s.).

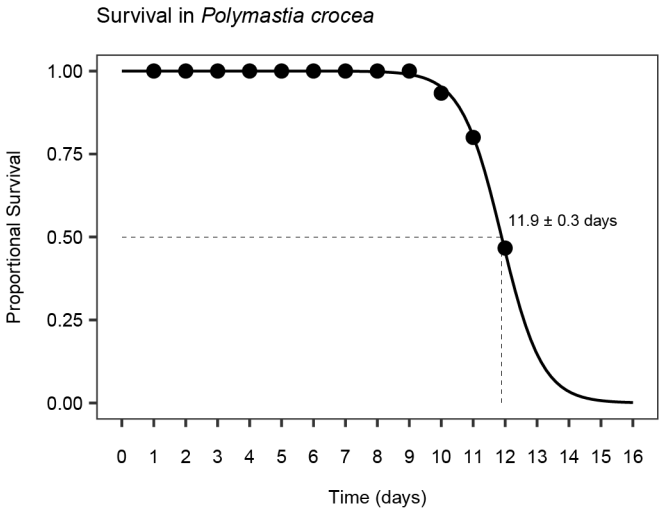

Figure S3.9. Logistic model of the survival in *P. crocea* sponges from experiment 3 (1.5% a.s.). Points indicate the recorded values, while the line indicates the model.

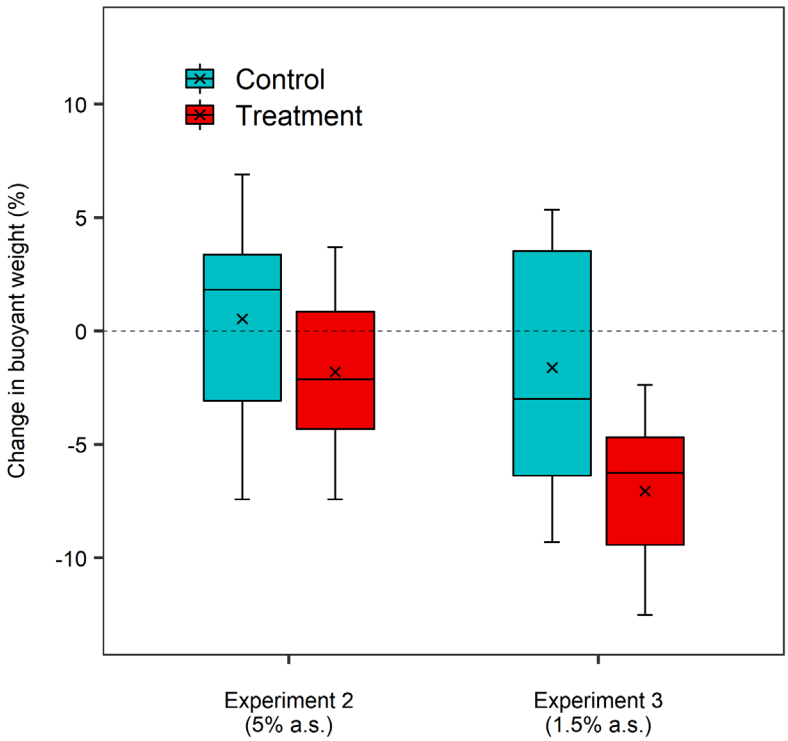

Figure S3.10. Change in buoyant weight relative to the initial value between *T*0 and *T-end* in *Polymastia crocea* in experiments 2 and 3 (severe hypoxia). Horizontal bars inside the boxplots represent medians; the symbol × represents means. The lower and upper hinges of the boxplots correspond to the first and third quartiles, respectively. The lower and upper whiskers represent the smallest and largest values, respectively. Single dots represent outliers.

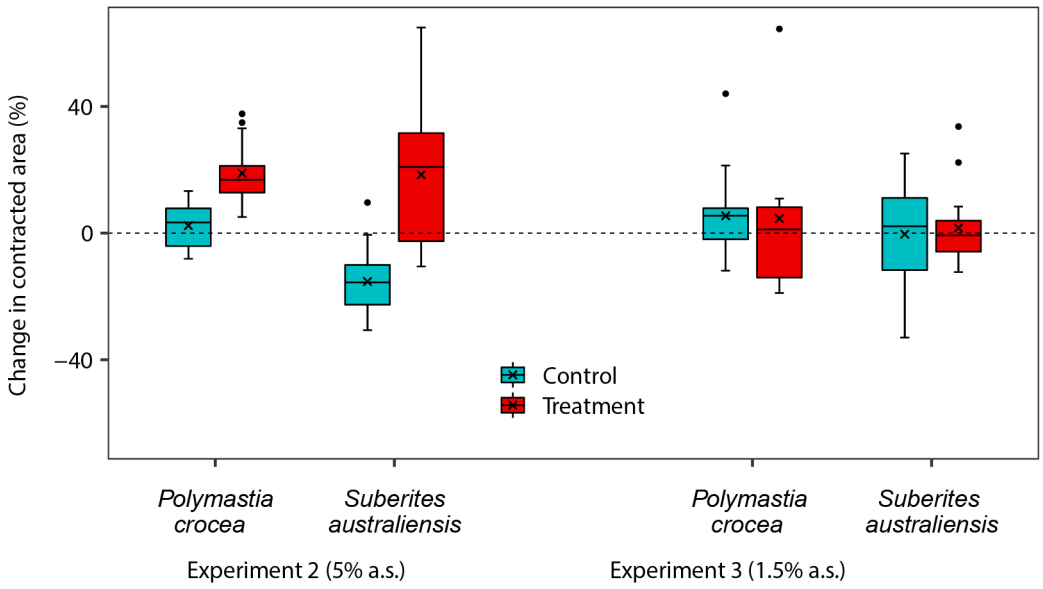

Figure S3.11. Change in contracted area relative to the initial value between *T*0 and *T-end* in *Polymastia crocea* and *Suberites australiensis* in experiments 2 and 3 (severe hypoxia). Horizontal bars inside the boxplots represent medians; the symbol × represents means. The lower and upper hinges of the boxplots correspond to the first and third quartiles, respectively. The lower and upper whiskers represent the smallest and largest values, respectively. Single dots represent outliers.

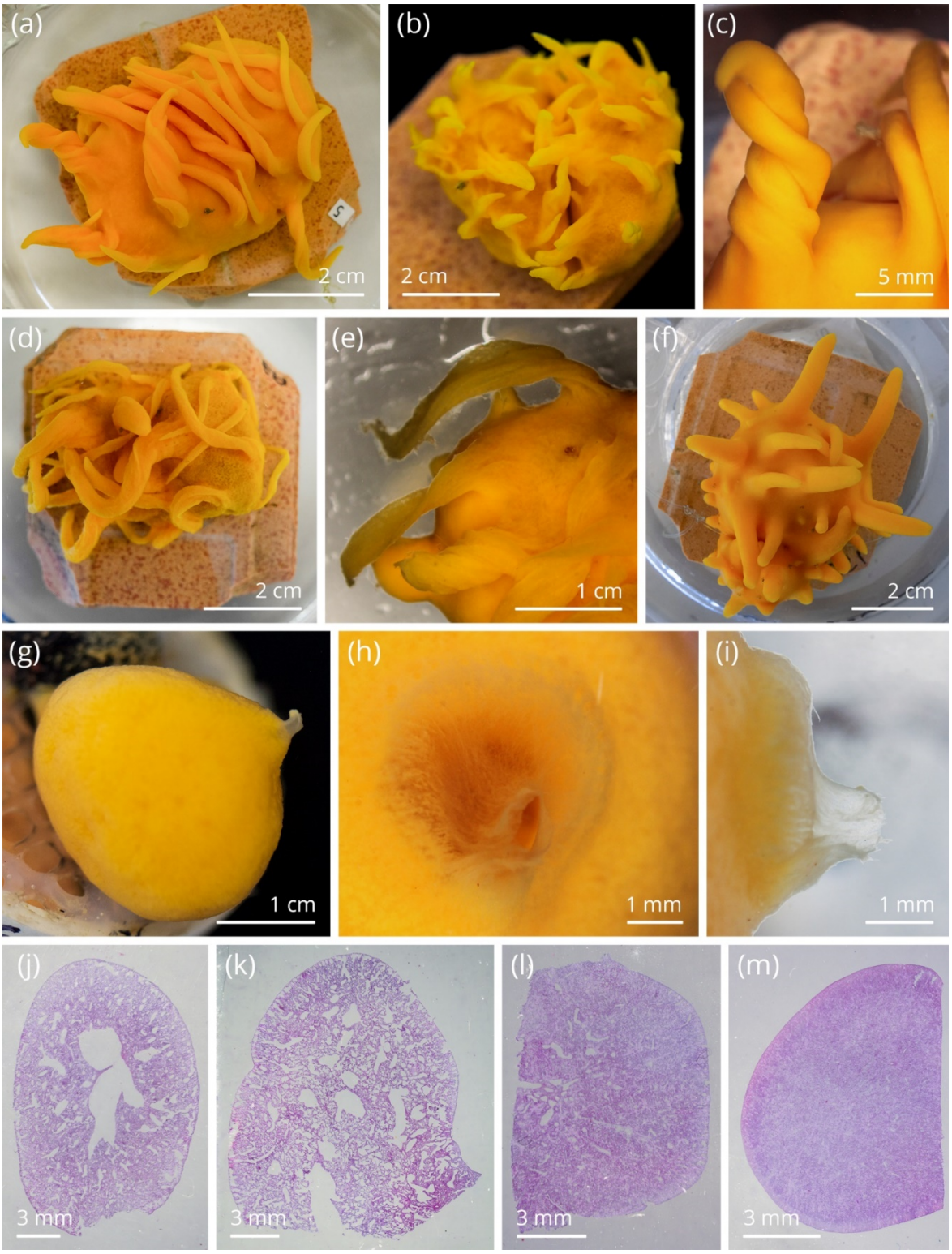

Figure S3.12. Morphological changes occurred in the sponges exposed to low dissolved oxygen in the severe hypoxia treatments. (a–c) *P. crocea* exposed to the 5% a.s. treatment; (d–e) *P. crocea* exposed to the 1.5% a.s. treatment; (f) *P. crocea* from the control treatment; (g–i) *S. australiensis* exposed to the 5% a.s. treatment. Histological sections of (j–k) *S. carnosus* exposed to the 5% a.s. treatment, (l) control, and (m) 1.5% a.s. treatment.

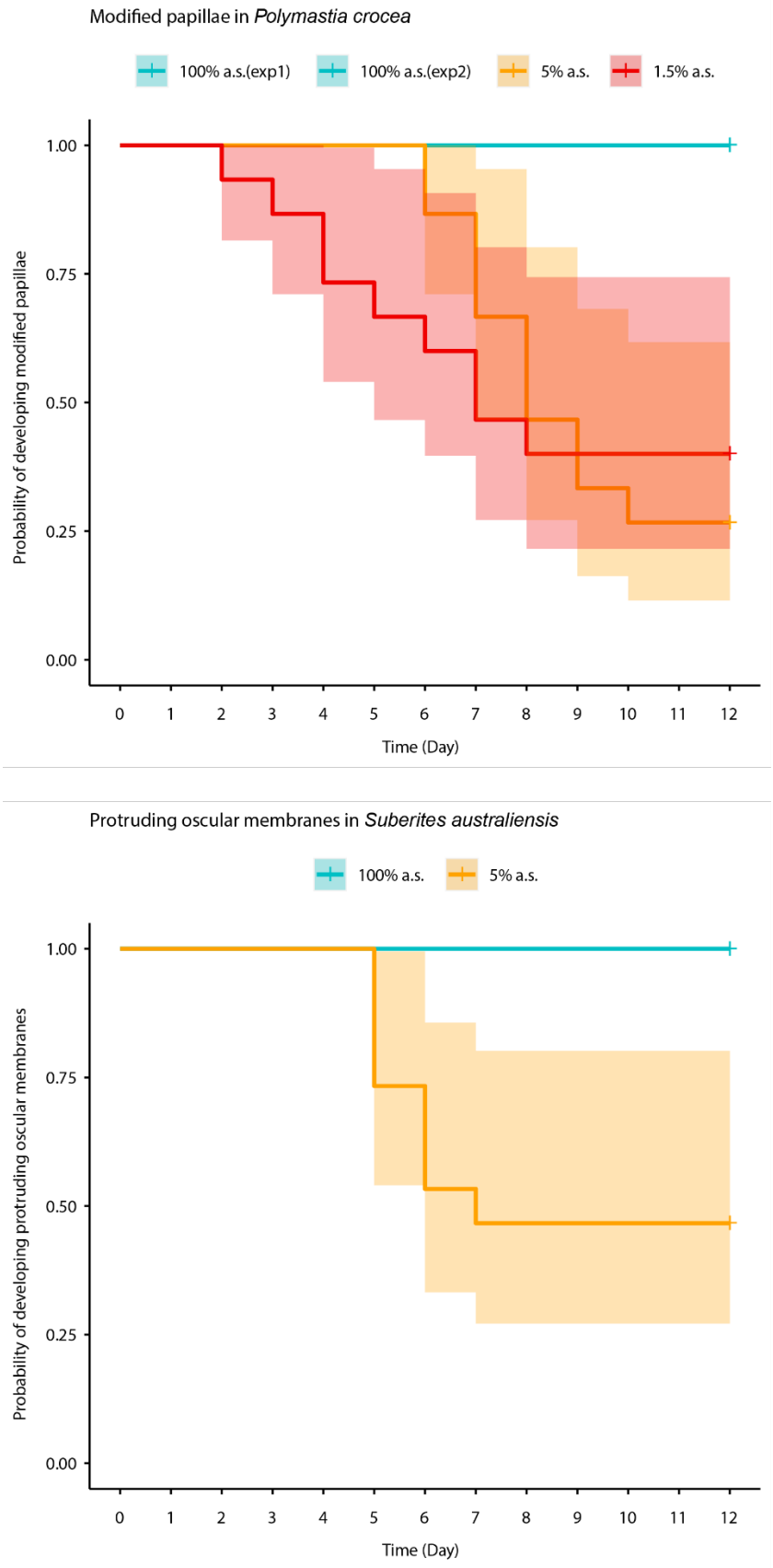

Figure S3.13. Kaplan-Meier Curve for development of modified papillae in *Polymastia crocea* and oscular protrusion in *S. australiensis* from Experiment 2 and 3 (severe hypoxia).

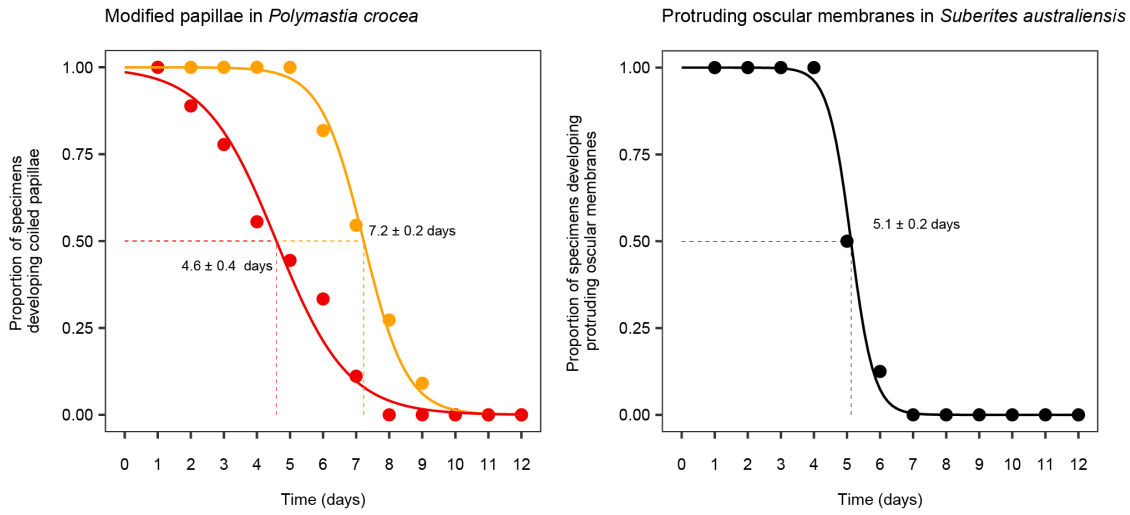

Figure S3.14. Logistic model of the development of modified papillae in *P. crocea* from the 5% (yellow) and 1.5% a.s. (red) treatments and protruding oscular membranes in *S. australiensis* from the 5% a.s. treatment. Points indicate the actual values. Sponges that did not develop these structures were excluded from this analysis.

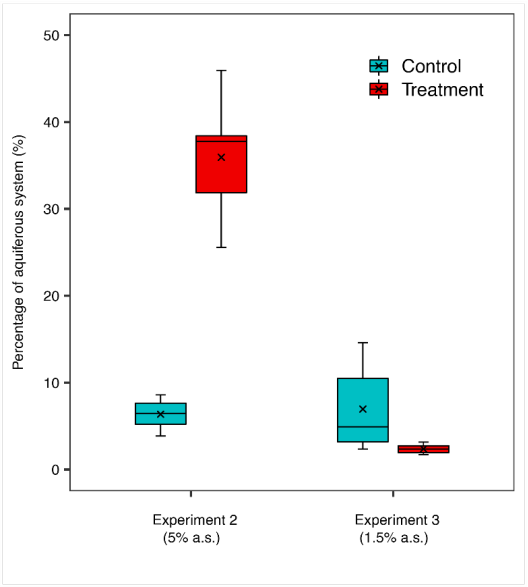

Figure S3.15. Percentage of sponge body occupied by the aquiferous system at the end of the experiment in *Suberites australiensis* from Experiment 2 and 3 (severe hypoxia). Horizontal bars inside the boxplots represent medians; the symbol × represents means. The lower and upper hinges of the boxplots correspond to the first and third quartiles, respectively. The lower and upper whiskers represent the smallest and largest values, respectively. Single dots represent outliers.

Table S3.1. Summary of the experiments performed for this study with measured (*) and calculated (**) seawater parameters represented as the mean (*SD*) of measurements.

Experiment	Type of System	Length	Treatments	Temp (°C)*	cO_2 (mg/L)*	O_2 (% a.s.)**	O_2 (%)**
1 (moderate hypoxia)	Flow-through	7 days	100% a.s.	15.47 (0.23)	7.71 (0.19)	95.41 (2.15)	19.99 (0.45)
			40% a.s.	15.56 (0.24)	3.34 (0.17)	41.45 (2.15)	8.68 (0.45)
			20% a.s.	15.61 (0.23)	1.56 (0.19)	19.38 (2.36)	4.06 (0.50)
			5% a.s.	15.64 (0.20)	0.48 (0.09)	6.01 (1.09)	1.26 (0.23)
2 (severe hypoxia)	Closed system	12 days	100% a.s.	13.25 (0.52)	8.34 (0.13)	98.89 (1.13)	20.72 (0.23)
			5% a.s.	13.26 (0.47)	0.40 (0.04)	4.77 (0.49)	1.00 (0.11)
3 (severe hypoxia)	Closed system	12 days	100% a.s.	14.33 (0.57)	8.15 (0.16)	98.34 (1.15)	20.61 (0.24)
			1.5% a.s.	14.31 (0.61)	0.13 (0.02)	1.55 (0.25)	0.33 (0.06)

Table S3.2. Summary of the analyses performed. LMM : linear mixed-effects model; GLMM: generalized linear mixed model

Experiment	**Species**	**Variable**	**Main model**	**Transformation**
1 (moderate hypoxia)	*C. celata*	Change in buoyant weight	Kruskal–Wallis test	-
1 (moderate hypoxia)	*S. carnosus*	Change in buoyant weight	Kruskal–Wallis test	-
1 (moderate hypoxia)	*C. celata*	Respiration rate	LMM	log (x + 1)
1 (moderate hypoxia)	*S. carnosus*	Respiration rate	LMM	log (x + 1)
2 (5% a.s.)	*P. crocea*	Change in buoyant weight	-	-
3 (1.5% a.s.)	*P. crocea*	Change in buoyant weight	-	-
2 (5% a.s.)	*P. crocea*	Change in contracted area	-	-
2 (5% a.s.)	*S. australiensis*	Change in contracted area	-	-
3 (1.5% a.s.)	*P. crocea*	Change in contracted area	-	-
3 (1.5% a.s.)	*S. australiensis*	Change in contracted area	-	-
2 (5% a.s.)	*P. crocea*	Ratio of expanded papillae	PERMANOVA	-
3 (1.5% a.s.)	*P. crocea*	Ratio of expanded papillae	GLMM (beta distribution)	-
2 (5% a.s.)	*S. australiensis*	Expansion ratio	LMM	-
3 (1.5% a.s.)	*S. australiensis*	Expansion ratio	PERMANOVA	-
2 (5% a.s.)	*S. australiensis*	Proportion of aquiferous system	-	-
3 (1.5% a.s.)	*S. australiensis*	Proportion of aquiferous system	-	-
2 (5% a.s.)	*S. australiensis*	Pumping rate	LMM with heterogeneous variance	Square root
3 (1.5% a.s.)	*S. australiensis*	Pumping rate	LMM with heterogeneous variance	Square root
2 (5% a.s.)	*P. crocea*	Respiration rate	LMM	-
2 (5% a.s.)	*S. australiensis*	Respiration rate	LMM	-

Table S3.3. Kruskal–Wallis, Dunn and One-Sample Wilcoxon Signed Rank tests evaluating the effect of treatment on the relative change in buoyant weight in *Cliona celata* and *Suberites carnosus* from experiment 1 (moderate hypoxia). Data are untransformed. P-values are uncorrected, but significance after correction with Benjamini-Hochberg Procedure (sign. corr.) is reported as: *$p < 0.05$; **$p < 0.01$; ***$p < 0.001$; ****$p < 0.0001$; *ns,* non-significant. *df* : degrees of freedom.

Relative change in Buoyant weight - *Cliona celata* & *Suberites carnosus*
Experiment 1 (moderate hypoxia)
Untransformed data

Kruskal-Wallis rank sum test

species	Kruskal-Wallis chi-squared	*p*-value	*df*
C. celata	1.305	0.7279	3
S. carnosus	0.767	0.8574	3

One-Sample Wilcoxon Signed-Rank Test (mu = 0)

species	treatment	*n*	*W*-statistic	*p*-value	sign. corr.
C. celata	100% a.s.	12	10	**0.0454**	*ns*
C. celata	6% a.s.	12	19	0.1290	*ns*
C. celata	40% a.s.	12	1	**0.0081**	*
C. celata	20% a.s.	12	1	**0.0081**	*
S. carnosus	100% a.s.	12	21	0.7260	*ns*
S. carnosus	6% a.s.	12	15	0.9330	*ns*
S. carnosus	40% a.s.	12	29.5	0.7880	*ns*
S. carnosus	20% a.s.	12	35	0.4750	*ns*

Table S3.4. Results of the linear mixed effect model (lmer) evaluating the effect of treatment and time on the respiration rate of *Cliona celata* from experiment 1 (moderate hypoxia). Data are Log (x + 1) transformed.

Respiration rate - *Cliona celata*

Experiment 1 (moderate hypoxia)

Linear mixed-effects model (lmer)

Formula: Respiration rate ~ treatment * time + (1|chamber/sponge)

Transformation: Log (x + 1)

Fixed effects test (anova)

	sum sq	mean sq	num*DF*	den*DF*	*F*-value	*p*-value
treatment	0.000	0.000	3	20	0.047	0.9861
time	0.011	0.005	2	40	2.212	0.1227
treatment:time	0.016	0.003	6	40	1.077	0.3922

Random effects test (ranova)

	npar	logLik	AIC	LRT	*df*	*p*-value
<none>	15	68.12	-106.24	#N/D	#N/D	#N/D
(1 | sponge:chamber)	14	66.36	-104.73	3.51	1.00	0.061
(1 | chamber)	14	68.12	-108.24	0.00	1.00	1.000

Pairwise comparis*ons,* time pairs (emmeans)

contrast	treatment	estimate	*SE*	*df*	*t*-ratio	*p*-value	sign. corr.
day 0 - day 2	100% a.s.	-0.01	0.03	40	-0.36	0.7195	*ns*
day 0 - day 7	100% a.s.	-0.01	0.03	40	-0.42	0.6800	*ns*
day 2 - day 7	100% a.s.	0.00	0.03	40	-0.05	0.9574	*ns*
day 0 - day 2	6% a.s.	0.04	0.03	40	1.39	0.1725	*ns*
day 0 - day 7	6% a.s.	-0.02	0.03	40	-0.87	0.3898	*ns*
day 2 - day 7	6% a.s.	-0.06	0.03	40	-2.26	**0.0294**	*ns*
day 0 - day 2	40% a.s.	0.01	0.03	40	0.36	0.7210	*ns*
day 0 - day 7	40% a.s.	0.01	0.03	40	0.45	0.6557	*ns*
day 2 - day 7	40% a.s.	0.00	0.03	40	0.09	0.9291	*ns*
day 0 - day 2	20% a.s.	0.07	0.03	40	2.28	**0.0283**	*ns*
day 0 - day 7	20% a.s.	0.03	0.03	40	0.87	0.3876	*ns*
day 2 - day 7	20% a.s.	-0.04	0.03	40	-1.40	0.1688	*ns*

Pairwise comparis*ons,* treatment pairs (emmeans)

contrast	time	estimate	*SE*	*df*	*t*-ratio	*p*-value	sign. corr.
100% a.s. - 6% a.s.	day 0	-0.01	0.03	13.92	-0.19	0.8529	*ns*
100% a.s. - 40% a.s.	day 0	-0.02	0.03	13.92	-0.46	0.6520	*ns*
100% a.s. - 20% a.s.	day 0	-0.03	0.03	13.92	-0.93	0.3693	*ns*
6% a.s. - 40% a.s.	day 0	-0.01	0.03	13.92	-0.27	0.7896	*ns*
6% a.s. - 20% a.s.	day 0	-0.02	0.03	13.92	-0.74	0.4722	*ns*
40% a.s. - 20% a.s.	day 0	-0.02	0.03	13.92	-0.47	0.6478	*ns*
100% a.s. - 6% a.s.	day 2	0.04	0.03	13.92	1.31	0.2126	*ns*
100% a.s. - 40% a.s.	day 2	0.01	0.03	13.92	0.16	0.8789	*ns*
100% a.s. - 20% a.s.	day 2	0.04	0.03	13.92	1.32	0.2067	*ns*
6% a.s. - 40% a.s.	day 2	-0.04	0.03	13.92	-1.15	0.2690	*ns*
6% a.s. - 20% a.s.	day 2	0.00	0.03	13.92	0.02	0.9860	*ns*
40% a.s. - 20% a.s.	day 2	0.04	0.03	13.92	1.17	0.2620	*ns*
100% a.s. - 6% a.s.	day 7	-0.02	0.03	13.92	-0.58	0.5734	*ns*
100% a.s. - 40% a.s.	day 7	0.01	0.03	13.92	0.28	0.7854	*ns*
100% a.s. - 20% a.s.	day 7	0.01	0.03	13.92	0.17	0.8650	*ns*
6% a.s. - 40% a.s.	day 7	0.03	0.03	13.92	0.85	0.4074	*ns*
6% a.s. - 20% a.s.	day 7	0.03	0.03	13.92	0.75	0.4658	*ns*
40% a.s. - 20% a.s.	day 7	0.00	0.03	13.92	-0.10	0.9183	*ns*

Table S3.5. Results of the linear mixed effect model (lmer) evaluating the effect of treatment and time on the respiration rate of *Suberites carnosus* from experiment 1 (moderate hypoxia). Data are Log (x + 1) transformed.

Linear mixed-effects model (lmer)
Formula: Respiration rate ~ treatment * time + (1|chamber/sponge)
Trasformation: Log (x + 1)

Fixed effects test (anova)

	sum sq	mean sq	num*DF*	den*DF*	*F*-value	*p*-value
treatment	0.326	0.109	3	20.000	1.700	0.1992
time	0.980	0.490	2	40.000	7.663	**0.0015**
treatment:time	1.350	0.225	6	40.000	3.521	**0.0068**

Random effects test (ranova)

	npar	logLik	AIC	LRT	*df*	*p*-value
<none>	15	-32.10	94.20	#N/D	#N/D	#N/D
(1 | sponge:chamber)	14	-35.81	99.61	7.41	1.00	**0.006**
(1 | chamber)	14	-32.10	92.20	0.00	1.00	1.000

Pairwise comparis*ons,* time pairs (emmeans)

contrast	treatment	estimate	*SE*	*df*	*t*-ratio	*p*-value	sign. corr.
day 0 - day 2	100% a.s.	0.10	0.15	40	0.70	0.4907	*ns*
day 0 - day 7	100% a.s.	0.04	0.15	40	0.26	0.7992	*ns*
day 2 - day 7	100% a.s.	-0.06	0.15	40	-0.44	0.6627	*ns*
day 0 - day 2	6% a.s.	-0.06	0.15	40	-0.43	0.6677	*ns*
day 0 - day 7	6% a.s.	0.68	0.15	40	4.64	**< 0.0001**	*****
day 2 - day 7	6% a.s.	0.74	0.15	40	5.07	**< 0.0001**	*****
day 0 - day 2	40% a.s.	0.06	0.15	40	0.40	0.6894	*ns*
day 0 - day 7	40% a.s.	0.06	0.15	40	0.44	0.6623	*ns*
day 2 - day 7	40% a.s.	0.01	0.15	40	0.04	0.9703	*ns*
day 0 - day 2	20% a.s.	0.01	0.15	40	0.07	0.9445	*ns*
day 0 - day 7	20% a.s.	0.26	0.15	40	1.78	0.0825	*ns*
day 2 - day 7	20% a.s.	0.25	0.15	40	1.71	0.0949	*ns*

Pairwise comparis*ons,* treatment pairs (emmeans)

contrast	time	estimate	*SE*	*df*	*t*-ratio	*p*-value	sign. corr.
100% a.s. - 6% a.s.	day 0	-0.20	0.18	11.29	-1.08	0.3019	*ns*
100% a.s. - 40% a.s.	day 0	0.21	0.18	11.29	1.14	0.2766	*ns*
100% a.s. - 20% a.s.	day 0	0.15	0.18	11.29	0.84	0.4187	*ns*
6% a.s. - 40% a.s.	day 0	0.41	0.18	11.29	2.22	**0.0473**	*ns*
6% a.s. - 20% a.s.	day 0	0.35	0.18	11.29	1.92	0.0803	*ns*
40% a.s. - 20% a.s.	day 0	-0.06	0.18	11.29	-0.30	0.7668	*ns*
100% a.s. - 6% a.s.	day 2	-0.36	0.18	11.29	-1.98	0.0730	*ns*
100% a.s. - 40% a.s.	day 2	0.17	0.18	11.29	0.91	0.3815	*ns*
100% a.s. - 20% a.s.	day 2	0.06	0.18	11.29	0.34	0.7379	*ns*
6% a.s. - 40% a.s.	day 2	0.53	0.18	11.29	2.89	**0.0144**	*ns*
6% a.s. - 20% a.s.	day 2	0.43	0.18	11.29	2.32	**0.0400**	*ns*
40% a.s. - 20% a.s.	day 2	-0.10	0.18	11.29	-0.57	0.5814	*ns*
100% a.s. - 6% a.s.	day 5	0.44	0.18	11.29	2.40	**0.0348**	*ns*
100% a.s. - 40% a.s.	day 5	0.24	0.18	11.29	1.29	0.2231	*ns*
100% a.s. - 20% a.s.	day 5	0.38	0.18	11.29	2.05	0.0644	*ns*
6% a.s. - 40% a.s.	day 5	-0.20	0.18	11.29	-1.11	0.2904	*ns*
6% a.s. - 20% a.s.	day 5	-0.06	0.18	11.29	-0.35	0.7336	*ns*
40% a.s. - 20% a.s.	day 5	0.14	0.18	11.29	0.76	0.4627	*Ns*

Table S3.6. Welch t-tests evaluating the effect of treatment on the relative change in buoyant weight in *Polymastia crocea & Suberites australiensis* from experiments 2 and 3 (severe hypoxia). Data are untransformed. P-values are uncorrected, but significance after correction with Benjamini-Hochberg Procedure (sign. corr.) is reported as: *$p < 0.05$; **$p < 0.01$; ***$p < 0.001$; ****$p < 0.0001$; *ns,* non-significant. *df* : degrees of freedom

Relative change in Buoyant weight - *Polymastia crocea* & *Suberites australiensis*
Experiments 2 and 3 (severe hypoxia)
Untransformed data

Two-Sample Welch t-test

experiment	species	group1	group2	*n* 1	*n* 2	*t*	*df*	*p*-value	sign. corr.
2 (5% a.s.)	*P. crocea*	100% a.s.	5% a.s.	15	15	1.6	25.8	0.1180	*ns*
3 (1.5% a.s.)	*P. crocea*	100% a.s.	1.5% a.s.	15	7	2.8	16.8	**0.0119**	*

One-Sample Welch t-test (mu = 0)

experiment	species	treatment	*n*	*t*	*df*	*p*-value	sign. corr.
2 (5% a.s.)	*P. crocea*	100% a.s.	15	0.5	14	0.6520	*ns*
2 (5% a.s.)	*P. crocea*	5% a.s.	15	-2.1	14	0.0545	*ns*
3 (1.5% a.s.)	*P. crocea*	100% a.s.	15	-1.2	14	0.2580	*ns*
3 (1.5% a.s.)	*P. crocea*	1.5% a.s.	7	-5.2	6	**0.0021**	**

Table S3.7. Wilcoxon signed-rank tests evaluating the effect of treatment on the relative change in contracted area in *Polymastia crocea & Suberites australiensis* from experiments 2 and 3 (severe hypoxia). Data are untransformed.

Relative change in Contracted area - *Polymastia crocea* & *Suberites australiensis*
Experiments 2 and 3 (severe hypoxia)
Untransformed data

Two-Sample Wilcoxon Signed-Rank Test

experiment	species	group1	group2	*n*1	*n*2	*W*-statistic	*p*-value	sign. corr.
2 (5% a.s.)	*P. crocea*	100% a.s.	5% a.s.	15	15	12	**< 0.0001**	****
2 (5% a.s.)	*S. australiensis*	100% a.s.	5% a.s.	15	15	13	**< 0.0001**	****
3 (1.5% a.s.)	*P. crocea*	100% a.s.	1.5% a.s.	15	7	54	0.9450	*ns*
3 (1.5% a.s.)	*S. australiensis*	100% a.s.	1.5% a.s.	15	15	123	0.6830	*ns*

One-Sample Wilcoxon Signed-Rank Test (mu = 0)

experiment	species	treatment	*n*	*W*-statistic	*p*-value	sign. corr.
2 (5% a.s.)	*P. crocea*	100% a.s.	15	80	0.2770	*ns*
2 (5% a.s.)	*P. crocea*	5% a.s.	15	120	**0.0001**	***
2 (5% a.s.)	*S. australiensis*	100% a.s.	15	3	**0.0003**	**
2 (5% a.s.)	*S. australiensis*	5% a.s.	15	105	**0.0084**	*
3 (1.5% a.s.)	*P. crocea*	100% a.s.	15	84	0.1880	*ns*
3 (1.5% a.s.)	*P. crocea*	1.5% a.s.	7	16	0.8130	*ns*
3 (1.5% a.s.)	*S. australiensis*	100% a.s.	15	60	0.6600	*ns*
3 (1.5% a.s.)	*S. australiensis*	1.5% a.s.	15	55	0.8040	*ns*

Table S3.8. Results of the PERMANOVA model, and permutation t-tests evaluating the effect of treatment and time on the ratio of expanded papillae in *Polymastia crocea* from experiment 2 (5% a.s.). Data are untransformed.

Ratio of expanded papillae - *Polymastia croceus*
Experiment 2 (5% a.s.)
Repeated Measures Univariate
PERMANOVA
Untransformed data

Factors	**Abbrev.**	**Type**
treatment	TR	Fixed
chamber	CH	Random
sponge	SP	Random
time	TI	Fixed

source	*df*	*SS*	*MS*	pseudo-*F*	*p*-value	perms
TR	1	7.6	7.6	18.4	0.1028	10
CH(TR)	4	1.7	0.4	1.5	0.2395	9957
SP(CH(TR))	24	6.8	0.3	19.8	**0.0001**	9898
TI	12	12.1	1.0	61.9	**0.0001**	9948
TRxTI	12	5.2	0.4	26.6	**0.0001**	9918
CH(TR)xTI	48	0.8	0.0	1.1	0.2642	9872
Res	288	4.1	0.0			
Total	389	38.3				

Pairwise permutation t-tests, pairs of times

treatment	comparison	*p*-value	sign. corr.
5% a.s.	T1 vs T0	0.4920	*ns*
5% a.s.	T2 vs T1	0.4994	*ns*
5% a.s.	T3 vs T2	0.2554	*ns*
5% a.s.	T4 vs T3	**0.0088**	*
5% a.s.	T5 vs T4	**0.0038**	*
5% a.s.	T6 vs T5	**0.0012**	*
5% a.s.	T7 vs T6	**0.0008**	*
5% a.s.	T8 vs T7	**0.0038**	*
5% a.s.	T9 vs T8	**0.0076**	*
5% a.s.	T10 vs T9	**0.0024**	*
5% a.s.	T11 vs T10	0.6480	*ns*
5% a.s.	T12 vs T0	**0.0002**	**
5% a.s.	T12 vs T11	0.1368	*ns*
100% a.s.	T1 vs T0	0.7442	*ns*
100% a.s.	T2 vs T1	0.4920	*ns*
100% a.s.	T3 vs T2	0.4938	*ns*
100% a.s.	T4 vs T3	0.1302	*ns*
100% a.s.	T5 vs T4	0.2494	*ns*
100% a.s.	T6 vs T5	0.7522	*ns*
100% a.s.	T7 vs T6	0.2014	*ns*
100% a.s.	T8 vs T7	0.6058	*ns*
100% a.s.	T9 vs T8	0.0580	*ns*
100% a.s.	T10 vs T9	**0.0248**	*ns*
100% a.s.	T11 vs T10	0.1494	*ns*
100% a.s.	T12 vs T0	**0.0024**	*
100% a.s.	T12 vs T11	0.5778	*ns*

Pairwise permutation t-tests, pairs of treatments

time	comparison	*p*-value	sign. corr.
T0	5% a.s. vs 100% a.s.	0.7412	*ns*
T1	5% a.s. vs 100% a.s.	0.4810	*ns*
T2	5% a.s. vs 100% a.s.	0.7980	*ns*
T3	5% a.s. vs 100% a.s.	0.2644	*ns*
T4	5% a.s. vs 100% a.s.	0.1754	*ns*
T5	5% a.s. vs 100% a.s.	**0.0346**	*ns*
T6	5% a.s. vs 100% a.s.	**0.0052**	**
T7	5% a.s. vs 100% a.s.	**0.0016**	**
T8	5% a.s. vs 100% a.s.	**0.0004**	**
T9	5% a.s. vs 100% a.s.	**0.0002**	***
T11	5% a.s. vs 100% a.s.	**0.0002**	***
T12	5% a.s. vs 100% a.s.	**0.0002**	***
T10	5% a.s. vs 100% a.s.	**0.0002**	***

Table S3.9. Results of the generalized linear mixed effect model evaluating the effect of treatment and time on the ratio of expanded papillae in *Polymastia crocea* from experiment 3 (1.5% a.s.).

Ratio of expanded papillae - *Polymastia crocea*
Experiment 3 (1.5% a.s.)
Generalized linear mixed models - Beta regression with logit link (glmmTMB)
Formula: Expansion ratio ~ treatment * time + (1|chamber/sponge)
Untransformed data

Fixed effects test (anova)

	chisq	*df*	*p*-value
(Intercept)	27	1	**< 0.0001**
treatment	4	1	0.0582
time	142	11	**< 0.0001**
treatment:time	21	11	**0.0303**

Pairwise comparis*ons,* time pairs (emmeans)

contrast	treatment	estimate	*SE*	*df*	*t*-ratio	*p*-value	sign. corr.
T0 - T1	100% a.s.	-0.02	0.36	333	-0.05	0.9622	*ns*
T0 - T11	100% a.s.	-1.48	0.36	333	-4.15	**< 0.0001**	***
T1 - T2	100% a.s.	0.13	0.36	333	0.35	0.7255	*ns*
T2 - T3	100% a.s.	-0.12	0.36	333	-0.33	0.7415	*ns*
T3 - T4	100% a.s.	-1.05	0.36	333	-2.90	**0.0040**	*
T4 - T5	100% a.s.	-0.36	0.34	333	-1.06	0.2911	*ns*
T5 - T6	100% a.s.	0.49	0.34	333	1.45	0.1474	*ns*
T6 - T7	100% a.s.	-0.36	0.35	333	-1.02	0.3096	*ns*
T7 - T8	100% a.s.	-0.09	0.33	333	-0.26	0.7965	*ns*
T8 - T9	100% a.s.	0.57	0.34	333	1.66	0.0969	*ns*
T9 - T10	100% a.s.	-0.80	0.33	333	-2.38	**0.0177**	*ns*
T10 - T11	100% a.s.	0.10	0.32	333	0.32	0.7503	*ns*
T0 - T1	1.5% a.s.	-0.56	0.43	333	-1.29	0.1966	*ns*
T0 - T11	1.5% a.s.	-2.48	0.41	333	-6.11	**< 0.0001**	****
T1 - T2	1.5% a.s.	-0.36	0.37	333	-0.97	0.3351	*ns*
T2 - T3	1.5% a.s.	-0.42	0.33	333	-1.25	0.2107	*ns*
T3 - T4	1.5% a.s.	-0.06	0.32	333	-0.17	0.8626	*ns*
T4 - T5	1.5% a.s.	-0.56	0.30	333	-1.85	0.0648	*ns*
T5 - T6	1.5% a.s.	0.39	0.31	333	1.23	0.2203	*ns*
T6 - T7	1.5% a.s.	-0.72	0.32	333	-2.24	**0.0256**	*ns*
T7 - T8	1.5% a.s.	-0.22	0.32	333	-0.69	0.4929	*ns*
T8 - T9	1.5% a.s.	-0.11	0.32	333	-0.33	0.7384	*ns*
T9 - T10	1.5% a.s.	-0.31	0.31	333	-1.02	0.3070	*ns*
T10 - T11	1.5% a.s.	0.45	0.31	333	1.48	0.1390	*ns*

Pairwise comparis*ons,* treatment pairs (emmeans)

contrast	time	estimate	*SE*	*df*	*t*-ratio	*p*-value	sign. corr.
100% a.s. - 1.5% a.s.	T0	-0.27	0.74	333	-0.37	0.7140	*ns*
100% a.s. - 1.5% a.s.	T1	-0.81	0.72	333	-1.13	0.2602	*ns*
100% a.s. - 1.5% a.s.	T2	-1.30	0.70	333	-1.85	0.0657	*ns*
100% a.s. - 1.5% a.s.	T3	-1.60	0.70	333	-2.27	**0.0237**	*ns*
100% a.s. - 1.5% a.s.	T4	-0.61	0.69	333	-0.88	0.3780	*ns*
100% a.s. - 1.5% a.s.	T5	-0.81	0.69	333	-1.18	0.2382	*ns*
100% a.s. - 1.5% a.s.	T6	-0.92	0.69	333	-1.33	0.1859	*ns*
100% a.s. - 1.5% a.s.	T7	-1.29	0.70	333	-1.85	0.0655	*ns*
100% a.s. - 1.5% a.s.	T8	-1.42	0.69	333	-2.05	**0.0412**	*ns*
100% a.s. - 1.5% a.s.	T9	-2.10	0.70	333	-3.01	**0.0028**	*
100% a.s. - 1.5% a.s.	T10	-1.62	0.68	333	-2.37	**0.0181**	*ns*
100% a.s. - 1.5% a.s.	T11	-1.27	0.69	333	-1.84	0.0667	*ns*

Table S3.10. Results of the linear mixed effect model (lmer) evaluating the effect of treatment and time on the expansion ratio in *Suberites australiensis* from experiment 2 (5% a.s.). Data are untransformed. P-values are uncorrected, but significance after correction with Benjamini-Hochberg Procedure (sign. corr.) is reported as: *$p < 0.05$; **$p < 0.01$; ***$p < 0.001$; ****$p < 0.0001$; *ns,* non-significant.

Expansion ratio - *Suberites australiensis*
Experiment 2 (5% a.s.)
Linear mixed-effects model (lmer)
Formula: Expansion ratio ~ treatment * time + (1|chamber/sponge)
Untransformed data

Fixed effects test (anova)

	sum sq	mean sq	num*DF*	den*DF*	*F*-value	*p*-value
treatment	1.82	1.82	1	4	67.3	**0.0012**
time	6.03	0.50	12	336	18.6	**< 0.0001**
treatment:time	4.62	0.39	12	336	14.2	**< 0.0001**

Random effects test (ranova)

	npar	logLik	AIC	LRT	*df*	*p*-value
<none>	29	49.24	-40.48	#N/D	#N/D	#N/D
(1 | sponge:chamber)	28	-59.18	174.36	216.84	1.00	**< 0.0001**
(1 | chamber)	28	49.19	-42.38	0.10	1.00	0.7516

Pairwise comparis*ons,* time pairs (emmeans)

contrast	treatment	estimate	*SE*	*df*	*t*-ratio	*p*-value	sign. corr.
T0 - T1	100% a.s.	-0.09	0.06	336	-1.49	0.1374	*ns*
T0 - T12	100% a.s.	0.31	0.06	336	5.11	**< 0.0001**	****
T1 - T2	100% a.s.	0.02	0.06	336	0.39	0.6987	*ns*
T2 - T3	100% a.s.	0.07	0.06	336	1.21	0.2254	*ns*
T3 - T4	100% a.s.	-0.01	0.06	336	-0.10	0.9200	*ns*
T4 - T5	100% a.s.	0.12	0.06	336	1.93	0.0549	*ns*
T5 - T6	100% a.s.	-0.10	0.06	336	-1.65	0.1009	*ns*
T6 - T7	100% a.s.	0.10	0.06	336	1.58	0.1145	*ns*
T7 - T8	100% a.s.	0.10	0.06	336	1.73	0.0841	*ns*
T8 - T9	100% a.s.	0.00	0.06	336	-0.04	0.9660	*ns*
T9 - T10	100% a.s.	0.06	0.06	336	0.96	0.3355	*ns*
T10 - T11	100% a.s.	0.03	0.06	336	0.50	0.6204	*ns*
T11 - T12	100% a.s.	0.00	0.06	336	0.08	0.9358	*ns*
T0 - T1	5% a.s.	-0.68	0.06	336	-11.26	**< 0.0001**	****
T0 - T12	5% a.s.	-0.41	0.06	336	-6.76	**< 0.0001**	****
T1 - T2	5% a.s.	-0.09	0.06	336	-1.43	0.1535	*ns*
T2 - T3	5% a.s.	0.16	0.06	336	2.74	**0.0065**	*
T3 - T4	5% a.s.	0.03	0.06	336	0.48	0.6347	*ns*
T4 - T5	5% a.s.	-0.09	0.06	336	-1.43	0.1536	*ns*
T5 - T6	5% a.s.	0.01	0.06	336	0.22	0.8256	*ns*
T6 - T7	5% a.s.	-0.12	0.06	336	-1.94	0.0533	*ns*
T7 - T8	5% a.s.	0.14	0.06	336	2.34	**0.0197**	*ns*
T8 - T9	5% a.s.	-0.05	0.06	336	-0.78	0.4352	*ns*
T9 - T10	5% a.s.	0.17	0.06	336	2.88	**0.0043**	*
T10 - T11	5% a.s.	0.01	0.06	336	0.09	0.9310	*ns*
T11 - T12	5% a.s.	0.08	0.06	336	1.34	0.1818	*ns*

Table S3.10. (Continued)

Pairwise comparis*ons*, treatment pairs (emmeans)

contrast	time	estimate	*SE*	*df*	*t*-ratio	*p*-value	sign. corr.
100% a.s. - 5% a.s.	T0	0.00	0.10	8.85	-0.05	0.9643	*ns*
100% a.s. - 5% a.s.	T1	-0.59	0.10	8.85	-5.88	**0.0003**	***
100% a.s. - 5% a.s.	T2	-0.70	0.10	8.85	-6.96	**0.0001**	***
100% a.s. - 5% a.s.	T3	-0.61	0.10	8.85	-6.05	**0.0002**	***
100% a.s. - 5% a.s.	T4	-0.57	0.10	8.85	-5.71	**0.0003**	***
100% a.s. - 5% a.s.	T5	-0.78	0.10	8.85	-7.71	**< 0.0001**	****
100% a.s. - 5% a.s.	T6	-0.66	0.10	8.85	-6.60	**0.0001**	***
100% a.s. - 5% a.s.	T7	-0.88	0.10	8.85	-8.70	**< 0.0001**	****
100% a.s. - 5% a.s.	T8	-0.84	0.10	8.85	-8.33	**< 0.0001**	****
100% a.s. - 5% a.s.	T9	-0.88	0.10	8.85	-8.78	**< 0.0001**	****
100% a.s. - 5% a.s.	T10	-0.77	0.10	8.85	-7.63	**< 0.0001**	****
100% a.s. - 5% a.s.	T11	-0.79	0.10	8.85	-7.88	**< 0.0001**	****
100% a.s. - 5% a.s.	T12	-0.72	0.10	8.85	-7.13	**0.0001**	***

Table S3.11. Results of the PERMANOVA model evaluating the effect of treatment and time on the expansion ratio in *Suberites australiensis* from experiment 3 (1.5% a.s.). Data are untransformed. P-values are uncorrected, but significance after correction with Benjamini-Hochberg Procedure (sign. corr.) is reported as: *$p < 0.05$; **$p < 0.01$; ***$p < 0.001$; ****$p <$ 0.0001; *ns,* non-significant.

Expansion ratio - *Suberites australiensis*
Experiment 3 (1.5% a.s.)
Repeated Measures Univariate PERMANOVA
Untransformed data
Resemblance: D1 Euclidean distance
Sums of squares type: Type I (sequential)
Permutation method: Permutation of residuals under a reduced model
Number of permutations: 9999

Factors	**Abbrev.**	**Type**
treatment	TR	Fixed
chamber	CH	Random
sponge	SP	Random
time	TI	Fixed

source	*df*	*SS*	*MS*	pseudo-*F*	*p*-value	perms
TR	1	0.3	0.33	0.4	0.8	10
CH(TR)	4	3.5	0.88	2.9	**0.0234**	9940
SP(CH(TR))	24	7.4	0.31	20.2	**0.0001**	9913
TI	14	0.7	0.05	2.4	**0.0118**	9921
TRxTI	14	0.1	0.01	0.5	0.9356	9937
CH(TR)xTI	56	1.2	0.02	1.4	**0.0418**	9853
Res	336	5.2	0.02			
Total	449	18.5				

Table S3.12. Results of the linear mixed effect model (lme) evaluating the effect of treatment and time on the pumping rate in *Suberites australiensis* from experiment 2 (5% a.s.). Data are square root trasformed. P-values are uncorrected, but significance after correction with Benjamini-Hochberg Procedure (sign. corr.) is reported as: *$p < 0.05$; **$p < 0.01$; ***$p < 0.001$; ****$p < 0.0001$; *ns,* non-significant. In fixed effect table: sum sq: sum of squares; mean sq: means quare; numDF: numerator degrees of freedom; denDF: denominator degrees of freedom; df : degrees of freedom.

Pumping rate - *Suberites australiensis*
Experiment 2 (5% a.s.)
Linear mixed-effects model (lme) with different variances per stratum
Formula: Pumping rate ~ treatment * time + (1|chamber/sponge)
Variance model: varIdent (form = ~ 1|time * treatment)
Trasformation: Square root

Fixed effects test (anova)

	num*DF*	den*DF*	*F*-value	*p*-value
(Intercept)	1	192	140.3	**< 0.0001**
treatment	1	4	16.7	**0.0151**
time	12	192	23.3	**< 0.0001**
treatment:time	12	192	9.3	**< 0.0001**

Pairwise comparisons, time pairs (emmeans)

contrast	treatment	estimate	*SE*	*df*	*t*-ratio	*p*-value	sign. corr.
T0 - T1	100% a.s.	-0.01	0.02	192	-0.37	0.7106	*ns*
T0 - T12	100% a.s.	0.04	0.01	192	3.84	**0.0002**	**
T1 - T2	100% a.s.	0.00	0.02	192	0.20	0.8384	*ns*
T2 - T3	100% a.s.	0.00	0.02	192	0.14	0.8892	*ns*
T3 - T4	100% a.s.	0.02	0.02	192	0.73	0.4687	*ns*
T4 - T5	100% a.s.	0.01	0.01	192	0.77	0.4410	*ns*
T5 - T6	100% a.s.	-0.01	0.02	192	-0.74	0.4578	*ns*
T6 - T7	100% a.s.	0.00	0.02	192	0.18	0.8563	*ns*
T7 - T8	100% a.s.	0.01	0.02	192	0.73	0.4658	*ns*
T8 - T9	100% a.s.	0.01	0.01	192	0.98	0.3294	*ns*
T9 - T10	100% a.s.	0.01	0.01	192	1.46	0.1451	*ns*
T10 - T11	100% a.s.	-0.01	0.00	192	-1.13	0.2587	*ns*
T11 - T12	100% a.s.	0.00	0.00	192	0.39	0.6980	*ns*
T0 - T1	5% a.s.	-0.24	0.04	192	-5.62	**< 0.0001**	****
T0 - T12	5% a.s.	0.03	0.01	192	2.20	**0.0293**	*ns*
T1 - T2	5% a.s.	-0.01	0.05	192	-0.21	0.8357	*ns*
T2 - T3	5% a.s.	0.16	0.03	192	4.56	**< 0.0001**	***
T3 - T4	5% a.s.	0.05	0.02	192	2.84	**0.0050**	*
T4 - T5	5% a.s.	0.02	0.01	192	1.90	0.0584	*ns*
T5 - T6	5% a.s.	0.00	0.01	192	-0.41	0.6841	*ns*
T6 - T7	5% a.s.	0.01	0.01	192	1.30	0.1967	*ns*
T7 - T8	5% a.s.	0.01	0.01	192	1.38	0.1688	*ns*
T8 - T9	5% a.s.	0.01	0.00	192	1.79	0.0754	*ns*
T9 - T10	5% a.s.	0.01	0.00	192	1.34	0.1825	*ns*
T10 - T11	5% a.s.	0.01	0.00	192	3.78	**0.0002**	**
T11 - T12	5% a.s.	0.00	0.00	192	-0.34	0.7365	*ns*

Table S3.12. (Continued)

Pairwise comparisons, treatment pairs (emmeans)

contrast	time	estimate	*SE*	*df*	*t*-ratio	*p*-value	sign. corr.
100% a.s. - 5% a.s.	T0	0.00	0.02	4.00	0.23	0.8326	*ns*
100% a.s. - 5% a.s.	T1	-0.23	0.04	4.00	-5.18	**0.0066**	*
100% a.s. - 5% a.s.	T2	-0.24	0.03	4.00	-7.51	**0.0017**	*
100% a.s. - 5% a.s.	T3	-0.09	0.03	4.00	-3.28	**0.0305**	*ns*
100% a.s. - 5% a.s.	T4	-0.05	0.02	4.00	-3.53	**0.0242**	*ns*
100% a.s. - 5% a.s.	T5	-0.04	0.01	4.00	-3.47	**0.0257**	*ns*
100% a.s. - 5% a.s.	T6	-0.03	0.02	4.00	-1.78	0.1501	*ns*
100% a.s. - 5% a.s.	T7	-0.02	0.01	4.00	-1.52	0.2039	*ns*
100% a.s. - 5% a.s.	T8	-0.02	0.01	4.00	-2.13	0.1000	*ns*
100% a.s. - 5% a.s.	T9	-0.03	0.01	4.00	-3.21	**0.0327**	*ns*
100% a.s. - 5% a.s.	T10	-0.03	0.01	4.00	-3.90	**0.0175**	*ns*
100% a.s. - 5% a.s.	T11	-0.01	0.01	4.00	-1.28	0.2688	*ns*
100% a.s. - 5% a.s.	T12	-0.01	0.01	4.00	-1.71	0.1619	*ns*

Table S3.13. Results of the PERMANOVA model, and permutation t-tests evaluating the effect of treatment and time on the pumping rate in *Suberites australiensis* from experiment 2 (5% a.s.). Data are square root transformed. P-values are uncorrected, but significance after correction with Benjamini-Hochberg Procedure (sign. corr.) is reported as: *$p < 0.05$; **$p < 0.01$; ***$p < 0.001$; ****$p < 0.0001$; *ns,* non-significant.

Pumping rate - *Suberites australiensis*
Experiment 2 (5% a.s.)
Repeated Measures Univariate PERMANOVA
Transformation: Square root

Factors	**Abbrev.**	**Type**
treatment	TR	Fixed
chamber	CH	Random
sponge	SP	Random
time	TI	Fixed

PERMANOVA

source	*df*	*SS*	*MS*	pseudo-*F*	*p*-value	perms
TR	1	42556	42556	50.9	0.0974	10
CH(TR)	4	3346	837	0.2	0.9929	9951
SP(CH(TR))	12	57026	4752	8.0	**0.0001**	9892
TI	12	78718	6560	13.4	**0.0001**	9922
TRxTI	12	39320	3277	6.7	**0.0001**	9910
CH(TR)xTI	48	23492	489	0.8	0.9067	9809
Res	144	85166	591			
Total	233	329620				

Pairwise permutation t-tests, time pairs

treatment	comparison	*p*-value	sign. corr.
5% a.s.	T1 vs T0	**0.0046**	*ns*
5% a.s.	T2 vs T1	0.7716	*ns*
5% a.s.	T3 vs T2	**0.0044**	*ns*
5% a.s.	T4 vs T3	**0.0090**	*ns*
5% a.s.	T5 vs T4	**0.0442**	*ns*
5% a.s.	T6 vs T5	0.4746	*ns*
5% a.s.	T7 vs T6	0.0746	*ns*
5% a.s.	T8 vs T7	0.2062	*ns*
5% a.s.	T9 vs T8	0.0786	*ns*
5% a.s.	T10 vs T9	0.2472	*ns*
5% a.s.	T11 vs T10	**0.0148**	*ns*
5% a.s.	T12 vs T0	0.0642	*ns*
5% a.s.	T12 vs T11	0.6956	*ns*
100% a.s.	T1 vs T0	0.8358	*ns*
100% a.s.	T2 vs T1	0.7748	*ns*
100% a.s.	T3 vs T2	0.8860	*ns*
100% a.s.	T4 vs T3	0.3416	*ns*
100% a.s.	T5 vs T4	**0.0458**	*ns*
100% a.s.	T6 vs T5	0.3480	*ns*
100% a.s.	T7 vs T6	0.7690	*ns*
100% a.s.	T8 vs T7	0.1670	*ns*
100% a.s.	T9 vs T8	0.5058	*ns*
100% a.s.	T10 vs T9	0.2648	*ns*
100% a.s.	T11 vs T10	0.3676	*ns*
100% a.s.	T12 vs T0	**0.0066**	*ns*
100% a.s.	T12 vs T11	0.6638	*ns*

Pairwise permutation t-tests, treatment pairs

time	comparison	*p*-value	sign. corr.
T0	5% a.s. vs 100% a.s.	0.8060	*ns*
T1	5% a.s. vs 100% a.s.	**0.0004**	**
T2	5% a.s. vs 100% a.s.	**0.0002**	**
T3	5% a.s. vs 100% a.s.	**0.0102**	*
T4	5% a.s. vs 100% a.s.	**0.0084**	*
T5	5% a.s. vs 100% a.s.	**0.0096**	*
T6	5% a.s. vs 100% a.s.	0.1270	*ns*
T7	5% a.s. vs 100% a.s.	0.1920	*ns*
T8	5% a.s. vs 100% a.s.	0.0680	*ns*
T9	5% a.s. vs 100% a.s.	**0.0046**	*
T10	5% a.s. vs 100% a.s.	**0.0018**	**
T11	5% a.s. vs 100% a.s.	0.1116	*ns*
T12	5% a.s. vs 100% a.s.	0.0932	*ns*

Table S3.14. Results of the linear mixed effect model (lme) evaluating the effect of treatment and time on the pumping rate in *Suberites australiensis* from experiment 3 (1.5% a.s.). Data are square root transformed. P-values are uncorrected, but significance after correction with Benjamini-Hochberg Procedure (sign. corr.) is reported as: *$p < 0.05$; **$p < 0.01$; ***$p < 0.001$; ****$p < 0.0001$; *ns,* non-significant.

Pumping rate - *Suberites australiensis*
Experiment 3 (1.5% a.s.)
Linear mixed-effects model (lme) with different variances per stratum
Formula: Pumping rate ~ treatment * time + (1|chamber/sponge)
Variance model: varIdent (form = ~ 1|time * treatment)
Transformation: Square root

Fixed effects test (anova)

	num*DF*	den*DF*	*F*-value	*p*-value
(Intercept)	1	224	42.5	**< 0.0001**
treatment	1	4	0.0	0.9499
time	14	224	3.7	**< 0.0001**
treatment:time	14	224	1.7	**0.0486**

Pairwise comparisons, time pairs (emmeans)

contrast	treatment	estimate	*SE*	*df*	*t*-ratio	*p*-value	sign. corr.
T0 - T1	100% a.s.	-0.01	0.02	224	-0.70	0.4858	*ns*
T0 - T14	100% a.s.	0.01	0.01	224	1.43	0.1549	*ns*
T1 - T2	100% a.s.	-0.01	0.03	224	-0.22	0.8267	*ns*
T2 - T3	100% a.s.	0.00	0.04	224	-0.11	0.9149	*ns*
T3 - T4	100% a.s.	0.03	0.03	224	1.07	0.2862	*ns*
T4 - T5	100% a.s.	0.00	0.00	224	-0.43	0.6661	*ns*
T5 - T6	100% a.s.	0.01	0.00	224	1.38	0.1682	*ns*
T6 - T7	100% a.s.	-0.01	0.00	224	-1.78	0.0763	*ns*
T7 - T8	100% a.s.	-0.01	0.01	224	-0.70	0.4856	*ns*
T8 - T9	100% a.s.	0.01	0.01	224	0.73	0.4655	*ns*
T9 - T10	100% a.s.	0.00	0.01	224	-0.41	0.6854	*ns*
T10 - T11	100% a.s.	0.01	0.01	224	0.84	0.4033	*ns*
T11 - T12	100% a.s.	0.00	0.00	224	0.71	0.4782	*ns*
T12 - T13	100% a.s.	0.00	0.00	224	2.34	**0.0201**	*ns*
T13 - T14	100% a.s.	0.00	0.00	224	-1.33	0.1855	*ns*
T0 - T1	1.5% a.s.	-0.02	0.02	224	-0.92	0.3589	*ns*
T0 - T14	1.5% a.s.	0.02	0.00	224	3.78	**0.0002**	**
T1 - T2	1.5% a.s.	0.02	0.02	224	0.83	0.4074	*ns*
T2 - T3	1.5% a.s.	0.00	0.02	224	0.31	0.7593	*ns*
T3 - T4	1.5% a.s.	0.00	0.02	224	-0.02	0.9860	*ns*
T4 - T5	1.5% a.s.	0.01	0.01	224	0.50	0.6149	*ns*
T5 - T6	1.5% a.s.	0.00	0.00	224	0.00	0.9971	*ns*
T6 - T7	1.5% a.s.	0.00	0.00	224	0.33	0.7420	*ns*
T7 - T8	1.5% a.s.	0.00	0.00	224	0.19	0.8522	*ns*
T8 - T9	1.5% a.s.	0.00	0.00	224	-0.19	0.8463	*ns*
T9 - T10	1.5% a.s.	0.00	0.00	224	1.83	0.0682	*ns*
T10 - T11	1.5% a.s.	0.00	0.00	224	-0.64	0.5197	*ns*
T11 - T12	1.5% a.s.	0.00	0.00	224	1.40	0.1636	*ns*
T12 - T13	1.5% a.s.	0.00	0.00	224	-2.10	**0.0365**	*ns*
T13 - T14	1.5% a.s.	0.00	0.00	224	1.56	0.1193	*ns*

Table S3.14. (Continued)

Pairwise comparison*s*, treatment pairs (emmeans)

contrast	time	estimate	*SE*	*df*	*t*-ratio	*p*-value	sign. corr.
100% a.s. - 1.5% a.s.	T0	-0.01	0.01	4.00	-0.69	0.5297	*ns*
100% a.s. - 1.5% a.s.	T1	-0.01	0.03	4.00	-0.41	0.7035	*ns*
100% a.s. - 1.5% a.s.	T2	0.02	0.03	4.00	0.52	0.6313	*ns*
100% a.s. - 1.5% a.s.	T3	0.02	0.03	4.00	0.89	0.4256	*ns*
100% a.s. - 1.5% a.s.	T4	0.00	0.01	4.00	-0.23	0.8300	*ns*
100% a.s. - 1.5% a.s.	T5	0.01	0.01	4.00	0.76	0.4910	*ns*
100% a.s. - 1.5% a.s.	T6	0.00	0.01	4.00	-0.15	0.8876	*ns*
100% a.s. - 1.5% a.s.	T7	0.01	0.01	4.00	1.29	0.2660	*ns*
100% a.s. - 1.5% a.s.	T8	0.02	0.01	4.00	1.49	0.2107	*ns*
100% a.s. - 1.5% a.s.	T9	0.01	0.01	4.00	1.36	0.2464	*ns*
100% a.s. - 1.5% a.s.	T10	0.02	0.01	4.00	1.57	0.1916	*ns*
100% a.s. - 1.5% a.s.	T11	0.01	0.01	4.00	0.97	0.3858	*ns*
100% a.s. - 1.5% a.s.	T12	0.01	0.00	4.00	1.45	0.2201	*ns*
100% a.s. - 1.5% a.s.	T13	0.00	0.00	4.00	-0.17	0.8717	*ns*
100% a.s. - 1.5% a.s.	T14	0.00	0.00	4.00	0.90	0.4185	*ns*

Table S3.15. Results of the PERMANOVA model, and permutation t-tests evaluating the effect of treatment and time on the pumping rate in *Suberites australiensis* from experiment 3 (1.5% a.s.). Data are square root transformed. P-values are uncorrected, but significance after correction with Benjamini-Hochberg Procedure (sign. corr.) is reported as: $*p < 0.05$; $**p < 0.01$; $***p < 0.001$; $****p < 0.0001$; *ns,* non-significant. *df* : degrees of freedom; *SS*: sum of squares; *MS*: mean squares; perms: number of permutations.

Pumping rate - *Suberites australiensis*
Experiment 3 (1.5% a.s.)
Repeated Measures Univariate PERMANOVA
Resemblance: D1 Euclidean distance
Sums of squares type: Type I (sequential)
Permutation method: Permutation of residuals under a reduced model
Number of permutations:
9999
Transformation: Square root

Factors	**Abbrev.**	**Type**
treatment	TR	Fixed
chamber	CH	Random
sponge	SP	Random
time	TI	Fixed

source	*df*	*SS*	*MS*	pseudo-*F*	*p*-value	perms
TR	1	5517.0	5517.0	0.8	0.5043	10
CH(TR)	4	27467.0	6866.7	0.8	0.5382	9945
SP(CH(TR))	12	98683.0	8223.6	19.6	**0.0001**	9888
TI	14	15644.0	1117.5	2.4	**0.0006**	9910
TRxTI	14	13409.0	957.8	2.1	**0.0023**	9901
CH(TR)xTI	56	26026.0	464.8	1.1	0.2108	9786
Res	168	70386.0	419.0			
Total	269	257130.0				

Table S3.15. (continued)

Pairwise permutation t-tests, time pairs

treatment	comparison	*p*-value	sign. corr.
1.5% a.s.	T1 vs T0	0.3106	*ns*
1.5% a.s.	T2 vs T1	**0.0044**	*ns*
1.5% a.s.	T3 vs T2	**0.0476**	*ns*
1.5% a.s.	T4 vs T3	0.8556	*ns*
1.5% a.s.	T5 vs T4	0.7006	*ns*
1.5% a.s.	T6 vs T5	0.9906	*ns*
1.5% a.s.	T7 vs T6	0.6656	*ns*
1.5% a.s.	T8 vs T7	0.6816	*ns*
1.5% a.s.	T9 vs T8	0.8134	*ns*
1.5% a.s.	T10 vs T9	0.1416	*ns*
1.5% a.s.	T11 vs T10	0.2038	*ns*
1.5% a.s.	T12 vs T11	**0.0038**	*ns*
1.5% a.s.	T13 vs T12	0.0634	*ns*
1.5% a.s.	T14 vs T0	**0.0064**	*ns*
1.5% a.s.	T14 vs T13	0.1464	*ns*
100% a.s.	T1 vs T0	0.6332	*ns*
100% a.s.	T2 vs T1	0.7626	*ns*
100% a.s.	T3 vs T2	0.5176	*ns*
100% a.s.	T4 vs T3	0.0704	*ns*
100% a.s.	T5 vs T4	0.6258	*ns*
100% a.s.	T6 vs T5	0.0610	*ns*
100% a.s.	T7 vs T6	**0.0246**	*ns*
100% a.s.	T8 vs T7	0.5062	*ns*
100% a.s.	T9 vs T8	0.7590	*ns*
100% a.s.	T10 vs T9	0.9840	*ns*
100% a.s.	T11 vs T10	0.2478	*ns*
100% a.s.	T12 vs T11	0.8248	*ns*
100% a.s.	T13 vs T12	**0.0416**	*ns*
100% a.s.	T14 vs T0	0.3148	*ns*
100% a.s.	T14 vs T13	0.1882	*ns*

Pairwise permutation t-tests, treatment pairs

time	comparison	*p*-value	sign. corr.
T0	1.5% a.s. vs 100% a.s.	0.5414	*ns*
T1	1.5% a.s. vs 100% a.s.	0.5072	*ns*
T2	1.5% a.s. vs 100% a.s.	0.6702	*ns*
T3	1.5% a.s. vs 100% a.s.	0.4812	*ns*
T4	1.5% a.s. vs 100% a.s.	0.9818	*ns*
T5	1.5% a.s. vs 100% a.s.	0.5304	*ns*
T6	1.5% a.s. vs 100% a.s.	0.9024	*ns*
T7	1.5% a.s. vs 100% a.s.	0.3368	*ns*
T8	1.5% a.s. vs 100% a.s.	0.1784	*ns*
T9	1.5% a.s. vs 100% a.s.	0.2734	*ns*
T10	1.5% a.s. vs 100% a.s.	0.1428	*ns*
T11	1.5% a.s. vs 100% a.s.	0.2474	*ns*
T12	1.5% a.s. vs 100% a.s.	**0.0146**	*ns*
T13	1.5% a.s. vs 100% a.s.	0.8450	*ns*
T14	1.5% a.s. vs 100% a.s.	0.1288	*ns*

Table S3.16. Results of the linear mixed effect model (lmer) evaluating the effect of treatment and time on the respiration rate of *Polymastia crocea* from experiment 2 (5% a.s.). Data are untransformed. P-values are uncorrected, but significance after correction with Benjamini-Hochberg Procedure (sign. corr.) is reported as: *$p < 0.05$; **$p < 0.01$; ***$p < 0.001$; ****$p < 0.0001$; *ns,* non-significant. In fixed effect table: sum sq: sum of squares; mean sq: means quare; num*DF*: numerator degrees of freedom; den*DF*: denominator degrees of freedom. In random effects table: npar: number of model parameters; logLik: log-likelihood; AIC: Akaike information criterion; LRT: likelihood ratio test statistic; *df* : degrees of freedom

Respiration Rate -*Polymastia crocea*
Experiment 2 (5% a.s.)
Linear mixed-effects model (lmer)
Formula: Respiration rate ~ treatment * time + (1|chamber/sponge)
Untransformed data

Fixed effects test (anova)

	sum sq	mean sq	num*DF*	den*DF*	*F*-value	*p*-value
treatment	0.00	0.00	1	4	0.4	0.5454
time	0.01	0.00	2	32	5.6	**0.0082**
treatment:time	0.00	0.00	2	32	1.4	0.2661

Random effects test (ranova)

	npar	logLik	AIC	LRT	*df*	*p*-value
<none>	9	83.79	-149.59	#N/D	#N/D	#N/D
(1 | sponge:chamber)	8	80.04	-144.08	7.51	1.00	**0.0061**
(1 | chamber)	8	83.74	-151.49	0.10	1.00	0.7552

Pairwise comparis*ons,* time pairs (emmeans)

contrast	treatment	estimate	*SE*	*df*	*t*-ratio	*p*-value	sign. corr.
day 0 - day 5	100% a.s.	0.00	0.01	32	0.28	0.7823	*ns*
day 0 - day 12	100% a.s.	-0.04	0.01	32	-2.81	**0.0084**	*
day 5 - day 12	100% a.s.	-0.04	0.01	32	-3.09	**0.0041**	*
day 0 - day 5	5% a.s.	-0.01	0.01	32	-0.78	0.4436	*ns*
day 0 - day 12	5% a.s.	-0.02	0.01	32	-1.52	0.1389	*ns*
day 5 - day 12	5% a.s.	-0.01	0.01	32	-0.74	0.4635	*ns*

Pairwise comparis*ons,* treatment pairs (emmeans)

contrast	time	estimate	*SE*	*df*	*t*-ratio	*p*-value	sign. corr.
100% a.s. - 5% a.s.	day 0	0.01	0.02	8.28	0.49	0.6352	*ns*
100% a.s. - 5% a.s.	day 5	0.00	0.02	8.28	-0.23	0.8232	*ns*
100% a.s. - 5% a.s.	day 12	0.03	0.02	8.28	1.38	0.2042	*ns*

Table S3.17. Results of the linear mixed effect model (lmer) evaluating the effect of treatment and time on the respiration rate of *Suberites australiensis* from experiment 2 (5% a.s.). Data are untransformed. P-values are uncorrected, but significance after correction with Benjamini-Hochberg Procedure (sign. corr.) is reported as: *$p < 0.05$; **$p < 0.01$; ***$p < 0.001$; ****$p < 0.0001$; *ns,* non-significant. In fixed effect table: sum sq: sum of squares; mean sq: means quare; num*DF*: numerator degrees of freedom; den*DF*: denominator degrees of freedom. In random effects table: npar: number of model parameters; logLik: log-likelihood; AIC: Akaike information criterion; LRT: likelihood ratio test statistic; *df* : degrees of freedom

Respiration Rate - *Suberites australiensis*
Experiment 2 (5% a.s.)
Linear mixed-effects model (lmer)
Formula: Respiration rate ~ treatment * time + (1|chamber/sponge)
Untransformed data

Fixed effects test (anova)

	sum sq	mean sq	num*DF*	den*DF*	*F*-value	*p*-value
treatment	0.02	0.02	1	16	2.1	0.1666
time	0.13	0.06	2	32	7.4	**0.0023**
treatment:time	0.04	0.02	2	32	2.2	0.1277

Random effects test (ranova)

	npar	logLik	AIC	LRT	*df*	*p*-value
<none>	9	25.61	-33.22	#N/D	#N/D	#N/D
(1 | sponge:chamber)	8	21.61	-27.21	8.01	1.00	**0.0047**
(1 | chamber)	8	25.61	-35.22	0.00	1.00	1.0000

Pairwise comparisons, time pairs (emmeans)

contrast	treatment	estimate	*SE*	*df*	*t*-ratio	*p*-value	sign. corr.
day 0 - day 7	100% a.s.	-0.01	0.04	32	-0.19	0.8535	*ns*
day 0 - day 14	100% a.s.	0.12	0.04	32	2.82	**0.0082**	*
day 7 - day 14	100% a.s.	0.13	0.04	32	3.00	**0.0051**	*
day 0 - day 7	5% a.s.	0.10	0.04	32	2.25	**0.0318**	*
day 0 - day 14	5% a.s.	0.11	0.04	32	2.57	**0.0152**	*
day 7 - day 14	5% a.s.	0.01	0.04	32	0.32	0.7510	*ns*

Pairwise comparisons, treatment pairs (emmeans)

contrast	time	estimate	*SE*	*df*	*t*-ratio	*p*-value	sign. corr.
100% a.s. - 5% a.s.	day 0	-0.10	0.06	9.65	-1.69	0.1227	*ns*
100% a.s. - 5% a.s.	day 7	0.01	0.06	9.65	0.12	0.9076	*ns*
100% a.s. - 5% a.s.	day 14	-0.11	0.06	9.65	-1.88	0.0907	*ns*

Appendix C - Resilience to disturbance and interannual dynamics of a rocky temperate mesophotic ecosystem.

Table S4.1. Schematic representations of the sampling design. Numbers in the tables indicate the number of replicate quadrats sampled for each combination of time and site.

Complete Sampling design		Historical data				Present data						
	Site	Apr-94	Oct-94	Mar-95	Aug-95	Jul-18	Nov-18	Jul-19	Nov-19	Sep-20	Mar-21	Aug-21
Innermost site	West Cliff	-	-	-	-	5	5	5	5	-	-	5
	Goleen	-	-	-	-	5	5	5	5	5	5	4
Internal sites	Labhra Cliff	5	5	5	5	5	5	5	5	5	5	4
	Glannafeen	5	5	5	5	5	5	5	5	5	4	-
Entrance site	Whirlpool Cliff	-	-	-	-	5	5	5	5	5	5	-

Table S4.2. Schematic representations of the data subsets used for the statistical analysis. Numbers in the tables indicate the number of replicate quadrats sampled for each combination of time and site.

Comparison across all sites (17 months)

	Site	Jul-18	Nov-18	Jul-19	Nov-19
Innermost site	West Cliff	5	5	5	5
	Goleen	5	5	5	5
Internal sites	Labhra Cliff	5	5	5	5
	Glannafeen	5	5	5	5
Entrance site	Whirlpool Cliff	5	5	5	5

2.5-year comparison (32 months)

	Site	Jul-18	Nov-18	Jul-19	Nov-19	Sep-20	Mar-21
	Goleen	4	4	4	4	4	4
Internal sites	Labhra Cliff	4	4	4	4	4	4
	Glannafeen	4	4	4	4	4	4
Entrance site	Whirlpool Cliff	4	4	4	4	4	4

3-year full comparison (36 months)

	Site	Jul-18	Nov-18	Jul-19	Nov-19	Sep-20	Mar-21	Aug-21
Internal sites	Goleen	4	4	4	4	4	4	4
	Labhra Cliff	4	4	4	4	4	4	4

Present-past comparison (16-17 months)

	Site	Apr-94	Oct-94	Mar-95	Aug-95	Jul-18	Nov-18	Jul-19	Nov-19
Internal sites	Labhra Cliff	5	5	5	5	5	5	5	5
	Glannafeen	5	5	5	5	5	5	5	5

Table S4.3. List of Taxa and OTUs recorded during this study. For sponges the morphology in reported in bracket: EN Encrusting Non-Raspailiidae, ER Erect, GO Globular, MA Massive, OT Other, PA Papillate, PE Pedunculate, RA Encrusting Raspailiidae, RE Repent. Some species of the genera *Eurypon* and *Polymastia* are currently being described. We assigned them a provisional name (in all caps, not to be confused with described species) to help in the analyses and in the identification.

Benthic group	taxon/OTU
Algae	CCA
	Encrusting non-calcified red algae
	Foliose red algae
	Turf red algae
Animal turf	Animal turf
Anthozoans	*Alcyonium hibernicum*
	Anthopleura ballii
	Caryophyllia spp-
	Corynactis viridis
	Cylista troglodytes
Ascidians	*Aplidium pallidum*
	Aplidium punctum
	Ascidia mentula
	Ascidiella spp-
	Botrylloides leachi
	Ciona intestinalis
	Clavelina lepadiformis
	Didemnum maculosum
	Didemnum maculosum var. *dentata*
	Diplosoma spongiforme
	Distaplia rosea
	Encrusting Red Ascidians
	Pyuridae ind.
	Trididemnum cereum
	Balanus spp-
Lophophorates	*Bugulina calathus*
	Encrusting bryozoans
	Other upright bryozoans
	Phoronida
Polychaetes	Non-calcifying polychaetes
	Serpulids
Sponges	*Amphilectus fucorum* (RE)
	Aplysilla sulfurea (EN)
	Axinella damicornis (ER)
	Axinella dissimilis (ER)
	Cliona celata (MA)

Benthic group	taxon/OTU
Sponges	*Dysidea* spp- (MA)
	Encrusting Suberitidae (EN)
	Eurypon BRIGHTRED (RA)
	Eurypon LIGHTYELLOWs (RA)
	Eurypon major (RA)
	Eurypon ORANGE (RA)
	Eurypon YELLOW (RA)
	Haliclona spp- (OT)
	Haliclona urceolus (OT)
	Halicnemia patera (EN)
	Hymedesmia paupertas (EN)
	Hymeniacidon kitchingi (MA)
	Hymeniacidon perlevis (MA)
	Hymeraphia stellifera (EN)
	Iophon sp- (EN)
	Leucosolenia complicata (OT)
	Mycale contareni (EN)
	Mycale ORANGE (EN)
	Paratimea spp- (EN)
	Phorbas dives (EN)
	Polymastia ACULEATA (PA)
	Polymastia boletiformis (PA)
	Polymastia conigera (PA)
	Polymastia ROSACEA (PA)
	Polymastia SPAGHETTI (PA)
	Polymastia svenseni (PA)
	Raspailia aculeata (EN)
	Raspailia ramosa (ER)
	Sphaerotylus renoufi (PA)
	Stelligera spp- (ER)
	Suberites carnosus (PE)
	Sycon ciliatum (OT)
	Tethya aurantium (GL)
	Tethyd ORANGE (EN)
	Tethyd YELLOW (EN)

C.1. PERMANOVA

Table S4.4. Results of the PERMANOVA models evaluating the effect of time and site on the benthic community, and sponge and ascidian assemblage structure. Comparison across all sites (June 2018 – November 2019). Significant *p*-values ($p < 0.05$) are in bold.

Benthic communities

Comparison across all sites (June 2018 – November 2019)

Log (x+1) transformed data, Bray Curtis dissimilarity, 9999 permutations

Two-way PERMANOVA with all sites (benthic communities)

	Df	SS	MS	Pseudo-*F*	R2	*p-value*
Site	4	13.80	3.45	89.56	0.78	**0.0001**
Time	1	0.15	0.15	3.89	0.01	**0.0079**
Site:Time	4	0.27	0.07	1.75	0.02	**0.0449**
Residuals	90	3.47	0.04		0.20	
Total	99	17.68			1.00	

PERMANOVA pairwise comparisons between pairs of sites (benthic communities)

pairs	Df	SS	Pseudo-*F*	R2	*p*-value	*p*-adjusted	sig.
Glannafeen vs Goleen	1	0.71	14.68	0.28	**0.0001**	**0.0001**	***
Glannafeen vs Labhra Cliff	1	2.03	36.35	0.49	**0.0001**	**0.0001**	***
Glannafeen vs West Cliff	1	3.36	73.18	0.66	**0.0001**	**0.0001**	***
Glannafeen vs Whirlpool Cliff	1	5.21	164.78	0.81	**0.0001**	**0.0001**	***
Goleen vs Labhra Cliff	1	1.28	25.05	0.40	**0.0001**	**0.0001**	***
Goleen vs West Cliff	1	3.97	96.29	0.72	**0.0001**	**0.0001**	***
Goleen vs Whirlpool Cliff	1	5.81	216.11	0.85	**0.0001**	**0.0001**	***
Labhra Cliff vs West Cliff	1	2.78	56.91	0.60	**0.0001**	**0.0001**	***
Labhra Cliff vs Whirlpool Cliff	1	5.03	145.70	0.79	**0.0001**	**0.0001**	***
West Cliff vs Whirlpool Cliff	1	4.31	175.65	0.82	**0.0001**	**0.0001**	***

Two-way PERMANOVA with only internal sites (benthic communities)

	Df	SS	MS	Pseudo-*F*	R2	*p-value*
Site	2	2.68	1.34	26.69	0.48	**0.0001**
Time	1	0.20	0.20	4.07	0.04	**0.0038**
Site:Time	2	0.03	0.02	0.34	0.01	0.9831
Residuals	54	2.72	0.05		0.48	
Total	59	5.64			1.00	

Table S4.4. (Continued)

One-way PERMANOVAs at each site (benthic communities)

			Df	SS	MS	Pseudo-*F*	R2	*p-value*
Entrance	Whirlpool Cliff	Time	1	0.07	0.07	10.63	0.37	**0.0001**
		Residuals	18	0.12	0.01		0.63	
		Total	19	0.19			1.00	

			Df	SS	MS	Pseudo-*F*	R2	*p*-value
Internal sites	Glannafeen	Time	1	0.09	0.09	1.79	0.09	0.1243
		Residuals	18	0.92	0.05		0.91	
		Total	19	1.01			1.00	

			Df	SS	MS	Pseudo-*F*	R2	*p-value*
	Labhra Cliff	Time	1	0.09	0.09	1.58	0.08	0.1827
		Residuals	18	1.03	0.06		0.92	
		Total	19	1.12			1.00	

			Df	SS	MS	Pseudo-*F*	R2	*p-value*
	Goleen	Time	1	0.06	0.06	1.35	0.07	0.2571
		Residuals	18	0.77	0.04		0.93	
		Total	19	0.83			1.00	

			Df	SS	MS	Pseudo-*F*	R2	*p-value*
Innermost site	West Cliff	Time	1	0.11	0.11	3.10	0.15	**0.0068**
		Residuals	18	0.63	0.03		0.85	
		Total	19	0.74			1.00	

Sponge assemblages

Comparison across all sites (June 2018 – November 2019)

Log (x+1) transformed data, Bray Curtis dissimilarity, 9999 permutations

Two-way PERMANOVA with all sites (sponge assemblage)

	Df	SS	MS	Pseudo-*F*	R2	*p-value*
Site	4	21.46	5.36	63.58	0.73	**0.0001**
Time	1	0.09	0.09	1.08	0.00	0.3417
Site:Time	4	0.18	0.05	0.54	0.01	0.9254
Residuals	90	7.59	0.08		0.26	
Total	99	29.32			1.00	

PERMANOVA pairwise comparisons between pairs of sites (sponge assemblages)

pairs	Df	SS	Pseudo-*F*	R2	*p*-value	*p*-adjusted	sig
Glannafeen vs Goleen	1	0.48	5.69	0.13	**0.0001**	**0.0001**	***
Glannafeen vs Labhra Cliff	1	1.58	12.57	0.25	**0.0001**	**0.0001**	***
Glannafeen vs West Cliff	1	5.60	70.11	0.65	**0.0001**	**0.0001**	***
Glannafeen vs Whirlpool Cliff	1	8.59	157.27	0.81	**0.0001**	**0.0001**	***
Goleen vs Labhra Cliff	1	1.74	14.77	0.28	**0.0001**	**0.0001**	***
Goleen vs West Cliff	1	5.48	75.42	0.66	**0.0001**	**0.0001**	***
Goleen vs Whirlpool Cliff	1	9.10	191.93	0.83	**0.0001**	**0.0001**	***
Labhra Cliff vs West Cliff	1	4.34	38.05	0.50	**0.0001**	**0.0001**	***
Labhra Cliff vs Whirlpool Cliff	1	7.63	86.00	0.69	**0.0001**	**0.0001**	***
West Cliff vs Whirlpool Cliff	1	9.11	210.62	0.85	**0.0001**	**0.0001**	***

Table S4.4. (Continued)

Two-way PERMANOVA with only internal sites (sponge assemblages)

	Df	SS	MS	Pseudo-*F*	R2	*p-value*
Site	2	2.53	1.27	11.20	0.29	**0.0001**
Time	1	0.07	0.07	0.63	0.01	0.6946
Site:Time	2	0.05	0.02	0.21	0.01	0.9985
Residuals	54	6.10	0.11		0.70	
Total	59	8.76			1.00	

One-way PERMANOVAs at each site (sponge assemblages)

			Df	SS	MS	Pseudo-*F*	R2	*p-value*
Entrance	Whirlpool Cliff	Time	1	0.09	0.09	6.15	0.25	**0.006**
		Residuals	18	0.25	0.01		0.75	
		Total	19	0.34			1.00	
Internal sites	Glannafeen	Time	1	0.04	0.04	0.46	0.02	0.7554
		Residuals	18	1.69	0.09		0.98	
		Total	19	1.73			1.00	
	Labhra Cliff	Time	1	0.06	0.06	0.37	0.02	0.7466
		Residuals	18	2.97	0.16		0.98	
		Total	19	3.03			1.00	
	Goleen	Time	1	0.02	0.02	0.19	0.01	0.9276
		Residuals	18	1.45	0.08		0.99	
		Total	19	1.46			1.00	
Innermost site	West Cliff	Time	1	0.07	0.07	0.99	0.05	0.399
		Residuals	18	1.23	0.07		0.95	
		Total	19	1.30			1.00	

Ascidian assemblages

Comparison across all sites (June 2018 – November 2019)

Log (x+1) transformed data, Bray Curtis dissimilarity, 9999 permutations

Two-way PERMANOVA with all sites (ascidian assemblages)

	Df	SS	MS	Pseudo-*F*	R2	*p-value*
Site	3	5.38	1.79	9.73	0.25	**0.0001**
Time	1	1.08	1.08	5.86	0.05	**0.0001**
Site:Time	3	1.74	0.58	3.14	0.08	**0.0003**
Residuals	72	13.27	0.18		0.62	
Total	79	21.47			1.00	

Table S4.4. (Continued)

PERMANOVA pairwise comparisons between pairs of sites (ascidian assemblages)

pairs	Df	SS	Pseudo-*F*	R2	*p-value*	*p*-adjusted	sig
Glannafeen vs Goleen	1	0.77	2.65	0.07	**0.0227**	**0.0227**	*
Glannafeen vs Labhra Cliff	1	0.86	4.07	0.10	**0.0054**	**0.00648**	**
Glannafeen vs West Cliff	1	2.68	14.60	0.28	**0.0001**	**0.0002**	***
Goleen vs Labhra Cliff	1	0.96	3.99	0.10	**0.0027**	**0.00405**	**
Goleen vs West Cliff	1	3.45	16.29	0.30	**0.0001**	**0.0002**	***
Labhra Cliff vs West Cliff	1	2.05	15.44	0.29	**0.0001**	**0.0002**	***

Two-way PERMANOVA with only internal sites (ascidian assemblages)

	Df	SS	MS	Pseudo-*F*	R2	*p-value*
Site	2	1.73	0.86	3.95	0.11	**0.0004**
Time	1	1.80	1.80	8.26	0.11	**0.0001**
Site:Time	2	0.51	0.26	1.17	0.03	0.2822
Residuals	54	11.79	0.22		0.74	
Total	59	15.83			1.00	

One-way PERMANOVAs at each site (ascidian assemblages)

			Df	SS	MS	Pseudo-*F*	R2	*p-value*
Internal sites	Glannafeen	Time	1	1.23	1.23	5.92	0.25	**0.0007**
		Residuals	18	3.75	0.21		0.75	
		Total	19	4.99			1.00	
	Labhra Cliff	Time	1	0.52	0.52	3.69	0.17	**0.0137**
		Residuals	18	2.53	0.14		0.83	
		Total	19	3.05			1.00	
	Goleen	Time	1	0.56	0.56	1.84	0.09	0.1001
		Residuals	18	5.50	0.31		0.91	
		Total	19	6.06			1.00	
Innermost site	West Cliff	Time	1	0.50	0.50	6.07	0.25	**0.0003**
		Residuals	18	1.48	0.08		0.75	
		Total	19	1.98			1.00	

Table S4.5. Results of the PERMANOVA models evaluating the effect of time and site on the benthic community, and sponge and ascidian assemblage structure. 2.5-year comparison (June 2018 – March 2021). Significant *p*-values ($p < 0.05$) are in bold.

Benthic communities

2.5-year comparison (June 2018 – March 2021)

Log (x+1) transformed data, Bray Curtis dissimilarity, 9999 permutations

Two-way PERMANOVA with all sites (benthic communities)

	Df	SS	MS	Pseudo-*F*	R2	*p-value*
Site	3	12.02	4.01	108.18	0.78	**0.0001**
Time	1	0.08	0.08	2.03	0.00	0.107
Site:Time	3	0.09	0.03	0.80	0.01	0.5876
Residuals	88	3.26	0.04		0.21	
Total	95	15.45			1.00	

Two-way PERMANOVA with only internal sites (benthic communities)

	Df	SS	MS	Pseudo-*F*	R2	*p-value*
Site	2	3.11	1.56	32.77	0.49	**0.0001**
Time	1	0.07	0.07	1.41	0.01	0.1979
Site:Time	2	0.03	0.01	0.27	0.00	0.9951
Residuals	66	3.13	0.05		0.49	
Total	71	6.34			1.00	

One-way PERMANOVAs at each site (benthic communities)

			Df	SS	MS	Pseudo-*F*	R2	*p-value*
Entrance	Whirlpool Cliff	Time	1	0.07	0.07	12.52	0.36	**0.0001**
		Residuals	22	0.13	0.01		0.64	
		Total	23	0.20			1.00	
			Df	SS	MS	Pseudo-*F*	R2	*p*-value
Internal sites	Glannafeen	Time	1	0.06	0.06	1.19	0.05	0.3133
		Residuals	22	1.04	0.05		0.95	
		Total	23	1.10			1.00	
			Df	SS	MS	Pseudo-*F*	R2	*p-value*
	Labhra Cliff	Time	1	0.02	0.02	0.33	0.01	0.8459
		Residuals	22	1.16	0.05		0.99	
		Total	23	1.18			1.00	
			Df	SS	MS	Pseudo-*F*	R2	*p-value*
	Goleen	Time	1	0.02	0.02	0.45	0.02	0.7769
		Residuals	22	0.93	0.04		0.98	
		Total	23	0.95			1.00	

Table S4.5. (Continued)

Sponge assemblages

2.5-year comparison (June 2018 – March 2021)

Log (x+1) transformed data, Bray Curtis dissimilarity, 9999 permutations

Two-way PERMANOVA with all sites (sponge assemblages)

	Df	SS	MS	Pseudo-*F*	R2	*p-value*
Site	3	17.79	5.93	67.84	0.69	**0.0001**
Time	1	0.06	0.06	0.64	0.00	0.5698
Site:Time	3	0.10	0.03	0.39	0.00	0.9575
Residuals	88	7.69	0.09		0.30	
Total	95	25.64			1.00	

Two-way PERMANOVA with only internal sites (sponge assemblages)

	Df	SS	MS	Pseudo-*F*	R2	*p-value*
Site	2	2.90	1.45	12.90	0.28	**0.0001**
Time	1	0.06	0.06	0.52	0.01	0.7709
Site:Time	2	0.04	0.02	0.18	0.00	0.9989
Residuals	66	7.43	0.11		0.71	
Total	71	10.43			1.00	

One-way PERMANOVAs at each site (sponge assemblages)

			Df	SS	MS	Pseudo-*F*	R2	*p-value*
Entrance	Whirlpool Cliff	Time	1	0.06	0.06	4.80	0.18	**0.0065**
		Residuals	22	0.26	0.01		0.82	
		Total	23	0.32			1.00	

			Df	SS	MS	Pseudo-*F*	R2	*p*-value
Internal sites	Glannafeen	Time	1	0.06	0.06	0.72	0.03	0.5512
		Residuals	22	1.92	0.09		0.97	
		Total	23	1.98			1.00	

			Df	SS	MS	Pseudo-*F*	R2	*p-value*
	Labhra Cliff	Time	1	0.01	0.01	0.07	0.00	0.9628
		Residuals	22	3.71	0.17		1.00	
		Total	23	3.72			1.00	

			Df	SS	MS	Pseudo-*F*	R2	*p-value*
	Goleen	Time	1	0.02	0.02	0.31	0.01	0.8295
		Residuals	22	1.80	0.08		0.99	
		Total	23	1.82			1.00	

Table S4.5. (Continued)

Ascidian assemblages

2.5-year comparison (June 2018 – March 2021)
Log (x+1) transformed data, Bray Curtis dissimilarity, 9999 permutations

Two-way PERMANOVA with only internal sites (ascidian assemblages)

	Df	SS	MS	Pseudo-*F*	R2	*p-value*
Site	2	1.76	0.88	3.46	0.09	**0.0006**
Time	1	0.73	0.73	2.85	0.04	**0.0139**
Site:Time	2	0.22	0.11	0.43	0.01	0.9573
Residuals	66	16.79	0.25		0.86	
Total	71	19.49			1.00	

One-way PERMANOVAs at each site (ascidian assemblages)

			Df	SS	MS	Pseudo-*F*	R2	*p*-value
Internal sites	Glannafeen	Time	1	0.56	0.56	2.26	0.09	0.0605
		Residuals	22	5.43	0.25		0.91	
		Total	23	5.99			1.00	
			Df	SS	MS	Pseudo-*F*	R2	*p-value*
	Labhra Cliff	Time	1	0.24	0.24	1.40	0.06	0.2418
		Residuals	22	3.81	0.17		0.94	
		Total	23	4.05			1.00	
			Df	SS	MS	Pseudo-*F*	R2	*p-value*
	Goleen	Time	1	0.14	0.14	0.42	0.02	0.9048
		Residuals	22	7.55	0.34		0.98	
		Total	23	7.70			1.00	

Table S4.6. Results of the PERMANOVA models evaluating the effect of time and site on the benthic community, and sponge and ascidian assemblage structure. 3-year full comparison (June 2018 – June 2021). Significant *p*-values ($p < 0.05$) are in bold.

Benthic communities

3-year full comparison (June 2018 – June 2021)

Log (x+1) transformed data, Bray Curtis dissimilarity, 9999 permutations

Two-way PERMANOVA with all sites (benthic communities)

	Df	SS	MS	Pseudo-*F*	R2	*p-value*
Site	1	1.61	1.61	34.48	0.39	**0.0001**
Time	1	0.06	0.06	1.26	0.01	0.2673
Site:Time	1	0.00	0.00	0.04	0.00	0.9962
Residuals	52	2.43	0.05		0.59	
Total	55	4.11			1.00	

One-way PERMANOVAs at each site (benthic communities)

			Df	SS	MS	Pseudo-*F*	R2	*p-value*
Internal sites	Labhra Cliff	Time	1	0.03	0.03	0.53	0.02	0.6941
		Residuals	26	1.35	0.05		0.98	
		Total	27	1.38			1.00	
			Df	SS	MS	Pseudo-*F*	R2	*p-value*
	Goleen	Time	1	0.03	0.03	0.81	0.03	0.5096
		Residuals	26	1.08	0.04		0.97	
		Total	27	1.12			1.00	

Table S4.6. (Continued)

Sponge assemblages

3-year full comparison (June 2018 – June 2021)

Log (x+1) transformed data, Bray Curtis dissimilarity, 9999 permutations

Two-way PERMANOVA with all sites (sponge assemblages)

	Df	SS	MS	Pseudo-*F*	R2	*p-value*
Site	1	2.23	2.23	18.00	0.26	**0.0001**
Time	1	0.06	0.06	0.48	0.01	0.7303
Site:Time	1	0.01	0.01	0.06	0.00	0.9932
Residuals	52	6.44	0.12		0.74	
Total	55	8.74			1.00	

One-way PERMANOVAs at each site (sponge assemblages)

			Df	SS	MS	Pseudo-*F*	R2	*p-value*
Internal sites	Labhra Cliff	Time	1	0.04	0.04	0.21	0.01	0.8405
		Residuals	26	4.34	0.17		0.99	
		Total	27	4.38			1.00	
			Df	SS	MS	Pseudo-*F*	R2	*p-value*
	Goleen	Time	1	0.03	0.03	0.40	0.01	0.7516
		Residuals	26	2.10	0.08		0.99	
		Total	27	2.13			1.00	

Ascidian assemblages

3-year full comparison (June 2018 – June 2021)

Log (x+1) transformed data, Bray Curtis dissimilarity, 9999 permutations

Two-way PERMANOVA with all sites (ascidian assemblages)

	Df	SS	MS	Pseudo-*F*	R2	*p-value*
Site	1	1.26	1.26	4.66	0.08	**0.0009**
Time	1	0.51	0.51	1.86	0.03	0.083
Site:Time	1	0.14	0.14	0.52	0.01	0.8118
Residuals	52	14.12	0.27		0.88	
Total	55	16.03			1.00	

One-way PERMANOVAs at each site (ascidian assemblages)

			Df	SS	MS	Pseudo-*F*	R2	*p-value*
Internal sites	Labhra Cliff	Time	1	0.38	0.38	1.90	0.07	0.0991
		Residuals	26	5.15	0.20		0.93	
		Total	27	5.52			1.00	
			Df	SS	MS	Pseudo-*F*	R2	*p-value*
	Goleen	Time	1	0.27	0.27	0.79	0.03	0.5812
		Residuals	26	8.98	0.35		0.97	
		Total	27	9.25			1.00	

Table S4.7. Results of the PERMANOVA models evaluating the effect of time and site and historical period on the benthic community, and sponge and ascidian assemblage structure. Present-past comparison (April 1994 – August 1995 and June 2018 – November 2019). Significant *p*-values ($p < 0.05$) are in bold.

Benthic communities

Present-past comparison (April 1994 – August 1995 and June 2018 – November 2019)
Log (x+1) transformed data, Bray Curtis dissimilarity, 9999 permutations

Three-way PERMANOVA with all sites (benthic communities)

	Df	SS	MS	Pseudo-*F*	R2	*p-value*
Site	1	3.36	3.36	63.92	0.35	**0.0001**
Period	1	1.09	1.09	20.83	0.11	**0.0001**
Time	1	0.20	0.20	3.81	0.02	**0.005**
Site:Period	1	1.08	1.08	20.52	0.11	**0.0001**
Site:Time	1	0.00	0.00	0.04	0.00	0.9998
Period:Time	1	0.09	0.09	1.63	0.01	0.1233
Site:Period:Time	1	0.04	0.04	0.73	0.00	0.5988
Residuals	72	3.79	0.05		0.39	
Total	79	9.65			1.00	

Two-way PERMANOVAs at each historical period (benthic communities)

		Df	SS	MS	Pseudo-*F*	R2	*p-value*
1994-1995	Site	1	2.41	2.41	47.05	0.55	**0.0001**
	Time	1	0.11	0.11	2.08	0.02	0.0981
	Site:Time	1	0.04	0.04	0.76	0.01	0.4949
	Residuals	36	1.84	0.05		0.42	
	Total	39	4.39			1.00	

		Df	SS	MS	Pseudo-*F*	R2	*p-value*
2018-2019	Site	1	2.03	2.03	37.64	0.49	**0.0001**
	Time	1	0.18	0.18	3.32	0.04	**0.0231**
	Site:Time	1	0.00	0.00	0.03	0.00	0.9969
	Residuals	36	1.95	0.05		0.47	
	Total	39	4.16			1.00	

Sponge assemblages

Present-past comparison (April 1994 – August 1995 and June 2018 – November 2019)
Log (x+1) transformed data, Bray Curtis dissimilarity, 9999 permutations

Three-way PERMANOVA with all sites (sponge assemblages)

	Df	SS	MS	Pseudo-*F*	R2	*p-value*
Site	1	4.46	4.46	45.17	0.32	**0.0001**
Period	1	1.19	1.19	12.10	0.09	**0.0001**
Time	1	0.03	0.03	0.27	0.00	0.9643
Site:Period	1	1.06	1.06	10.72	0.08	**0.0001**
Site:Time	1	0.03	0.03	0.29	0.00	0.9541
Period:Time	1	0.05	0.05	0.49	0.00	0.8164
Site:Period:Time	1	0.03	0.03	0.33	0.00	0.9377
Residuals	72	7.10	0.10		0.51	
Total	79	13.95			1.00	

Table S4.7. (Continued)

Two-way PERMANOVAs at each historical period (sponge assemblages)

		Df	SS	MS	Pseudo-*F*	R2	*p-value*
1994-1995	Site	1	3.94	3.94	58.03	0.61	**0.0001**
	Time	1	0.01	0.01	0.21	0.00	0.9308
	Site:Time	1	0.02	0.02	0.27	0.00	0.8821
	Residuals	36	2.44	0.07		0.38	
	Total	39	6.41			1.00	

		Df	SS	MS	Pseudo-*F*	R2	*p-value*
2018-2019	Site	1	1.58	1.58	12.17	0.25	**0.0001**
	Time	1	0.06	0.06	0.47	0.01	0.795
	Site:Time	1	0.04	0.04	0.33	0.01	0.8954
	Residuals	36	4.66	0.13		0.74	
	Total	39	6.34			1.00	

Ascidian assemblages

Present-past comparison (April 1994 – August 1995 and June 2018 – November 2019)
Log (x+1) transformed data, Bray Curtis dissimilarity, 9999 permutations

Three-way PERMANOVA with all sites (ascidian assemblages)

	Df	SS	MS	Pseudo-*F*	R2	*p-value*
Site	1	1.81	1.81	10.17	0.09	**0.0001**
Period	1	2.17	2.17	12.20	0.11	**0.0001**
Time	1	2.25	2.25	12.61	0.11	**0.0001**
Site:Period	1	0.59	0.59	3.30	0.03	**0.0069**
Site:Time	1	0.20	0.20	1.10	0.01	0.3538
Period:Time	1	0.58	0.58	3.27	0.03	**0.006**
Site:Period:Time	1	0.21	0.21	1.17	0.01	0.3081
Residuals	72	12.82	0.18		0.62	
Total	79	20.63			1.00	

Two-way PERMANOVAs at each historical period (ascidian assemblages)

		Df	SS	MS	Pseudo-*F*	R2	*p-value*
1994-1995	Site	1	1.54	1.54	8.47	0.16	**0.0001**
	Time	1	1.40	1.40	7.73	0.15	**0.0001**
	Site:Time	1	0.08	0.08	0.42	0.01	0.8414
	Residuals	36	6.53	0.18		0.68	
	Total	39	9.55			1.00	

		Df	SS	MS	Pseudo-*F*	R2	*p-value*
2018-2019	Site	1	0.86	0.86	4.94	0.10	**0.0014**
	Time	1	1.43	1.43	8.16	0.16	**0.0002**
	Site:Time	1	0.33	0.33	1.88	0.04	0.1144
	Residuals	36	6.29	0.17		0.71	
	Total	39	8.91			1.00	

C.2. Rate of community and assemblage changes

Table S4.8. Results of the linear mixed effect model (lmer) testing rates and patterns of variability in benthic communities, and ascidian and sponge assemblages. Comparison across all sites (June 2018 – November 2019). *P*-adjusted: *p*-value adjusted with Benjamini-Hochberg Procedure. Significant *p*-values ($p < 0.05$) are in bold.

Benthic communities

Linear mixed-effects model (lmer)

Comparison across all sites (June 2018 – November 2019)

*Formula: Euclidean distance ~ TimeLag * Site + (1|Quadrat)*

Fixed effects test (Anova)

	Chi-sq	df	*p*-value
(Intercept)	6.69	1	**0.0097**
TimeLag	0.07	1	0.7933
Site	26.22	4	**< 0.0001**
TimeLag:Site	9.85	4	**0.0431**

Testing rate and nature of community change over time at each site (emtrends)

Site	trend	SE	df	*t*-ratio	*p*-value	*p*-adjusted	Sign.
Glannafeen	-0.53	2.02	120	-0.26	0.7937	0.8406	ns
Goleen	1.35	2.02	120	0.67	0.5064	0.8406	ns
Labhra Cliff	1.05	2.02	120	0.52	0.6052	0.8406	ns
West Cliff	0.41	2.02	120	0.20	0.8406	0.8406	ns
Whirlpool Cliff	7.48	2.02	120	3.70	**0.0003**	**0.0016**	**

Pairwise comparisons of temporal trends, sites pairs (emtrends)

contrast	estimate	SE	df	*t*-ratio	*p*-value	*p*-adjusted	Sign.
Glannafeen - Goleen	-1.88	2.86	120	-0.66	0.9651	1.0000	ns
Glannafeen - Labhra Cliff	-1.58	2.86	120	-0.55	0.9815	1.0000	ns
Glannafeen - West Cliff	-0.94	2.86	120	-0.33	0.9975	1.0000	ns
Glannafeen - Whirlpool Cliff	-8.01	2.86	120	-2.80	**0.0462**	0.4617	ns
Goleen - Labhra Cliff	0.30	2.86	120	0.10	1.0000	1.0000	ns
Goleen - West Cliff	0.94	2.86	120	0.33	0.9974	1.0000	ns
Goleen - Whirlpool Cliff	-6.13	2.86	120	-2.14	0.2088	0.5220	ns
Labhra Cliff - West Cliff	0.64	2.86	120	0.22	0.9994	1.0000	ns
Labhra Cliff - Whirlpool Cliff	-6.43	2.86	120	-2.25	0.1694	0.5220	ns
West Cliff - Whirlpool Cliff	-7.07	2.86	120	-2.47	0.1039	0.5197	ns

Pairwise comparisons, sites pairs (emmeans)

contrast	estimate	SE	df	*t*-ratio	*p*-value	*p*-adjusted	Sign.
Glannafeen - Goleen	-8.28	2.39	20	-3.46	**0.0025**	**0.0041**	**
Glannafeen - Labhra Cliff	-5.46	2.39	20	-2.28	**0.0336**	**0.0479**	*
Glannafeen - West Cliff	-23.47	2.39	20	-9.81	**< 0.0001**	**< 0.0001**	****
Glannafeen - Whirlpool Cliff	-10.70	2.39	20	-4.47	**0.0002**	**0.0005**	***
Goleen - Labhra Cliff	2.82	2.39	20	1.18	0.2526	0.2807	ns
Goleen - West Cliff	-15.19	2.39	20	-6.35	**< 0.0001**	**< 0.0001**	****
Goleen - Whirlpool Cliff	-2.42	2.39	20	-1.01	0.3244	0.3244	ns
Labhra Cliff - West Cliff	-18.01	2.39	20	-7.52	**< 0.0001**	**< 0.0001**	****
Labhra Cliff - Whirlpool Cliff	-5.24	2.39	20	-2.19	**0.0407**	0.0509	ns
West Cliff - Whirlpool Cliff	12.77	2.39	20	5.34	**< 0.0001**	**0.0001**	****

Table S4.8. (Continued)

Sponge assemblages

Linear mixed-effects model (lmer)

Comparison across all sites (June 2018 – November 2019)

*Formula: Euclidean distance ~ TimeLag * Site + (1|Quadrat)*

Fixed effects test (Anova)

	Chi-sq	df	*p*-value
(Intercept)	0.46	1	0.4999
TimeLag	0.00	1	0.9886
Site	32.06	4	**< 0.0001**
TimeLag:Site	16.03	4	**0.0030**

Testing rate and nature of community change over time at each site (emtrends)

Site	trend	SE	df	*t*-ratio	*p*-value	*p*-adjusted	Sign.
Glannafeen	0.01	0.86	120	0.01	0.9886	0.9886	ns
Goleen	0.14	0.86	120	0.17	0.8677	0.9886	ns
Labhra Cliff	1.16	0.86	120	1.34	0.1820	0.3033	ns
West Cliff	-2.37	0.86	120	-2.75	**0.0068**	**0.0229**	*
Whirlpool Cliff	2.28	0.86	120	2.65	**0.0091**	**0.0229**	*

Pairwise comparisons of temporal trends, sites pairs (emtrends)

contrast	estimate	SE	df	*t*-ratio	*p*-value	*p*-adjusted	Sign.
Glannafeen - Goleen	-0.13	1.22	120	-0.11	1.0000	1.0000	ns
Glannafeen - Labhra Cliff	-1.14	1.22	120	-0.94	0.8810	1.0000	ns
Glannafeen - West Cliff	2.38	1.22	120	1.96	0.2935	0.6740	ns
Glannafeen - Whirlpool Cliff	-2.27	1.22	120	-1.86	0.3427	0.6740	ns
Goleen - Labhra Cliff	-1.01	1.22	120	-0.83	0.9204	1.0000	ns
Goleen - West Cliff	2.52	1.22	120	2.06	0.2422	0.6740	ns
Goleen - Whirlpool Cliff	-2.14	1.22	120	-1.76	0.4044	0.6740	ns
Labhra Cliff - West Cliff	3.53	1.22	120	2.90	**0.0357**	0.1783	ns
Labhra Cliff - Whirlpool Cliff	-1.13	1.22	120	-0.92	0.8870	1.0000	ns
West Cliff - Whirlpool Cliff	-4.65	1.22	120	-3.82	**0.0020**	**0.0195**	*

Pairwise comparisons, sites pairs (emmeans)

contrast	estimate	SE	df	*t*-ratio	*p*-value	*p*-adjusted	Sign.
Glannafeen - Goleen	-0.08	1.61	20	-0.05	0.9616	0.9616	ns
Glannafeen - Labhra Cliff	-1.53	1.61	20	-0.95	0.3543	0.4739	ns
Glannafeen - West Cliff	-7.83	1.61	20	-4.86	**0.0001**	**0.0005**	***
Glannafeen - Whirlpool Cliff	-6.71	1.61	20	-4.17	**0.0005**	**0.0013**	**
Goleen - Labhra Cliff	-1.45	1.61	20	-0.90	0.3791	0.4739	ns
Goleen - West Cliff	-7.75	1.61	20	-4.81	**0.0001**	**0.0005**	***
Goleen - Whirlpool Cliff	-6.63	1.61	20	-4.12	**0.0005**	**0.0013**	**
Labhra Cliff - West Cliff	-6.30	1.61	20	-3.91	**0.0009**	**0.0017**	**
Labhra Cliff - Whirlpool Cliff	-5.18	1.61	20	-3.22	**0.0043**	**0.0072**	**
West Cliff - Whirlpool Cliff	1.12	1.61	20	0.70	0.4945	0.5494	ns

Table S4.8. (Continued)

Ascidian assemblages

Linear mixed-effects model (lmer)

Comparison across all sites (June 2018 – November 2019)

*Formula: Euclidean distance ~ TimeLag * Site + (1|Quadrat)*

Fixed effects test (Anova)

	Chi-sq	df	*p*-value
(Intercept)	0.46	1	0.4989
TimeLag	1.30	1	0.2535
Site	32.92	3	**< 0.0001**
TimeLag:Site	5.80	3	0.1219

Testing rate and nature of community change over time at each site (emtrends)

Site	trend	SE	df	*t*-ratio	*p*-value	*p*-adjusted	Sign.
Glannafeen	1.54	1.35	96	1.14	0.2564	0.5128	ns
Goleen	0.88	1.35	96	0.65	0.5171	0.5576	ns
Labhra Cliff	0.80	1.35	96	0.59	0.5576	0.5576	ns
West Cliff	-2.63	1.35	96	-1.94	0.0550	0.2202	ns

Pairwise comparisons, sites pairs (emmeans)

contrast	estimate	SE	df	*t*-ratio	*p*-value	*p*-adjusted	Sign.
Glannafeen - Goleen	2.16	1.84	16	1.18	0.2560	0.3072	ns
Glannafeen - Labhra Cliff	-1.06	1.84	16	-0.57	0.5737	0.5737	ns
Glannafeen - West Cliff	-10.47	1.84	16	-5.70	**< 0.0001**	**0.0001**	****
Goleen - Labhra Cliff	-3.22	1.84	16	-1.75	0.0988	0.1483	ns
Goleen - West Cliff	-12.64	1.84	16	-6.88	**< 0.0001**	**< 0.0001**	****
Labhra Cliff - West Cliff	-9.42	1.84	16	-5.13	**0.0001**	**0.0002**	***

Table S4.9. Results of the linear mixed effect model (lmer) testing rates and patterns of variability in benthic communities, and ascidian and sponge assemblages. 2.5-year comparison (June 2018 – March 2021). *P*-adjusted: *p*-value adjusted with Benjamini-Hochberg Procedure. Significant *p*-values ($p < 0.05$) are in bold.

Linear mixed-effects model (lmer)
2.5-year comparison (June 2018 – March 2021)
*Formula: Euclidean distance ~ TimeLag * Site + (1|Quadrat)*

Benthic communities

Fixed effects test (Anova)

	Chi-sq	df	*p*-value
(Intercept)	10.10	1	**0.0015**
TimeLag	0.38	1	0.5380
Site	23.85	3	**< 0.0001**
TimeLag:Site	41.56	3	**< 0.0001**

Testing rate and nature of community change over time at each site (emtrends)

Site	trend	SE	df	*t*-ratio	*p*-value	*p*-adjusted	Sign.
Glannafeen	0.42	0.69	220	0.62	0.5387	0.7182	ns
Goleen	-1.81	0.69	220	-2.62	**0.0094**	**0.0188**	*
Labhra Cliff	-0.24	0.69	220	-0.36	0.7229	0.7229	ns
Whirlpool Cliff	4.24	0.69	220	6.15	**< 0.0001**	**< 0.0001**	****

Pairwise comparisons of temporal trends, sites pairs (emtrends)

contrast	estimate	SE	df	*t*-ratio	*p*-value	*p*-adjusted	Sign.
Glannafeen - Goleen	2.23	0.98	220	2.29	0.1040	0.1560	ns
Glannafeen - Labhra Cliff	0.67	0.98	220	0.69	0.9022	0.9022	ns
Glannafeen - Whirlpool Cliff	-3.81	0.98	220	-3.91	**0.0007**	**0.0014**	**
Goleen - Labhra Cliff	-1.56	0.98	220	-1.60	0.3800	0.4560	ns
Goleen - Whirlpool Cliff	-6.04	0.98	220	-6.20	**< 0.0001**	**< 0.0001**	****
Labhra Cliff - Whirlpool Cliff	-4.48	0.98	220	-4.60	**< 0.0001**	**0.0001**	***

Sponge assemblages

Fixed effects test (Anova)

	Chi-sq	df	*p*-value
(Intercept)	1.44	1	0.2297
TimeLag	0.56	1	0.4544
Site	36.90	3	**< 0.0001**
TimeLag:Site	6.42	3	0.0930

Testing rate and nature of community change over time at each site (emtrends)

Site	trend	SE	df	*t*-ratio	*p*-value	*p*-adjusted	Sign.
Glannafeen	0.16	0.22	220	0.75	0.4552	0.8830	ns
Goleen	0.03	0.22	220	0.15	0.8819	0.8830	ns
Labhra Cliff	0.03	0.22	220	0.15	0.8830	0.8830	ns
Whirlpool Cliff	0.71	0.22	220	3.22	**0.0015**	**0.0059**	**

Table S4.9. (Continued)

Ascidian assemblages

Fixed effects test (Anova)

	Chi-sq	df	*p*-value
(Intercept)	5.60	1	**0.0180**
TimeLag	2.09	1	0.1482
Site	5.45	2	0.0654
TimeLag:Site	1.17	2	0.5567

Testing rate and nature of community change over time at each site (emtrends)

Site	trend	SE	df	*t*-ratio	*p*-value	*p*-adjusted	Sign.
Glannafeen	0.36	0.25	165	1.45	0.1501	0.4502	ns
Goleen	0.19	0.25	165	0.75	0.4561	0.6842	ns
Labhra Cliff	-0.02	0.25	165	-0.08	0.9342	0.9342	ns

Table S4.10. Results of the linear mixed effect model (lmer) testing rates and patterns of variability in benthic communities, and ascidian and sponge assemblages. 3-year full comparison (June 2018 – June 2021). *P*-adjusted: *p*-value adjusted with Benjamini-Hochberg Procedure. Significant *p*-values ($p < 0.05$) are in bold.

Linear mixed-effects model (lmer)
3-year full comparison (June 2018 – June 2021)
*Formula: Euclidean distance ~ TimeLag * Site + (1|Quadrat)*

Benthic communities

Fixed effects test (Anova)

	Chi-sq	df	*p*-value
(Intercept)	87.64	1	**< 0.0001**
TimeLag	0.24	1	0.6220
Site	4.71	1	**0.0299**
TimeLag:Site	0.22	1	0.6415

Testing rate and nature of community change over time at each site (emtrends)

Site	trend	SE	df	*t*-ratio	*p*-value	*p*-adjusted	Sign.
Goleen	-0.25	0.51	158	-0.49	0.6227	0.8689	ns
Labhra Cliff	0.08	0.51	158	0.17	0.8689	0.8689	ns

Sponge assemblages

Fixed effects test (Anova)

	Chi-sq	df	*p*-value
(Intercept)	26.52	1	**< 0.0001**
TimeLag	1.16	1	0.2814
Site	0.34	1	0.5601
TimeLag:Site	0.49	1	0.4821

Testing rate and nature of community change over time at each site (emtrends)

Site	trend	SE	df	*t*-ratio	*p*-value	*p*-adjusted	Sign.
Goleen	0.06	0.05	158	1.08	0.2831	0.5661	ns
Labhra Cliff	0.00	0.05	158	0.08	0.9340	0.9340	ns

Ascidian assemblages

Fixed effects test (Anova)

	Chi-sq	df	*p*-value
(Intercept)	0.76	1	0.3827
TimeLag	0.44	1	0.5067
Site	5.34	1	**0.0208**
TimeLag:Site	1.15	1	0.2843

Testing rate and nature of community change over time at each site (emtrends)

Site	trend	SE	df	*t*-ratio	*p*-value	*p*-adjusted	Sign.
Goleen	0.12	0.18	158	0.66	0.5076	0.5076	ns
Labhra Cliff	-0.15	0.18	158	-0.85	0.3965	0.5076	ns

Table S4.11. Results of the linear mixed effect model (lmer) testing rates and patterns of variability in benthic communities, and ascidian and sponge assemblages. Present*-*past comparison (April 1994 – August 1995 and June 2018 – November 2019). *P*-adjusted: *p*-value adjusted with Benjamini-Hochberg Procedure. Significant *p*-values ($p < 0.05$) are in bold.

Linear mixed-effects model (lmer)
Present-past comparison (April 1994 – August 1995 and June 2018 – November 2019)
*Formula: Euclidean distance ~ TimeLag * Period * Site + (1|Quadrat)*

Benthic communities

Fixed effects test (Anova)

	Chi-sq	df	*p*-value
(Intercept)	25.94	1	**< 0.0001**
TimeLag	0.31	1	0.5777
Period	0.94	1	0.3324
Site	2.63	1	0.1047
TimeLag:Period	0.01	1	0.9357
TimeLag:Site	3.94	1	**0.0471**
Period:Site	2.85	1	0.0916
TimeLag:Period:Site	0.55	1	0.4566

Testing rate and nature of community change over time at each site (emtrends)

Site	Period	trend	SE	df	*t*-ratio	*p*-value	*p*-adjusted	Sign.
Glannafeen	1994-1995	-0.67	1.20	96	-0.56	0.5790	0.6590	ns
Labhra Cliff	1994-1995	2.69	1.20	96	2.25	**0.0267**	0.1068	ns
Glannafeen	2018-2021	-0.53	1.20	96	-0.44	0.6590	0.6590	ns
Labhra Cliff	2018-2021	1.05	1.20	96	0.88	0.3834	0.6590	ns

Sponge assemblages

Fixed effects test (Anova)

	Chi-sq	df	*p*-value
(Intercept)	0.64	1	0.4222
TimeLag	0.09	1	0.7583
Period	0.02	1	0.8853
Site	0.82	1	0.3666
TimeLag:Period	0.04	1	0.8422
TimeLag:Site	0.53	1	0.4684
Period:Site	0.63	1	0.4276
TimeLag:Period:Site	0.49	1	0.4833

Testing rate and nature of community change over time at each site (emtrends)

Site	Period	trend	SE	df	*t*-ratio	*p*-value	*p*-adjusted	Sign.
Glannafeen	1994-1995	0.14	0.47	96	0.31	0.7590	0.9792	ns
Labhra Cliff	1994-1995	0.63	0.47	96	1.33	0.1857	0.3714	ns
Glannafeen	2018-2021	0.01	0.47	96	0.03	0.9792	0.9792	ns
Labhra Cliff	2018-2021	1.16	0.47	96	2.45	**0.0159**	0.0638	ns

Table S4.20. (Continued)

Ascidian assemblages

Fixed effects test (Anova)

	Chi-sq	df	*p*-value
(Intercept)	0.85	1	0.3567
TimeLag	0.01	1	0.9271
Period	0.07	1	0.7911
Site	1.54	1	0.2142
TimeLag:Period	4.77	1	**0.0290**
TimeLag:Site	0.02	1	0.8755
Period:Site	0.00	1	0.9760
TimeLag:Period:Site	0.70	1	0.4026

Testing rate and nature of community change over time at each site (emtrends)

Site	Period	trend	SE	df	*t*-ratio	*p*-value	*p*-adjusted	Sign.
Glannafeen	1994-1995	-0.05	0.52	96	-0.09	0.9273	0.9273	ns
Labhra Cliff	1994-1995	0.07	0.52	96	0.13	0.8968	0.9273	ns
Glannafeen	2018-2021	1.54	0.52	96	3.00	**0.0035**	**0.0139**	*
Labhra Cliff	2018-2021	0.80	0.52	96	1.54	0.1258	0.2516	ns

C.3. Turnover

Table S4.12. Pairwise Wilcoxon signed-rank tests testing differences in compositional turnover between pairs of biological communities at each period and site. B. community: benthic community; Spo. assem: sponge assemblage; Asc. assem.: ascidian assemblage.

Wilcoxon signed-rank test between pairs of biological communities
Turnover

Comparison across all sites (June 2018 – November 2019)

Site	group1	group2	n1	n2	*W*-statistic	*p*-value	*p*-adjusted	Sign.
Glannafeen	Asc. assem.	B. community	15	15	205	**0.0001**	**0.0003**	***
Glannafeen	Asc. assem.	Spo. assem.	15	15	224	**< 0.0001**	**< 0.0001**	****
Glannafeen	B. community	Spo. assem.	15	15	200	**0.0003**	**0.0006**	***
Goleen	Asc. assem.	B. community	15	15	209	**0.0001**	**0.0002**	***
Goleen	Asc. assem.	Spo. assem.	15	15	224	**< 0.0001**	**< 0.0001**	****
Goleen	B. community	Spo. assem.	15	15	210	**0.0001**	**0.0002**	***
Labhra Cliff	Asc. assem.	B. community	15	15	168	**0.0220**	**0.0238**	*
Labhra Cliff	Asc. assem.	Spo. assem.	15	15	192	**0.0010**	**0.0016**	**
Labhra Cliff	B. community	Spo. assem.	15	15	186	**0.0030**	**0.0039**	**
West Cliff	Asc. assem.	B. community	15	15	184	**0.0030**	**0.0039**	**
West Cliff	Asc. assem.	Spo. assem.	15	15	205	**0.0001**	**0.0003**	***
West Cliff	B. community	Spo. assem.	15	15	178	**0.0070**	**0.0083**	**
Whirlpool Cliff	B. community	Spo. assem.	15	15	116	0.9000	0.9000	ns

2.5-year comparison (June 2018 – March 2021)

Site	group1	group2	n1	n2	*W*-statistic	*p*-value	*p*-adjusted	Sign.
Glannafeen	Asc. assem.	B. community	20	20	373	**< 0.0001**	**< 0.0001**	****
Glannafeen	Asc. assem.	Spo. assem.	20	20	398	**< 0.0001**	**< 0.0001**	****
Glannafeen	B. community	Spo. assem.	20	20	359	**< 0.0001**	**< 0.0001**	****
Goleen	Asc. assem.	B. community	20	20	346	**0.0001**	**0.0001**	***
Goleen	Asc. assem.	Spo. assem.	20	20	365	**< 0.0001**	**< 0.0001**	****
Goleen	B. community	Spo. assem.	20	20	356	**< 0.0001**	**0.0001**	****
Labhra Cliff	Asc. assem.	B. community	20	20	272	0.0530	0.0589	ns
Labhra Cliff	Asc. assem.	Spo. assem.	20	20	324	**0.0008**	**0.0012**	**
Labhra Cliff	B. community	Spo. assem.	20	20	307	**0.0040**	**0.0050**	**
Whirlpool Cliff	B. community	Spo. assem.	20	20	184	0.6610	0.6610	ns

3-year full comparison (June 2018 – June 2021)

Site	group1	group2	n1	n2	*W*-statistic	*p*-value	*p*-adjusted	Sign.
Goleen	Asc. assem.	B. community	24	24	510	**< 0.0001**	**< 0.0001**	****
Goleen	Asc. assem.	Spo. assem.	24	24	532	**< 0.0001**	**< 0.0001**	****
Goleen	B. community	Spo. assem.	24	24	510	**< 0.0001**	**< 0.0001**	****
Labhra Cliff	Asc. assem.	B. community	24	24	424	**0.0050**	**0.0050**	**
Labhra Cliff	Asc. assem.	Spo. assem.	24	24	492	**< 0.0001**	**< 0.0001**	****
Labhra Cliff	B. community	Spo. assem.	24	24	456	**0.0006**	**0.0007**	***

Table S4.12. (Continued)

Present-past comparison (April 1994 – August 1995 and June 2018 – November 2019)

Period	Site	group1	group2	n1	n2	*W*-statistic	*p*-value	*p*-adjusted	Sign.
199x	Glannafeen	Asc. assem.	B. communities	15	15	208	**0.0001**	**0.0002**	***
199x	Glannafeen	Asc. assem.	Spo. assem.	15	15	211	**< 0.0001**	**0.0001**	***
199x	Glannafeen	B. communities	Spo. assem.	15	15	190	**0.0010**	**0.0012**	**
199x	Labhra Cliff	Asc. assem.	B. communities	15	15	225	**< 0.0001**	**< 0.0001**	****
199x	Labhra Cliff	Asc. assem.	Spo. assem.	15	15	225	**< 0.0001**	**< 0.0001**	****
199x	Labhra Cliff	B. communities	Spo. assem.	15	15	224	**< 0.0001**	**< 0.0001**	****
20xx	Glannafeen	Asc. assem.	B. communities	15	15	205	**0.0001**	**0.0002**	***
20xx	Glannafeen	Asc. assem.	Spo. assem.	15	15	224	**< 0.0001**	**< 0.0001**	****
20xx	Glannafeen	B. communities	Spo. assem.	15	15	200	**0.0003**	**0.0005**	***
20xx	Labhra Cliff	Asc. assem.	B. communities	15	15	168	**0.0220**	**0.0220**	*
20xx	Labhra Cliff	Asc. assem.	Spo. assem.	15	15	192	**0.0010**	**0.0012**	**
20xx	Labhra Cliff	B. communities	Spo. assem.	15	15	186	**0.0030**	**0.0033**	**

Table S4.13. Kruskal–Wallis and Dunn's post hoc tests evaluating the differences in turnover between sites, independently for benthic communities, and sponge and ascidian assemblages. Comparison across all sites (June 2018 – November 2019). Significant *p*-values ($p < 0.05$) are in bold.

Comparison across all sites (June 2018 – November 2019)

Kruskal–Wallis test

Differences in turnover between all sites

	factor	H-statistic	*p*-value	df
Benthic communities	Site	14.46	**0.0060**	4
Sponge assemblages	Site	4.45	0.3484	4
Ascidian assemblages	Site	4.43	0.2185	3

Kruskal–Wallis test

Differences in turnover between internal sites

	factor	H-statistic	*p*-value	df
Benthic communities	Site	3.98	0.1368	2
Sponge assemblages	Site	0.09	0.9551	2
Ascidian assemblages	Site	3.09	0.2129	2

Dunn's Test between pairs of sites

Benthic communities

group1	group2	n1	n2	*Z*-statistic	*p*-value	*p*-adjusted	Sign.
Glannafeen	Goleen	15	15	1.60	0.1104	0.2209	ns
Glannafeen	Labhra Cliff	15	15	1.37	0.1707	0.2845	ns
Glannafeen	West Cliff	15	15	3.62	**0.0003**	**0.0029**	**
Glannafeen	Whirlpool Cliff	15	15	2.46	**0.0139**	0.0696	ns
Goleen	Labhra Cliff	15	15	-0.23	0.8210	0.8210	ns
Goleen	West Cliff	15	15	2.03	**0.0426**	0.1064	ns
Goleen	Whirlpool Cliff	15	15	0.86	0.3881	0.4312	ns
Labhra Cliff	West Cliff	15	15	2.25	**0.0242**	0.0806	ns
Labhra Cliff	Whirlpool Cliff	15	15	1.09	0.2760	0.3450	ns
West Cliff	Whirlpool Cliff	15	15	-1.16	0.2441	0.3450	ns

Table S4.14. Kruskal–Wallis and Dunn's post hoc tests evaluating the differences in turnover between sites, independently for benthic communities, and sponge and ascidian assemblages. 2.5-year comparison (June 2018 – March 2021). Significant *p*-values ($p < 0.05$) are in bold.

2.5-year comparison (June 2018 – March 2021)

Kruskal–Wallis test

Differences in turnover between all sites

	factor	H-statistic	*p*-value	df
Benthic communities	Site	1.24	0.7443	3
Sponge assemblages	Site	4.85	0.1835	3

Kruskal–Wallis test

Differences in turnover between internal sites

	factor	H-statistic	*p*-value	df
Benthic communities	Site	0.24	0.8876	2
Sponge assemblages	Site	2.76	0.2513	2
Ascidian assemblages	Site	10.44	**0.0054**	2

Dunn's Test between pairs of sites

Ascidian assemblages

group1	group2	n1	n2	*Z*-statistic	*p*-value	*p*-adjusted	Sign.
Glannafeen	Goleen	20	20	-1.30	0.1939	0.1939	ns
Glannafeen	Labhra Cliff	20	20	-3.21	**0.0013**	**0.0040**	**
Goleen	Labhra Cliff	20	20	-1.91	0.0558	0.0837	ns

Table S4.15. Dunn's post hoc tests evaluating the differences in turnover between Goleen and Labhra Cliff, independently for benthic communities, and sponge and ascidian assemblages. 3-year full comparison (June 2018 – June 2021). Significant *p*-values ($p < 0.05$) are in bold.

Dunn's Test

Differences in turnover

3-year full comparison (June 2018 – June 2021)

	group1	group2	n1	n2	*Z*-statistic	*p*-value
Benthic communities	Goleen	Labhra Cliff	24	24	-0.77	0.4392
Sponge assemblages	Goleen	Labhra Cliff	24	24	0.85	0.3939
Ascidian assemblages	Goleen	Labhra Cliff	24	24	-2.11	0.0347

Table S4.16. Non-parametric ANOVA and Pairwise Wilcoxon post hoc tests evaluating the differences in turnover between sites, independently for benthic communities, and sponge and ascidian assemblages. Present-past comparison (April 1994 – August 1995 and June 2018 – November 2019). Significant *p*-values ($p < 0.05$) are in bold.

Non-parametric ANOVA

Differences in turnover

Present-past comparison (April 1994 – August 1995 and June 2018 – November 2019)

Benthic communities

	df	*F*-statistic	*p*-value
Period	1	0.34	0.5595
Site	1	10.36	**0.0021**
Period:Site	1	2.02	0.1612

Sponge assemblages

	df	*F*-statistic	*p*-value
Period	1	0.00	1.0000
Site	1	0.00	1.0000
Period:Site	1	0.00	1.0000

Ascidian assemblage

	df	*F*-statistic	*p*-value
Period	1	9.71	**0.0029**
Site	1	0.01	0.9357
Period:Site	1	3.27	0.0760

Pairwise Wilcoxon signed-rank test between pairs of sites

Benthic communities

Period	group1	group2	n1	n2	*W*-statistic	*p*-value	*p*-adjusted	Sign.
199x	Glannafeen	Labhra Cliff	15	15	40	**0.0028**	**0.0056**	**
20xx	Glannafeen	Labhra Cliff	15	15	78.5	0.1650	0.1650	ns

Pairwise Wilcoxon signed-rank test between pairs of Periods

Ascidian assemblage

Site	group1	group2	n1	n2	*W*-statistic	*p*-value	*p*-adjusted	Sign.
Glannafeen	199x	20xx	15	15	134	0.3780	0.3780	ns
Labhra Cliff	199x	20xx	15	15	187.5	**0.0019**	**0.0038**	**

C.4. Diversity indices

Table S4.17. Results of the linear mixed effect model (lmer) testing the effects of time and site on three diversity indices separately (taxa richness, Shannon diversity index, and Simpson diversity index). Comparison across all sites (June 2018 – November 2019). *P*-adjusted: *p*-value adjusted with Benjamini-Hochberg Procedure. Significant *p*-values ($p < 0.05$) are in bold.

Linear mixed-effects model (lmer)
Benthic communities
Comparison across all sites (June 2018 – November 2019)
*Formula: Diversity index ~ Time * Site + (1|Quadrat)*

Taxa richness

Fixed effects test (Anova)

	Chi-sq	df	*p*-value
(Intercept)	570.03	1	**< 0.0001**
Site	253.87	4	**< 0.0001**
Time	2.15	1	0.1428
Site:Time	12.55	4	**0.0137**

Tests of temporal trends in taxa richness at each individual site (emtrends)

Site	trend	SE	df	*t*-ratio	*p*-value	*p*-adjusted	Sign.
Glannafeen	0.0571	0.04	70	1.47	0.1473	0.1473	ns
Goleen	0.1541	0.06	70	2.38	**0.0202**	**0.0253**	*
Labhra Cliff	0.2301	0.03	70	7.55	**< 0.0001**	**< 0.0001**	****
West Cliff	0.1786	0.02	70	10.51	**< 0.0001**	**< 0.0001**	****
Whirlpool Cliff	0.1718	0.01	70	12.46	**< 0.0001**	**< 0.0001**	****

Pairwise comparisons of temporal trends in taxa richness, between pairs of sites (emmeans)

contrast	estimate	SE	df	*t*-ratio	*p*-value	*p*-adjusted	Sign.
Glannafeen - Goleen	-0.0970	0.08	70	-1.28	0.7030	0.9989	ns
Glannafeen - Labhra Cliff	-0.1730	0.05	70	-3.50	**0.0071**	0.0715	ns
Glannafeen - West Cliff	-0.1215	0.04	70	-2.86	**0.0431**	0.1780	ns
Glannafeen - Whirlpool Cliff	-0.1147	0.04	70	-2.77	0.0534	0.1780	ns
Goleen - Labhra Cliff	-0.0760	0.07	70	-1.06	0.8262	0.9989	ns
Goleen - West Cliff	-0.0245	0.07	70	-0.37	0.9961	0.9989	ns
Goleen - Whirlpool Cliff	-0.0177	0.07	70	-0.27	0.9989	0.9989	ns
Labhra Cliff - West Cliff	0.0514	0.03	70	1.47	0.5827	0.9989	ns
Labhra Cliff - Whirlpool Cliff	0.0583	0.03	70	1.74	0.4150	0.9989	ns
West Cliff - Whirlpool Cliff	0.0069	0.02	70	0.31	0.9978	0.9989	ns

Pairwise comparisons of taxa richness, between pairs of sites (emmeans)

contrast	estimate	SE	df	*t*-ratio	*p*-value	*p*-adjusted	Sign.
Glannafeen - Goleen	4.7109	1.77	20	2.66	**0.0151**	**0.0189**	*
Glannafeen - Labhra Cliff	3.7805	1.76	20	2.15	**0.0442**	**0.0491**	*
Glannafeen - West Cliff	14.1296	1.75	20	8.08	**< 0.0001**	**< 0.0001**	****
Glannafeen - Whirlpool Cliff	23.7819	1.71	20	13.87	**< 0.0001**	**< 0.0001**	****
Goleen - Labhra Cliff	-0.9303	1.79	20	-0.52	0.6082	0.6082	ns
Goleen - West Cliff	9.4188	1.77	20	5.31	**< 0.0001**	**< 0.0001**	****
Goleen - Whirlpool Cliff	19.0710	1.74	20	10.96	**< 0.0001**	**< 0.0001**	****
Labhra Cliff - West Cliff	10.3491	1.76	20	5.88	**< 0.0001**	**< 0.0001**	****
Labhra Cliff - Whirlpool Cliff	20.0013	1.73	20	11.58	**< 0.0001**	**< 0.0001**	****
West Cliff - Whirlpool Cliff	9.6522	1.72	20	5.63	**< 0.0001**	**< 0.0001**	****

Table S4.17. (Continued)

Shannon diversity index (H)

Fixed effects test (Anova)

	Chi-sq	df	*p*-value
(Intercept)	1051.95	1	**< 0.0001**
Site	28.83	4	**< 0.0001**
Time	0.13	1	0.7227
Site:Time	137.88	4	**< 0.0001**

Tests of temporal trends in Shannon diversity index at each individual site (emtrends)

Site	trend	SE	df	*t*-ratio	*p*-value	*p*-adjusted	Sign.
Glannafeen	-0.0008	0.00	70	-0.35	0.7237	0.7237	ns
Goleen	0.0021	0.00	70	0.51	0.6090	0.7237	ns
Labhra Cliff	0.0155	0.00	70	5.57	**< 0.0001**	**< 0.0001**	****
West Cliff	0.0331	0.00	70	7.14	**< 0.0001**	**< 0.0001**	****
Whirlpool Cliff	-0.0164	0.00	70	-7.45	**< 0.0001**	**< 0.0001**	****

Pairwise comparisons of temporal trends in Shannon diversity index, between pairs of sites (emmeans)

contrast	estimate	SE	df	*t*-ratio	*p*-value	*p*-adjusted	Sign.
Glannafeen - Goleen	-0.0029	0.00	70	-0.62	0.9710	0.9710	ns
Glannafeen - Labhra Cliff	-0.0163	0.00	70	-4.50	**0.0003**	**0.0004**	***
Glannafeen - West Cliff	-0.0339	0.01	70	-6.54	**< 0.0001**	**< 0.0001**	****
Glannafeen - Whirlpool Cliff	0.0156	0.00	70	4.85	**0.0001**	**0.0001**	***
Goleen - Labhra Cliff	-0.0134	0.00	70	-2.74	0.0585	0.0650	ns
Goleen - West Cliff	-0.0310	0.01	70	-5.04	**< 0.0001**	**0.0001**	****
Goleen - Whirlpool Cliff	0.0185	0.00	70	4.01	**0.0014**	**0.0019**	**
Labhra Cliff - West Cliff	-0.0176	0.01	70	-3.25	**0.0149**	**0.0186**	*
Labhra Cliff - Whirlpool Cliff	0.0319	0.00	70	8.99	**< 0.0001**	**< 0.0001**	****
West Cliff - Whirlpool Cliff	0.0495	0.01	70	9.65	**< 0.0001**	**< 0.0001**	****

Pairwise comparisons of Shannon diversity index, between pairs of sites (emmeans)

contrast	estimate	SE	df	*t*-ratio	*p*-value	*p*-adjusted	Sign.
Glannafeen - Goleen	-0.2050	0.07	20	-3.00	**0.0070**	**0.0140**	*
Glannafeen - Labhra Cliff	-0.0738	0.07	20	-1.06	0.3018	0.3772	ns
Glannafeen - West Cliff	-0.1456	0.07	20	-1.99	0.0601	0.1002	ns
Glannafeen - Whirlpool Cliff	0.3381	0.07	20	5.11	**0.0001**	**0.0001**	***
Goleen - Labhra Cliff	0.1312	0.07	20	1.86	0.0781	0.1115	ns
Goleen - West Cliff	0.0594	0.07	20	0.80	0.4317	0.4317	ns
Goleen - Whirlpool Cliff	0.5430	0.07	20	8.07	**< 0.0001**	**< 0.0001**	****
Labhra Cliff - West Cliff	-0.0718	0.08	20	-0.95	0.3517	0.3908	ns
Labhra Cliff - Whirlpool Cliff	0.4119	0.07	20	6.00	**< 0.0001**	**< 0.0001**	****
West Cliff - Whirlpool Cliff	0.4836	0.07	20	6.70	**< 0.0001**	**< 0.0001**	****

Table S4.17. (Continued)

Simpson's diversity index

Fixed effects test (Anova)

	Chi-sq	df	*p*-value
(Intercept)	1345.93	1	**< 0.0001**
Site	14.30	4	**0.0064**
Time	14.54	1	**0.0001**
Site:Time	152.13	4	**< 0.0001**

Tests of temporal trends in Simpson's diversity index at each individual site (emtrends)

Site	trend	SE	df	*t*-ratio	*p*-value	*p*-adjusted	Sign.
Glannafeen	-0.0037	0.00	70	-3.81	**0.0003**	**0.0005**	***
Goleen	0.0012	0.00	70	0.98	0.3284	0.3284	ns
Labhra Cliff	0.0033	0.00	70	3.39	**0.0012**	**0.0015**	**
West Cliff	0.0096	0.00	70	6.59	**< 0.0001**	**< 0.0001**	****
Whirlpool Cliff	-0.0057	0.00	70	-10.97	**< 0.0001**	**< 0.0001**	****

Pairwise comparisons of temporal trends in Simpson's diversity index, between pairs of sites (emmeans)

contrast	estimate	SE	df	*t*-ratio	*p*-value	*p*-adjusted	Sign.
Glannafeen - Goleen	-0.0049	0.00	70	-3.11	**0.0219**	**0.0273**	*
Glannafeen - Labhra Cliff	-0.0070	0.00	70	-5.09	**< 0.0001**	**0.0001**	****
Glannafeen - West Cliff	-0.0133	0.00	70	-7.60	**< 0.0001**	**< 0.0001**	****
Glannafeen - Whirlpool Cliff	0.0020	0.00	70	1.85	0.3512	0.3902	ns
Goleen - Labhra Cliff	-0.0021	0.00	70	-1.34	0.6693	0.6693	ns
Goleen - West Cliff	-0.0084	0.00	70	-4.39	**0.0004**	**0.0006**	***
Goleen - Whirlpool Cliff	0.0069	0.00	70	5.14	**< 0.0001**	**0.0001**	****
Labhra Cliff - West Cliff	-0.0063	0.00	70	-3.57	**0.0057**	**0.0081**	**
Labhra Cliff - Whirlpool Cliff	0.0090	0.00	70	8.10	**< 0.0001**	**< 0.0001**	****
West Cliff - Whirlpool Cliff	0.0153	0.00	70	9.88	**< 0.0001**	**< 0.0001**	****

Pairwise comparisons of Simpson's diversity index, between pairs of sites (emmeans)

contrast	estimate	SE	df	*t*-ratio	*p*-value	*p*-adjusted	Sign.
Glannafeen - Goleen	-0.1198	0.02	20	-5.05	**0.0001**	**0.0006**	***
Glannafeen - Labhra Cliff	-0.0560	0.03	20	-2.22	**0.0378**	0.0631	ns
Glannafeen - West Cliff	-0.1094	0.03	20	-4.12	**0.0005**	**0.0027**	**
Glannafeen - Whirlpool Cliff	-0.0337	0.02	20	-1.42	0.1711	0.2139	ns
Goleen - Labhra Cliff	0.0638	0.03	20	2.55	**0.0190**	**0.0379**	*
Goleen - West Cliff	0.0104	0.03	20	0.40	0.6970	0.6970	ns
Goleen - Whirlpool Cliff	0.0862	0.02	20	3.66	**0.0016**	**0.0052**	**
Labhra Cliff - West Cliff	-0.0534	0.03	20	-1.93	0.0683	0.0975	ns
Labhra Cliff - Whirlpool Cliff	0.0223	0.02	20	0.89	0.3823	0.4247	ns
West Cliff - Whirlpool Cliff	0.0757	0.03	20	2.87	**0.0095**	**0.0237**	*

Table S4.18. Results of the linear mixed effect model (lmer) testing the effects of time and site on three diversity indices separately (taxa richness, Shannon diversity index, and Simpson diversity index). 2.5-year comparison (June 2018 – March 2021). *P*-adjusted: *p*-value adjusted with Benjamini-Hochberg Procedure. Significant *p*-values ($p < 0.05$) are in bold.

Linear mixed-effects model (lmer)
Benthic communities
2.5-year comparison (June 2018 – March 2021)
*Formula: Diversity index ~ Time * Site + (1|Quadrat)*

Taxa richness

Fixed effects test (Anova)

	Chi-sq	df	*p*-value
(Intercept)	269.14	1	< **0.0001**
Site	112.79	3	< **0.0001**
Time	0.94	1	0.3327
Site:Time	1.72	3	0.6336

Pairwise comparisons of taxa richness, between pairs of sites (emmeans)

contrast	estimate	SE	df	*t*-ratio	*p*-value	*p*-adjusted	Sign.
Glannafeen - Goleen	4.9376	2.41	12	2.05	0.0630	0.0945	ns
Glannafeen - Labhra Cliff	4.0349	2.47	12	1.63	0.1283	0.1540	ns
Glannafeen - Whirlpool Cliff	23.3720	2.39	12	9.80	**< 0.0001**	**< 0.0001**	****
Goleen - Labhra Cliff	-0.9028	2.44	12	-0.37	0.7179	0.7179	ns
Goleen - Whirlpool Cliff	18.4344	2.35	12	7.83	**< 0.0001**	**< 0.0001**	****
Labhra Cliff - Whirlpool Cliff	19.3372	2.42	12	8.00	**< 0.0001**	**< 0.0001**	****

Shannon diversity index (H)

Fixed effects test (Anova)

	Chi-sq	df	*p*-value
(Intercept)	657.15	1	< **0.0001**
Site	23.23	3	< **0.0001**
Time	0.00	1	0.9555
Site:Time	20.31	3	**0.0001**

Tests of temporal trends in Shannon diversity index at each individual site (emtrends)

Site	trend	SE	df	*t*-ratio	*p*-value	*p*-adjusted	Sign.
Glannafeen	0.0001	0.00	76	0.06	0.9556	0.9891	ns
Goleen	-0.0007	0.00	76	-0.31	0.7548	0.9891	ns
Labhra Cliff	< 0.0001	0.00	76	0.01	0.9891	0.9891	ns
Whirlpool Cliff	-0.0094	0.00	76	-5.78	**< 0.0001**	**< 0.0001**	****

Pairwise comparisons of temporal trends in Shannon diversity index, between pairs of sites (emmeans)

contrast	estimate	SE	df	*t*-ratio	*p*-value	*p*-adjusted	Sign.
Glannafeen - Goleen	0.0008	0.00	76	0.29	0.9918	1.0000	ns
Glannafeen - Labhra Cliff	0.0001	0.00	76	0.02	1.0000	1.0000	ns
Glannafeen - Whirlpool Cliff	0.0095	0.00	76	3.98	**0.0009**	**0.0054**	**
Goleen - Labhra Cliff	-0.0008	0.00	76	-0.21	0.9966	1.0000	ns
Goleen - Whirlpool Cliff	0.0087	0.00	76	3.01	**0.0183**	**0.0497**	*
Labhra Cliff - Whirlpool Cliff	0.0095	0.00	76	2.90	**0.0249**	**0.0497**	*

Table S4.18. (Continued)

Pairwise comparisons of Shannon diversity index, between pairs of sites (emmeans)

contrast	estimate	SE	df	*t*-ratio	*p*-value	*p*-adjusted	Sign.
Glannafeen - Goleen	-0.2255	0.08	12	-2.76	**0.0171**	**0.0257**	*
Glannafeen - Labhra Cliff	-0.0852	0.09	12	-1.00	0.3377	0.3377	ns
Glannafeen - Whirlpool Cliff	0.3448	0.08	12	4.32	**0.0010**	**0.0020**	**
Goleen - Labhra Cliff	0.1403	0.09	12	1.61	0.1331	0.1597	ns
Goleen - Whirlpool Cliff	0.5702	0.08	12	6.99	**< 0.0001**	**0.0001**	****
Labhra Cliff - Whirlpool Cliff	0.4300	0.09	12	5.04	**0.0003**	**0.0009**	***

Simpson's diversity index

Fixed effects test (Anova)

	Chi-sq	df	*p*-value
(Intercept)	677.65	1	**< 0.0001**
Site	14.35	3	**0.0025**
Time	0.14	1	0.7103
Site:Time	22.37	3	**0.0001**

Tests of temporal trends in Simpson's diversity index at each individual site (emtrends)

Site	trend	SE	df	*t*-ratio	*p*-value	*p*-adjusted	Sign.
Glannafeen	-0.0002	0.00	76	-0.37	0.7113	0.9982	ns
Goleen	< 0.0001	0.00	76	0.02	0.9813	0.9982	ns
Labhra Cliff	< 0.0001	0.00	76	0.00	0.9982	0.9982	ns
Whirlpool Cliff	-0.0031	0.00	76	-5.96	**< 0.0001**	**< 0.0001**	****

Pairwise comparisons of temporal trends in Simpson's diversity index, between pairs of sites (emmeans)

contrast	estimate	SE	df	*t*-ratio	*p*-value	*p*-adjusted	Sign.
Glannafeen - Goleen	-0.0003	0.00	76	-0.28	0.9923	1.0000	ns
Glannafeen - Labhra Cliff	-0.0002	0.00	76	-0.25	0.9942	1.0000	ns
Glannafeen - Whirlpool Cliff	0.0029	0.00	76	3.50	**0.0043**	**0.0086**	**
Goleen - Labhra Cliff	< 0.0001	0.00	76	0.01	1.0000	1.0000	ns
Goleen - Whirlpool Cliff	0.0031	0.00	76	3.81	**0.0016**	**0.0086**	**
Labhra Cliff - Whirlpool Cliff	0.0031	0.00	76	3.60	**0.0031**	**0.0086**	**

Pairwise comparisons of Simpson's diversity index, between pairs of sites (emmeans)

contrast	estimate	SE	df	*t*-ratio	*p*-value	*p*-adjusted	Sign.
Glannafeen - Goleen	-0.1353	0.03	12	-4.26	**0.0011**	**0.0066**	**
Glannafeen - Labhra Cliff	-0.0699	0.03	12	-2.11	0.0569	0.1069	ns
Glannafeen - Whirlpool Cliff	-0.0279	0.03	12	-0.87	0.4029	0.4029	ns
Goleen - Labhra Cliff	0.0654	0.03	12	1.98	0.0712	0.1069	ns
Goleen - Whirlpool Cliff	0.1075	0.03	12	3.36	**0.0057**	**0.0171**	*
Labhra Cliff - Whirlpool Cliff	0.0420	0.03	12	1.26	0.2326	0.2791	ns

Table S4.19. Results of the linear mixed effect model (lmer) testing the effects of time and site on three diversity indices separately (taxa richness, Shannon diversity index, and Simpson diversity index). 3-year full comparison (June 2018 – June 2021). *P*-adjusted: *p*-value adjusted with Benjamini-Hochberg Procedure. Significant *p*-values ($p < 0.05$) are in bold.

Linear mixed-effects model (lmer)
Benthic communities
3-year full comparison (June 2018 – June 2021)
*Formula: Diversity index ~ Time * Site + (1|Quadrat)*

Taxa richness

Fixed effects test (Anova)

	Chi-sq	df	*p*-value
(Intercept)	124.24	1	< **0.0001**
Site	0.00	1	0.9604
Time	6.42	1	**0.0113**
Site:Time	0.16	1	0.6913

Tests of temporal trends in taxa richness at each individual site (emtrends)

Site	trend	SE	df	*t*-ratio	*p*-value	*p*-adjusted	Sign.
Goleen	-0.0739	0.03	46	-2.53	**0.0147**	**0.0295**	*
Labhra Cliff	-0.0535	0.04	46	-1.26	0.2127	0.2127	ns

Shannon diversity index (H)

Fixed effects test (Anova)

	Chi-sq	df	*p*-value
(Intercept)	443.52	1	< **0.0001**
Site	1.78	1	0.1826
Time	4.75	1	**0.0292**
Site:Time	0.00	1	0.9862

Tests of temporal trends in Shannon diversity index at each individual site (emtrends)

Site	trend	SE	df	*t*-ratio	*p*-value	*p*-adjusted	Sign.
Goleen	-0.0038	0.00	46	-2.18	**0.0344**	0.0688	ns
Labhra Cliff	-0.0038	0.00	46	-1.66	0.1034	0.1034	ns

Simpson's diversity index

Fixed effects test (Anova)

	Chi-sq	df	*p*-value
(Intercept)	921.60	1	< **0.0001**
Site	4.72	1	**0.0298**
Time	4.29	1	**0.0382**
Site:Time	0.39	1	0.5337

Tests of temporal trends in Simpson's diversity index at each individual site (emtrends)

Site	trend	SE	df	*t*-ratio	*p*-value	*p*-adjusted	Sign.
Goleen	-0.0011	0.00	46	-2.07	**0.0439**	0.0877	ns
Labhra Cliff	-0.0006	0.00	46	-1.15	0.2556	0.2556	ns

Pairwise comparisons of Simpson's diversity index, between pairs of sites (emmeans)

contrast	estimate	SE	df	*t*-ratio	*p*-value	*p*-adjusted	Sign.
Goleen - Labhra Cliff	0.0733	0.03	6	2.09	0.0812	0.0812	ns

Table S4.20. Results of the linear mixed effect model (lmer) testing the effects of time, site and historical period on three diversity indices separately (taxa richness, Shannon diversity index, and Simpson diversity index). Present-past comparison (April 1994 – August 1995 and June 2018 – November 2019). *P*-adjusted: *p*-value adjusted with Benjamini-Hochberg Procedure. Significant *p*-values ($p < 0.05$) are in bold.

Linear mixed-effects model (lmer)
Benthic communities
Present-past comparison (April 1994 – August 1995 and June 2018 – November 2019)
*Formula: Diversity index ~ Time * Site * Period + (1|Quadrat)*

Taxa richness

Fixed effects test (Anova)

	Chi-sq	df	*p*-value
(Intercept)	563.84	1	**< 0.0001**
Period	0.08	1	0.7796
Site	3.98	1	**0.0462**
Time	2.53	1	0.1118
Period:Site	0.44	1	0.5054
Period:Time	0.04	1	0.8455
Site:Time	8.59	1	**0.0034**
Period:Site:Time	20.53	1	**< 0.0001**

Tests of temporal trends in taxa richness at each individual site and historical period (emtrends)

Site	Period	trend	SE	df	*t*-ratio	*p*-value	*p*-adjusted	Sign.
Glannafeen	199x	0.0684	0.04	56	1.59	0.1174	0.1484	ns
Labhra Cliff	199x	-0.0841	0.03	56	-2.87	**0.0058**	**0.0115**	*
Glannafeen	20xx	0.0571	0.04	56	1.47	0.1484	0.1484	ns
Labhra Cliff	20xx	0.2300	0.03	56	7.54	**< 0.0001**	**< 0.0001**	****

Pairwise comparisons of temporal trends in taxa richness, between pairs of sites at each historical period (emtrends)

contrast	Period	estimate	SE	df	*t*-ratio	*p*-value	*p*-adjusted	Sign.
Glannafeen - Labhra Cliff	199x	0.1525	0.05	56	2.93	**0.0049**	**0.0049**	**
Glannafeen - Labhra Cliff	20xx	-0.1729	0.05	56	-3.49	**0.0009**	**0.0019**	**

Pairwise comparisons of temporal trends in taxa richness, between historical periods at each site (emtrends)

contrast	Site	estimate	SE	df	*t*-ratio	*p*-value	*p*-adjusted	Sign.
199x - 20xx	Glannafeen	0.0113	0.06	56	0.19	0.8462	0.8462	ns
199x - 20xx	Labhra Cliff	-0.3141	0.04	56	-7.43	**< 0.0001**	**< 0.0001**	****

Pairwise comparisons of taxa richness, between pairs of sites, at each historical period (emmeans)

contrast	Period	estimate	SE	df	*t*-ratio	*p*-value	*p*-adjusted	Sign.
Glannafeen - Labhra Cliff	199x	4.7290	1.70	16	2.79	**0.0132**	**0.0264**	*
Glannafeen - Labhra Cliff	20xx	3.7425	1.72	16	2.17	**0.0454**	**0.0454**	*

Pairwise comparisons of taxa richness, between, historical period at each site (emmeans)

contrast	Site	estimate	SE	df	*t*-ratio	*p*-value	*p*-adjusted	Sign.
199x - 20xx	Glannafeen	-0.4046	1.71	16	-0.24	0.8160	0.8160	ns
199x - 20xx	Labhra Cliff	-1.3910	1.71	16	-0.81	0.4281	0.8160	ns

Table S4.20. (Continued)

Shannon diversity index (H)

Fixed effects test (Anova)

	Chi-sq	df	*p*-value
(Intercept)	603.93	1	**< 0.0001**
Period	7.20	1	**0.0073**
Site	0.08	1	0.7760
Time	3.83	1	0.0504
Period:Site	0.71	1	0.3999
Period:Time	3.21	1	0.0734
Site:Time	47.99	1	**< 0.0001**
Period:Site:Time	57.85	1	**< 0.0001**

Tests of temporal trends in taxa richness at each individual site and historical period (emtrends)

Site	Period	trend	SE	df	*t*-ratio	*p*-value	*p*-adjusted	Sign.
Glannafeen	199x	0.0066	0.00	56	1.96	0.0553	0.0738	ns
Labhra Cliff	199x	-0.0173	0.00	56	-22.72	**< 0.0001**	**< 0.0001**	****
Glannafeen	20xx	-0.0010	0.00	56	-0.39	0.6979	0.6979	ns
Labhra Cliff	20xx	0.0151	0.00	56	5.00	**< 0.0001**	**< 0.0001**	****

Pairwise comparisons of temporal trends in taxa richness, between pairs of sites at each historical period (emtrends)

contrast	Period	estimate	SE	df	*t*-ratio	*p*-value	*p*-adjusted	Sign.
Glannafeen - Labhra Cliff	199x	0.0238	0.00	56	6.93	**< 0.0001**	**< 0.0001**	****
Glannafeen - Labhra Cliff	20xx	-0.0161	0.00	56	-4.06	**0.0002**	**0.0002**	***

Pairwise comparisons of temporal trends in taxa richness, between historical periods at each site (emtrends)

contrast	Site	estimate	SE	df	*t*-ratio	*p*-value	*p*-adjusted	Sign.
199x - 20xx	Glannafeen	0.0076	0.00	56	1.79	0.0788	0.0788	ns
199x - 20xx	Labhra Cliff	-0.0324	0.00	56	-10.38	**< 0.0001**	**< 0.0001**	****

Pairwise comparisons of taxa richness, between pairs of sites, at each historical period (emmeans)

contrast	Period	estimate	SE	df	*t*-ratio	*p*-value	*p*-adjusted	Sign.
Glannafeen - Labhra Cliff	199x	0.1636	0.10	16	1.60	0.1286	0.2571	ns
Glannafeen - Labhra Cliff	20xx	-0.0343	0.10	16	-0.33	0.7427	0.7427	ns

Pairwise comparisons of taxa richness, between, historical period at each site (emmeans)

contrast	Site	estimate	SE	df	*t*-ratio	*p*-value	*p*-adjusted	Sign.
199x - 20xx	Glannafeen	0.3532	0.10	16	3.42	**0.0035**	**0.0070**	**
199x - 20xx	Labhra Cliff	0.1553	0.10	16	1.53	0.1456	0.1456	ns

Table S4.20. (Continued)

Simpson's diversity index

Fixed effects test (Anova)

	Chi-sq	df	*p*-value
(Intercept)	692.62	1	**< 0.0001**
Period	4.46	1	**0.0348**
Site	0.10	1	0.7460
Time	0.87	1	0.3514
Period:Site	0.00	1	0.9551
Period:Time	8.10	1	**0.0044**
Site:Time	31.32	1	**< 0.0001**
Period:Site:Time	52.81	1	**< 0.0001**

Tests of temporal trends in taxa richness at each individual site and historical period (emtrends)

Site	Period	trend	SE	df	*t*-ratio	*p*-value	*p*-adjusted	Sign.
Glannafeen	199x	0.0010	0.00	56	0.93	0.3554	0.3554	ns
Labhra Cliff	199x	-0.0061	0.00	56	-9.88	**< 0.0001**	**< 0.0001**	****
Glannafeen	20xx	-0.0032	0.00	56	-3.24	**0.0020**	**0.0027**	**
Labhra Cliff	20xx	0.0033	0.00	56	3.44	**0.0011**	**0.0022**	**

Pairwise comparisons of temporal trends in taxa richness, between pairs of sites at each historical period (emtrends)

contrast	Period	estimate	SE	df	*t*-ratio	*p*-value	*p*-adjusted	Sign.
Glannafeen - Labhra Cliff	199x	0.0071	0.00	56	5.60	**< 0.0001**	**< 0.0001**	****
Glannafeen - Labhra Cliff	20xx	-0.0065	0.00	56	-4.72	**< 0.0001**	**< 0.0001**	****

Pairwise comparisons of temporal trends in taxa richness, between historical periods at each site (emtrends)

contrast	Site	estimate	SE	df	*t*-ratio	*p*-value	*p*-adjusted	Sign.
199x - 20xx	Glannafeen	0.0042	0.00	56	2.85	**0.0062**	**0.0062**	**
199x - 20xx	Labhra Cliff	-0.0094	0.00	56	-8.24	**< 0.0001**	**< 0.0001**	****

Pairwise comparisons of taxa richness, between pairs of sites, at each historical period (emmeans)

contrast	Period	estimate	SE	df	*t*-ratio	*p*-value	*p*-adjusted	Sign.
Glannafeen - Labhra Cliff	199x	0.0707	0.04	16	1.87	0.0805	0.1611	ns
Glannafeen - Labhra Cliff	20xx	-0.0432	0.04	16	-1.12	0.2805	0.2805	ns

Pairwise comparisons of taxa richness, between, historical period at each site (emmeans)

contrast	Site	estimate	SE	df	*t*-ratio	*p*-value	*p*-adjusted	Sign.
199x - 20xx	Glannafeen	0.1188	0.04	16	3.12	**0.0066**	**0.0132**	*
199x - 20xx	Labhra Cliff	0.0049	0.04	16	0.13	0.9000	0.9000	ns

C.5. Temporal dynamics of benthic taxonomic groups

Table S4.21. Results of the linear mixed effect model (lmer) testing the effects of time and site on the percentage cover of the main benthic taxonomic groups. Comparison across all sites (June 2018 – November 2019). *P*-adjusted: *p*-value adjusted with Benjamini-Hochberg Procedure. Significant *p*-values ($p < 0.05$) are in bold.

Linear mixed-effects model (lme)
Benthic categories
Comparison across all sites (June 2018 – November 2019)
*Formula: Percentage cover ~ Time * Site + (1|Quadrat)*

Sponges
Fixed effects test (Anova)

	Chi-sq	df	*p*-value
(Intercept)	64.89	1	**< 0.0001**
Site	5.82	4	0.2133
Time	8.96	1	**0.0028**
Site:Time	25.84	4	**< 0.0001**

Tests of temporal trends in sponge cover at each individual site (emtrends)

Site	trend	SE	df	*t*-ratio	*p*-value	*p*-adjusted	Sign.
Glannafeen	0.1037	0.03	70	2.99	**0.0038**	**0.0095**	**
Goleen	0.0504	0.02	70	2.09	**0.0403**	0.0672	ns
Labhra Cliff	0.2061	0.02	70	10.20	**< 0.0001**	**< 0.0001**	****
West Cliff	0.2484	0.24	70	1.03	0.3053	0.3816	ns
Whirlpool Cliff	0.0705	0.17	70	0.41	0.6857	0.6857	ns

Pairwise comparisons of temporal trends in sponge percentage cover, between pairs of sites (emmeans)

contrast	estimate	SE	df	*t*-ratio	*p*-value	*p*-adjusted	Sign.
Glannafeen - Goleen	0.0533	0.04	70	1.26	0.7152	1.0000	ns
Glannafeen - Labhra Cliff	-0.1024	0.04	70	-2.55	0.0906	0.4530	ns
Glannafeen - West Cliff	-0.1447	0.24	70	-0.60	0.9753	1.0000	ns
Glannafeen - Whirlpool Cliff	0.0332	0.18	70	0.19	0.9997	1.0000	ns
Goleen - Labhra Cliff	-0.1557	0.03	70	-4.95	**< 0.0001**	**0.0005**	***
Goleen - West Cliff	-0.1980	0.24	70	-0.82	0.9239	1.0000	ns
Goleen - Whirlpool Cliff	-0.0201	0.18	70	-0.11	1.0000	1.0000	ns
Labhra Cliff - West Cliff	-0.0423	0.24	70	-0.18	0.9998	1.0000	ns
Labhra Cliff - Whirlpool Cliff	0.1356	0.17	70	0.78	0.9365	1.0000	ns
West Cliff - Whirlpool Cliff	0.1779	0.30	70	0.60	0.9746	1.0000	ns

Pairwise comparisons of sponge percentage cover, between pairs of sites (emmeans)

contrast	estimate	SE	df	*t*-ratio	*p*-value	*p*-adjusted	Sign.
Glannafeen - Goleen	6.6882	4.46	20	1.50	0.1493	0.4976	ns
Glannafeen - Labhra Cliff	7.5778	4.52	20	1.68	0.1092	0.4976	ns
Glannafeen - West Cliff	10.0173	4.79	20	2.09	**0.0496**	0.4955	ns
Glannafeen - Whirlpool Cliff	5.0717	4.61	20	1.10	0.2842	0.6551	ns
Goleen - Labhra Cliff	0.8897	4.52	20	0.20	0.8458	0.8458	ns
Goleen - West Cliff	3.3291	4.79	20	0.70	0.4949	0.7752	ns
Goleen - Whirlpool Cliff	-1.6164	4.60	20	-0.35	0.7292	0.8103	ns
Labhra Cliff - West Cliff	2.4394	4.85	20	0.50	0.6202	0.7752	ns
Labhra Cliff - Whirlpool Cliff	-2.5061	4.66	20	-0.54	0.5970	0.7752	ns
West Cliff - Whirlpool Cliff	-4.9455	4.93	20	-1.00	0.3276	0.6551	ns

Table S4.21. (Continued)

Ascidians

Fixed effects test (Anova)

	Chi-sq	df	*p*-value
(Intercept)	10.29	1	**0.0013**
Site	0.99	3	0.8031
Time	3.14	1	0.0763
Site:Time	19.14	3	**0.0003**

Tests of temporal trends in ascidian percentage cover at each individual site (emtrends)

Site	trend	SE	df	*t*-ratio	*p*-value	*p*-adjusted	Sign.
Glannafeen	-0.1251	0.07	56	-1.77	0.0817	0.1634	ns
Goleen	0.0005	0.01	56	0.04	0.9656	0.9656	ns
Labhra Cliff	0.1277	0.11	56	1.17	0.2485	0.3314	ns
West Cliff	1.1399	0.30	56	3.83	**0.0003**	**0.0013**	**

Pairwise comparisons of temporal trends in ascidian percentage cover, between pairs of sites (emmeans)

contrast	estimate	SE	df	*t*-ratio	*p*-value	*p*-adjusted	Sign.
Glannafeen - Goleen	-0.1256	0.07	56	-1.76	0.3055	0.3666	ns
Glannafeen - Labhra Cliff	-0.2527	0.13	56	-1.94	0.2232	0.3349	ns
Glannafeen - West Cliff	-1.2649	0.31	56	-4.13	**0.0007**	**0.0041**	**
Goleen - Labhra Cliff	-0.1271	0.11	56	-1.15	0.6576	0.6576	ns
Goleen - West Cliff	-1.1394	0.30	56	-3.82	**0.0019**	**0.0056**	**
Labhra Cliff - West Cliff	-1.0122	0.32	56	-3.19	**0.0122**	**0.0243**	*

Pairwise comparisons of ascidian percentage cover, between pairs of sites (emmeans)

contrast	estimate	SE	df	*t*-ratio	*p*-value	*p*-adjusted	Sign.
Glannafeen - Goleen	-0.1140	1.70	16	-0.07	0.9472	0.9472	ns
Glannafeen - Labhra Cliff	-2.5548	1.86	16	-1.38	0.1876	0.2306	ns
Glannafeen - West Cliff	-12.0212	2.57	16	-4.68	**0.0002**	**0.0007**	***
Goleen - Labhra Cliff	-2.4408	1.79	16	-1.36	0.1921	0.2306	ns
Goleen - West Cliff	-11.9071	2.52	16	-4.72	**0.0002**	**0.0007**	***
Labhra Cliff - West Cliff	-9.4664	2.63	16	-3.60	**0.0024**	**0.0048**	**

Table S4.21. (Continued)

TurF-Forming animals

Fixed effects test (Anova)

	Chi-sq	df	*p*-value
(Intercept)	209.64	1	**< 0.0001**
Site	45.07	4	**< 0.0001**
Time	4.74	1	**0.0294**
Site:Time	61.90	4	**< 0.0001**

Tests of temporal trends in turf percentage cover at each individual site (emtrends)

Site	trend	SE	df	*t*-ratio	*p*-value	*p*-adjusted	Sign.
Glannafeen	0.2618	0.12	70	2.18	**0.0328**	0.0547	ns
Goleen	-0.2820	0.14	70	-1.96	0.0537	0.0671	ns
Labhra Cliff	0.0423	0.15	70	0.28	0.7796	0.7796	ns
West Cliff	-1.4794	0.51	70	-2.89	**0.0051**	**0.0127**	*
Whirlpool Cliff	0.7155	0.07	70	9.89	**< 0.0001**	**< 0.0001**	****

Pairwise comparisons of temporal trends in turf percentage cover, between pairs of sites (emmeans)

contrast	estimate	SE	df	*t*-ratio	*p*-value	*p*-adjusted	Sign.
Glannafeen - Goleen	0.5438	0.19	70	2.90	**0.0385**	0.0623	ns
Glannafeen - Labhra Cliff	0.2195	0.19	70	1.14	0.7854	0.7854	ns
Glannafeen - West Cliff	1.7412	0.53	70	3.31	**0.0123**	**0.0308**	*
Glannafeen - Whirlpool Cliff	-0.4537	0.14	70	-3.23	**0.0156**	**0.0311**	*
Goleen - Labhra Cliff	-0.3244	0.21	70	-1.56	0.5290	0.5878	ns
Goleen - West Cliff	1.1974	0.53	70	2.25	0.1726	0.2158	ns
Goleen - Whirlpool Cliff	-0.9975	0.16	70	-6.20	**< 0.0001**	**< 0.0001**	****
Labhra Cliff - West Cliff	1.5218	0.53	70	2.85	**0.0436**	0.0623	ns
Labhra Cliff - Whirlpool Cliff	-0.6732	0.17	70	-4.03	**0.0013**	**0.0043**	**
West Cliff - Whirlpool Cliff	-2.1949	0.52	70	-4.25	**0.0006**	**0.0030**	**

Pairwise comparisons of turf percentage cover, between pairs of sites (emmeans)

contrast	estimate	SE	df	*t*-ratio	*p*-value	*p*-adjusted	Sign.
Glannafeen - Goleen	21.5189	4.43	20	4.86	**0.0001**	**0.0003**	***
Glannafeen - Labhra Cliff	31.1402	4.41	20	7.06	**< 0.0001**	**< 0.0001**	****
Glannafeen - West Cliff	15.7643	5.38	20	2.93	**0.0083**	**0.0161**	*
Glannafeen - Whirlpool Cliff	7.7833	4.51	20	1.73	0.0996	0.1245	ns
Goleen - Labhra Cliff	9.6213	4.42	20	2.18	**0.0417**	0.0596	ns
Goleen - West Cliff	-5.7546	5.39	20	-1.07	0.2983	0.2983	ns
Goleen - Whirlpool Cliff	-13.7356	4.52	20	-3.04	**0.0065**	**0.0161**	*
Labhra Cliff - West Cliff	-15.3759	5.38	20	-2.86	**0.0097**	**0.0161**	*
Labhra Cliff - Whirlpool Cliff	-23.3569	4.50	20	-5.19	**< 0.0001**	**0.0002**	***
West Cliff - Whirlpool Cliff	-7.9810	5.45	20	-1.46	0.1589	0.1766	ns

Table S4.21. (Continued)

Anthozoans

Fixed effects test (Anova)

	Chi-sq	df	*p*-value
(Intercept)	96.83	1	**< 0.0001**
Site	198.68	4	**< 0.0001**
Time	0.90	1	0.3426
Site:Time	16.21	4	**0.0027**

Tests of temporal trends in anthozoan percentage cover at each individual site (emtrends)

Site	trend	SE	df	*t*-ratio	*p*-value	*p*-adjusted	Sign.
Glannafeen	0.0066	0.01	70	0.95	0.3459	0.5765	ns
Goleen	0.0006	0.01	70	0.12	0.9017	0.9017	ns
Labhra Cliff	0.0341	0.02	70	1.41	0.1616	0.4039	ns
West Cliff	0.3561	0.10	70	3.74	**0.0004**	**0.0019**	**
Whirlpool Cliff	0.0646	0.09	70	0.71	0.4777	0.5972	ns

Pairwise comparisons of temporal trends in anthozoan percentage cover, between pairs of sites (emmeans)

contrast	estimate	SE	df	*t*-ratio	*p*-value	*p*-adjusted	Sign.
Glannafeen - Goleen	0.0060	0.01	70	0.69	0.9590	0.9975	ns
Glannafeen - Labhra Cliff	-0.0275	0.03	70	-1.10	0.8079	0.9975	ns
Glannafeen - West Cliff	-0.3495	0.10	70	-3.66	**0.0043**	**0.0215**	*
Glannafeen - Whirlpool Cliff	-0.0580	0.09	70	-0.64	0.9681	0.9975	ns
Goleen - Labhra Cliff	-0.0335	0.02	70	-1.36	0.6570	0.9975	ns
Goleen - West Cliff	-0.3554	0.10	70	-3.73	**0.0035**	**0.0215**	*
Goleen - Whirlpool Cliff	-0.0639	0.09	70	-0.71	0.9546	0.9975	ns
Labhra Cliff - West Cliff	-0.3219	0.10	70	-3.28	**0.0137**	**0.0457**	*
Labhra Cliff - Whirlpool Cliff	-0.0304	0.09	70	-0.33	0.9975	0.9975	ns
West Cliff - Whirlpool Cliff	0.2915	0.13	70	2.22	0.1848	0.4620	ns

Pairwise comparisons of anthozoan percentage cover, between pairs of sites (emmeans)

contrast	estimate	SE	df	*t*-ratio	*p*-value	*p*-adjusted	Sign.
Glannafeen - Goleen	0.8310	0.22	20	3.80	**0.0011**	**0.0022**	**
Glannafeen - Labhra Cliff	-0.5729	0.51	20	-1.12	0.2762	0.2762	ns
Glannafeen - West Cliff	-5.0101	1.88	20	-2.66	**0.0149**	**0.0186**	*
Glannafeen - Whirlpool Cliff	-26.0749	1.79	20	-14.59	**< 0.0001**	**< 0.0001**	****
Goleen - Labhra Cliff	-1.4039	0.50	20	-2.79	**0.0114**	**0.0162**	*
Goleen - West Cliff	-5.8412	1.88	20	-3.11	**0.0055**	**0.0092**	**
Goleen - Whirlpool Cliff	-26.9059	1.79	20	-15.07	**< 0.0001**	**< 0.0001**	****
Labhra Cliff - West Cliff	-4.4373	1.93	20	-2.29	**0.0328**	**0.0364**	*
Labhra Cliff - Whirlpool Cliff	-25.5020	1.84	20	-13.83	**< 0.0001**	**< 0.0001**	****
West Cliff - Whirlpool Cliff	-21.0647	2.58	20	-8.15	**< 0.0001**	**< 0.0001**	****

Table S4.21. (Continued)

Polychaetes

Fixed effects test (Anova)

	Chi-sq	df	*p*-value
(Intercept)	5.71	1	**0.0168**
Site	18.53	4	**0.0010**
Time	0.16	1	0.6890
Site:Time	22.66	4	**0.0001**

Tests of temporal trends in polychaete percentage cover at each individual site (emtrends)

Site	trend	SE	df	*t*-ratio	*p*-value	*p*-adjusted	Sign.
Glannafeen	0.0511	0.13	70	0.40	0.6902	0.9684	ns
Goleen	0.6076	0.13	70	4.76	**< 0.0001**	**0.0001**	****
Labhra Cliff	0.0255	0.13	70	0.20	0.8424	0.9684	ns
West Cliff	-0.2077	0.13	70	-1.63	0.1081	0.2703	ns
Whirlpool Cliff	0.0051	0.13	70	0.04	0.9684	0.9684	ns

Pairwise comparisons of temporal trends in polychaete percentage cover, between pairs of sites (emmeans)

contrast	estimate	SE	df	*t*-ratio	*p*-value	*p*-adjusted	Sign.
Glannafeen - Goleen	-0.5565	0.18	70	-3.08	**0.0237**	0.0593	ns
Glannafeen - Labhra Cliff	0.0256	0.18	70	0.14	0.9999	1.0000	ns
Glannafeen - West Cliff	0.2588	0.18	70	1.43	0.6082	1.0000	ns
Glannafeen - Whirlpool Cliff	0.0460	0.18	70	0.25	0.9990	1.0000	ns
Goleen - Labhra Cliff	0.5821	0.18	70	3.22	**0.0159**	0.0531	ns
Goleen - West Cliff	0.8154	0.18	70	4.52	**0.0002**	**0.0024**	**
Goleen - Whirlpool Cliff	0.6025	0.18	70	3.34	**0.0115**	0.0531	ns
Labhra Cliff - West Cliff	0.2332	0.18	70	1.29	0.6970	1.0000	ns
Labhra Cliff - Whirlpool Cliff	0.0204	0.18	70	0.11	1.0000	1.0000	ns
West Cliff - Whirlpool Cliff	-0.2128	0.18	70	-1.18	0.7633	1.0000	ns

Pairwise comparisons of polychaete percentage cover, between pairs of sites (emmeans)

contrast	estimate	SE	df	*t*-ratio	*p*-value	*p*-adjusted	Sign.
Glannafeen - Goleen	-6.6321	1.21	20	-5.47	**< 0.0001**	**0.0001**	****
Glannafeen - Labhra Cliff	3.3523	1.21	20	2.77	**0.0119**	**0.0149**	*
Glannafeen - West Cliff	-0.8423	1.21	20	-0.69	0.4951	0.5502	ns
Glannafeen - Whirlpool Cliff	3.5450	1.21	20	2.92	**0.0084**	**0.0120**	*
Goleen - Labhra Cliff	9.9844	1.21	20	8.24	**< 0.0001**	**< 0.0001**	****
Goleen - West Cliff	5.7897	1.21	20	4.78	**0.0001**	**0.0003**	***
Goleen - Whirlpool Cliff	10.1771	1.21	20	8.40	**< 0.0001**	**< 0.0001**	****
Labhra Cliff - West Cliff	-4.1946	1.21	20	-3.46	**0.0025**	**0.0041**	**
Labhra Cliff - Whirlpool Cliff	0.1927	1.21	20	0.16	0.8753	0.8753	ns
West Cliff - Whirlpool Cliff	4.3873	1.21	20	3.62	**0.0017**	**0.0034**	**

Table S4.22. Results of the linear mixed effect model (lmer) testing the effects of time and site on the percentage cover of the main benthic taxonomic groups. 2.5-year comparison (June 2018 – March 2021). *P*-adjusted: *p*-value adjusted with Benjamini-Hochberg Procedure. Significant *p*-values ($p < 0.05$) are in bold.

Linear mixed-effects model (lme)
Benthic categories
2.5-year comparison (June 2018 – March 2021)
*Formula: Percentage cover ~ Time * Site + (1|Quadrat)*

Sponges

Fixed effects test (Anova)

	Chi-sq	df	*p*-value
(Intercept)	37.18	1	**< 0.0001**
Site	2.57	3	0.4626
Time	43.53	1	**< 0.0001**
Site:Time	21.17	3	**0.0001**

Tests of temporal trends in sponge cover at each individual site (emtrends)

Site	trend	SE	df	*t*-ratio	*p*-value	*p*-adjusted	Sign.
Glannafeen	0.0912	0.01	76	6.60	**< 0.0001**	**< 0.0001**	****
Goleen	0.0500	0.02	76	3.33	**0.0013**	**0.0018**	**
Labhra Cliff	0.0294	0.01	76	4.03	**0.0001**	**0.0003**	***
Whirlpool Cliff	-0.1722	0.09	76	-1.85	0.0679	0.0679	ns

Pairwise comparisons of temporal trends in sponge percentage cover, between pairs of sites (emmeans)

contrast	estimate	SE	df	*t*-ratio	*p*-value	*p*-adjusted	Sign.
Glannafeen - Goleen	0.0412	0.02	76	2.02	0.1909	0.2290	ns
Glannafeen - Labhra Cliff	0.0617	0.02	76	3.95	**0.0010**	**0.0059**	**
Glannafeen - Whirlpool Cliff	0.2633	0.09	76	2.80	**0.0320**	0.0959	ns
Goleen - Labhra Cliff	0.0206	0.02	76	1.23	0.6086	0.6086	ns
Goleen - Whirlpool Cliff	0.2222	0.09	76	2.36	0.0938	0.1877	ns
Labhra Cliff - Whirlpool Cliff	0.2016	0.09	76	2.16	0.1432	0.2149	ns

Pairwise comparisons of sponge percentage cover, between pairs of sites (emmeans)

contrast	estimate	SE	df	*t*-ratio	*p*-value	*p*-adjusted	Sign.
Glannafeen - Goleen	6.5174	5.78	12	1.13	0.2813	0.7726	ns
Glannafeen - Labhra Cliff	8.9286	5.77	12	1.55	0.1480	0.7726	ns
Glannafeen - Whirlpool Cliff	4.9895	5.87	12	0.85	0.4122	0.7726	ns
Goleen - Labhra Cliff	2.4112	5.78	12	0.42	0.6838	0.7992	ns
Goleen - Whirlpool Cliff	-1.5279	5.88	12	-0.26	0.7992	0.7992	ns
Labhra Cliff - Whirlpool Cliff	-3.9390	5.87	12	-0.67	0.5151	0.7726	ns

Table S4.22. (Continued)

Ascidians

Fixed effects test (Anova)

	Chi-sq	df	*p*-value
(Intercept)	4.00	1	**0.0456**
Site	3.36	2	0.1863
Time	0.65	1	0.4199
Site:Time	0.83	2	0.6588

TurF-Forming animals

Fixed effects test (Anova)

	Chi-sq	df	*p*-value
(Intercept)	234.58	1	**< 0.0001**
Site	43.20	3	**< 0.0001**
Time	0.67	1	0.4145
Site:Time	33.76	3	**< 0.0001**

Tests of temporal trends in turf percentage cover at each individual site (emtrends)

Site	trend	SE	df	*t*-ratio	*p*-value	*p*-adjusted	Sign.
Glannafeen	0.0613	0.08	76	0.82	0.4170	0.8341	ns
Goleen	-0.0129	0.10	76	-0.13	0.8986	0.8986	ns
Labhra Cliff	-0.0132	0.08	76	-0.16	0.8735	0.8986	ns
Whirlpool Cliff	0.5235	0.07	76	7.17	**< 0.0001**	**< 0.0001**	****

Pairwise comparisons of temporal trends in turf percentage cover, between pairs of sites (emmeans)

contrast	estimate	SE	df	*t*-ratio	*p*-value	*p*-adjusted	Sign.
Glannafeen - Goleen	0.0742	0.13	76	0.59	0.9350	1.0000	ns
Glannafeen - Labhra Cliff	0.0744	0.11	76	0.67	0.9089	1.0000	ns
Glannafeen - Whirlpool Cliff	-0.4622	0.10	76	-4.41	**0.0002**	**0.0006**	***
Goleen - Labhra Cliff	0.0002	0.13	76	0.00	1.0000	1.0000	ns
Goleen - Whirlpool Cliff	-0.5364	0.12	76	-4.30	**0.0003**	**0.0006**	***
Labhra Cliff - Whirlpool Cliff	-0.5366	0.11	76	-4.88	**< 0.0001**	**0.0002**	***

Pairwise comparisons of turf percentage cover, between pairs of sites (emmeans)

contrast	estimate	SE	df	*t*-ratio	*p*-value	*p*-adjusted	Sign.
Glannafeen - Goleen	24.6338	4.47	12	5.51	**0.0001**	**0.0004**	***
Glannafeen - Labhra Cliff	29.9836	4.41	12	6.80	**< 0.0001**	**0.0001**	***
Glannafeen - Whirlpool Cliff	6.3486	4.47	12	1.42	0.1813	0.2176	ns
Goleen - Labhra Cliff	5.3499	4.50	12	1.19	0.2571	0.2571	ns
Goleen - Whirlpool Cliff	-18.2852	4.56	12	-4.01	**0.0017**	**0.0026**	**
Labhra Cliff - Whirlpool Cliff	-23.6350	4.50	12	-5.26	**0.0002**	**0.0004**	***

Table S4.22. (Continued)

Anthozoans

Fixed effects test (Anova)

	Chi-sq	df	*p*-value
(Intercept)	48.03	1	**< 0.0001**
Site	108.29	3	**< 0.0001**
Time	0.43	1	0.5117
Site:Time	0.53	3	0.9120

Pairwise comparisons of anthozoan percentage cover, between pairs of sites (emmeans)

contrast	estimate	SE	df	*t*-ratio	*p*-value	*p*-adjusted	Sign.
Glannafeen - Goleen	0.7087	0.34	12	2.10	0.0579	0.0868	ns
Glannafeen - Labhra Cliff	0.5187	0.38	12	1.35	0.2010	0.2412	ns
Glannafeen - Whirlpool Cliff	-24.4012	1.99	12	-12.25	**< 0.0001**	**< 0.0001**	****
Goleen - Labhra Cliff	-0.1900	0.37	12	-0.51	0.6201	0.6201	ns
Goleen - Whirlpool Cliff	-25.1099	1.99	12	-12.62	**< 0.0001**	**< 0.0001**	****
Labhra Cliff - Whirlpool Cliff	-24.9199	2.00	12	-12.47	**< 0.0001**	**< 0.0001**	****

Polychaetes

Fixed effects test (Anova)

	Chi-sq	df	*p*-value
(Intercept)	10.36	1	**0.0013**
Site	33.98	3	**< 0.0001**
Time	0.50	1	0.4797
Site:Time	0.65	3	0.8843

Pairwise comparisons of polychaete percentage cover, between pairs of sites (emmeans)

contrast	estimate	SE	df	*t*-ratio	*p*-value	*p*-adjusted	Sign.
Glannafeen - Goleen	-6.4394	1.15	12	-5.60	**0.0001**	**0.0002**	***
Glannafeen - Labhra Cliff	3.3632	1.15	12	2.92	**0.0127**	**0.0153**	*
Glannafeen - Whirlpool Cliff	3.4778	1.15	12	3.02	**0.0106**	**0.0153**	*
Goleen - Labhra Cliff	9.8025	1.15	12	8.52	**< 0.0001**	**< 0.0001**	****
Goleen - Whirlpool Cliff	9.9172	1.15	12	8.62	**< 0.0001**	**< 0.0001**	****
Labhra Cliff - Whirlpool Cliff	0.1147	1.15	12	0.10	0.9222	0.9222	ns

Table S4.23. Results of the linear mixed effect model (lmer) testing the effects of time and site on the percentage cover of the main benthic taxonomic groups. 3-year full comparison (June 2018 – June 2021). *P*-adjusted: *p*-value adjusted with Benjamini-Hochberg Procedure. Significant *p*-values ($p < 0.05$) are in bold.

Linear mixed-effects model (lme)
Benthic categories
3-year full comparison (June 2018 – June 2021)
*Formula: Percentage cover ~ Time * Site + (1|Quadrat)*

Sponges

Fixed effects test (Anova)

	Chi-sq	df	*p*-value
(Intercept)	26.72	1	**< 0.0001**
Site	0.10	1	0.7523
Time	9.74	1	**0.0018**
Site:Time	1.46	1	0.2262

Tests of temporal trends in sponge cover at each individual site (emtrends)

Site	trend	SE	df	*t*-ratio	*p*-value	*p*-adjusted	Sign.
Goleen	0.0375	0.01	46	2.53	**0.0148**	**0.0296**	*
Labhra Cliff	0.0166	0.01	46	1.84	0.0716	0.0716	ns

Pairwise comparisons of temporal trends in sponge percentage cover, between pairs of sites (emmeans)

contrast	estimate	SE	df	*t*-ratio	*p*-value	*p*-adjusted	Sign.
Goleen - Labhra Cliff	0.0210	0.02	46	1.21	0.2323	0.2323	ns

Ascidians

Fixed effects test (Anova)

	Chi-sq	df	*p*-value
(Intercept)	12.05	1	**0.0005**
Site	3.06	1	0.0800
Time	4.27	1	**0.0387**
Site:Time	2.30	1	0.1290

Tests of temporal trends in ascidian percentage cover at each individual site (emtrends)

Site	trend	SE	df	*t*-ratio	*p*-value	*p*-adjusted	Sign.
Goleen	-0.0136	0.02	46	-0.87	0.3889	0.3889	ns
Labhra Cliff	-0.0889	0.05	46	-1.89	0.0652	0.1304	ns

TurF-Forming animals

Fixed effects test (Anova)

	Chi-sq	df	*p*-value
(Intercept)	135.05	1	**< 0.0001**
Site	2.99	1	0.0837
Time	1.42	1	0.2334
Site:Time	2.67	1	0.1021

Table S4.23. (Continued)

Anthozoans

Fixed effects test (Anova)

	Chi-sq	df	*p*-value
(Intercept)	12.74	1	**0.0004**
Site	1.30	1	0.2536
Time	1.54	1	0.2149
Site:Time	0.27	1	0.6031

Polychaetes

Fixed effects test (Anova)

	Chi-sq	df	*p*-value
(Intercept)	19.97	1	< **0.0001**
Site	19.55	1	< **0.0001**
Time	0.55	1	0.4584
Site:Time	0.50	1	0.4781

Pairwise comparisons of polychaete percentage cover, between pairs of sites (emmeans)

contrast	estimate	SE	df	*t*-ratio	*p*-value	*p*-adjusted	Sign.
Goleen - Labhra Cliff	8.6052	1.30	6	6.60	**0.0006**	**0.0006**	***

Table S4.24. Results of the linear mixed effect model (lmer) testing the effects of time historical period and site on the percentage cover of the main benthic taxonomic groups. Present-past comparison (April 1994 – August 1995 and June 2018 – November 2019). *P*-adjusted: *p*-value adjusted with Benjamini-Hochberg Procedure. Significant *p*-values ($p < 0.05$) are in bold.

Linear mixed-effects model (lme)
Benthic categories
Present-past comparison (April 1994 – August 1995 and June 2018 – November 2019)
*Formula: Percentage cover ~ Time * Site * Period + (1|Quadrat)*

Sponges

Fixed effects test (Anova)

	Chi-sq	df	*p*-value
(Intercept)	158.08	1	**< 0.0001**
Period	11.69	1	**0.0006**
Site	2.12	1	0.1456
Time	1.12	1	0.2895
Period:Site	0.09	1	0.7698
Period:Time	113.03	1	**< 0.0001**
Site:Time	18.39	1	**< 0.0001**
Period:Site:Time	53.16	1	**< 0.0001**

Tests of temporal trends in sponge percentage cover at each individual site and historical period (emtrends)

Site	Period	trend	SE	df	*t*-ratio	*p*-value	*p*-adjusted	Sign.
Glannafeen	199x	-0.0018	0.02	56	-0.10	0.9177	0.9177	ns
Labhra Cliff	199x	-0.3808	0.05	56	-8.23	**< 0.0001**	**< 0.0001**	****
Glannafeen	20xx	0.1075	0.04	56	2.90	**0.0053**	**0.0070**	**
Labhra Cliff	20xx	0.2057	0.02	56	9.49	**< 0.0001**	**< 0.0001**	****

Pairwise comparisons of temporal trends in sponge percentage cover, between pairs of sites at each historical period (emtrends)

contrast	Period	estimate	SE	df	*t*-ratio	*p*-value	*p*-adjusted	Sign.
Glannafeen - Labhra Cliff	199x	0.3789	0.05	56	7.67	**< 0.0001**	**< 0.0001**	****
Glannafeen - Labhra Cliff	20xx	-0.0983	0.04	56	-2.29	**0.0258**	**0.0258**	*

Pairwise comparisons of temporal trends in sponge percentage cover, between historical periods at each site (emtrends)

contrast	Site	estimate	SE	df	*t*-ratio	*p*-value	*p*-adjusted	Sign.
199x - 20xx	Glannafeen	-0.1093	0.04	56	-2.67	**0.0099**	**0.0099**	**
199x - 20xx	Labhra Cliff	-0.5865	0.05	56	-11.48	**< 0.0001**	**< 0.0001**	****

Pairwise comparisons of sponge percentage cover, between pairs of sites, at each historical period (emmeans)

contrast	Period	estimate	SE	df	*t*-ratio	*p*-value	*p*-adjusted	Sign.
Glannafeen - Labhra Cliff	199x	8.5147	6.58	16	1.29	0.2139	0.2820	ns
Glannafeen - Labhra Cliff	20xx	7.3730	6.62	16	1.11	0.2820	0.2820	ns

Pairwise comparisons of sponge percentage cover, between, historical period at each site (emmeans)

contrast	Site	estimate	SE	df	*t*-ratio	*p*-value	*p*-adjusted	Sign.
199x - 20xx	Glannafeen	13.7286	6.57	16	2.09	0.0529	0.0760	ns
199x - 20xx	Labhra Cliff	12.5870	6.63	16	1.90	0.0760	0.0760	ns

Table S4.24. (Continued)

Ascidians

Fixed effects test (Anova)

	Chi-sq	df	*p*-value
(Intercept)	60.14	1	**< 0.0001**
Period	2.97	1	0.0846
Site	2.70	1	0.1004
Elapsed_Time	0.10	1	0.7563
Period:Site	0.80	1	0.3700
Period:Elapsed_Time	0.05	1	0.8253
Site:Elapsed_Time	2.68	1	0.1013
Period:Site:Elapsed_Time	3.31	1	0.0689

TurF-Forming animals

Fixed effects test (Anova)

	Chi-sq	df	*p*-value
(Intercept)	290.75	1	**< 0.0001**
Period	3.07	1	0.0799
Site	5.79	1	**0.0162**
Time	9.67	1	**0.0019**
Period:Site	19.34	1	**< 0.0001**
Period:Time	0.98	1	0.3214
Site:Time	6.91	1	**0.0086**
Period:Site:Time	17.59	1	**< 0.0001**

Tests of temporal trends in turf percentage cover at each individual site and historical period (emtrends)

Site	Period	trend	SE	df	*t*-ratio	*p*-value	*p*-adjusted	Sign.
Glannafeen	199x	-0.1936	0.20	56	-0.97	0.3340	0.4454	ns
Labhra Cliff	199x	0.7775	0.07	56	11.02	**< 0.0001**	**< 0.0001**	****
Glannafeen	20xx	0.2623	0.12	56	2.19	**0.0324**	0.0649	ns
Labhra Cliff	20xx	0.0393	0.15	56	0.26	0.7934	0.7934	ns

Pairwise comparisons of temporal trends in turf percentage cover, between pairs of sites at each historical period (emtrends)

contrast	Period	estimate	SE	df	*t*-ratio	*p*-value	*p*-adjusted	Sign.
Glannafeen - Labhra Cliff	199x	-0.9711	0.21	56	-4.61	**< 0.0001**	**< 0.0001**	****
Glannafeen - Labhra Cliff	20xx	0.2230	0.19	56	1.17	0.2487	0.2487	ns

Pairwise comparisons of temporal trends in turf percentage cover, between historical periods at each site (emtrends)

contrast	Site	estimate	SE	df	*t*-ratio	*p*-value	*p*-adjusted	Sign.
199x - 20xx	Glannafeen	-0.4559	0.23	56	-1.97	0.0543	0.0543	ns
199x - 20xx	Labhra Cliff	0.7382	0.17	56	4.47	**< 0.0001**	**0.0001**	****

Pairwise comparisons of turf percentage cover, between pairs of sites, at each historical period (emmeans)

contrast	Period	estimate	SE	df	*t*-ratio	*p*-value	*p*-adjusted	Sign.
Glannafeen - Labhra Cliff	199x	-16.3459	5.83	16	-2.80	**0.0127**	**0.0127**	*
Glannafeen - Labhra Cliff	20xx	30.6822	5.72	16	5.37	**0.0001**	**0.0001**	***

Pairwise comparisons of turf percentage cover, between, historical period at each site (emmeans)

contrast	Site	estimate	SE	df	*t*-ratio	*p*-value	*p*-adjusted	Sign.
199x - 20xx	Glannafeen	-14.9368	5.89	16	-2.53	**0.0221**	**0.0221**	*
199x - 20xx	Labhra Cliff	32.0913	5.65	16	5.68	**< 0.0001**	**0.0001**	****

Table S4.24. (Continued)

Anthozoans

Fixed effects test (Anova)

	Chi-sq	df	*p*-value
(Intercept)	70.93	1	**< 0.0001**
Period	5.17	1	**0.0230**
Site	3.34	1	0.0678
Time	54.59	1	**< 0.0001**
Period:Site	0.10	1	0.7530
Period:Time	7.76	1	**0.0053**
Site:Time	3.68	1	0.0552
Period:Site:Time	9.79	1	**0.0018**

Tests of temporal trends in anthozoan percentage cover at each individual site and historical period (emtrends)

Site	Period	trend	SE	df	*t*-ratio	*p*-value	*p*-adjusted	Sign.
Glannafeen	199x	0.0096	0.00	56	28.60	**< 0.0001**	**< 0.0001**	****
Labhra Cliff	199x	0.0122	0.00	56	6.63	**< 0.0001**	**< 0.0001**	****
Glannafeen	20xx	0.0103	0.00	56	3.62	**0.0006**	**0.0008**	***
Labhra Cliff	20xx	-0.0005	0.00	56	-0.18	0.8553	0.8553	ns

Pairwise comparisons of temporal trends in anthozoan percentage cover, between pairs of sites at each historical period (emtrends)

contrast	Period	estimate	SE	df	*t*-ratio	*p*-value	*p*-adjusted	Sign.
Glannafeen - Labhra Cliff	199x	-0.0026	0.00	56	-1.39	0.1705	0.1705	ns
Glannafeen - Labhra Cliff	20xx	0.0108	0.00	56	2.80	**0.0069**	**0.0138**	*

Pairwise comparisons of temporal trends in anthozoan percentage cover, between historical periods at each site (emtrends)

contrast	Site	estimate	SE	df	*t*-ratio	*p*-value	*p*-adjusted	Sign.
199x - 20xx	Glannafeen	-0.0007	0.00	56	-0.26	0.7987	0.7987	ns
199x - 20xx	Labhra Cliff	0.0126	0.00	56	3.98	**0.0002**	**0.0004**	***

Pairwise comparisons of anthozoan percentage cover, between pairs of sites, at each historical period (emmeans)

contrast	Period	estimate	SE	df	*t*-ratio	*p*-value	*p*-adjusted	Sign.
Glannafeen - Labhra Cliff	199x	-0.8267	0.53	16	-1.57	0.1369	0.2739	ns
Glannafeen - Labhra Cliff	20xx	-0.4812	0.54	16	-0.90	0.3820	0.3820	ns

Pairwise comparisons of anthozoan percentage cover, between, historical period at each site (emmeans)

contrast	Site	estimate	SE	df	*t*-ratio	*p*-value	*p*-adjusted	Sign.
199x - 20xx	Glannafeen	-0.9802	0.53	16	-1.86	0.0817	0.1634	ns
199x - 20xx	Labhra Cliff	-0.6348	0.54	16	-1.19	0.2533	0.2533	ns

Table S4.24. (Continued)

Polychaetes

Fixed effects test (Anova)

	Chi-sq	df	*p*-value
(Intercept)	44.70	1	**< 0.0001**
Period	0.13	1	0.7145
Site	2.83	1	0.0927
Time	0.00	1	0.9752
Period:Site	20.10	1	**< 0.0001**
Period:Time	5.41	1	**0.0201**
Site:Time	3.30	1	0.0695
Period:Site:Time	1.10	1	0.2946

Tests of temporal trends in polychaete percentage cover at each individual site and historical period (emtrends)

Site	Period	trend	SE	df	*t*-ratio	*p*-value	*p*-adjusted	Sign.
Glannafeen	199x	0.0085	0.04	56	0.24	0.8106	0.8106	ns
Labhra Cliff	199x	-0.0871	0.04	56	-2.48	**0.0163**	0.0650	ns
Glannafeen	20xx	0.0511	0.03	56	1.62	0.1105	0.2210	ns
Labhra Cliff	20xx	0.0255	0.03	56	0.81	0.4221	0.5628	ns

Pairwise comparisons of temporal trends in polychaete percentage cover, between pairs of sites at each historical period (emtrends)

contrast	Period	estimate	SE	df	*t*-ratio	*p*-value	*p*-adjusted	Sign.
Glannafeen - Labhra Cliff	199x	0.0956	0.05	56	1.92	0.0596	0.1193	ns
Glannafeen - Labhra Cliff	20xx	0.0256	0.04	56	0.57	0.5677	0.5677	ns

Pairwise comparisons of temporal trends in polychaete percentage cover, between historical periods at each site (emtrends)

contrast	Site	estimate	SE	df	*t*-ratio	*p*-value	*p*-adjusted	Sign.
199x - 20xx	Glannafeen	-0.0426	0.05	56	-0.90	0.3704	0.3704	ns
199x - 20xx	Labhra Cliff	-0.1126	0.05	56	-2.39	**0.0205**	**0.0410**	*

Pairwise comparisons of polychaete percentage cover, between pairs of sites, at each historical period (emmeans)

contrast	Period	estimate	SE	df	*t*-ratio	*p*-value	*p*-adjusted	Sign.
Glannafeen - Labhra Cliff	199x	-0.6542	0.61	16	-1.06	0.3028	0.3028	ns
Glannafeen - Labhra Cliff	20xx	3.3555	0.61	16	5.52	**< 0.0001**	**0.0001**	****

Pairwise comparisons of polychaete percentage cover, between, historical period at each site (emmeans)

contrast	Site	estimate	SE	df	*t*-ratio	*p*-value	*p*-adjusted	Sign.
199x - 20xx	Glannafeen	-2.4486	0.61	16	-4.01	**0.0010**	**0.0020**	**
199x - 20xx	Labhra Cliff	1.5611	0.61	16	2.55	**0.0212**	**0.0212**	*

C.6. Temporal dynamics of sponge morphologies

Table S4.25. Results of the linear mixed effect model (lmer) testing the effects of time and site on the percentage cover of the main sponge morphologies. Comparison across all sites (June 2018 – November 2019). *P*-adjusted: *p*-value adjusted with Benjamini-Hochberg Procedure. Significant *p*-values ($p < 0.05$) are in bold.

Linear mixed-effects model (lme)
Benthic categories
Comparison across all sites (June 2018 – November 2019)
*Formula: Percentage cover ~ Time * Site + (1|Quadrat)*

Encrusting Raspaiilidae
Fixed effects test (Anova)

	Chi-sq	df	*p*-value
(Intercept)	29.02	1	**< 0.0001**
Site	15.31	3	**0.0016**
Time	0.06	1	0.8064
Site:Time	4.62	3	0.2020

Pairwise comparisons of Encrusting Raspaiilidae percentage cover, between pairs of sites (emmeans)

contrast	estimate	SE	df	*t*-ratio	*p*-value	*p*-adjusted	Sign.
Glannafeen - Goleen	3.0067	4.80	16	0.63	0.5403	0.6483	ns
Glannafeen - Labhra Cliff	3.7970	4.80	16	0.79	0.4405	0.6483	ns
Glannafeen - West Cliff	17.3734	4.80	16	3.62	**0.0023**	**0.0138**	*
Goleen - Labhra Cliff	0.7903	4.80	16	0.16	0.8713	0.8713	ns
Goleen - West Cliff	14.3666	4.80	16	2.99	**0.0086**	**0.0241**	*
Labhra Cliff - West Cliff	13.5764	4.80	16	2.83	**0.0121**	**0.0241**	*

Table S4.25. (Continued)

Encrusting non-Raspaiilidae

Fixed effects test (Anova)

	Chi-sq	df	*p*-value
(Intercept)	9.10	1	**0.0026**
Site	17.50	4	**0.0015**
Time	1.75	1	0.1862
Site:Time	73.83	4	**< 0.0001**

Tests of temporal trends in encrusting non-Raspaiilidae percentage cover at each individual site (emtrends)

Site	trend	SE	df	*t*-ratio	*p*-value	*p*-adjusted	Sign.
Glannafeen	-0.0099	0.01	70	-1.32	0.1905	0.3174	ns
Goleen	-0.0016	0.01	70	-0.12	0.9083	0.9083	ns
Labhra Cliff	0.1002	0.02	70	6.15	**< 0.0001**	**< 0.0001**	****
West Cliff	0.2216	0.23	70	0.95	0.3469	0.4336	ns
Whirlpool Cliff	0.6372	0.11	70	5.98	**< 0.0001**	**< 0.0001**	****

Pairwise comparisons of temporal trends in encrusting non-Raspaiilidae percentage cover, between pairs of sites (emmeans)

contrast	estimate	SE	df	*t*-ratio	*p*-value	*p*-adjusted	Sign.
Glannafeen - Goleen	-0.0083	0.02	70	-0.52	0.9856	0.9856	ns
Glannafeen - Labhra Cliff	-0.1101	0.02	70	-6.14	**< 0.0001**	**< 0.0001**	****
Glannafeen - West Cliff	-0.2315	0.23	70	-0.99	0.8595	0.9856	ns
Glannafeen - Whirlpool Cliff	-0.6471	0.11	70	-6.06	**< 0.0001**	**< 0.0001**	****
Goleen - Labhra Cliff	-0.1018	0.02	70	-4.71	**0.0001**	**0.0002**	***
Goleen - West Cliff	-0.2232	0.23	70	-0.95	0.8752	0.9856	ns
Goleen - Whirlpool Cliff	-0.6389	0.11	70	-5.94	**< 0.0001**	**< 0.0001**	****
Labhra Cliff - West Cliff	-0.1214	0.23	70	-0.52	0.9853	0.9856	ns
Labhra Cliff - Whirlpool Cliff	-0.5370	0.11	70	-4.98	**< 0.0001**	**0.0001**	***
West Cliff - Whirlpool Cliff	-0.4157	0.26	70	-1.62	0.4920	0.8200	ns

Pairwise comparisons of encrusting non-Raspaiilidae percentage cover, between pairs of sites (emmeans)

contrast	estimate	SE	df	*t*-ratio	*p*-value	*p*-adjusted	Sign.
Glannafeen - Goleen	1.7579	2.32	20	0.76	0.4583	0.5729	ns
Glannafeen - Labhra Cliff	2.7847	2.32	20	1.20	0.2447	0.3496	ns
Glannafeen - West Cliff	-8.9318	2.86	20	-3.13	**0.0053**	**0.0088**	**
Glannafeen - Whirlpool Cliff	-10.2619	2.55	20	-4.02	**0.0007**	**0.0017**	**
Goleen - Labhra Cliff	1.0267	2.32	20	0.44	0.6629	0.6664	ns
Goleen - West Cliff	-10.6897	2.85	20	-3.75	**0.0013**	**0.0025**	**
Goleen - Whirlpool Cliff	-12.0199	2.55	20	-4.72	**0.0001**	**0.0007**	***
Labhra Cliff - West Cliff	-11.7164	2.85	20	-4.11	**0.0005**	**0.0017**	**
Labhra Cliff - Whirlpool Cliff	-13.0466	2.55	20	-5.12	**0.0001**	**0.0005**	***
West Cliff - Whirlpool Cliff	-1.3302	3.04	20	-0.44	0.6664	0.6664	ns

Massive

Fixed effects test (Anova)

	Chi-sq	df	*p*-value
(Intercept)	0.71	1	0.3989
Site	0.30	3	0.9609
Time	0.19	1	0.6627
Site:Time	2.26	3	0.5201

Table S4.25. (Continued)

Papillate

Fixed effects test (Anova)

	Chi-sq	df	*p*-value
(Intercept)	14.30	1	**0.0002**
Site	10.82	3	**0.0127**
Time	65.91	1	**< 0.0001**
Site:Time	48.52	3	**< 0.0001**

Tests of temporal trends in papillate sponge percentage cover at each individual site (emtrends)

Site	trend	SE	df	*t*-ratio	*p*-value	*p*-adjusted	Sign.
Glannafeen	0.0253	0.00	56	8.12	**< 0.0001**	**< 0.0001**	****
Goleen	-0.0025	0.00	56	-0.81	0.4213	0.5618	ns
Labhra Cliff	0.0050	0.00	56	1.60	0.1145	0.2289	ns
West Cliff	0.0006	0.00	56	0.18	0.8599	0.8599	ns

Pairwise comparisons of temporal trends in papillate sponge percentage cover, between pairs of sites (emmeans)

contrast	estimate	SE	df	*t*-ratio	*p*-value	*p*-adjusted	Sign.
Glannafeen - Goleen	0.0279	0.00	56	6.31	**< 0.0001**	**< 0.0001**	****
Glannafeen - Labhra Cliff	0.0203	0.00	56	4.61	**0.0001**	**0.0003**	***
Glannafeen - West Cliff	0.0248	0.00	56	5.62	**< 0.0001**	**< 0.0001**	****
Goleen - Labhra Cliff	-0.0075	0.00	56	-1.71	0.3300	0.4949	ns
Goleen - West Cliff	-0.0031	0.00	56	-0.70	0.8974	0.8974	ns
Labhra Cliff - West Cliff	0.0044	0.00	56	1.01	0.7452	0.8942	ns

Pairwise comparisons of papillate sponge percentage cover, between pairs of sites (emmeans)

contrast	estimate	SE	df	*t*-ratio	*p*-value	*p*-adjusted	Sign.
Glannafeen - Goleen	0.2239	0.13	16	1.76	0.0974	0.1461	ns
Glannafeen - Labhra Cliff	0.4034	0.13	16	3.17	**0.0059**	**0.0177**	*
Glannafeen - West Cliff	0.5515	0.13	16	4.34	**0.0005**	**0.0031**	**
Goleen - Labhra Cliff	0.1795	0.13	16	1.41	0.1771	0.2126	ns
Goleen - West Cliff	0.3276	0.13	16	2.58	**0.0203**	**0.0406**	*
Labhra Cliff - West Cliff	0.1480	0.13	16	1.16	0.2614	0.2614	ns

Table S4.25. (Continued)

Pedunculate

Fixed effects test (Anova)

	Chi-sq	df	*p*-value
(Intercept)	1.99	1	0.1581
Site	3.76	2	0.1523
Time	17.95	1	**< 0.0001**
Site:Time	18.60	2	**0.0001**

Tests of temporal trends in pedunculate sponge percentage cover at each individual site (emtrends)

Site	trend	SE	df	*t*-ratio	*p*-value	*p*-adjusted	Sign.
Glannafeen	0.0288	0.01	42	4.24	**0.0001**	**0.0004**	***
Goleen	-0.0003	0.00	42	-0.22	0.8305	0.8305	ns
Labhra Cliff	-0.0021	0.00	42	-0.79	0.4319	0.6479	ns

Pairwise comparisons of temporal trends in pedunculate sponge percentage cover, between pairs of sites (emmeans)

contrast	estimate	SE	df	*t*-ratio	*p*-value	*p*-adjusted	Sign.
Glannafeen - Goleen	0.0290	0.01	42	4.21	**0.0004**	**0.0006**	***
Glannafeen - Labhra Cliff	0.0308	0.01	42	4.24	**0.0003**	**0.0006**	***
Goleen - Labhra Cliff	0.0018	0.00	42	0.62	0.8078	0.8078	ns

Pairwise comparisons of pedunculate sponge percentage cover, between pairs of sites (emmeans)

contrast	estimate	SE	df	*t*-ratio	*p*-value	*p*-adjusted	Sign.
Glannafeen - Goleen	0.3353	0.08	12	4.26	**0.0011**	**0.0033**	**
Glannafeen - Labhra Cliff	0.2813	0.08	12	3.39	**0.0054**	**0.0080**	**
Goleen - Labhra Cliff	-0.0540	0.03	12	-1.63	0.1285	0.1285	ns

Table S4.26. Results of the linear mixed effect model (lmer) testing the effects of time and site on the percentage cover of the main sponge morphologies. 2.5-year comparison (June 2018 – March 2021). *P*-adjusted: *p*-value adjusted with Benjamini-Hochberg Procedure. Significant *p*-values ($p < 0.05$) are in bold.

Linear mixed-effects model (lme)
Benthic categories
2.5-year comparison (June 2018 – March 2021)
*Formula: Percentage cover ~ Time * Site + (1|Quadrat)*

Encrusting Raspaiilidae

Fixed effects test (Anova)

	Chi-sq	df	*p*-value
(Intercept)	12.79	1.000	**0.0003**
Site	0.37	2.000	0.8318
Time	10.95	1.000	**0.0009**
Site:Time	1.03	2.000	0.5985

Tests of temporal trends in encrusting Raspaiilidae cover at each individual site (emtrends)

Site	trend	SE	df	*t*-ratio	*p*-value	*p*-adjusted	Sign.
Glannafeen	0.0342	0.010	57	3.31	**0.0016**	**0.0049**	**
Goleen	0.0256	0.016	57	1.60	0.1142	0.1142	ns
Labhra Cliff	0.0214	0.007	57	2.92	**0.0051**	**0.0076**	**

Pairwise comparisons of temporal trends in encrusting Raspaiilidae percentage cover, between pairs of sites (emmeans)

contrast	estimate	SE	df	*t*-ratio	*p*-value	*p*-adjusted	Sign.
Glannafeen - Goleen	0.0086	0.019	57	0.45	0.8927	0.9688	ns
Glannafeen - Labhra Cliff	0.0128	0.013	57	1.01	0.5716	0.9688	ns
Goleen - Labhra Cliff	0.0042	0.018	57	0.24	0.9688	0.9688	ns

Encrusting non-Raspaiilidae

Fixed effects test (Anova)

	Chi-sq	df	*p*-value
(Intercept)	5.92	1.000	**0.0150**
Site	11.96	3.000	**0.0075**
Time	0.02	1.000	0.8769
Site:Time	1.18	3.000	0.7586

Pairwise comparisons of encrusting non-Raspaiilidae percentage cover, between pairs of sites (emmeans)

contrast	estimate	SE	df	*t*-ratio	*p*-value	*p*-adjusted	Sign.
Glannafeen - Goleen	2.0452	3.087	12	0.66	0.5201	0.6241	ns
Glannafeen - Labhra Cliff	3.3496	3.089	12	1.08	0.2996	0.4493	ns
Glannafeen - Whirlpool Cliff	-9.3539	3.286	12	-2.85	**0.0147**	**0.0294**	*
Goleen - Labhra Cliff	1.3044	3.089	12	0.42	0.6803	0.6803	ns
Goleen - Whirlpool Cliff	-11.3991	3.286	12	-3.47	**0.0046**	**0.0139**	*
Labhra Cliff - Whirlpool Cliff	-12.7035	3.289	12	-3.86	**0.0023**	**0.0135**	*

Table S4.26. (Continued)

Massive

Fixed effects test (Anova)

	Chi-sq	df	*p*-value
(Intercept)	0.00	1.000	0.9478
Site	2.76	2.000	0.2514
Time	0.03	1.000	0.8675
Site:Time	0.10	2.000	0.9495

Papillate

Fixed effects test (Anova)

	Chi-sq	df	*p*-value
(Intercept)	1.37	1.000	0.2427
Site	2.83	2.000	0.2431
Time	20.05	1.000	**< 0.0001**
Site:Time	19.23	2.000	**0.0001**

Tests of temporal trends in papillate cover at each individual site (emtrends)

Site	trend	SE	df	*t*-ratio	*p*-value	*p*-adjusted	Sign.
Glannafeen	0.0234	0.005	57	4.48	**< 0.0001**	**0.0001**	***
Goleen	-0.0010	0.003	57	-0.30	0.7615	0.7615	ns
Labhra Cliff	-0.0007	0.002	57	-0.32	0.7521	0.7615	ns

Pairwise comparisons of temporal trends in papillate sponge percentage cover, between pairs of sites (emmeans)

contrast	estimate	SE	df	*t*-ratio	*p*-value	*p*-adjusted	Sign.
Glannafeen - Goleen	0.0244	0.006	57	3.97	**0.0006**	**0.0009**	***
Glannafeen - Labhra Cliff	0.0241	0.006	57	4.28	**0.0002**	**0.0006**	***
Goleen - Labhra Cliff	-0.0003	0.004	57	-0.08	0.9961	0.9961	ns

Pairwise comparisons of papillate sponge percentage cover, between pairs of sites (emmeans)

contrast	estimate	SE	df	*t*-ratio	*p*-value	*p*-adjusted	Sign.
Glannafeen - Goleen	0.2476	0.200	9	1.24	0.2465	0.2465	ns
Glannafeen - Labhra Cliff	0.4740	0.183	9	2.59	**0.0291**	0.0874	ns
Goleen - Labhra Cliff	0.2264	0.125	9	1.82	0.1026	0.1539	ns

Table S4.26. (Continued)

Erect

Fixed effects test (Anova)

	Chi-sq	df	*p*-value
(Intercept)	1.03	1.000	0.3111
Site	0.75	2.000	0.6873
Time	15.95	1.000	**0.0001**
Site:Time	4.94	2.000	0.0845

Tests of temporal trends in erect cover at each individual site (emtrends)

Site	trend	SE	df	*t*-ratio	*p*-value	*p*-adjusted	Sign.
Glannafeen	0.0069	0.002	57	3.99	**0.0002**	**0.0006**	***
Goleen	0.0015	0.002	57	0.85	0.3975	0.3975	ns
Labhra Cliff	0.0044	0.002	57	2.54	**0.0140**	**0.0210**	*

Pairwise comparisons of temporal trends in erect sponge percentage cover, between pairs of sites (emmeans)

contrast	estimate	SE	df	*t*-ratio	*p*-value	*p*-adjusted	Sign.
Glannafeen - Goleen	0.0055	0.002	57	2.22	0.0762	0.2285	ns
Glannafeen - Labhra Cliff	0.0025	0.002	57	1.03	0.5605	0.5605	ns
Goleen - Labhra Cliff	-0.0029	0.002	57	-1.19	0.4639	0.5605	ns

Pedunculate

Fixed effects test (Anova)

	Chi-sq	df	*p*-value
(Intercept)	1.06	1.000	0.3025
Site	3.49	2.000	0.1750
Time	9.20	1.000	**0.0024**
Site:Time	10.85	2.000	**0.0044**

Tests of temporal trends in pedunculate cover at each individual site (emtrends)

Site	trend	SE	df	*t*-ratio	*p*-value	*p*-adjusted	Sign.
Glannafeen	0.0174	0.006	57	3.03	**0.0036**	**0.0109**	*
Goleen	-0.0007	0.001	57	-0.92	0.3628	0.3628	ns
Labhra Cliff	-0.0023	0.002	57	-1.35	0.1818	0.2727	ns

Pairwise comparisons of temporal trends in pedunculate sponge percentage cover, between pairs of sites (emmeans)

contrast	estimate	SE	df	*t*-ratio	*p*-value	*p*-adjusted	Sign.
Glannafeen - Goleen	0.0181	0.006	57	3.13	**0.0077**	**0.0116**	*
Glannafeen - Labhra Cliff	0.0198	0.006	57	3.29	**0.0048**	**0.0116**	*
Goleen - Labhra Cliff	0.0016	0.002	57	0.88	0.6553	0.6553	ns

Pairwise comparisons of pedunculate sponge percentage cover, between pairs of sites (emmeans)

contrast	estimate	SE	df	*t*-ratio	*p*-value	*p*-adjusted	Sign.
Glannafeen - Goleen	0.3980	0.121	9	3.28	**0.0096**	**0.0287**	*
Glannafeen - Labhra Cliff	0.3385	0.126	9	2.69	**0.0246**	**0.0369**	*
Goleen - Labhra Cliff	-0.0595	0.039	9	-1.52	0.1617	0.1617	ns

Table S4.27. Results of the linear mixed effect model (lmer) testing the effects of time and site on the percentage cover of the main sponge morphologies. 3-year full comparison (June 2018 – June 2021). *P*-adjusted: *p*-value adjusted with Benjamini-Hochberg Procedure. Significant *p*-values ($p < 0.05$) are in bold.

Linear mixed-effects model (lme)
Benthic categories
3-year full comparison (June 2018 – June 2021)
*Formula: Percentage cover ~ Time * Site + (1|Quadrat)*

Encrusting Raspailiidae

Fixed effects test (Anova)

	Chi-sq	df	*p*-value
(Intercept)	9.47	1.000	**0.0021**
Site	0.02	1.000	0.8826
Time	6.17	1.000	**0.0130**
Site:Time	0.75	1.000	0.3872

Tests of temporal trends in encrusting Raspailiidae cover at each individual site (emtrends)

Site	trend	SE	df	*t*-ratio	*p*-value		*p*-adjusted	Sign.
Goleen	0.0301	0.012	46	2.48	**0.0167**	*	**0.0167**	*
Labhra Cliff	0.0186	0.005	46	3.43	**0.0013**	**	**0.0026**	**

Pairwise comparisons of temporal trends in encrusting Raspailiidae percentage cover, between pairs of sites (emtrends)

contrast	estimate	SE	df	*t*-ratio	*p*-value		*p*-adjusted	Sign.
Goleen - Labhra Cliff	0.0115	0.013	46	0.86	0.3917	ns	0.3917	ns

Encrusting non-Raspailiidae

Fixed effects test (Anova)

	Chi-sq	df	*p*-value
(Intercept)	42.17	1.000	**< 0.0001**
Site	4.31	1.000	**0.0380**
Time	2.24	1.000	0.1341
Site:Time	0.59	1.000	0.4424

Pairwise comparisons of encrusting non-Raspailiidae percentage cover, between pairs of sites (emmeans)

contrast	estimate	SE	df	*t*-ratio	*p*-value		*p*-adjusted	Sign.
Goleen - Labhra Cliff	1.5267	0.619	6	2.47	**0.0487**	*	**0.0487**	*

Massive

Fixed effects test (Anova)

	Chi-sq	df	*p*-value
(Intercept)	2.86	1.000	0.0906
Site	0.01	1.000	0.9286
Time	0.02	1.000	0.8783
Site:Time	0.01	1.000	0.9418

Table S4.27. (Continued)

Papillate

Fixed effects test (Anova)

	Chi-sq	df	*p*-value
(Intercept)	16.12	1.000	**0.0001**
Site	3.48	1.000	0.0623
Time	0.02	1.000	0.8993
Site:Time	0.10	1.000	0.7550

Erect

Fixed effects test (Anova)

	Chi-sq	df	*p*-value
(Intercept)	0.01	1.000	0.9114
Site	1.19	1.000	0.2756
Time	0.93	1.000	0.3348
Site:Time	5.38	1.000	**0.0203**

Tests of temporal trends in erect cover at each individual site (emtrends)

Site	trend	SE	df	*t*-ratio	*p*-value		*p*-adjusted	Sign.
Goleen	0.0011	0.001	46	0.96	0.3399	ns	0.3399	ns
Labhra Cliff	0.0047	0.001	46	4.25	**0.0001**	***	**0.0002**	***

Pairwise comparisons of temporal trends in erect sponge percentage cover, between pairs of sites (emmeans)

contrast	estimate	SE	df	*t*-ratio	*p*-value		*p*-adjusted	Sign.
Goleen - Labhra Cliff	-0.003604	0.002	46	-2.32002	0.02483	*	0.024830286	*

Pairwise comparisons of erect sponge percentage cover, between pairs of sites (emmeans)

contrast	estimate	SE	df	*t*-ratio	*p*-value		*p*-adjusted	Sign.
Goleen - Labhra Cliff	-0.1505	0.073	6	-2.07	0.0836	ns	0.0836	ns

Pedunculate

Fixed effects test (Anova)

	Chi-sq	df	*p*-value
(Intercept)	2.76	1.000	0.0964
Site	3.72	1.000	0.0538
Time	0.51	1.000	0.4759
Site:Time	1.24	1.000	0.2648

Table S4.28. Results of the linear mixed effect model (lmer) testing the effects of time historical period and site on the percentage cover of the main sponge morphologies. Present-past comparison (April 1994 – August 1995 and June 2018 – November 2019). *P*-adjusted: *p*-value adjusted with Benjamini-Hochberg Procedure. Significant *p*-values ($p < 0.05$) are in bold.

Linear mixed-effects model (lme)
Benthic categories
Present-past comparison (April 1994 – August 1995 and June 2018 – November 2019)
*Formula: Percentage cover ~ Time * Site * Period + (1|Quadrat)*

Encrusting Raspailiidae

Fixed effects test (Anova)

	Chi-sq	df	*p*-value
(Intercept)	34.03	1	**< 0.0001**
Period	2.37	1	0.1238
Site	5.52	1	**0.0188**
Time	3.45	1	0.0634
Period:Site	1.68	1	0.1955
Period:Time	5.50	1	**0.0190**
Site:Time	0.02	1	0.8824
Period:Site:Time	0.95	1	0.3293

Tests of temporal trends in encr. Ras*p*- percentage cover at each individual site and historical period (emtrends)

Site	Period	trend	SE	df	*t*-ratio	*p*-value	*p*-adjusted	Sign.
Glannafeen	199x	-0.0272	0.01	56	-1.86	0.0686	0.1113	ns
Labhra Cliff	199x	-0.0246	0.01	56	-2.61	**0.0116**	**0.0466**	*
Glannafeen	20xx	0.0201	0.01	56	1.45	0.1524	0.1524	ns
Labhra Cliff	20xx	0.0009	0.00	56	1.76	0.0835	0.1113	ns

Pairwise comparisons of temporal trends in encr. Ras*p*- percentage cover, between pairs of sites at each historical period (emtrends)

contrast	Period	estimate	SE	df	*t*-ratio	*p*-value	*p*-adjusted	Sign.
Glannafeen - Labhra Cliff	199x	-0.0026	0.02	56	-0.15	0.8830	0.8830	ns
Glannafeen - Labhra Cliff	20xx	0.0191	0.01	56	1.38	0.1722	0.3443	ns

Pairwise comparisons of temporal trends in encr. Ras*p*- percentage cover, between historical periods at each site (emtrends)

contrast	Site	estimate	SE	df	*t*-ratio	*p*-value	*p*-adjusted	Sign.
199x - 20xx	Glannafeen	-0.0473	0.02	56	-2.35	**0.0225**	**0.0225**	*
199x - 20xx	Labhra Cliff	-0.0256	0.01	56	-2.70	**0.0091**	**0.0182**	*

Pairwise comparisons of encr. Ras*p*- percentage cover, between pairs of sites, at each historical period (emmeans)

contrast	Period	estimate	SE	df	*t*-ratio	*p*-value	*p*-adjusted	Sign.
Glannafeen - Labhra Cliff	199x	16.5295	7.05	16	2.35	**0.0322**	0.0644	ns
Glannafeen - Labhra Cliff	20xx	3.8050	7.05	16	0.54	0.5966	0.5966	ns

Pairwise comparisons of encr. Ras*p*- percentage cover, between, historical period at each site (emmeans)

contrast	Site	estimate	SE	df	*t*-ratio	*p*-value	*p*-adjusted	Sign.
199x - 20xx	Glannafeen	10.4636	7.05	16	1.48	0.1570	0.3140	ns
199x - 20xx	Labhra Cliff	-2.2609	7.04	16	-0.32	0.7524	0.7524	ns

Table S4.27. (Continued).

Encrusting non-Raspaiilidae

Fixed effects test (Anova)

	Chi-sq	df	*p*-value
(Intercept)	5.79	1	**0.0161**
Period	0.16	1	0.6858
Site	1.25	1	0.2630
Time	0.60	1	0.4379
Period:Site	3.54	1	0.0600
Period:Time	2.03	1	0.1540
Site:Time	16.62	1	**< 0.0001**
Period:Site:Time	42.15	1	**< 0.0001**

Tests of temporal trends in encrusting percentage cover at each individual site and historical period (emtrends)

Site	Period	trend	SE	df	*t*-ratio	*p*-value	*p*-adjusted	Sign.
Glannafeen	199x	0.0054	0.01	56	0.78	0.4412	0.4412	ns
Labhra Cliff	199x	-0.1178	0.03	56	-4.01	**0.0002**	**0.0004**	***
Glannafeen	20xx	-0.0100	0.01	56	-1.21	0.2309	0.3078	ns
Labhra Cliff	20xx	0.0996	0.02	56	5.71	**< 0.0001**	**< 0.0001**	****

Pairwise comparisons of temporal trends in encrusting percentage cover, between pairs of sites at each historical period (emtrends)

contrast	Period	estimate	SE	df	*t*-ratio	*p*-value	*p*-adjusted	Sign.
Glannafeen - Labhra Cliff	199x	0.1232	0.03	56	4.08	**0.0001**	**0.0001**	***
Glannafeen - Labhra Cliff	20xx	-0.1096	0.02	56	-5.68	**< 0.0001**	**< 0.0001**	****

Pairwise comparisons of temporal trends in encrusting percentage cover, between historical periods at each site (emtrends)

contrast	Site	estimate	SE	df	*t*-ratio	*p*-value	*p*-adjusted	Sign.
199x - 20xx	Glannafeen	0.0154	0.01	56	1.43	0.1596	0.1596	ns
199x - 20xx	Labhra Cliff	-0.2174	0.03	56	-6.36	**< 0.0001**	**< 0.0001**	****

Pairwise comparisons of encrusting percentage cover, between pairs of sites, at each historical period (emmeans)

contrast	Period	estimate	SE	df	*t*-ratio	*p*-value	*p*-adjusted	Sign.
Glannafeen - Labhra Cliff	199x	-1.6742	2.38	16	-0.70	0.4914	0.4914	ns
Glannafeen - Labhra Cliff	20xx	2.7540	2.36	16	1.17	0.2596	0.4914	ns

Pairwise comparisons of encrusting percentage cover, between, historical period at each site (emmeans)

contrast	Site	estimate	SE	df	*t*-ratio	*p*-value	*p*-adjusted	Sign.
199x - 20xx	Glannafeen	-0.8276	2.35	16	-0.35	0.7298	0.7298	ns
199x - 20xx	Labhra Cliff	3.6006	2.38	16	1.51	0.1497	0.2994	ns

Table S4.28. (Continued)

Massive

Fixed effects test (Anova)

	Chi-sq	df	*p*-value
(Intercept)	0.08	1	0.7735
Period	0.00	1	0.9739
Site	73.23	1	**< 0.0001**
Time	0.00	1	0.9748
Period:Site	35.18	1	**< 0.0001**
Period:Time	0.01	1	0.9032
Site:Time	4.80	1	**0.0285**
Period:Site:Time	2.68	1	0.1017

Tests of temporal trends in massive percentage cover at each individual site and historical period (emtrends)

Site	Period	trend	SE	df	*t*-ratio	*p*-value	*p*-adjusted	Sign.
Glannafeen	199x	0.0013	0.04	56	0.03	0.9749	0.9749	ns
Labhra Cliff	199x	-0.1229	0.04	56	-3.07	**0.0033**	**0.0133**	*
Glannafeen	20xx	0.0081	0.04	56	0.21	0.8381	0.9749	ns
Labhra Cliff	20xx	0.0142	0.04	56	0.36	0.7199	0.9749	ns

Pairwise comparisons of temporal trends in massive percentage cover, between pairs of sites at each historical period (emtrends)

contrast	Period	estimate	SE	df	*t*-ratio	*p*-value	*p*-adjusted	Sign.
Glannafeen - Labhra Cliff	199x	0.1241	0.06	56	2.19	**0.0326**	0.0653	ns
Glannafeen - Labhra Cliff	20xx	-0.0061	0.06	56	-0.11	0.9130	0.9130	ns

Pairwise comparisons of temporal trends in massive percentage cover, between historical periods at each site (emtrends)

contrast	Site	estimate	SE	df	*t*-ratio	*p*-value	*p*-adjusted	Sign.
199x - 20xx	Glannafeen	-0.0068	0.06	56	-0.12	0.9036	0.9036	ns
199x - 20xx	Labhra Cliff	-0.1371	0.06	56	-2.44	**0.0180**	**0.0361**	*

Pairwise comparisons of massive percentage cover, between pairs of sites, at each historical period (emmeans)

contrast	Period	estimate	SE	df	*t*-ratio	*p*-value	*p*-adjusted	Sign.
Glannafeen - Labhra Cliff	199x	-9.0302	1.08	16	-8.36	**< 0.0001**	**< 0.0001**	****
Glannafeen - Labhra Cliff	20xx	-0.2587	1.08	16	-0.24	0.8140	0.8140	ns

Pairwise comparisons of massive percentage cover, between, historical period at each site (emmeans)

contrast	Site	estimate	SE	df	*t*-ratio	*p*-value	*p*-adjusted	Sign.
199x - 20xx	Glannafeen	-0.0172	1.08	16	-0.02	0.9875	0.9875	ns
199x - 20xx	Labhra Cliff	8.7543	1.08	16	8.10	**< 0.0001**	**< 0.0001**	****

Table S4.28. (Continued)

Papillate

Fixed effects test (Anova)

	Chi-sq	df	*p*-value
(Intercept)	46.08	1	**< 0.0001**
Period	19.34	1	**< 0.0001**
Site	21.72	1	**< 0.0001**
Time	15.19	1	**0.0001**
Period:Site	9.63	1	**0.0019**
Period:Time	20.77	1	**< 0.0001**
Site:Time	5.45	1	**0.0195**
Period:Site:Time	7.28	1	**0.0070**

Tests of temporal trends in papillate percentage cover at each individual site and historical period (emtrends)

Site	Period	trend	SE	df	*t*-ratio	*p*-value	*p*-adjusted	Sign.
Glannafeen	199x	-0.0405	0.01	56	-3.90	**0.0003**	**0.0010**	**
Labhra Cliff	199x	-0.0062	0.01	56	-0.60	0.5540	0.6516	ns
Glannafeen	20xx	0.0265	0.01	56	2.55	**0.0136**	**0.0272**	*
Labhra Cliff	20xx	0.0047	0.01	56	0.45	0.6516	0.6516	ns

Pairwise comparisons of temporal trends in papillate percentage cover, between pairs of sites at each historical period (emtrends)

contrast	Period	estimate	SE	df	*t*-ratio	*p*-value	*p*-adjusted	Sign.
Glannafeen - Labhra Cliff	199x	-0.0343	0.01	56	-2.33	**0.0232**	**0.0463**	*
Glannafeen - Labhra Cliff	20xx	0.0218	0.01	56	1.48	0.1443	0.1443	ns

Pairwise comparisons of temporal trends in papillate percentage cover, between historical periods at each site (emtrends)

contrast	Site	estimate	SE	df	*t*-ratio	*p*-value	*p*-adjusted	Sign.
199x - 20xx	Glannafeen	-0.0670	0.01	56	-4.56	**< 0.0001**	**0.0001**	****
199x - 20xx	Labhra Cliff	-0.0109	0.01	56	-0.74	0.4612	0.4612	ns

Pairwise comparisons of papillate percentage cover, between pairs of sites, at each historical period (emmeans)

contrast	Period	estimate	SE	df	*t*-ratio	*p*-value	*p*-adjusted	Sign.
Glannafeen - Labhra Cliff	199x	3.5936	0.82	16	4.37	**0.0005**	**0.0010**	***
Glannafeen - Labhra Cliff	20xx	0.4034	0.82	16	0.49	0.6305	0.6305	ns

Pairwise comparisons of papillate percentage cover, between, historical period at each site (emmeans)

contrast	Site	estimate	SE	df	*t*-ratio	*p*-value	*p*-adjusted	Sign.
199x - 20xx	Glannafeen	3.1089	0.82	16	3.78	**0.0016**	**0.0033**	**
199x - 20xx	Labhra Cliff	-0.0812	0.82	16	-0.10	0.9226	0.9226	ns

Table S4.28. (Continued)

Erect

Fixed effects test (Anova)

	Chi-sq	df	*p*-value
(Intercept)	5.63	1	**0.0177**
Period	1.84	1	0.1748
Site	0.12	1	0.7324
Time	1.43	1	0.2316
Period:Site	0.19	1	0.6639
Period:Time	1.03	1	0.3110
Site:Time	9.97	1	**0.0016**
Period:Site:Time	11.03	1	**0.0009**

Tests of temporal trends in erect percentage cover at each individual site and historical period (emtrends)

Site	Period	trend	SE	df	*t*-ratio	*p*-value	*p*-adjusted	Sign.
Glannafeen	199x	0.0104	0.01	56	1.20	0.2366	0.3155	ns
Labhra Cliff	199x	-0.0611	0.02	56	-2.92	**0.0050**	**0.0196**	*
Glannafeen	20xx	< 0.0001	0.01	56	-0.01	0.9947	0.9947	ns
Labhra Cliff	20xx	0.0063	0.00	56	2.67	**0.0098**	**0.0196**	*

Pairwise comparisons of temporal trends in erect percentage cover, between pairs of sites at each historical period (emtrends)

contrast	Period	estimate	SE	df	*t*-ratio	*p*-value	*p*-adjusted	Sign.
Glannafeen - Labhra Cliff	199x	0.0715	0.02	56	3.16	**0.0026**	**0.0051**	**
Glannafeen - Labhra Cliff	20xx	-0.0063	0.01	56	-1.05	0.2981	0.2981	ns

Pairwise comparisons of temporal trends in erect percentage cover, between historical periods at each site (emtrends)

contrast	Site	estimate	SE	df	*t*-ratio	*p*-value	*p*-adjusted	Sign.
199x - 20xx	Glannafeen	0.0104	0.01	56	1.01	0.3153	0.3153	ns
199x - 20xx	Labhra Cliff	-0.0673	0.02	56	-3.20	**0.0023**	**0.0045**	**

Pairwise comparisons of erect percentage cover, between pairs of sites, at each historical period (emmeans)

contrast	Period	estimate	SE	df	*t*-ratio	*p*-value	*p*-adjusted	Sign.
Glannafeen - Labhra Cliff	199x	0.0137	1.65	16	0.01	0.9935	0.9935	ns
Glannafeen - Labhra Cliff	20xx	0.3908	1.63	16	0.24	0.8130	0.9935	ns

Pairwise comparisons of erect percentage cover, between, historical period at each site (emmeans)

contrast	Site	estimate	SE	df	*t*-ratio	*p*-value	*p*-adjusted	Sign.
199x - 20xx	Glannafeen	2.2975	1.63	16	1.41	0.1774	0.1774	ns
199x - 20xx	Labhra Cliff	2.6746	1.64	16	1.63	0.1234	0.1774	ns

Table S4.28. (Continued)

Pedunculate

Fixed effects test (Anova)

	Chi-sq	df	*p*-value
(Intercept)	6.41	1	**0.0113**
Period	1.20	1	0.2728
Site	0.10	1	0.7509
Time	0.04	1	0.8501
Period:Site	0.01	1	0.9247
Period:Time	11.45	1	**0.0007**
Site:Time	0.73	1	0.3914
Period:Site:Time	3.45	1	0.0632

Tests of temporal trends in pedunculate percentage cover at each individual site and historical period (emtrends)

Site	Period	trend	SE	df	*t*-ratio	*p*-value	*p*-adjusted	Sign.
Glannafeen	199x	-0.0012	0.01	56	-0.19	0.8507	0.8507	ns
Labhra Cliff	199x	-0.0088	0.01	56	-1.40	0.1667	0.3334	ns
Glannafeen	20xx	0.0288	0.01	56	4.60	< **0.0001**	**0.0001**	****
Labhra Cliff	20xx	-0.0021	0.01	56	-0.33	0.7412	0.8507	ns

Pairwise comparisons of temporal trends in pedunculate percentage cover, between pairs of sites at each historical period (emtrends)

contrast	Period	estimate	SE	df	*t*-ratio	*p*-value	*p*-adjusted	Sign.
Glannafeen - Labhra Cliff	199x	0.0076	0.01	56	0.86	0.3951	0.3951	ns
Glannafeen - Labhra Cliff	20xx	0.0309	0.01	56	3.49	**0.0010**	**0.0019**	**

Pairwise comparisons of temporal trends in pedunculate percentage cover, between historical periods at each site (emtrends)

contrast	Site	estimate	SE	df	*t*-ratio	*p*-value	*p*-adjusted	Sign.
199x - 20xx	Glannafeen	-0.0300	0.01	56	-3.38	**0.0013**	**0.0026**	**
199x - 20xx	Labhra Cliff	-0.0067	0.01	56	-0.76	0.4527	0.4527	ns

Pairwise comparisons of pedunculate percentage cover, between pairs of sites, at each historical period (emmeans)

contrast	Period	estimate	SE	df	*t*-ratio	*p*-value	*p*-adjusted	Sign.
Glannafeen - Labhra Cliff	199x	0.1230	0.18	16	0.69	0.5025	0.5025	ns
Glannafeen - Labhra Cliff	20xx	0.2867	0.18	16	1.60	0.1296	0.2592	ns

Pairwise comparisons of pedunculate percentage cover, between, historical period at each site (emmeans)

contrast	Site	estimate	SE	df	*t*-ratio	*p*-value	*p*-adjusted	Sign.
199x - 20xx	Glannafeen	-0.0324	0.18	16	-0.18	0.8590	0.8590	ns
199x - 20xx	Labhra Cliff	0.1313	0.18	16	0.73	0.4749	0.8590	ns